



# THE UNIVERSITY *of* EDINBURGH

Investigating the role of the Rad51 regulation by  
Srs2 and Rad54 during DNA replication and repair

Tadas Andriuskevicius

Thesis submitted for the Degree of Doctor of Philosophy

School of Biological Sciences

The University of Edinburgh

November 2021

## Table of contents

Declaration.....	6
Acknowledgements.....	7
Abstract.....	8
Lay summary.....	10
Abbreviations.....	11
Chapter 1. General introduction .....	13
1.1. DNA damage and repair.....	13
1.1.1. Base excision repair.....	13
1.1.2. Nucleotide excision repair.....	15
1.1.3. Ribonucleotide excision repair.....	17
1.1.4. Mismatch repair .....	17
1.1.5. DNA double-strand breaks.....	19
1.1.5.1. Non-homologous end joining .....	20
1.1.5.2. Homology-directed repair.....	23
1.1.5.2.1. DNA end resection.....	23
1.1.5.2.2. Rad51 recombinase .....	25
1.1.5.2.3. Rad51 nucleofilament formation.....	26
1.1.5.2.4. Strand invasion .....	27
1.1.5.2.5. Gene conversion.....	28
1.1.5.2.6. Break-induced replication .....	30
1.1.5.2.7. Single-strand annealing .....	30
1.1.5.2.8. DSB repair in meiosis .....	31
1.1.6. DNA damage tolerance .....	33
1.1.6.1. Translesion synthesis.....	33
1.1.6.2. Template switching .....	34
1.1.6.3. DNA damage tolerance at replication forks .....	36
1.1.6.4. Postreplicative gap repair .....	38
1.1.7. DNA damage checkpoint.....	42
1.2. The disassembly of Rad51 nucleofilaments and its role in the DNA maintenance .....	47
1.2.1 PCNA loading.....	47

1.2.2. Damage-associated DNA synthesis and Rad51 .....	48
1.2.3. Rad51 removal from ssDNA .....	50
1.2.4. Rad51 removal from dsDNA.....	51
1.2.5. The <i>srs2Δ</i> and <i>rad54Δ</i> synthetic lethality.....	53
Chapter 2. Materials and Methods.....	55
2.1. Yeast strains .....	55
2.2. Oligonucleotides.....	55
2.3. Plasmids .....	55
2.4. Restriction enzymes.....	55
2.5. Propagation and manipulation of yeast and bacteria .....	74
2.5.1. Growth media .....	74
2.5.2. Cell stocks.....	77
2.5.3. Yeast transformation .....	77
2.5.4. Yeast mating, sporulation, and tetrad dissection .....	78
2.5.5. Measuring the yeast doubling time .....	80
2.5.6. Yeast spot assay .....	80
2.5.7. <i>E. coli</i> competent cells preparation.....	81
2.5.8. <i>E. coli</i> transformation .....	82
2.6. General manipulation of DNA .....	83
2.6.1. The amplification of cassettes for gene deletions and truncations, protein tagging and placing genes under a galactose-inducible promoter .....	83
2.6.2. Yeast colony PCR .....	85
2.6.3. Molecular cloning .....	86
2.6.4. Agarose gel electrophoresis .....	88
2.7. General manipulation of proteins.....	89
2.7.1. TCA protein precipitation.....	89
2.7.2. SDS polyacrylamide gel electrophoresis .....	90
2.7.3. Western blotting .....	91
2.7.4. Antibodies .....	92
2.8. SSA assays .....	93
2.8.1. Plating assay .....	93
2.8.2. Time-course experiments to assay SSA .....	94

2.8.2.1. Cell synchronisation, $P_{GAL1}$ induction and sample collection.....	94
2.8.2.2. Genomic DNA extraction .....	95
2.8.2.3. Labelling of Southern blotting DNA probes with $^{32}P$ .....	96
2.8.2.4. Southern blotting.....	97
2.8.2.5. Analysis of flap cleavage by qPCR .....	99
2.9. Analysis of the cell cycle progression in $P_{GAL1}\text{-RAD55 } srs2\Delta \ rad54\Delta \ rad53\text{-13Myc}$ cells .....	100
2.9.1. Cell synchronisation, $P_{GAL1}$ induction and sample collection .....	100
2.9.2. FACS .....	102
2.10. Detection of persistent Rad51 chromatin binding in $P_{GAL1}\text{-RAD55 } srs2\Delta \ rad54\Delta$ cells .....	103
2.10.1. Cell synchronisation, $P_{GAL1}$ induction and sample collection .....	103
2.10.2. Cell fractionation.....	105
2.11. Statistical analyses .....	106
Chapter 3. The functional relationship between Srs2 and Rad54 in the regulation of Rad51 during damage-associated DNA synthesis.....	107
3.1. Introduction .....	107
3.2. The SSA system used to study the damage-associated DNA synthesis .....	109
3.3. The lack of Srs2 and/or Rad54 leads to a decreased SSA efficiency in the $P_{GAL1}\text{-RAD51}$ background .....	114
3.4. The elimination of Srs2 and/or Rad54 affects the earlier stages of SSA in the $P_{GAL1}\text{-RAD51}$ background .....	117
3.5. $RAD51$ expression from $P_{GAL1}$ leads to excessive protein levels.....	119
3.6. In the $P_{GAL1}\text{-RAD55}$ background, the deletion of $RAD54$ decreases the efficiency of SSA only when combined with $srs2\Delta$ .....	122
3.7. Rad54 cannot effectively substitute for the Srs2 function in damage-associated DNA synthesis .....	126
3.8. Discussion .....	129
Chapter 4. The molecular aspects of the $srs2\Delta$ and $rad54\Delta$ synthetic lethality.....	133
4.1. Introduction .....	133

4.2. <i>P<sub>GAL1</sub>-RAD55 srs2Δ rad54Δ</i> cells grown in galactose accumulate chromatin-bound Rad51 .....	134
4.3. After the addition of galactose, <i>P<sub>GAL1</sub>-RAD55 srs2Δ rad54Δ</i> mutants activate the DNA damage checkpoint in the first cell cycle.....	137
4.4. Postreplicative repair by HR and TLS is not essential for cell viability.....	141
4.5. Discussion.....	147
Chapter 5. Suppressors of the <i>srs2Δ</i> and <i>rad54Δ</i> synthetic lethality .....	150
5.1. Introduction .....	150
5.2. Rad51-II3A cannot effectively inhibit damage-associated DNA synthesis .....	151
5.3. The lack of the Rad54 function in the damage-associated DNA synthesis significantly contributes to the <i>srs2Δ</i> and <i>rad54Δ</i> synthetic lethality .....	154
5.4. NER and MMR do not significantly contribute to the generation of expanded ssDNA gaps in unchallenged yeast cells.....	157
5.5. The 9-1-1 complex may primarily cause the cell death of <i>srs2Δ rad54Δ</i> mutants through Exo1-dependent resection rather than DNA damage checkpoint signalling .....	158
5.6. Identifying the hypothetical Mec3-interacting regions in Exo1 ....	161
5.7. <i>HED1</i> expression suppresses the <i>srs2Δ</i> and <i>rad54Δ</i> synthetic lethality .....	164
5.8. Discussion.....	170
Chapter 6. Summary and general discussion .....	174
6.1. Srs2 and Rad54 have complementary functions in the negative regulation of Rad51.....	175
6.2. In the absence of the strand invasion, Rad51 nucleofilaments need to be enzymatically disassembled to complete the genome duplication.....	176
6.3. Enzymatic Rad51 removal might be required for the completion of genome duplication even when strand invasion is functional .....	179
6.4. The synthetic lethality of <i>srs2Δ</i> and <i>rad54Δ</i> is suppressed when the formation of stable Rad51 nucleofilaments is prevented.....	181
6.5. The mechanistic model explaining the synthetic lethality of <i>srs2Δ</i> and <i>rad54Δ</i> .....	183
References .....	186

## **Declaration**

I declare that this thesis has been composed by myself and the work presented here is my own, unless stated otherwise. This work has not been submitted for any other degree or professional qualification.

A handwritten signature in black ink, appearing to read "Tadas Andriuskevicius". A small, stylized "D" is written at the end of the signature.

Tadas Andriuskevicius

November 2021

## Acknowledgements

I would like to express my gratitude to my supervisor Dr Sveta Makovets for being a role model of an excellent scientist and supporting me throughout my PhD journey by both providing guidance when I am hesitant and encouraging independent thinking and creativity.

I would also like to thank Prof David Leach, Dr Elizabeth Bayne and Dr Sara Buonomo for providing feedback on my work every year and helping me to make the most out of my PhD studies.

I would like to express appreciation to my labmates Alexey Kotenko, Andrei Sukhareuski, Dmitry Degtev, John Hutchinson, Anton Dubenko, Alex Postrach, Prashant Pandit, Hayat Anu Ranjani and Tanya Kardash for a caring and supportive atmosphere that contributed greatly towards my constructive and enjoyable time in the lab.

I am also very grateful for the financial and academic support provided by the EASTBIO Doctoral Training Partnership and the University of Edinburgh.

I would also like to express my gratitude to one of my best friends Kristina Stakyte who greatly contributed to all my academic achievements. I could never forget my partner in crime Raminta Kazlauskaitė who is always there to keep me grounded and entertained. I would also like to thank my friends back in Lithuania who make home feel so much closer keeping the homesickness at bay. I want to say thank you to my flatmates Adam Dykes, Leon Matkovics and Mihail Dishev for always having my back and making Edinburgh my second home.

I owe everything that I have ever achieved to my amazing parents who have moved mountains for me and my siblings. Along with my brother, sister, grandparents, aunts, uncles and cousins they gave me a marvellous life that I am very grateful for every day.

## Abstract

DNA carries the information necessary for the continuity of life. However, its integrity is constantly threatened by genotoxic stress exerted by various exogenous and endogenous factors. DNA damage may lead to genetic instability, which can disrupt normal cellular processes and cause cell death. Therefore, multiple mechanisms have evolved to protect the genome integrity.

Replication and many DNA repair mechanisms require the formation of single-stranded DNA (ssDNA) intermediates which eventually must be converted back to double-stranded DNA (dsDNA). The results of the experiments performed on the budding yeast *Saccharomyces cerevisiae* in this study suggest that DNA replication routinely generates ssDNA gaps, most likely at the regions with obstacles for DNA polymerases. These gaps must be filled in postreplicatively to restore the doublestrandedness of DNA, thereby completing the genome duplication.

Postreplicative gaps are preferentially repaired by an error-free recombination-based mechanism. This involves the formation of Rad51 nucleofilaments required for the identification of homologous donor sequences which are used as templates for the reconstitution of dsDNA. The elimination of two Rad51 regulators, Srs2 and Rad54, causes the death of *Saccharomyces cerevisiae* cells. In *srs2Δ rad54Δ* double mutants, postreplicative gaps cannot be resolved by recombination as Rad54 is necessary for this type of repair.

The alternative pathway to restore doublestrandedness involves a simple filling of ssDNA gaps by DNA polymerases. However, although necessary for the establishment of recombination intermediates, Rad51 filaments can hinder the recruitment and loading of DNA synthesis machinery at DNA damage sites. Srs2 helicase can promote damage-associated DNA synthesis by disassembling Rad51 nucleofilaments formed on ssDNA. It was demonstrated in this study that Rad54 translocase capable of removing Rad51 from dsDNA can facilitate the DNA synthesis during DNA repair along with Srs2. Further analysis has revealed that the activities of Srs2 and Rad54 in the

said process are mostly complementary rather than redundant. This is most likely because the two proteins work on different substrates – Rad51 filaments formed on ssDNA and dsDNA respectively.

The *srs2Δ rad54Δ* mutants were found to accumulate chromatin-bound Rad51 after a single round of DNA replication suggesting that Rad51 filaments cannot be effectively disassembled in these cells. Furthermore, extensive DNA loss was observed after the double mutants attempted to divide and entered the second round of DNA replication. The elimination of the DNA end resection nuclease Exo1 rescued the viability of the *srs2Δ rad54Δ* cells. The nucleolytic processing of ssDNA gaps is known to be required for an efficient formation of Rad51 nucleofilaments. Thus, the excessive expansion of ssDNA gaps by Exo1 and the failure to repair them due to the inability to disassemble Rad51 nucleofilaments is the likely explanation of the DNA loss and cell death in the absence of both Srs2 and Rad54.

Overall, this study provides evidence that the disassembly of Rad51 nucleofilaments by Srs2 and/or Rad54 is necessary to enable the filling of postreplicative ssDNA gaps by DNA polymerases and is likely required for the routine genome maintenance.

## Lay summary

DNA contains the instructions required for the living organisms to grow, survive and reproduce. However, many factors, like radiation and chemicals, including those formed during normal cellular processes, can damage DNA, threatening the integrity of the information it carries. In order to counteract these threats, multiple mechanisms have evolved to protect and maintain DNA inside the living cells.

To ensure the continuity of life, DNA needs to be replicated. During replication, the two DNA strands of the double helix serve as templates to produce two new copies of double-stranded DNA (dsDNA). The experiments performed in this study using budding yeast suggest that when replication enzymes encounter natural barriers for DNA synthesis, single-stranded DNA (ssDNA) gaps are frequently formed. These ssDNA gaps must be converted to dsDNA for cells to survive. However, the binding of a DNA repair protein called Rad51 to DNA inhibits the filling of these ssDNA gaps. It has previously been discovered that an enzyme Srs2 capable of removing Rad51 from ssDNA can promote the restoration of dsDNA. This study provides the evidence that another enzyme, Rad54, also participates in this process. The absence of both Srs2 and Rad54 was found to result in the accumulation of Rad51 bound to DNA and the failure to fill in ssDNA gaps, which led to cell death.

Overall, this study provides molecular insights into the regulation of the important DNA repair protein Rad51 and elucidates the role of this regulation in genome maintenance and cell survival.

## Abbreviations

<b>aNHEJ</b>	alternative non-homologous end joining
<b>AP</b>	apurinic/apyrimidinic
<b>APS</b>	ammonium persulfate
<b>ATP</b>	adenosine triphosphate
<b>BER</b>	base excision repair
<b>BIR</b>	break-induced replication
<b>bp</b>	base pair(s)
<b>BSA</b>	bovine serum albumin
<b>cNHEJ</b>	classical non-homologous end joining
<b>DNA</b>	deoxyribonucleic acid
<b>dNTP</b>	deoxynucleoside triphosphate
<b>DSB</b>	double-strand break
<b>DSBR</b>	double-strand break repair
<b>dsDNA</b>	double-stranded DNA
<b>GAL</b>	galactose
<b>GC</b>	gene conversion
<b>h</b>	hour(s)
<b>HDR</b>	homology-directed repair
<b>HJ</b>	Holliday junction
<b>HR</b>	homologous recombination
<b>indel</b>	insertion-deletion
<b>kDa</b>	kilodalton(s)
<b>min</b>	minute(s)
<b>MIP</b>	MLh1-interacting-peptide box
<b>MMR</b>	mismatch repair
<b>MMS</b>	methyl methanesulfonate
<b>NEB</b>	New England Biolabs
<b>NER</b>	nucleotide excision repair
<b>NHEJ</b>	non-homologous end joining
<b>OD<sub>600</sub></b>	optical density at 600 nm

<b>PCNA</b>	proliferating cell nuclear antigen
<b>PCR</b>	polymerase chain reaction
<b>PEG</b>	polyethylene glycol
<b>PIP</b>	PCNA-interacting peptide box
<b>PVP</b>	polyvinylpyrrolidone
<b>qPCR</b>	quantitative PCR
<b>RAF</b>	raffinose
<b>RER</b>	ribonucleotide excision repair
<b>RFC</b>	replication factor C
<b>RPA</b>	replication protein A
<b>RT</b>	room temperature
<b>SD</b>	standard deviation
<b>SDS</b>	sodium dodecyl sulphate
<b>SDSA</b>	synthesis-dependent strand annealing
<b>SDS-PAGE SDS</b>	SDS polyacrylamide gel electrophoresis
<b>SHIP</b>	Msh2-interacting-peptide box
<b>SIM</b>	SUMO-interacting motif
<b>SSA</b>	single-strand annealing
<b>ssDNA</b>	single-stranded DNA
<b>TCA</b>	trichloroacetic acid
<b>TEMED</b>	tetramethylethylenediamine
<b>TLS</b>	translesion synthesis
<b>TS</b>	template switching
<b>v/v</b>	volume per volume
<b>w/v</b>	weight per volume
<b>WT</b>	wild-type
<b>YP</b>	yeast extract-peptone
<b>YPD</b>	yeast extract-peptone-glucose
<b>YPRAF</b>	yeast extract-peptone-raffinose
<b>YPGAL</b>	yeast extract-peptone-galactose

# **Chapter 1. General introduction**

## **1.1. DNA damage and repair**

The secret of life lies within DNA. Made up of only four basic building blocks, the DNA underpins the overwhelming biodiversity found on our planet. However, its integrity inside the cells is constantly threatened by a genotoxic stress exerted by both environmental and endogenous factors. It is estimated that each human cell suffers tens of thousands of DNA lesions every day (1). Without appropriate repair, DNA damage might lead to mutations, the disruption of normal physiological processes and cell death (1-3). Thus, cells have evolved multiple mechanisms to ensure the repair and maintenance of their genetic material. These appear to be well conserved among eukaryotes and the overview of the major repair pathways is provided below, with the focus on a model organism *Saccharomyces cerevisiae* (4).

### **1.1.1. Base excision repair**

Damage to the individual bases is one of the most common types of DNA lesions (5, 6). This includes oxidative and other chemical modifications of the DNA bases as well as the formation of abasic sites (3, 5, 6). These lesions can be produced by exogenous factors such as alkylating drugs as well as reactive oxygen species generated during normal cellular metabolism (3, 5, 6). The instances of this kind of damage which do not lead to a significant distortion of the DNA helix are generally corrected by base excision repair (BER; Figure 1.1) (3). In such cases, the lesions are detected by a range of DNA glycosylases which cleave the glycosidic bond between the deoxyribose and its damaged nitrogenous base. The resulting abasic site is then recognized by apurinic/apyrimidinic (AP) endonucleases which introduce a nick in the phosphate backbone on the 5' end of the lesion. In human cells, the remnants of the damaged nucleotide can be removed and simultaneously replaced with a new nucleotide by polymerase  $\beta$ . Alternatively, polymerases  $\epsilon$

and  $\delta$  can catalyse DNA synthesis displacing a stretch of the 5' ended DNA containing the abasic site. The displaced DNA flap is then removed by a structure-specific endonuclease Rad27/FEN1. In both cases, the resulting nick is ligated by a DNA ligase to complete the repair (3, 7, 8). It appears that in *S. cerevisiae* the base excision repair does not involve polymerase  $\beta$  and mostly occurs by strand displacement (8).

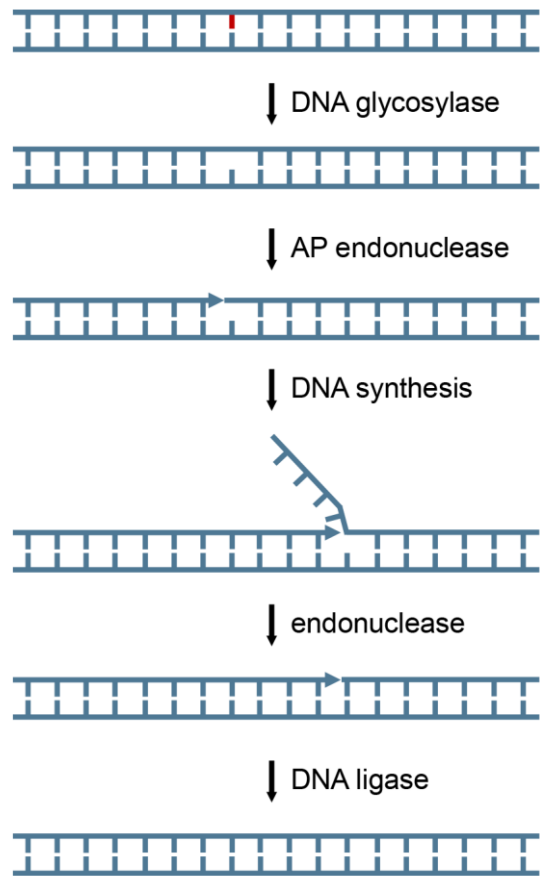


**Figure 1.1. Base excision repair**

IN BER pathway, DNA glycosylases detect a damaged DNA base and cleave its glycosidic bond with the associated deoxyribose. The resulting abasic site is recognised and cleaved by AP endonucleases. DNA synthesis is then initiated at the nick displacing a stretch of 5' ended DNA containing the abasic site. The DNA flap is then cleaved, and the resulting nick is ligated. Horizontal blue lines represent DNA backbone while vertical lines depict DNA bases. Arrow heads symbolise the 3' ends of DNA. A red vertical line represents a damaged DNA base.

### 1.1.2. Nucleotide excision repair

Bulkier lesions that significantly distort the DNA helix are usually corrected by nucleotide excision repair (NER; Figure 1.2). These include cyclobutane pyrimidine dimers induced by ultraviolet radiation as well as adducts and crosslinks produced by chemical agents (7, 9). NER can be divided into two sub-pathways. The first one, the global-genome NER, resolves lesions throughout the genome. In *S. cerevisiae*, it requires the Rad7-Rad16 complex which detects and specifically binds to damaged DNA (7, 9). The second sub-pathway, the transcription-coupled NER, corrects lesions on the transcribed strands of active genes. The repair is triggered by the damage-associated stalling of RNA polymerase and is mediated by either Rad26 or a nonessential subunit of RNA polymerase II, Rpb9. The two mediators seem to work independently, and their relative importance depends on the transcribed gene in question (7, 9). The genetic requirements of NER converge on *RAD4* which is essential for both sub-pathways (7, 9). Rad4 interacts with Rad23 and Rad33 which stimulate its function and protect it from degradation (10, 11). Similar to Rad7-Rad16, the Rad4-Rad23-Rad33 complex also detects and binds damaged DNA (7, 9). The exact recruitment order of the DNA damage sensing factors in NER is not fully understood. The fate of a stalled RNA polymerase during transcription-coupled NER in *S. cerevisiae* is not clear either, but based on the evidence in human cells, it seems that the polymerase is backtracked providing access for the repair factors (7).

Once the DNA damage is recognised, a small opening around the lesion is generated, most likely by the Rad4-Rad23-Rad33 complex. This enables the recruitment of the transcription factor TFIIH which extends the DNA opening further by using the helicase activities of its subunits Rad3 and Rad25. The damage detection proteins are then most likely released, and the unwound DNA is stabilised by the Replication Protein A (RPA) (7, 9). The lesion is bound and reassessed by Rad14 which is believed to be testing the bendability of the DNA to confirm the presence of a damage in a lesion-unspecific manner (12). This verification step is required for the further progression of the repair (13).

After the lesion has been verified, the structure-dependent nucleases Rad2 and Rad1-Rad10, recruited by TFIID and Rad14 respectively, incise the DNA strand around the lesion releasing a 24-27 nucleotide fragment. The resulting ssDNA gap is filled in by DNA polymerases and sealed by a DNA ligase completing the repair (7, 9).

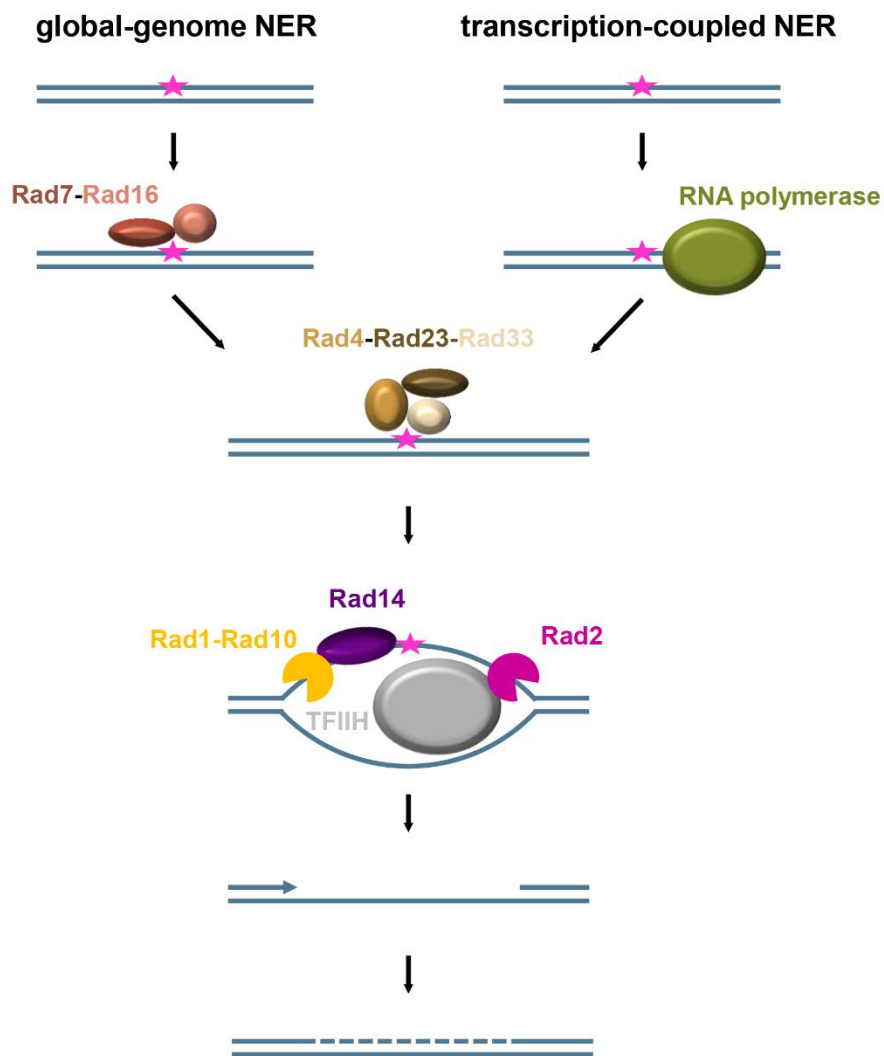


**Figure 1.2. Nucleotide excision repair**

In the NER pathway, DNA damage is detected either by Rad7-Rad16 throughout the genome or by RNA polymerases stalling at actively transcribed regions. The lesions are further recognised by Rad4-Rad23-Rad33 complex which introduces a small opening at the damage site. This enables the recruitment of TFIID which extends the opening further. Rad14 then verifies the presence of the DNA damage and a nucleotide fragment containing the lesion is excised from the affected DNA strand by Rad1-Rad10 and Rad2 endonucleases. The resulting ssDNA gap is then filled in and

ligated completing the repair. Solid blue lines represent the strands of the double helix and arrow heads indicate their 3' ends. Dashed lines specify newly synthesised DNA. The pink star represents a DNA lesion. Figure adapted from Tatum and Li (2011) (9).

### 1.1.3. Ribonucleotide excision repair

During replication, ribonucleotides can erroneously be incorporated into the newly synthesised DNA potentially compromising genome integrity (14). Such abnormalities are resolved by the ribonucleotide excision repair (RER) which is initiated by RNase H2. RNase H2 is able to detect mis-incorporated ribonucleotides and introduce a nick on their 5' side. DNA polymerases can then extend the 3'-terminated strand at the nick displacing the DNA strand containing the ribonucleotide. The DNA flap is then removed by a structure-specific endonuclease and the resulting nick is sealed by a DNA ligase completing the repair (7, 15).

### 1.1.4. Mismatch repair

Mismatch repair (MMR) corrects DNA helix distortions caused by base pairing issues (Figure 1.3). These include opposing non-complementary bases as well as loops formed by nucleotide insertions or deletions on one of the two strands. Mismatches can result from DNA synthesis errors or recombination events between non-identical sequences (7). MMR starts with a detection and verification of a mismatch. This is carried out by a class of protein complexes referred to as MutS. In *S. cerevisiae*, two nuclear MutS complexes are present in mitotic cells – Msh2-Msh6 and Msh2-Msh3. The former is believed to be specialised in the repair of mismatched base-pairs (bp), while the latter is important for the removal of large insertion-deletion (indel) loops. The two complexes are mostly redundant in the repair of smaller indels (7).

To ensure the appropriate repair of replicative DNA mismatches, cells must distinguish between parental and newly synthesised DNA strands. This is most likely achieved by the MMR dependence on DNA nicks and the coupling of some MMR factors to DNA replication. MutS complexes can

interact with Proliferating Cell Nuclear Antigen (PCNA) – a processivity factor which acts as a platform for the DNA replication machinery. This interaction targets them to the DNA replication sites and freshly made DNA strands (7). Once MutS recognises and binds a mismatch, another protein complex generally referred to as MutL is recruited. Mlh1-Pms1 is the main MutL complex in *S. cerevisiae* although two other complexes are known with either meiosis-specific or unidentified functions (7). Exonuclease Exo1 is then recruited to the repair site via its interactions with Msh2 and Mlh1 and removes the affected stretch of the newly synthesised strand (7). Exo1 has a 5' → 3' directionality and thus requires a nick on the 5' end of the mismatch to access the lesion and perform the strand resection in the right direction. During the lagging strand synthesis, nicks are inherently formed as a result of discontinuous synthesis and can be utilised by the MMR machinery. In contrast, the leading strand synthesis is mostly continuous. Pms1 has been implicated in introducing the nicks during the repair of mismatches on the leading strand. Pms1 has a latent endonuclease activity which is triggered by PCNA (7). Naturally, PCNA is located on the 3' end of the mismatch where the new DNA is being synthesised. It is postulated, that once activated, Mlh1-Pms1 can migrate to the other side of the lesion and introduce one or multiple nicks enabling mismatch removal by Exo1 (16). It appears that the inherent structural asymmetry of PCNA dictates which strand is newly synthesised and needs to be nicked by Pms1 (17). The DNA gap created by Exo1 can then be filled by DNA polymerases and sealed by a DNA ligase (7). It has also been proposed that DNA nicks introduced by RNase H2 during RER can be exploited by MMR as well (18, 19).

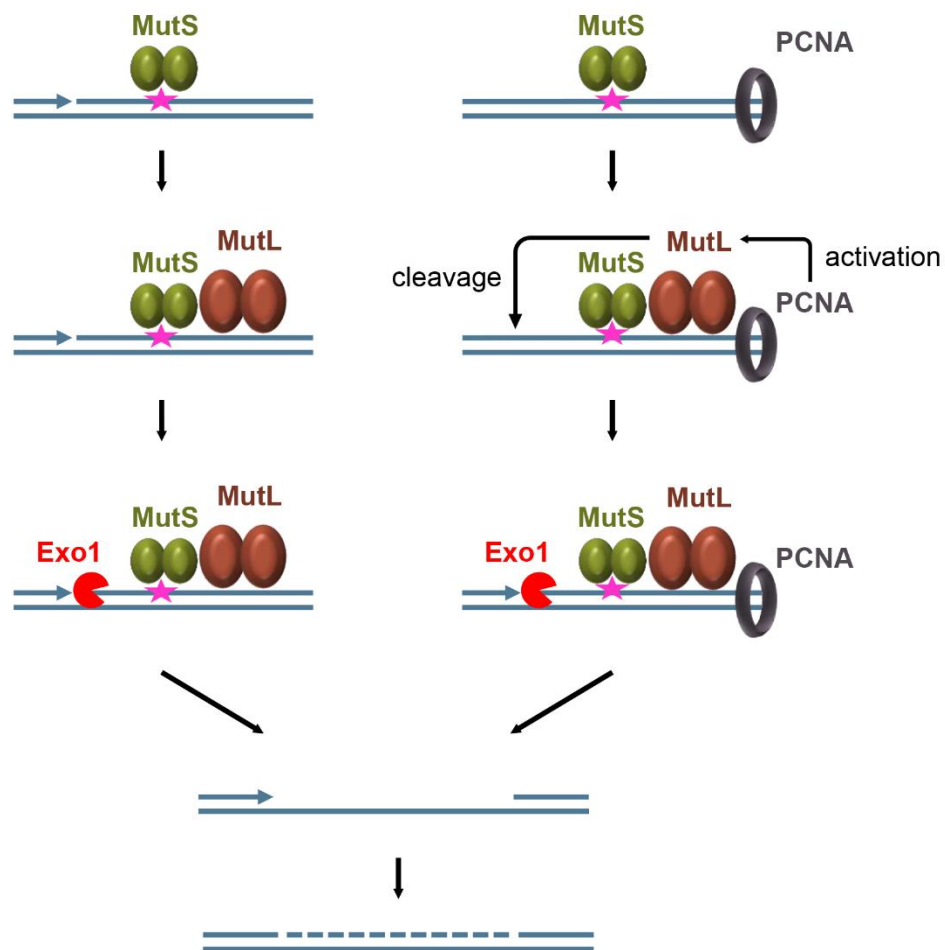


**Figure 1.3. Mismatch repair**

In the MMR pathway, DNA helix distortions caused by mismatches are detected by MutS. Consequentially, the MutL complex is recruited to the site. If a DNA nick resulting from the RNase H2 activity or the discontinuous synthesis of a lagging strand is present on the 5' end of the mismatch, it can directly act as an entry point for Exo1 nuclease. Alternatively, PCNA at the 3' end of the newly synthesised DNA strand can activate the endonuclease activity of MutL which can then introduce a nick on the 5' end of the mismatch. Exo1 recruited to the nick degrades a stretch of the DNA strand containing the mismatch. The resulting gap is then filled in and ligated completing the repair. Solid blue lines represent strands of the double helix and arrow heads indicate their 3' ends. Dashed lines specify newly synthesised DNA. The pink star represents a DNA mismatch.

### 1.1.5. DNA double-strand breaks

One of the most dangerous types of DNA lesions is considered to be a double-strand break (DSB). It occurs when the both strands of the double helix are broken close enough to prevent the base-pairing from holding the ends together. Exogenous factors like ionising radiation, mutagenic chemicals and

mechanical stress as well as reactive oxygen species generated during normal cellular metabolism may cause DSBs. Furthermore, single-ended DSBs may be formed after the collapse of replication forks prompted by other kinds of DNA lesions (6, 20). DSBs may lead to DNA loss, chromosomal rearrangements and cell death. The lack of the appropriate DSB repair has been implicated in multiple human disorders as well as the carcinogenesis (21). However, DSBs may also be genetically programmed and required for the normal cellular function. The examples of biological processes which include programmed DSB induction are the formation of chiasmata during meiosis, mating type switching in yeasts and VDJ recombination during the differentiation of T and B lymphocytes in animals (22).

Regardless of the origin, DSBs must be repaired. They are first detected by Ku and MRX complexes which rapidly and independently localise to DSBs *in vivo* (23-25). Ku is a ring-shaped heterodimer which has a high affinity for dsDNA ends and is comprised of Yku70 and Yku80 in *S. cerevisiae*. Ku blocks access to the ends of DSBs by other proteins and prevents the nucleolytic degradation of DNA (23). The MRX complex in *S. cerevisiae* consists of Mre11, Rad50 and Xrs2. The Rad50 molecules in the MRX complexes bound to the broken DNA ends can dimerise and tether the ends together facilitating the subsequent repair (23, 25). From this point on, multiple repair mechanisms can be employed to fix DSBs. These can generally be categorised as non-homologous end joining (NHEJ) and homology-directed repair (HDR).

#### **1.1.5.1. Non-homologous end joining**

NHEJ is a simpler repair pathway and basically involves a direct rejoining of broken DNA ends. The outcome of NHEJ depends on the nature of DSBs and the stochastic events of DNA degradation and synthesis prior to the ligation step, but this repair pathway is generally considered to be more mutagenic than HDR (23). Nonetheless, NHEJ is useful when homologous sequences suitable for repair are not available, for example, in the absence of homologous chromosomes and sister chromatids. NHEJ machinery is active

throughout the cell cycle but mostly occurs during the G1 stage in haploid yeasts as HDR is favoured in most other situations (23, 26). Interestingly, the prevalence of NHEJ is species-specific. In human cells, NHEJ is the predominant DSB repair pathway outside of the mid S phase during which sister chromatid recombination can be used to restore broken replication forks (27). A large portion of the human genome is highly repetitive and the attempts to repair DSBs by HR using these non-unique sequences could lead to gross chromosomal rearrangements.

NHEJ can be divided into classical (cNHEJ) and alternative (aNHEJ) sub-pathways (28). However, aNHEJ is rare in *S. cerevisiae* and thus will not be discussed here (28).

DSB repair by cNHEJ is initiated by Ku (Figure 1.4). Ku inhibits DSB resection which would make the DNA ends unsuitable for the repair by cNHEJ (23, 26, 29). Ku also recruits two other repair factors Dnl4-Lif1 and Nej1 to the DSB sites. Dnl4 is a DNA ligase IV of *S. cerevisiae* and is required strictly for cNHEJ. Dnl4 is strongly bound by Lif1 and is unstable without it. Dnl4-Lif1 DNA binding strongly depends on Ku but also requires MRX for stable association with DSBs (23, 26, 29). Another core cNHEJ protein of *S. cerevisiae*, Nej1, is haploid-specific. In diploid cells, *NEJ1* expression is inhibited effectively inactivating cNHEJ. Nej1 interacts with Lif1 and Ku supporting the formation of a stable cNHEJ complex at DSBs (23, 26, 29).

DSBs with compatible undamaged ends can be re-joined by cNHEJ machinery recreating the authentic sequence (23, 26, 29). However, some DSBs cannot be readily ligated by Dnl4 and require processing by different nucleases and DNA polymerases, which introduces indels at the repair site. The end-processing factors are generally recruited via the interactions with Dnl4-Lif1 and Nej1 (23, 26, 29).

Once the ends of a DSB are ligatable, Dnl4 can catalyse their re-joining. This step is assisted by the MRX-mediated end tethering. During the ligation Dnl4 undergoes auto-adenylation in its active site preventing it from catalysing

another reaction. Nej1 enhances Dnl4 deadenylation promoting its reactivation (23).

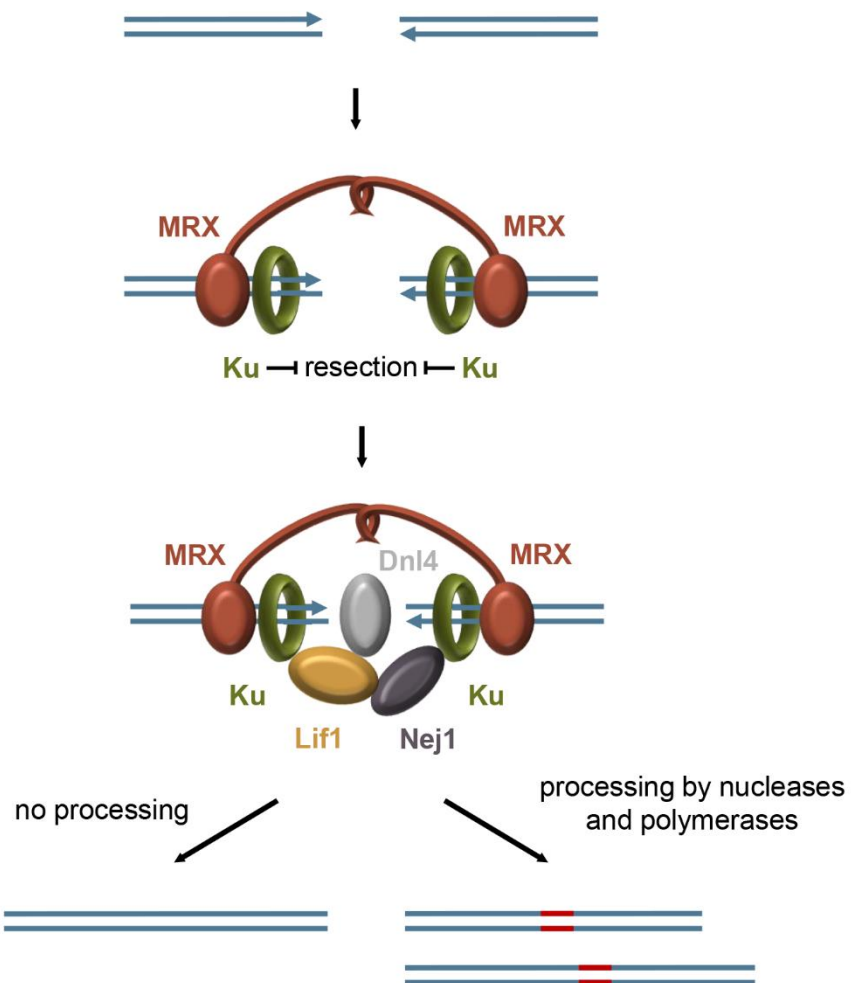


**Figure 1.4. Classical non-homologous end joining**

Inside the cells, DSBs are rapidly bound by the MRX and Ku complexes which tether the broken DNA ends and inhibit resection respectively. During cNHEJ, Ku further recruits Lif1-Dnl4 and Nej1. If the broken DNA ends are undamaged and compatible, Dnl4 can directly re-join them recreating the authentic sequence. However, if the ends are non-ligatable they must be processed by nucleases and polymerases first introducing indels at the break site. The schematic is not meant to accurately represent the exact structure of the cNHEJ complex or the stoichiometric amount of its components. Solid blue lines represent strands of the double helix and arrow heads indicate their 3' ends. Solid red lines represent indels.

### **1.1.5.2. Homology-directed repair**

#### **1.1.5.2.1. DNA end resection**

HDR involves sequences outside of the loci of DSBs. Those contain intact homologous templates and thus the repair can recreate authentic sequences of broken DNA molecules. Furthermore, unlike cNHEJ, HDR can also be used to fix single-ended DSBs. HDR requires DNA end resection in order to generate a ssDNA 3' overhang which is later used for base-pairing between homologous sequences (Figure 1.5A) (30, 31). However, the access of the resecting nucleases to the broken DNA ends is generally blocked by Ku. The Ku-dependent inhibition of DNA resection is overcome by the MRX complex (32). The MRX subunit Mre11 has a dsDNA exonuclease activity but due to its 3' → 5' polarity it cannot generate a 3' DNA overhang by resecting DSBs from their ends which are also protected by Ku. This conundrum is solved by Mre11 endonuclease activity which is greatly stimulated by another *S. cerevisiae* protein called Sae2. Upon activation, Mre11 can nick the 5'-terminated strand of a DSB and then use its exonuclease activity to generate a short 3' overhang. This results in the dissociation of Ku from the DNA ends (24, 32). The Mre11-activating function of Sae2 requires CDK-dependent phosphorylation which occurs only outside of the G1 phase of the cell cycle (32). This inhibits the resection in the absence of sister chromatids, likely minimising the risk of failed HDR due to the lack of a template in haploid cells. In diploid cells of higher eukaryotes, the inhibition of HDR in G1 might decrease the likelihood of a potentially dangerous loss of heterozygosity occurring when a homologous chromosome rather than a sister chromatid is used for the repair (30, 33). The MRX function in resection is limited to the initiation and further processing is carried out by other proteins which can access the DNA ends after the Ku removal (34). Two players have been implicated in the long-range resection – Exo1 and Dna2-Sgs1. Exo1 is a 5' → 3' exonuclease and can resect DNA on its own, while Dna2 operates as an endonuclease and functions in concert with Sgs1 helicase which requires Top3 and Rmi1 for its activity *in vivo* (32, 34). A resected DSB can be further funnelled into the gene conversion

(GC), break-induced replication (BIR) or single-strand annealing (SSA) pathways.

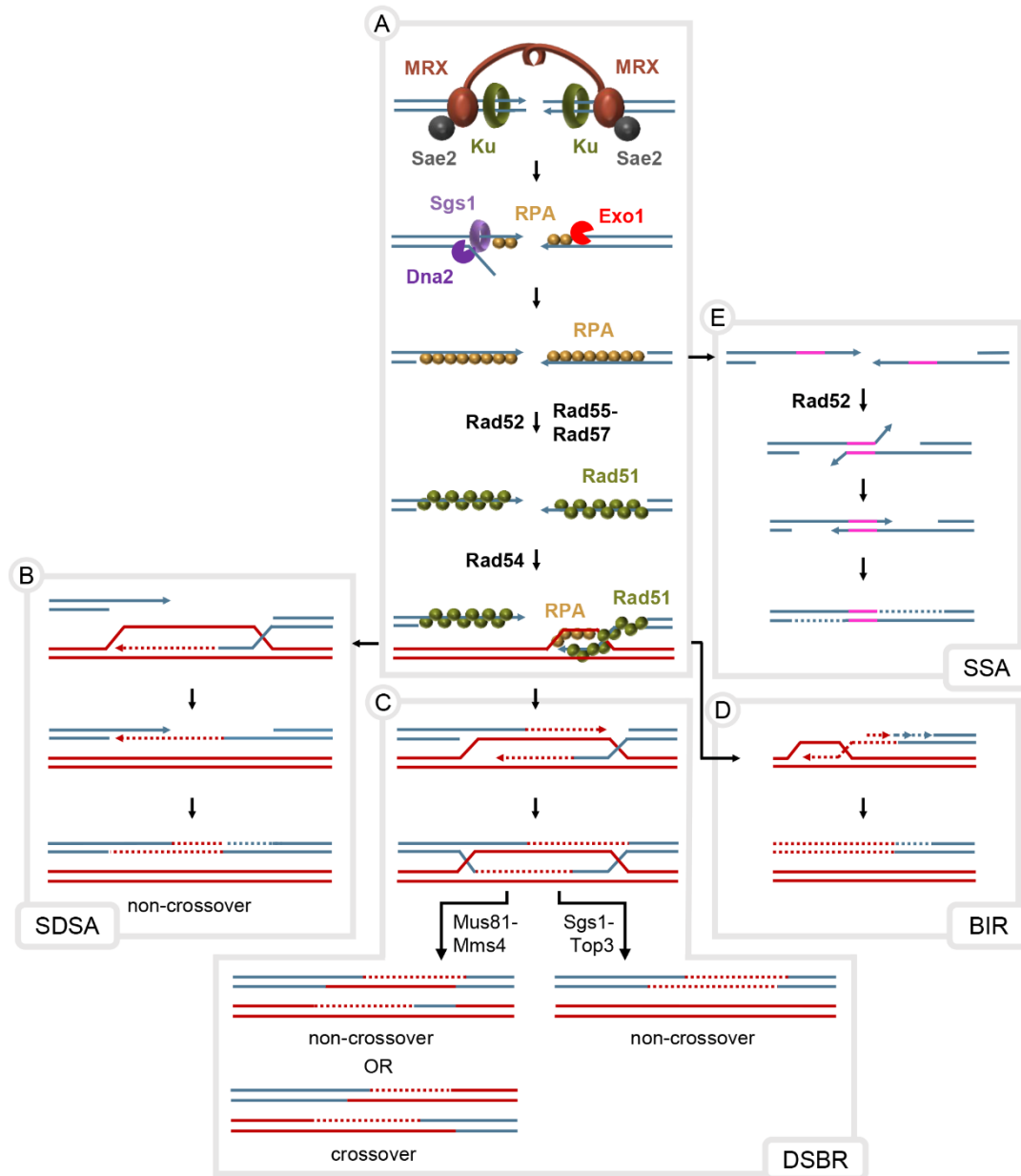


**Figure 1.5. Homology-directed repair**

**A.** Inside the cells, DSBs are rapidly bound by MRX and Ku which tether the broken DNA ends and inhibit resection respectively. Outside of G1, CDK-mediated phosphorylation of Sae2 allows it to activate the endonuclease activity of MRX subunit Mre11. Mre11 can then create short 3' overhangs causing the dissociation of Ku. Exposed DNA ends are resected further by Sgs1-Dna2 and Exo1. The ssDNA generated during the resection is rapidly bound and protected by RPA. Rad52 and Rad55-Rad57 can then mediate the formation of Rad51 nucleofilaments. Provided there is a suitable donor, Rad54 facilitates Rad51 filament invasion into the homologous template leading to the forming of a D-loop. The displaced strand is

stabilised by RPA binding. From this point onwards, multiple repair pathways can be employed depending on the circumstances. For simplicity, RPA and Rad51 bound to the DNA are not shown for the later repair steps.

**B.** During SDSA, the invading strand is extended using homologous donor as a template and then displaced allowing it to anneal to ssDNA on the other side of the break. The resulting gaps are then filled in and sealed completing the repair.

**C.** During DSBR, the second end of the break is captured by the growing D-loop and also extended forming a double HJ intermediate. This structure can then be resolved by Mus81-Mms4-mediated nucleolytic cleavage or Sgs1-Top3-mediated dissolution.

**D.** Single-ended DSBs are repaired by BIR. In this case, the D-loop migrates along the homologous donor as the invading strand is being extended. The newly synthesised DNA is displaced and serves as a template for the complementary strand synthesis. The homologous donor is copied to the end of a chromosome or until a replication bubble is encountered.

**E.** SSA can occur before the formation of Rad51 filaments or after they were disassembled due to the failure of other repair pathways. During SSA, Rad52 anneals direct homologous repeats flanking the DSB. Non-homologous DNA flaps are then cleaved off creating two ssDNA gaps which are filled in and sealed completing the repair. For simplicity, RPA bound to ssDNA is not shown.

Solid blue and red lines represent the strands of a broken DNA molecule and a homologous donor respectively. Arrow heads depict the 3' ends of DNA. Dotted lines represent newly synthesised DNA and their colour indicates which DNA molecule was used as a template. Solid pink lines specify direct repeat sequences.

#### 1.1.5.2.2. Rad51 recombinase

GC and BIR, also referred to as homologous recombination (HR) pathways, require the formation of a Rad51 nucleofilament. Rad51 is a well-conserved eukaryotic recombinase essential for the homology search during repair as well as the strand exchange reaction between a damaged DNA molecule and a homologous donor. Rad51 is defined as one of the key DNA repair proteins necessary for genome stability (31). Rad51 deficient eukaryotic cells exhibit increased sensitivity to ionising radiation, accumulation of spontaneous DSBs and higher rates of chromosome loss, all of which can be explained by the compromised DSB repair (35-38). Although Rad51 is not essential in *S. cerevisiae*, the lack of the recombinase leads to a lethality in mammalian and avian cells (36-38). The increased reliance of higher eukaryotes on Rad51 might be explained by a greater number of spontaneous DSBs they experience per cell cycle due to the larger genomes (37).

*In vitro*, Rad51 can cooperatively polymerise on ssDNA and dsDNA to form a right-handed nucleofilament in which DNA is stretched and extended facilitating homology search and base pairing (39-44). Rad51 has primary and secondary DNA binding sites allowing it to bind two DNA molecules simultaneously, which is necessary for its recombinase activity. The primary site binds DNA during the formation of the filament and accommodates the heteroduplex DNA formed after the strand exchange. The secondary DNA binding site is responsible for the interactions with a homologous donor (45-47).

Rad51 binds and hydrolyses ATP in a DNA-dependent manner. ATP binding is essential for the Rad51 catalytic activity while the hydrolysis is partially dispensable but is still necessary for the full Rad51 function *in vivo* (48-54). The purpose of the ATP hydrolysis is not completely understood. It might be important for the disassembly and recycling of the nucleofilaments as Rad51 exhibits a lower affinity to DNA when bound to ADP instead of ATP (44, 55-57).

#### **1.1.5.2.3. Rad51 nucleofilament formation**

As mentioned above, the DSB repair by HR requires the formation of Rad51 nucleofilaments on resected DNA. However, ssDNA inside the cells is more rapidly coated by RPA which is more abundant and has a higher affinity to ssDNA than Rad51 (58). Rad51 cannot readily replace RPA bound to ssDNA and requires assistance from additional factors (31). Multiple proteins can support the formation of Rad51 nucleofilaments but only three are essential for this process *in vivo* in *S. cerevisiae* and are called mediators (Figure 1.5A) (31).

Arguably the most important Rad51 mediator Rad52 has been established to promote Rad51 nucleofilament formation by recruiting Rad51 and helping it to replace RPA on ssDNA (59-62). The N-terminus of Rad51 has been discovered to interact with the DNA binding domain of RPA, possibly

promoting its dissociation (63). Thus, Rad51 nucleated by Rad52 might help free Rad51 monomers to compete with RPA for ssDNA binding leading to the extension of the filament. This is consistent with the *in vitro* reconstitution studies suggesting that RPA mainly inhibits the nucleation but not the elongation of Rad51 nucleofilaments (44, 64). *S. cerevisiae* cells lacking Rad52 are sensitive to DNA damaging agents, deficient in HR and cannot form detectable DNA damage-induced Rad51 foci, demonstrating that Rad52 is essential for the Rad51 filament formation (65-67).

Rad55 and Rad57 are two other Rad51 mediators in *S. cerevisiae*. They function as an obligate heterodimer and the removal of either one leads to an increased sensitivity to DNA damaging agents, impaired DNA repair by HR and compromised localisation of Rad51 to DSBs *in vivo* (65, 68, 69). This highlights the importance of the Rad55-Rad57 heterodimer in the formation of the functional extended Rad51 nucleofilaments. Rad55-Rad57 functions downstream of Rad52 and might facilitate Rad51 filament formation by stabilising it via protein-protein interactions (70, 71). It has also been suggested that Rad55-Rad57 bound to Rad51 filaments might antagonise and physically impede the movement of the Srs2 helicase which has the ability to remove Rad51 from ssDNA (71). However, a recent study suggests that Rad55-Rad57 does not block the translocation of Srs2 and might not be incorporated into the mature Rad51 nucleofilaments. Instead, Rad55-Rad57 might be facilitating Rad51 nucleofilament formation via transient interactions in a chaperone-like fashion and counteract Srs2 by supporting a rapid Rad51 rebinding to DNA after the removal (72). Consistent with their antagonistic roles, the removal of Srs2 can suppress some of the DNA repair defects exhibited by the cells lacking Rad55-Rad57 (73).

#### 1.1.5.2.4. Strand invasion

Successfully formed Rad51 nucleofilaments (pre-synapsis) need to locate a homologous donor sequence for the repair to proceed via HR. The exact mechanism of homology search is not fully understood but it appears to

involve transient sampling of dsDNA (74-77). The homology search greatly depends on Snf2/Swi2 translocases Rad54 and Rdh54 which might have overlapping activities in this process (65, 76). Some research suggests that Rad51 filaments are virtually unable to sample DNA for homology in the absence of the two enzymes (74, 76). However, Rad51 can be immunoprecipitated at the *HML* donor locus during the mating type switching in *S. cerevisiae* even in the absence of both Rad54 and Rdh54, albeit at lower efficiency (65). This suggests that Rad51, to an extent, has an intrinsic ability to search for homology. However, the involvement of other proteins in this process cannot be excluded.

Once the homology is located, Rad51 mediates the formation of a paranemic joint between the invading ssDNA and the dsDNA donor (synapsis). This joint is unstable as it is primarily held together by Rad51 rather than base-pairing and does not support the extension of the invading strand by DNA polymerases (65, 78-80). Rad54 appears to be essential to convert this intermediate into a fully interwound plectonemic joint (65, 78-80). The Rad54 translocation activity has been demonstrated to induce supercoiling leading to a transient opening of the double-helix (81-83). This might allow for the invading ssDNA to form a properly interwound heteroduplex with the complementary strand of the homologous donor sequence. Meanwhile, the other strand of the donor molecules is displaced creating an intermediate called a D-loop. After a D-loop is formed, the invading strand can be extended by DNA polymerases using the homologous donor as a template (post-synapsis) and the DSB repair can proceed via GC or BIR (Figure 1.5A).

#### 1.1.5.2.5. Gene conversion

GC is employed when both ends of a DSB are available and share homology with a template. It involves copying of the genetic information from the homologous donor to the broken molecule. Gene conversion can recover the authentic sequence of a broken DNA molecule if a sister chromatid is used as a template. However, in diploids, the original sequence around the DSB can

be converted into that of a homologous chromosome (hence the name of the repair pathway) if it is used as a template for the repair (84, 85). This chromosome may contain some sequence diversity stemming from silent single nucleotide polymorphisms to mutations that affect the gene function.

GC can proceed via two mechanistically different sub-pathways, double-strand break repair (DSBR; Figure 1.5C) or synthesis-dependent strand annealing (SDSA; Figure 1.5B). The current model of DSBR suggests that the Rad51 nucleofilament formed on one end of a DSB invades a homologous donor forming a D-loop. As the D-loop is extended by DNA synthesis, the displaced strand pairs with the Rad51 nucleofilament on the other side of the break capturing the second end which is then also extended. The subsequent ligation of the DNA strands forms an intermediate with two four-way junctions called Holliday Junctions (HJs) (84, 85). These can be resolved by structure-specific endonucleases Mus81-Mms4 and Yen1 (86-88). Srs2 helicase has been shown to promote the Mus81-Mms4 activity by stimulating it directly and by removing Rad51 from HJs to provide access for the nuclease (89, 90). Depending on the strands cleaved to resolve the HJs, two outcomes are possible: a crossover, when the donor and recipient chromosomes exchange their arms, or non-crossover, when the genetic exchange is limited to the sequence between the HJs (84, 85). HJs can also be dissolved by the topoisomerase Top3 which functions in concert with the helicase Sgs1 and only produces non-crossover events (84, 86, 87).

During SDSA, the invading strand is extended but the second end is not captured. Instead, the extended strand is displaced from the donor and anneals to the resected DNA on the other end of the DSB. The resulting ssDNA gaps are then filled in by DNA polymerases and sealed by DNA ligases forming a non-crossover repaired product (84, 85). Several *S. cerevisiae* helicases have been implicated in the promotion of strand displacement during SDSA including Srs2, Sgs1 and Mph1 (91-93).

#### **1.1.5.2.6. Break-induced replication**

BIR is used when only one end of a DSB is present or matches a homologous donor, for example, when breaks are formed after a collapse of a replication fork or in a close proximity to a telomere (Figure 1.5D). In this case, the template molecule is copied from the invasion site to the telomere or an adjacent replication bubble (33, 94). Break-induced replication occurs via conservative DNA synthesis. After the initial formation, D-loop migrates along the template as the invading strand is extended. Extended strand is then used as a template for the synthesis of a complementary strand (33, 94).

Both GC and BIR are often referred to as error-free. However, if a homologous chromosome or an ectopic homology site are used as templates, HR might result in a loss of heterozygosity and translocations (33). Furthermore, the DNA repair synthesis appears to be less faithful than that of the conventional DNA replication (95).

#### **1.1.5.2.7. Single-strand annealing**

SSA exploits direct repeats flanking a DSB. Unlike HR, SSA is intrinsically mutagenic as one copy of the repeats and any intervening sequences between the repeats are lost during the repair. However, it might be useful when other HDR mechanisms are not available, for example, in the absence of a homologous donor (96).

SSA can take place after the direct repeats are exposed by resection (Figure 1.5E). The repeats are annealed by Rad52 which possesses an ability to anneal complementary ssDNA coated by RPA (97, 98). The Rad52 activity in this process is augmented by its paralog Rad59 (99). After the annealing, non-homologous DNA flaps can be generated and are cleaved by the Rad1-Rad10 structure-specific endonuclease creating an intermediate with two ssDNA gaps which are then filled in by DNA polymerases and sealed by DNA ligases completing the repair (31, 96, 100).

SSA does not require Rad51 and is, in fact, inhibited by it (101-103). Rad51 binding to both resected strands blocks the ability of Rad52 to anneal ssDNA (98). This contrasts with the Rad52-mediated second end capture during DSBR where only resected but not displaced strand is covered by Rad51 (98, 104, 105). The Rad51-dependent inhibition of SSA might be important to channel DSBs to the non-mutagenic HR pathways. However, while it takes 5-10 minutes for Rad51 filaments to form *in vitro*, the Rad52-mediated ssDNA annealing is completed within a few minutes (104). This suggests that under the right circumstances, the annealing step of SSA might occur before the formation of Rad51 nucleofilaments. Furthermore, Rad59 has been demonstrated to mitigate Rad51-dependent inhibition of the Rad52-mediated ssDNA annealing *in vitro* (104). Consistently, SSA is also promoted by Srs2 known to remove Rad51 from ssDNA (101, 103, 106). As SSA requires direct repeats for the repair, it is unusable for most DSBs in yeast. In contrast, human genome contains a lot of repetitive sequences and SSA can play a more significant role in DSB repair there.

#### **1.1.5.2.8. DSB repair in meiosis**

Apart from the maintenance of genomic stability, DSB repair is also important for the creation of genetic diversity by meiosis which is the key step in the sexual reproduction in eukaryotes. The programmed induction of DSBs followed by their repair provides not only genetic recombination between homologous chromosomes from different parents but is also crucial for the establishment of chiasmata which is essential for accurate chromosome segregation during meiosis (107). In *S. cerevisiae*, the programmed meiotic DSBs are induced by Spo11 (108). These breaks are then resected by a cooperative action of MRX complex and Exo1. In contrast to the mitotic DSB repair, Sgs1-Dna2 does not appear to participate in the end resection in meiosis (109). To ensure the creation of new genetic combinations and the formation of chiasmata, it is essential that the programmed DSBs are repaired by GC, preferentially using a homologous chromosome rather than a sister

chromatid as a template. Multiple proteins were found to be required to ensure this, but the mechanism of the donor preference has not been fully elucidated yet. However, it is clear that a meiosis-specific Rad51 homolog Dmc1 is necessary to create the donor preference towards homologous chromosomes (107).

After the Spo11-induced DSBs have been resected, they are covered by RPA which is later replaced by Rad51 and Dmc1. Although both recombinases are required for efficient meiosis, the strand exchange activity of Rad51 is dispensable. Instead, Rad51 appears to be important for the assembly of Dmc1 on ssDNA. It has been suggested that Dmc1 filaments are primarily initiated at the ends of nucleated Rad51. The Dmc1 filament formation is also dependent on its specific mediator Mei5–Sae3 which helps it to replace RPA on resected DNA (107). Once extended Dmc1 filaments are formed, the recombinase mediates a homology search and strand invasion with the preference for homologous chromosomes. This process depends on the Dmc1 accessory factor Hop2–Mnd1 (107). Snf2/Swi2 translocases also participate in meiosis but, in contrast to the mitotic DSB repair, Rad54 appears to have only a minor role while Rdh54 is more important in the promotion of the Dmc1-mediated recombination (110-112).

Both outcomes of GC occur during meiotic DSB repair (113, 114). However, some crossovers are absolutely necessary to establish the chiasmata providing the pairing of homologous chromosomes during meiosis I. It is known that cells ensure an appropriate number of crossovers between every chromosome pair, but the molecular mechanism of this process is still enigmatic (114, 115). It appears that the decision on the repair outcome for each DSB might be made well before the HJ resolution step (114).

For the meiotic recombination to preferentially occur between homologous chromosomes, Dmc1 must guide the homology search and strand invasion as the Rad51-mediated DSB repair has a strong donor preference towards sister chromatids (115). In *S. cerevisiae*, this is ensured by a meiosis-specific protein Hed1 which specifically binds Rad51 (111, 115-

117). Hed1 functions by blocking the interaction between Rad51 and Rad54 (111, 116, 117). As Rad54 is essential for the Rad51-mediated DSB repair, the meiotic recombination can predominantly be guided by Dmc1. Hed1 also downregulates the Rdh54 interaction with Rad51 but to a much smaller extent (116). Hed1 does not alter the Rad51 binding to DNA and might even have a stabilising effect *in vitro*, depending on the experimental conditions (111, 117). All in all, the DSB repair consist of a multitude of branches tailored for the specific cellular circumstances.

### **1.1.6. DNA damage tolerance**

Certain DNA lesions can block replicative DNA polymerases stalling the replication forks or uncoupling DNA synthesis on the leading and lagging strands. Long-lived ssDNA at challenged replication forks might be susceptible to passive breakage and cleavage by endonucleases, thereby threatening genomic integrity (118). Thus, additional mechanisms, collectively called DNA damage tolerance, have evolved to deal with DNA lesions that escape other repair pathways and hinder DNA replication. These include translesion synthesis (TLS) and template switching (TS) and are curated by post-translational modifications of PCNA (119, 120).

#### **1.1.6.1. Translesion synthesis**

TLS involves specialised polymerases that can synthesise DNA across different lesions. However, incorrect bases might be incorporated at the site of DNA damage making TLS error-prone (119, 120). *S. cerevisiae* has three translesion polymerases Rev1, Rev3-Rev7 (Pol  $\zeta$ ) and Rad30 (Pol  $\eta$ ). Rev3-Rev7 is considered the main translesion polymerase, while Rad30 is specialised in bypassing UV-induced damage and can, in fact, replicate across cyclobutane pyrimidine dimers without introducing mutations. Rev1 primarily acts as a regulatory scaffold required for the function of other translesion polymerases, while its own catalytic activity is mostly dispensable (121). The

recruitment of the translesion polymerases to the sites of blocked DNA synthesis is facilitated by mono-ubiquitination of PCNA carried out by the Rad6-Rad18 complex in response to DNA damage. The lesion bypass by TLS mostly occurs during the late S or G2/M phases (119, 120).

#### **1.1.6.2. Template switching**

TS exploits sister chromatids to bypass replication blocks and requires Rad51 as well as its mediators. Generally, it is very similar to the canonical HR but is genetically distinguishable by the requirement of some additional factors. TS depends on the polyubiquitination of PCNA. This involves the Rad5-Ubc13-Mms2 complex which adds ubiquitin molecules to the pre-existing one on the PCNA monoubiquitinated by Rad6-Rad18. Similar to the canonical HR, the homology search and strand invasion during TS are carried out by Rad51 and Rad54 (119, 120, 122). However, it has been demonstrated that Rad5 might also participate in the D-loop formation. As it involves a homologous donor, TS is generally regarded error-free and predominantly occurs during the early S phase (119, 120).

The canonical HR can act as a backup for TS during the lesion bypass and is referred to as the salvage pathway (119, 120). Although very similar to TS, it has some differences. The salvage pathway might be more prone to crossovers and thus has a higher propensity for undesirable genomic rearrangements (119, 120). It has been suggested that the salvage pathway primarily creates an intermediate with two HJs and these can be resolved to produce both crossover and non-crossover products. In contrast, the Rad5- and Rad51-mediated TS is thought to predominantly form hemicatenane intermediates which can be processed only by the Sgs1-Top3-mediated dissolution resulting in non-crossovers (119, 120). In support of this model, some evidence suggests that the ectopic expression of structure-specific endonucleases cannot prevent the accumulation of early recombination intermediates formed in *sgs1Δ* cells exposed to the ssDNA gap-inducing drug methyl methanesulfonate (MMS) but can promote their removal later on (119,

123). Perhaps, the persistent hemicatenanes are converted to HJ-containing intermediates during the later stages of the cell cycle enabling their resolution by nucleolytic cleavage. However, the ectopic endonuclease expression does decrease the overall level of early recombination intermediates (123). Same is observed when the mechanisms restricting the Mus81-Mms4 activity to G2/M are disrupted in *sgs1Δ* cells treated with MMS (124). This suggests that at least a fraction of early recombination intermediates is structurally susceptible for the endonuclease-mediated resolution. Thus, further research is required to clearly define the mechanistic differences between TS and canonical HR. Either way, it appears that TS intermediates are primarily processed by Sgs1-Top3 in early S phase but can also be resolved by Mus81-Mms4 in G2/M. Yen1 nuclease is activated only in the later stages of mitosis and does not appear to significantly contribute to the processing of these structures (86, 87).

During the bulk DNA replication, the salvage pathway is generally inhibited and does not contribute to damage bypass in *S. cerevisiae*. This is achieved by PCNA SUMOylation which is upregulated during the S phase (125, 126). Srs2 helicase capable of removing Rad51 from ssDNA binds SUMOylated PCNA and inhibits unscheduled HR during replication (119, 120). It is not entirely clear how PCNA SUMOylation is orchestrated with the TS which also requires Rad51. Possibly, the Srs2 levels are decreased timely and locally at the damage sites allowing TS to occur. This might be achieved by targeting of the replication fork-bound Srs2 for proteasomal degradation. Srs2 might also be untethered from the lesion bypass sites via the unloading of SUMOylated PCNA which is mediated by the Elg1-containing Replication Factor C (RFC) complex (127).

To summarise, the error-free TS is the preferred mechanism to bypass DNA lesions during the early S phase. However, if it is not available or unsuccessful, the more recombinogenic salvage pathway or error-prone TLS might be employed instead during the late S and G2/M phases.

### **1.1.6.3. DNA damage tolerance at replication forks**

DNA lesions may be bypassed directly at stalled replication forks. During TS, Rad51-mediated strand invasion allows a blocked DNA strand to be extended beyond the lesion using the newly synthesised complementary strand as a template (Figure 1.6A). Alternatively, TLS machinery can be recruited to synthesise DNA across the lesion (Figure 1.6B) (119, 120).

DNA damage can also be bypassed by rewinding a replication fork, which forms an X-shaped structure with the newly synthesised strands paired with each other (Figure 1.6C). The blocked strand can be extended pass the lesion using the other strand as a template. The conversion of the reversed fork back to its normal state would then enable further replication bypassing DNA damage. It is not exactly clear how the fork reversal is mediated but Rad5 and the helicases Rrm3, Pif1 and Mph1 as well as the main HR factors Rad51 and Rad54 have been suggested to participate in the process. However, the physiological importance of reversed replication forks is enigmatic as they appear to be largely inhibited or prevented by the DNA damage checkpoint in normal *S. cerevisiae* cells (118, 128, 129).

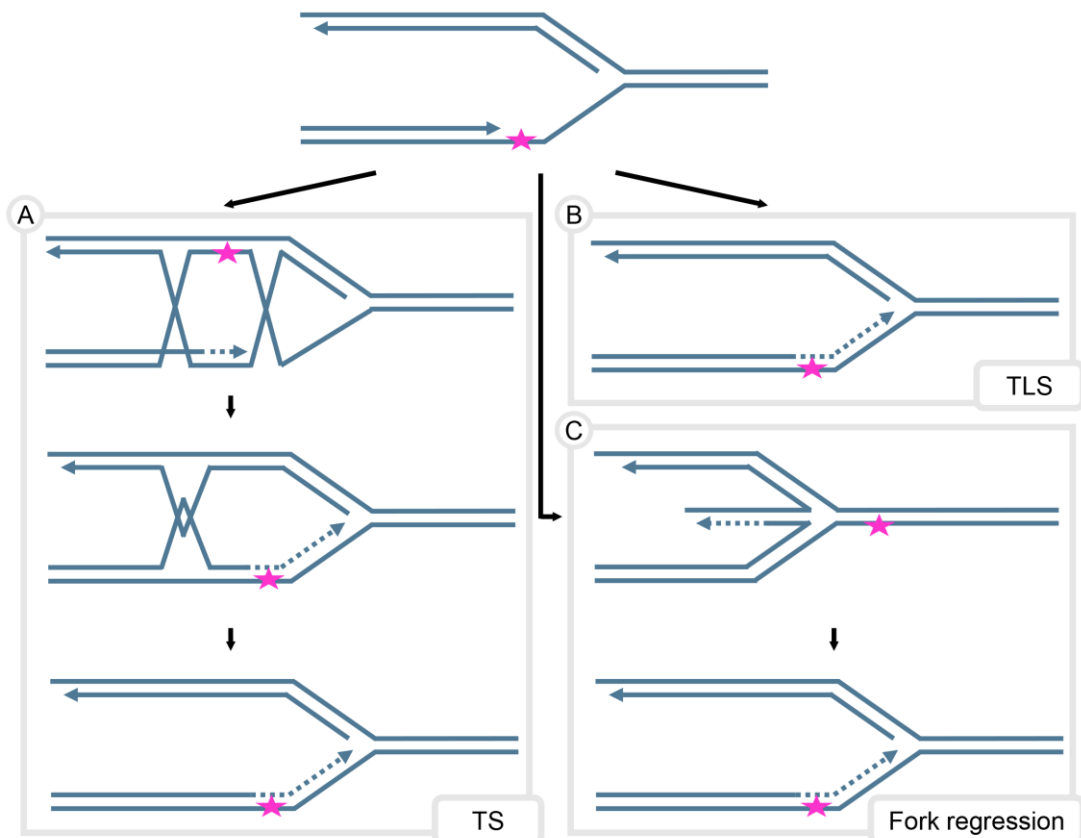


**Figure 1.6. DNA damage tolerance at replication forks**

**A.** DNA lesions can be bypassed at replication forks via TS. In this pathway, Rad51 filaments formed on ssDNA accumulated after the blockage of DNA synthesis catalyse strand invasion into the other arm of the replication fork. This allows for the newly synthesised complementary strand to serve as a template for the extension of blocked strand beyond the lesion. The resulting hemicatenane intermediate is resolved by Sgs1-Top3.

**B.** TLS can be used to extend the blocked DNA strand across the lesion directly. In this case, replicative polymerases are exchanged for translesion polymerases which can synthesise across the lesion. This bypasses DNA damage allowing replication to continue. However, translesion polymerases are less faithful and thus mutations might be introduced opposite to the lesion.

**C.** Replication forks can also be regressed annealing newly synthesised daughter strands. The blocked strand can then be extended beyond the lesion using the other one as a template.

Solid blue lines represent the DNA strands and arrow heads depict their 3' ends. Dotted lines indicate newly synthesised DNA. The pink star represents a DNA lesion.

#### **1.1.6.4. Postreplicative gap repair**

Instead of engaging with a DNA lesion directly, a replication fork might simply restart the synthesis downstream of the lesion leaving behind a ssDNA gap which can then be filled in by post-replicative repair (Figure 1.7). It is easy to imagine this happening on the lagging strand due to its discontinuous nature. However, previous research shows that in the presence of DNA damage, postreplicative gaps also form on the leading strand (130-132). Furthermore, although Rad18 and Rad5 are necessary for efficient replication through DNA damage in *S. cerevisiae*, their artificial restriction to G2/M does not significantly affect the bulk DNA replication in the presence of polymerase-blocking lesions (119, 130, 133). DNA damage tolerance events represented by the foci of fluorescently tagged RPA and Rad52 formed in response to DNA damaging agents are also primarily resolved behind replication forks (134). This suggests that the synthesis repriming downstream of the lesions might be quite prevalent and that the cells might prioritise the completion of bulk genome duplication leaving the DNA damage to be dealt with postreplicatively.

It appears that the formation of postreplicative ssDNA gaps can also be prompted by non-damage polymerase blocks. Naturally occurring secondary DNA structures and RNA:DNA hybrids can hinder DNA synthesis (135). As demonstrated in avian cells, a specialised DNA primase-polymerase PrimPol promotes processive and timely genome duplication by repriming DNA synthesis downstream of G-quadruplexes and R-loops (136, 137). *S. cerevisiae* cells do not contain PrimPol and thus most likely rely on the replicative primase Pol $\alpha$  (138). This makes it more difficult to study the repriming of the DNA synthesis in response to non-damage replication blocks as Pol $\alpha$  is essential. However, it was demonstrated that Pif1 helicase involved in G-quadruplex resolution reaches its maximum binding to these structures after the passage of replication forks in *S. cerevisiae* (139). Similarly, it was suggested that the RNase H2 activity in G2 and not the S phase is required for an adequate removal of R-loops in yeasts (140). Furthermore, it was previously observed that the RPA and Rad52 foci spontaneously formed in the absence of exogenous DNA damage in *S. cerevisiae* predominantly represent

ssDNA gaps rather than DSBs or stalled replication forks (134). Thus, yeasts may resemble higher eukaryotes where the non-damage DNA polymerase blocks are skipped by the replication forks leaving their resolution and the subsequent gap filling to occur postreplicatively.

It is not entirely clear, but it appears that the ssDNA gaps left behind replication forks are rather small. PrimPol has been shown to restarts DNA synthesis about 14 nucleotides downstream of DNA lesions *in vitro* (141). Furthermore, the experiments with Xenopus egg extracts suggest that the ssDNA gaps smaller than 40 nucleotides long are initially formed behind replication forks in response to polymerase-blocking lesions (131, 142). Although the situation might be similar, additional research is required to estimate the size of these gaps in *S. cerevisiae*.

The gaps left behind replication forks as a result of DNA damage are repaired by TLS and TS. It is likely that these gaps are initially too small to support the formation of multiprotein complexes required for postreplicative repair. They might be detected and initially expanded by the MRX complex which was found to be involved in both TLS and TS pathways (143). The MMS-induced PCNA monoubiquitylation is almost abolished in the absence of MRX and the complex has been demonstrated to physically interact with Rad18 supporting its early role in postreplicative repair (143). The MRX-mediated expansion of ssDNA gaps likely enables the loading of PCNA as well as 9-1-1 complex involved in the DNA damage checkpoint (Figure 1.7A) (144, 145).

The 9-1-1 complex has been implicated in both branches of the postreplicative repair (144, 145). It might promote TLS via the DNA damage checkpoint-dependent phosphorylation of Rev1, which increases the proficiency of the polymerase  $\zeta$ -mediated lesion bypass (144). The role of the 9-1-1 complex in TS appears to be more direct and likely involves the recruitment of Exo1 as it has been demonstrated to physically interact with the nuclease and stimulate its activity (145-147). Exo1 participates exclusively in the TS pathway and is involved in the further expansion of postreplicative gaps (Figure 1.7A) (145, 148, 149). This is likely required for Rad52-, Rad55- and

Rad57- mediated assembly of Rad51 nucleofilaments which then conduct homology search and strand invasion along with Rad54 (Figure 1.7B). The accumulation of TS intermediates observed in *sgs1Δ* cells treated with MMS is drastically reduced in the absence of either Exo1 or 9-1-1 reiterating the importance of their involvement in the process (145, 148, 149).

Pif1 helicase was also demonstrated to play a role in expanding postreplicative gaps. However, its function in the process appears to be auxiliary and is more apparent only in the absence of Exo1 (150). The participation of Sgs1-Dna2 in the resection of postreplicative gaps is rather enigmatic and difficult to study due to the role of Sgs1 in the later stages of TS. Unlike that of Exo1 and Pif1, the involvement of Sgs1-Dna2 in the process cannot be investigated by looking at the formation of TS intermediates as such assays are performed in *sgs1Δ* cells.

As TS is the preferred DNA damage tolerance pathway during early S phase, it is likely that the majority of postreplicative gaps are initially resected and covered by Rad51 (119, 120). However, in the absence of successful repair, the Rad51 filaments can be disassembled by Srs2 helicase channelling the ssDNA gaps into the TLS pathway (Figure 1.7C) (151).

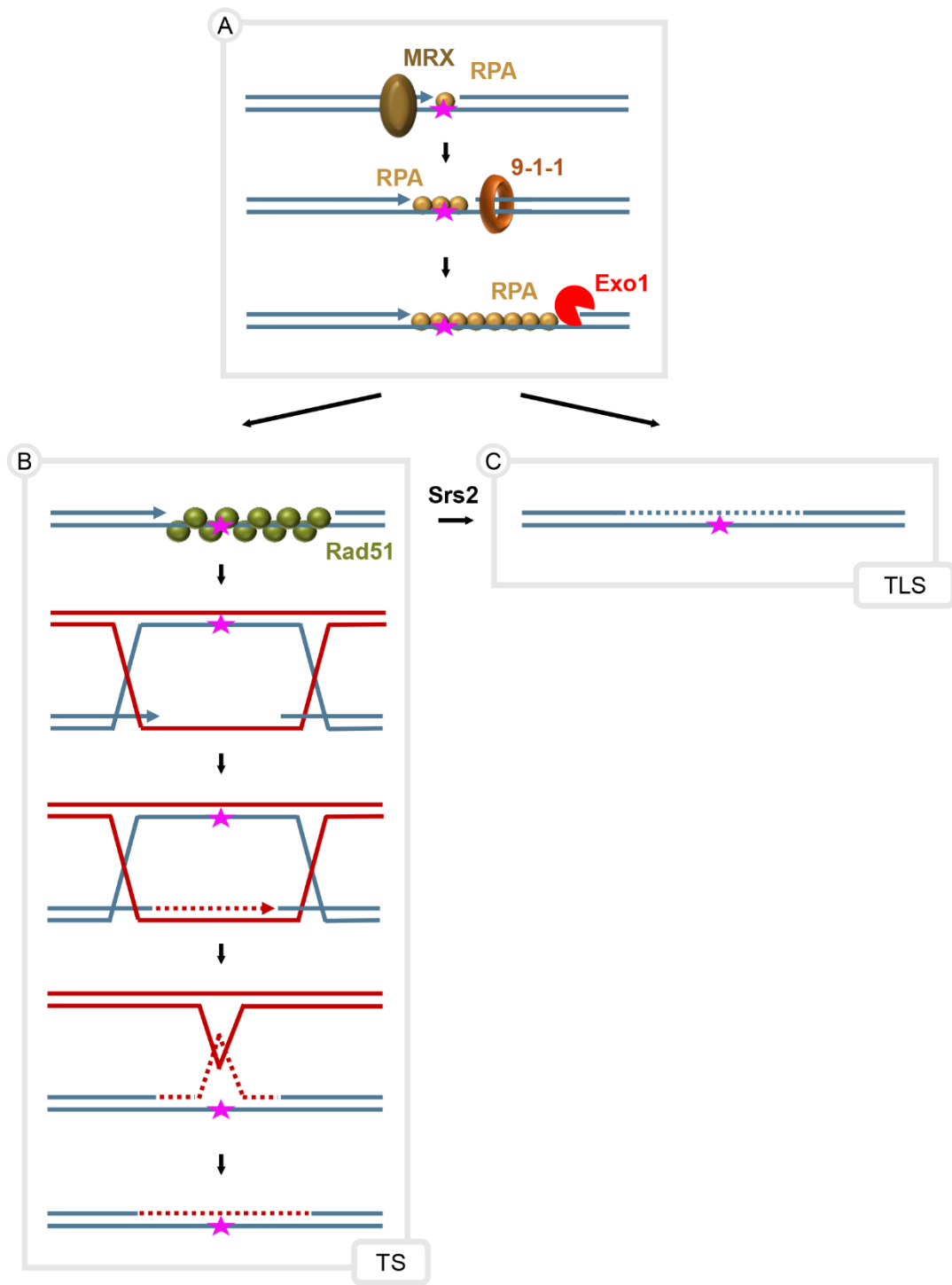


**Figure 1.7. Postreplicative gap repair**

**A.** Postreplicative gaps are initially detected and processed by MRX. This most likely enables the loading of the 9-1-1 complex which recruits Exo1 stimulating further expansion of the ssDNA gaps.

**B.** The extended post-replicative gaps can be repaired by TS. In this case, Rad51 filaments catalyse the invasion of ssDNA into a homologous donor represented by the sister chromatid. The displaced donor strand can then be used as a template to

fill in the ssDNA gap. TS primarily proceeds via hemicatenane intermediates resolved by Sgs1-Top3. For simplicity, Rad51 and RPA bound to the recombination structures are not shown.

C. The gaps left behind the replication forks as a result of DNA replication block can also be fixed by TLS. If TS fails, Srs2 can disassemble Rad51 filaments allowing the gaps to be filled in by translesion polymerases.

Solid blue and red lines represent the strands of a gapped DNA molecule and a homologous donor respectively. Arrow heads depict the 3' ends of the DNA. Dotted lines represent DNA repair synthesis and their colour indicates which DNA molecule was used as a template. Pink star represents a DNA synthesis block.

### 1.1.7. DNA damage checkpoint

The maintenance of genome integrity is crucial for life thus DNA repair needs to be well controlled and coordinated with other cellular processes. This is ensured by the DNA damage checkpoint primarily initiated by the serine/threonine protein kinases Tel1 and Mec1 in *S. cerevisiae*. The standard paradigm of the process is usually described in the context of DSBs (Figure 1.8A). Tel1 is recruited to broken DNA ends via a physical interaction with the MRX complex, while Mec1 localises to the damage sites after DNA resection (152). Although they appear to have overlapping phosphorylation consensus sites (SQ/TQ) and substrates, Mec1 is the main checkpoint kinase in *S. cerevisiae* (32). This contrasts with the mammalian cells where the Tel1 homolog ATM is necessary for the DNA damage checkpoint activation in response to DSBs. The difference likely arises from the higher propensity of yeasts to resect DSBs and thus enable the Mec1-mediated signalling. While ATM is necessary for this process in mammals, the elimination of *S. cerevisiae* Tel1 causes only a modest delay in the initiation of DSB resection (32, 153, 154). Nonetheless, it was demonstrated that Tel1 can activate DNA damage checkpoint in response to DSBs independently of Mec1 in *S. cerevisiae*. However, this response is weaker and becomes apparent only at higher levels of DNA damage (154).

While Tel1 is both recruited and activated by MRX, the Mec1 recruitment and activation requires multiple factors. Mec1 localises to DNA damage sites via its obligate partner Lcd1 (Ddc2) which binds RPA-coated

ssDNA. The 9-1-1 complex composed of Rad17, Mec3, and Ddc1 in *S. cerevisiae* is one of the Mec1 activators and is essential for the DNA damage checkpoint activation in response to DSBs (147). The 9-1-1 complex, also called the checkpoint clamp, is a ring-shaped heterotrimer which is loaded on 5' terminated ssDNA-dsDNA junctions (152). Once recruited, the 9-1-1 complex stimulates Exo1 and Dna2 activities promoting DSB resection and thus further recruitment of Mec1 (147). Furthermore, the 9-1-1 subunit Ddc1 directly induces partial activation of Mec1 kinase and is phosphorylated by it (155). The Ddc1 phosphorylation enables the recruitment of Dpb11 responsible for the full activation of Mec1 (155-157).

Once activated, Tel1 and Mec1 phosphorylate histone H2B in the nucleosomes around the DSB break. This modified histone is referred to as γ-H2AX and, along with Dpb11, is required for the recruitment of the DNA damage checkpoint adaptor protein Rad9 (152). Rad9 has an inhibitory effect on resection and thus provides a feedback loop contributing to the control of ssDNA accumulation (146). Furthermore, Rad9 localised to resected DSBs is phosphorylated by Mec1 and can then serve as a docking platform for the downstream effector kinase Rad53. Mec1 phosphorylates Rad53 brought in the proximity by Rad9 inducing Rad53's trans-autophosphorylation, full activation and the subsequent dissociation from Rad9. Rad53 phosphorylates and activates its parologue Dun1, while Mec1 along with Rad9 activate another downstream kinase Chk1 (152, 158, 159). Upon activation, Rad53, Dun1 and Chk1 phosphorylate numerous downstream targets including proteins involved in DNA repair and the regulation of the cell cycle progression. This ultimately results in the optimisation of DNA repair systems and a G2/M cell cycle arrest providing time for the DSB repair to occur before mitosis (152). The absence of ssDNA after the successful completion of repair leads to the cessation of the Mec1-dependent signalling, dephosphorylation of the downstream effectors and the termination of the DNA damage checkpoint (152). In the presence of persistent DSBs, *S. cerevisiae* cells can override the DNA damage checkpoint and resume the progression of the cell cycle entering mitosis with

unrepaired DNA damage. This process is called adaptation and depends on multiple conditions (152, 160).

Although the paradigm of the DNA damage checkpoint described above considers the response to DSBs and the subsequent arrest at G2/M, it also applies in other situations. The DNA damage checkpoint is generally weaker during G1 due to the cell-cycle dependent repression of resection (152). While G2-arrested *S. cerevisiae* cells activate Rad53 in response to a single DSB, G1 synchronised cells fail to do the same (160). However, multiple DSBs induced by  $\gamma$  rays can lead to Rad53 phosphorylation in G1. Exo1 and Sgs1 were found to be required for the DNA damage signalling in G1 suggesting that it is activated the same way as in G2 and mediated by Mec1 (161, 162). Furthermore, the G1 checkpoint response to UV-inflicted damage requires NER (162). This suggests that ssDNA gaps formed during the lesion processing also activate the DNA damage checkpoint in a manner similar to that of DSBs. Consistent with this hypothesis, 9-1-1 and Rad9 were found to be required for the DNA damage checkpoint activation during both G1 and G2 (155, 163).

The DNA damage checkpoint can also be activated during the S-phase in response to replication problems and is often referred to as replication checkpoint (Figure 1.8B). Replication fork stalling or the uncoupling of the leading and lagging strands prompted by DNA damage leads to the accumulation of long-lived RPA-coated ssDNA which is bound by Mec1-Lcd1 (164). In contrast to the previously described situations, the replication checkpoint does not absolutely depend on the 9-1-1 complex and Rad9 (165). This is because of their functional redundancy with other proteins involved in the process. In addition to 9-1-1 and Dpb11, Mec1 can be activated by Dna2 at replication forks, possibly via direct physical stimulation (166, 167). During the replication checkpoint, the Rad9 function is undertaken by Mrc1 which is a structural component in normal replication forks. Upon DNA damage, it is phosphorylated by Mec1 and serves an analogous function to that of Rad9 in supporting the Rad53 and Chk1 activation (164). Although the 9-1-1 complex and Rad9 are not essential, they are still required for the full robust activation

of the replication checkpoint (165, 167). The replication checkpoint promotes genome stability by inhibiting the firing of late replication origins, stabilising replication forks, optimising DNA repair and upregulating deoxynucleotide triphosphate (dNTP) pools (164).

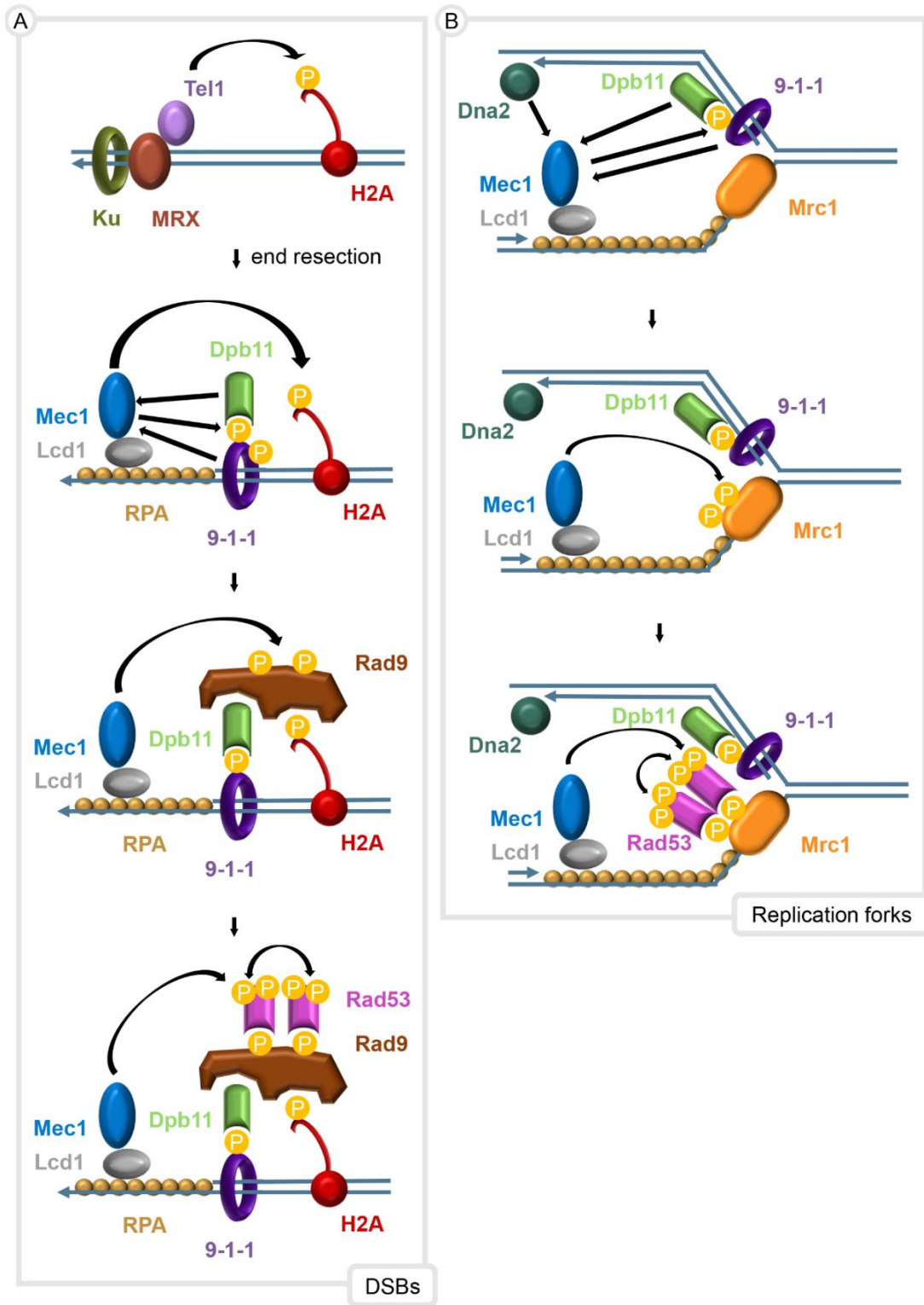


**Figure 1.8. The activation of the DNA damage checkpoint**

**A.** In the context of DSBs, Tel1 is recruited by MRX and phosphorylates histones H2A. After resection is initiated, the 9-1-1 complex is loaded at the ssDNA-dsDNA junction. Mec1 is recruited to damage sites by Lcd1 which binds RPA-coated ssDNA. The 9-1-1 complex partially activates Mec1 and is phosphorylated by it, which enables

the recruitment of Dpb11. Dpb11 fully activates Mec1 which then further phosphorylates histones H2A around the DSB. The adaptor protein Rad9 localises to the DSB via its interactions with Dpb11 and phosphorylated histones. Mec1 phosphorylates Rad9 enabling it to serve as a platform for Rad53 recruitment. Rad53 brought into the proximity by Rad9 is phosphorylated by Mec1. Rad53 molecules brought into a close proximity by Rad9 phosphorylate each other. This leads to the full activation of Rad53 which then phosphorylates downstream targets exerting the effects of the DNA damage checkpoint.

**B.** In the context of stalled replication forks, Mec1-Lcd1 localises to accumulated ssDNA covered by RPA. Mec1 can then be activated by the 9-1-1 complex and Dpb11 the same ways as at DSBs. Alternatively, it can be activated by Dna2 present at replication forks. After the activation, Mec1 phosphorylates a structural component of replication forks Mrc1 which then acts as a platform for Rad53 recruitment. Rad53 bound to Mrc1 is phosphorylated by Mec1 and trans-autophosphorylates, leading to its activation and the subsequent transduction of the DNA damage signalling.

Solid blue lines represent the DNA strands and arrow heads depict their 3' ends. Yellow circles containing a letter P indicate phosphorylation.

## 1.2. The disassembly of Rad51 nucleofilaments and its role in the DNA maintenance

### 1.2.1. PCNA loading

Most major DNA repair pathways described in the previous sections involve at least some DNA resection which then required DNA synthesis to reconstitute the double-stranded nature of the DNA *in vivo*. The DNA synthesis in eukaryotes depends on PCNA. PCNA, also called a sliding clamp, is a homotrimeric protein complex essential for DNA replication. It tethers replicative polymerases δ and ε to DNA drastically enhancing their processivity and thus enabling efficient synthesis. Furthermore, it coordinates other aspects of genome duplication by serving as a platform for additional components of the replication machinery including helicases, nucleases and ligases (168-170). PCNA is also involved in multiple repair pathways and required for TLS as well as recombination-associated DNA synthesis by polymerase δ (121, 168, 169, 171, 172).

PCNA is loaded on DNA by a chaperone-like protein complex RFC composed of five subunits Rfc1-5. RFC catalyses the opening and closing of the PCNA clamp placing it around dsDNA in an ATP-dependent manner. There are also alternative RFC complexes. They have different functions

defined by specific proteins which replace Rfc1 in the complex. For example, Elg1-RFC is involved in the unloading of PCNA, whereas Rad24-RFC controls the loading of another DNA clamp, the 9-1-1 complex, in *S. cerevisiae* (173).

Consistent with its pivotal role in DNA synthesis, PCNA can be loaded on both nicked and gapped DNA *in vitro* (103, 174-176). *In vitro* reconstitution studies have demonstrated that the extension of the 3' terminated strand at DNA nicks during BER and RER requires RFC and PCNA (15, 177). Efficient PCNA loading on gapped DNA additionally requires RPA. RPA physically interacts with RFC and promotes PCNA loading on dsDNA at the dsDNA-ssDNA junction *in vitro* (103, 176, 178-180).

### **1.2.2. Damage-associated DNA synthesis and Rad51**

DNA synthesis prompted by DNA damage and referred to as damage-associated DNA synthesis is involved in multiple repair pathways. This includes the extension of invading strands during HR, the filling of ssDNA gaps, and the restoration of resected DNA. Ironically, Rad51, required for HR and TS, can hinder damage-associated DNA synthesis (103, 178, 181). The Rad51 binding to gapped substrates as well as heteroduplex DNA in the D-loop inhibits PCNA loading *in vitro* (103, 178). The observed inhibitory effect might be a combination of two factors. Firstly, the replacement of RPA by Rad51 on ssDNA eliminates the RPA-mediated stimulation of PCNA loading by RFC (103). Secondly, the Rad51 binding to dsDNA at the dsDNA-ssDNA junction might physically obstruct PCNA loading (178).

The inhibitory effect of Rad51 on damage-associated DNA synthesis has been also studied *in vivo* using a SSA system in *S. cerevisiae*. It was discovered that the efficiency of DNA synthesis during SSA drops from nearly 100% to approximately 60% when the Rad51-removing helicase Srs2 is absent. Consistent with Rad51 playing an inhibitory role on the DNA synthesis, the defect observed in the *srs2Δ* mutants can be suppressed by the deletion of *RAD51* (103). Taking all of this evidence into account, it has been suggested

that Srs2 promotes the damage-associated DNA synthesis by removing Rad51 from ssDNA, thereby promoting RPA binding and the consequential PCNA loading via the RPA-RFC interactions (Figure 1.9) (31, 103). As mentioned earlier, Rad51 is not required for SSA. However, like all ssDNA-containing intermediates, gaps formed during SSA are potential substrates for the Rad51 filament formation. This suggests that the Rad51-mediated inhibition of damage-associated DNA synthesis might be a universal phenomenon relevant to all situations involving ssDNA rather than something specific to the repair pathways dependent on Rad51.

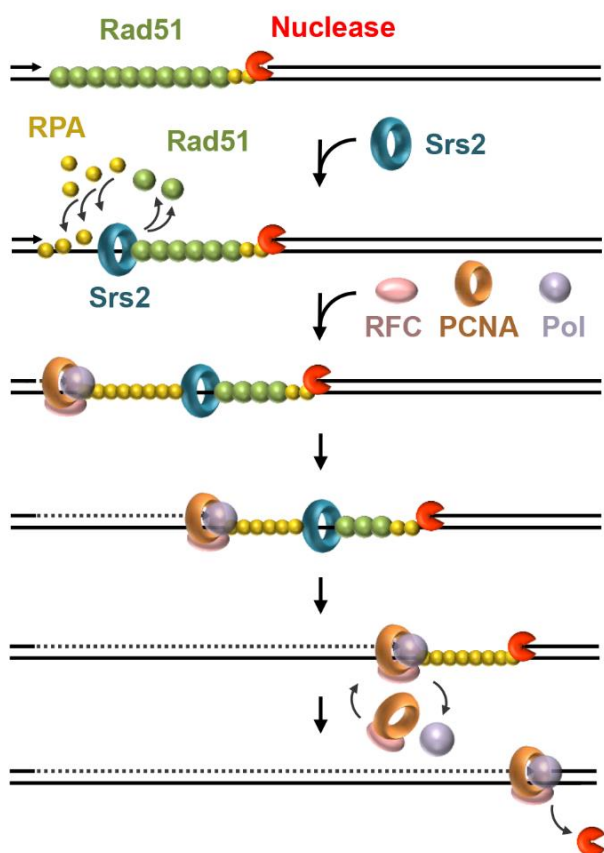


**Figure 1.9. Srs2-mediated Rad51 removal facilitates DNA synthesis during SSA**

A model proposed by Vasianovich *et al.* (2017) (103) suggests that Srs2 facilitates DNA synthesis during SSA by removing Rad51 from ssDNA and thus enabling a rapid PCNA loading and reloading via RFC-RPA interactions. Possibly, this allows DNA synthesis to catch up with a resecting nuclease and displace it completing the repair. Drawing adapted from Vasianovich *et al.* (2017) (103).

### 1.2.3. Rad51 removal from ssDNA

Several *S. cerevisiae* proteins have been implicated in Rad51 removal from ssDNA with the main one being Srs2. Srs2 is a helicase with a 3' → 5' polarity capable of removing Rad51 from ssDNA both *in vitro* and *in vivo* (103, 182). This activity depends on species-specific Srs2-Rad51 interactions and ATP hydrolysis by both proteins (55, 183). It has been suggested that Srs2 might allosterically activate ATP hydrolysis by Rad51 monomers which, in turn, decreases their affinity to ssDNA (55). The Srs2 mutant protein lacking the Rad51-interacting domain has a severely impaired Rad51 clearance activity *in vitro*. However, it appears that this is due to the disrupted Srs2 association with Rad51 nucleofilaments. Once loaded, the mutant Srs2 can remove Rad51 from ssDNA even in the absence of the Rad51-interacting domain, albeit at a decreased efficiency (55, 183).

Srs2 also contains a SUMO-interacting motif (SIM) and a PCNA-interacting peptide box (PIP) which are both required for its recruitment to replication forks by SUMOylated PCNA (184). The removal of SIM was shown to disrupt the localisation of Srs2 to replication foci *in vivo* (185). It is not entirely clear how Srs2 is recruited to DNA repair sites. As mentioned, the interaction with Rad51 possibly promotes the Srs2 association with Rad51 filaments, however, Srs2 has been shown to localise to DNA damage sites even in *rad51Δ* cells (183, 185). This might be explained by the observation that Srs2 can be recruited to DSBs by then NHEJ protein Nej1 (186). However, Srs2-(1-860) mutant protein lacking both Rad51- and Nej1-interacting domains is still capable of suppressing the Rad51-dependent inhibition of the damage-associated DNA synthesis during SSA suggesting it can still localise to and disassemble Rad51 filaments *in vivo* (103). *S. cerevisiae* cells lacking Srs2 show a paradoxical phenotype as they are hyper-recombinogenic but also have a defective HDR (179). This is most likely because the Srs2-mediated Rad51 removal suppresses the unscheduled HR events at DNA lesions early on but promotes damage-associated DNA synthesis during the later stages of repair (102, 177).

A member of the RecQ helicase family, Sgs1, is another budding yeast protein confirmed to have the ability of removing Rad51 from ssDNA *in vitro*. Mechanistically it appears to function differently from Srs2 as the ATP hydrolysis by Rad51 is irrelevant for the Sgs1-mediated filament disassembly (187). *S. cerevisiae* cells lacking Sgs1 activity exhibit hyper-recombinogenic phenotype (188-190). However, the relevance of the Sgs1-mediated Rad51 removal *in vivo* has not been investigated.

A clear Srs2 homolog has not been identified in higher eukaryotes. However, a human protein called PARI has been shown to remove Rad51 from ssDNA *in vitro*. Although it does not have an ATPase activity itself, PARI appears to stimulate ATP hydrolysis by Rad51, thereby promoting its dissociation. PARI binds PCNA and this interaction is enhanced by PCNA SUMOylation suggesting that PARI might be performing a function analogous to that of Srs2 at replication forks (191). In addition, the human homologue of Sgs1, BLM, along with the helicases FBH1, RECQL5 and FANCJ have been demonstrated to remove RAD51 from ssDNA *in vitro* (192-195). Mammalian cells lacking PARI, BLM, FBH1 and RECQL5 exhibit hyper-recombinogenic phenotypes highlighting their role in the negative regulation of HR (191, 194, 196-198).

#### 1.2.4. Rad51 removal from dsDNA

As mentioned earlier, Rad51 can also bind to and polymerise on dsDNA (39, 45). Two *S. cerevisiae* Snf2/Swi2 family translocases, Rad54 and Rdh54, have been demonstrated to remove Rad51 from dsDNA *in vitro* (199, 200). Another member of the family, Uls1, may have a similar ability, but it has not been investigated enough (201).

Rad54 is believed to be primarily responsible for Rad51 clearance at DNA repair sites. It is likely required to remove Rad51 from heteroduplex DNA formed after the strand invasion during DNA repair. This might be necessary to expose the 3' hydroxyl of the invading strand enabling its subsequent

extension (181). The Rad51 filaments formed on ssDNA at the damage sites might also spread into the surrounding dsDNA regions and need to be disassembled by Rad54. The exposure of *uls1Δ*, *uls1Δ rdh54Δ* and *uls1Δ rad54Δ* *S. cerevisiae* mutants to  $\gamma$  radiation revealed that the elimination of Rad54 leads to the highest accumulation of fluorescently tagged Rad51 in DNA damage foci visualised by cell microscopy (201). This is consistent with the notion that the Rad51 removal from dsDNA at the damage sites is primarily performed by Rad54. However, as mentioned before, Rad54 is also required for the strand invasion step during HR. Thus, it is difficult to dissect whether the accumulation of Rad51 foci in cells lacking Rad54 and exposed to  $\gamma$  radiation is due to a repair defect, the lack of Rad51 removal or both.

Rad51 can also bind undamaged DNA. If this binding is not reversed, Rad51 cellular pool might be depleted leaving fewer monomers for DNA repair (65). Furthermore, the dsDNA coated by Rad51 cannot serve as a donor during HR (50, 199). Thus, non-damage-associated Rad51 binding might disrupt DNA repair leading to genome instability (201, 202). However, the Rad51 binding to undamaged chromatin is cytologically undetectable in wild-type (WT) *S. cerevisiae* cells as it is actively antagonised by Rad54, Rdh54 and Uls1 (201). Rdh54 is believed to be the most important in this process as the lack of this translocase but not the other two leads to the accumulation of non-damage-associated Rad51 foci. However, a simultaneous elimination of all three proteins produces the most severe phenotype suggesting that Rdh54 can be partially substituted by Rad54 and Uls1 (201).

Two Rad54 homologs have been identified in human cells – RAD54 and RAD54B (203). Like its yeast counterpart, human RAD54 has been demonstrated to remove RAD51 from dsDNA *in vitro* (202). The simultaneous depletion of RAD54 and RAD54B leads to the accumulation of RAD51 on chromatin in cancer cells (202). This suggests that the aforementioned functions of Snf2/Swi2 translocases are conserved from yeasts to humans highlighting the importance of Rad51 removal from dsDNA *in vivo*.

### **1.2.5. The *srs2Δ* and *rad54Δ* synthetic lethality**

As mentioned earlier, the elimination of Srs2 has been shown to decrease the efficiency of the damage-associated DNA synthesis during SSA (103). Although this process was significantly affected in *srs2Δ* cells, it was not completely disrupted suggesting a possible involvement of the additional proteins. Rad54 is one of the best candidates to be considered.

*S. cerevisiae* cells lacking Srs2 and Rad54 are inviable unless Rad51 or its mediators are eliminated (204). It is generally believed that *srs2Δ rad54Δ* double mutants die due to unproductive long-lived Rad51 nucleofilaments formed during DNA repair (151, 205-208). It was estimated that *S. cerevisiae* cells suffer only 0.12 spontaneous DSBs per cell cycle (209-211). Furthermore, it was demonstrated that *srs2* alleles coding for the helicases that cannot interact with PCNA are not synthetically lethal with *rad54Δ* (212, 213). Together, this argues that the defective DNA repair in *srs2Δ rad54Δ* double mutants is not initiated by any problems at replication forks or by DSBs which are simply not frequent enough to underlie the lethality. Thus, the Rad51 filaments which become toxic in the absence of Srs2 and Rad54 might be primarily formed on ssDNA gaps in *S. cerevisiae*. Rad54 is required to catalyse the invasion of these filaments into homologous donor sequences for the repair to proceed via recombination-based mechanisms. Alternatively, Srs2 is needed to disassemble Rad51 filaments allowing the ssDNA gaps to be filled in by DNA polymerases. Thus, in the absence of both proteins, the ssDNA gaps remain unrepaired (151). However, the fact that the damage-associated DNA synthesis during SSA is still reasonably effective in the absence of Srs2 begs the question of why it is not sufficient to fill in the ssDNA gaps in *srs2Δ rad54Δ* double mutants. Possibly, the Rad51-dependent inhibition of DNA synthesis is stronger at these ssDNA gaps in question rather than those formed during SSA. Alternatively, Rad54 might also be involved in the facilitation of the damage-associated DNA synthesis. In this case, the lack of Rad54 would not only prevent the recombination-based repair but it would also decrease the efficiency of ssDNA gap filling by DNA polymerases possibly making it not effective enough to support cell viability. Thus, in this study, the

possible Srs2 and Rad54 functional relationship during the facilitation of the damage-associated DNA synthesis was investigated by reassessing the possible reasons underlying the *srs2Δ* and *rad54Δ* synthetic lethality.

## **Chapter 2. Materials and Methods**

### **2.1. Yeast strains**

Yeast strains used in this study are described in the Table 2.1.

### **2.2. Oligonucleotides**

DNA oligonucleotides used in this study are described in the Table 2.2. Oligonucleotides were designed using SerialCloner software and the gene reference sequences from <https://www.yeastgenome.org/>. Oligonucleotides (synthesised by Integrated DNA Technologies, IDT) were dissolved in Milli-Q H<sub>2</sub>O to the final concentration of 100 µM. The oligonucleotide solutions were kept at room temperature (RT) if in use or at -20°C for long-term storage.

### **2.3. Plasmids**

Plasmids used in this study are described in the Table 2.3.

### **2.4. Restriction enzymes**

Restriction enzymes used in this study were purchased from New England Biolabs (NEB) and stored according to the manufacturer's guidelines.

Table 2.1. *S. cerevisiae* A364a strains used in this study

<b>Strain number</b>	<b>Genotype</b>	<b>Origin/References</b>
NK1	<i>MATa ura3-52 trp1-289 leu2-3,112 bar1::LEU2</i>	(214)
NK78	<i>MATa ura3-52 trp1-289 leu2-3,112 bar1::LEU2 rad51::TRP1</i>	NK1 <i>rad51::TRP1</i>
NK79	<i>MATa ura3-52 trp1-289 leu2-3,112 bar1::LEU2 rad51::TRP1</i>	
NK219	<i>MATa ura3-52 trp1-289 leu2-3,112 bar1::LEU2</i>	Makovets' lab collection
NK1542	<i>MATa sst2::KAN</i>	Makovets' lab collection

NK4691	<i>MATa-inc trp1-289 leu2::P<sub>GAL1</sub>-HO-LEU2</i>	(103)
NK4692	<i>ura3-52::KAN-HO site-URA3</i>	
NK4693		
NK4694	<i>MATa-inc bar1::LEU2 trp1-289 leu2::P<sub>GAL1</sub>-HO-LEU2</i>	(103)
NK4695	<i>ura3-52::KAN-HO site-URA3</i>	
NK4805		(103)
NK4806	<i>MATa-inc trp1-289 leu2::P<sub>GAL1</sub>-HO-LEU2</i>	
NK4807	<i>ura3-52::KAN-HO site-URA3 srs2::TRP1</i>	
NK4808		
NK5081	<i>MATa-inc trp1-289 leu2::P<sub>GAL1</sub>-HO-LEU2</i>	(103)
	<i>ura3-52::KAN-HO site-URA3 rad51::HYG</i>	
NK5854		NK4805 srs2::HYG
NK5855	<i>MATa-inc trp1-289 leu2::P<sub>GAL1</sub>-HO-LEU2</i>	
NK5856	<i>ura3-52::KAN-HO site-URA3 srs2::HYG</i>	NK4807 srs2::HYG
NK5857		
NK5858	<i>MATa-inc trp1-289 leu2::P<sub>GAL1</sub>-HO-LEU2</i>	NK4691 rad51::TRP1-
NK5859	<i>ura3-52::KAN-HO site-URA3 rad51::TRP1-</i>	<i>P<sub>GAL1</sub>-RAD51</i>
NK5860	<i>P<sub>GAL1</sub>-RAD51</i>	NK4692 rad51::TRP1-
		<i>P<sub>GAL1</sub>-RAD51</i>
NK5861	<i>MATa-inc trp1-289 leu2::P<sub>GAL1</sub>-HO-LEU2</i>	NK5854 rad51::TRP1-
NK5862	<i>ura3-52::KAN-HO site-URA3 rad51::TRP1-</i>	<i>P<sub>GAL1</sub>-RAD51</i>
NK5863	<i>P<sub>GAL1</sub>-RAD51 srs2::HYG</i>	NK5856 rad51::TRP1-
		<i>P<sub>GAL1</sub>-RAD51</i>
NK5864	<i>MATa-inc trp1-289 leu2::P<sub>GAL1</sub>-HO-LEU2</i>	NK5858 rad54::NAT
NK5865	<i>ura3-52::KAN-HO site-URA3 rad51::TRP1-</i>	
NK5866	<i>P<sub>GAL1</sub>-RAD51 rad54::NAT</i>	NK5860 rad54::NAT
NK5868	<i>MATa-inc trp1-289 leu2::P<sub>GAL1</sub>-HO-LEU2</i>	NK5861 rad54::NAT
NK5869	<i>ura3-52::KAN-HO site-URA3 rad51::TRP1-</i>	
NK5870	<i>P<sub>GAL1</sub>-RAD51 srs2::HYG rad54::NAT</i>	NK5863 rad54::NAT
NK5871		
NK5895	<i>MATa ura3-52 trip1-289 leu2-3,112</i>	NK1 rad54:NAT
	<i>bar1::LEU2 rad54::NAT</i>	
NK6390	<i>MATa-inc trp1-289 leu2::P<sub>GAL1</sub>-HO-LEU2</i>	4691 rad54::NAT
NK6391	<i>ura3-52::KAN-HO site-URA3 rad54::NAT</i>	4692 rad54::NAT
NK6392		
NK6397	<i>MATa-inc trp1-289 leu2::P<sub>GAL1</sub>-HO-LEU2</i>	4691 rad54-13Myc-
	<i>ura3-52::KAN-HO site-URA3 rad54::rad54-</i>	<i>NAT via rad54-13Myc-TRP1</i>
NK6399	<i>13Myc-NAT</i>	4692 rad54-13Myc-
		<i>NAT via rad54-13Myc-TRP1</i>
NK6505		NK4691 pYT570/Clal
NK6506	<i>MATa-inc trp1-289 leu2::P<sub>GAL1</sub>-HO-LEU2</i>	
NK6507	<i>ura3-52::KAN-HO site-URA3</i>	NK4692 pYT570/Clal
NK6508	<i>rad51::RAD51-TRP1</i>	
NK6509	<i>MATa-inc trp1-289 leu2::P<sub>GAL1</sub>-HO-LEU2</i>	NK4691 pYT571/Clal
NK6510	<i>ura3-52::KAN-HO site-URA3 rad51::rad51-</i>	
NK6511	<i>K342E-TRP1</i>	NK4692 pYT571/Clal
NK6513	<i>MATa-inc trp1-289 leu2::P<sub>GAL1</sub>-HO-LEU2</i>	NK5854 pYT570/Clal
NK6514	<i>ura3-52::KAN-HO site-URA3 srs2::HYG</i>	
NK6515	<i>rad51::RAD51-TRP1</i>	NK5856 pYT570/Clal
NK6517		NK5854 pYT571/Clal

NK6518	<i>MATa-inc trp1-289 leu2::P<sub>GAL1</sub>-HO-LEU2</i>	
NK6519	<i>ura3-52::KAN-HO site-URA3 srs2::HYG</i> <i>rad51::rad51-K342E-TRP1</i>	NK5856 pYT571/Clal
NK6520	<i>MATa-inc trp1-289 leu2::P<sub>GAL1</sub>-HO-LEU2</i>	NK6397 pYT477/Ncol
NK6521	<i>ura3-52::KAN-HO site-URA3</i>	
NK6522	<i>rad54::RAD54-TRP1-P<sub>GAL1</sub>-rad54-13Myc-NAT</i>	NK6399 pYT477/Ncol
NK6524	<i>MATa-inc trp1-289 leu2::P<sub>GAL1</sub>-HO-LEU2</i> <i>ura3-52::KAN-HO site-URA3</i>	NK6520 srs2::HYG
NK6525	<i>rad54::RAD54-TRP1-P<sub>GAL1</sub>-rad54-13Myc-NAT</i>	NK6522 srs2::HYG
NK6526	<i>srs2::HYG</i>	
NK6527		NK6517 <i>rad54::NAT</i>
NK6528		
NK6529	<i>MATa-inc trp1-289 leu2::P<sub>GAL1</sub>-HO-LEU2</i> <i>ura3-52::KAN-HO site-URA3 srs2::HYG</i> <i>rad51::rad51-K342E-TRP1 rad54::NAT</i>	NK6519 <i>rad54::NAT</i>
NK6530		
NK6531		
NK6590	<i>MATa-inc trp1-289 leu2::P<sub>GAL1</sub>-HO-LEU2</i>	NK6397 srs2::HYG
NK6591	<i>ura3-52::KAN-HO site-URA3 rad54::rad54-13Myc-NAT</i>	NK6399 srs2::HYG
NK6592	<i>srs2::HYG</i>	
NK6724	<i>MATa-inc trp1-289 leu2::P<sub>GAL1</sub>-HO-LEU2</i> <i>ura3-52::KAN-HO site-URA3 rad55::TRP1-P<sub>GAL1</sub>-RAD55</i>	4691 <i>rad55::TRP1-P<sub>GAL1</sub>-RAD55</i>
NK6725		4692 <i>rad55::TRP1-P<sub>GAL1</sub>-RAD55</i>
NK6726		
NK6735	<i>MATa-inc trp1-289 leu2::P<sub>GAL1</sub>-HO-LEU2</i>	NK5854 <i>rad55::TRP1-P<sub>GAL1</sub>-RAD55</i>
NK6736	<i>ura3-52::KAN-HO site-URA3 srs2::HYG</i>	NK5856 <i>rad55::TRP1-P<sub>GAL1</sub>-RAD55</i>
NK6738	<i>rad55::TRP1-P<sub>GAL1</sub>-RAD55</i>	
NK6809		NK6520 srs2::HYG
NK6810		
NK6811	<i>MATa-inc trp1-289 leu2::P<sub>GAL1</sub>-HO-LEU2</i> <i>ura3-52::KAN-HO site-URA3</i>	NK6521 srs2::HYG
NK6813	<i>rad54::RAD54-TRP1-P<sub>GAL1</sub>-rad54-13Myc-NAT</i>	
NK6814		
NK6815	<i>srs2::HYG</i>	
NK6933	<i>MATa ura3-52 trp1-289 leu2-3,112 bar1::LEU2 rad55::TRP1-P<sub>GAL1</sub>-RAD55</i>	NK1 <i>rad55::TRP1-P<sub>GAL1</sub>-RAD55</i>
NK6934		
NK6935		
NK7182	<i>MATa-inc trp1-289 leu2::P<sub>GAL1</sub>-HO-LEU2</i>	NK6505 <i>rad54::NAT</i>
NK7183	<i>ura3-52::KAN-HO site-URA3</i>	
NK7184	<i>rad51::RAD51-TRP1 rad54::NAT</i>	NK6507 <i>rad54::NAT</i>
NK7185	<i>MATa-inc trp1-289 leu2::P<sub>GAL1</sub>-HO-LEU2</i> <i>ura3-52::KAN-HO site-URA3 rad51::rad51-K342E-TRP1 rad54::NAT</i>	NK6507 <i>rad54::NAT</i>
NK7186		NK6511 <i>rad54::NAT</i>
NK7187		
NK7188	<i>MATa-inc trp1-289 leu2::P<sub>GAL1</sub>-HO-LEU2</i>	NK6724 <i>rad54::NAT</i>
NK7189	<i>ura3-52::KAN-HO site-URA3 rad55::TRP1-P<sub>GAL1</sub>-RAD55</i>	NK6725 <i>rad54::NAT</i>
NK7190	<i>rad54::NAT</i>	
NK7200	<i>MATa ura3-52 trp1-289 leu2-3,112 bar1::LEU2 rad55::TRP1-P<sub>GAL1</sub>-RAD55</i>	NK6933 <i>rad54::NAT</i>
NK7201		
NK7202	<i>rad54::NAT</i>	NK6934 <i>rad54::NAT</i>
NK7204	<i>MATa ura3-52 trp1-289 leu2-3,112 bar1::LEU2 rad55::TRP1-P<sub>GAL1</sub>-RAD55</i>	NK6933 srs2::HYG
NK7205		
NK7206	<i>srs2::HYG</i>	NK6934 srs2::HYG

NK7208		NK7204 <i>rad54::NAT</i>
NK7209	<i>MATa ura3-52 trp1-289 leu2-3,112 bar1::LEU2 rad55:TRP1-P<sub>GAL1</sub>-RAD55 srs2::HYG rad54::NAT</i>	
NK7210		NK7206 <i>rad54::NAT</i>
NK7211		
NK7291	<i>MATa-inc trp1-289 leu2::P<sub>GAL1</sub>-HO-LEU2 ura3-52::KAN-HO site-URA3 rad55::TRP1-P<sub>GAL1</sub>-RAD55 srs2::HYG</i>	NK6724 <i>srs2::HYG</i>
NK7292		
NK7293		
NK7295	<i>MATa-inc trp1-289 leu2::P<sub>GAL1</sub>-HO-LEU2 ura3-52::KAN-HO site-URA3 rad55::TRP1-P<sub>GAL1</sub>-RAD55 rad54::NAT srs2::HYG</i>	NK7188 <i>srs2::HYG</i>
NK7296		
NK7297		
NK7424	<i>MATa-inc trp1-289 leu2::P<sub>GAL1</sub>-HO-LEU2 ura3-52::KAN-HO site-URA3 rad55::TRP1-P<sub>GAL1</sub>-RAD55 srs2::HYG</i>	NK6726 <i>srs2::HYG</i>
NK7425		
NK7426		
NK7427		
NK7428		
NK7580	<i>MATa-inc trp1-289 leu2::P<sub>GAL1</sub>-HO-LEU2 ura3-52::KAN-HO site-URA3 rad51::rad51-K342E-TRP1 srs2::HYG</i>	NK6509 <i>srs2::HYG</i>
NK7581		
NK7582		NK6510 <i>srs2::HYG</i>
NK7583		
NK8276	<i>MATa ura3-52 trp1-289 leu2-3,112 bar1::LEU2 rad55:TRP1-P<sub>GAL1</sub>-RAD55 srs2::HYG rad54::NAT sgs1::KAN</i>	NK7208 <i>sgs1::KAN</i>
NK8279	<i>MATa ura3-52 trp1-289 leu2-3,112 bar1::LEU2 rad55:TRP1-P<sub>GAL1</sub>-RAD55 srs2::HYG rad54::NAT exo1::URA3</i>	NK7208 <i>exo1::URA3</i>
NK8285	<i>MATa ura3-52 trp1-289 leu2-3,112 bar1::LEU2 rad55:TRP1-P<sub>GAL1</sub>-RAD55 srs2::HYG rad54::NAT msh2::KAN</i>	NK7208 <i>msh2::KAN</i>
NK8288	<i>MATa ura3-52 trp1-289 leu2-3,112 bar1::LEU2 rad55:TRP1-P<sub>GAL1</sub>-RAD55 srs2::HYG rad54::NAT rad4::URA3</i>	NK7208 <i>rad4::URA3</i>
NK8419	<i>MATa ura3-52 trp1-289 leu2-3,112 bar1::LEU2 rad55:TRP1-P<sub>GAL1</sub>-RAD55 srs2::HYG rad54::NAT rad51::KAN</i>	NK7208 <i>rad51::KAN</i>
NK8420		
NK8421	<i>MATa ura3-52 trp1-289 leu2-3,112 bar1::LEU2 rad55:TRP1-P<sub>GAL1</sub>-RAD55 srs2::HYG rad54::NAT rad51::KAN</i>	NK7210 <i>rad51::KAN</i>
NK8425	<i>MATa ura3-52 trp1-289 leu2-3,112 bar1::LEU2 rad55:TRP1-P<sub>GAL1</sub>-RAD55 srs2::HYG rad54::NAT rad17::KAN</i>	NK7210 <i>rad17::KAN</i>
NK8435	<i>MATa ura3-52 trp1-289 leu2-3,112 bar1::LEU2 rad55:TRP1-P<sub>GAL1</sub>-RAD55 srs2::HYG rad54::NAT exo1::URA3</i>	NK7210 <i>exo1::URA3</i>
NK8443	<i>MATa ura3-52 trp1-289 leu2-3,112 bar1::LEU2 rad55:TRP1-P<sub>GAL1</sub>-RAD55 srs2::HYG rad54::NAT rad4::URA3 msh2::KAN</i>	NK8288 <i>msh2::KAN</i>
NK8478	<i>MATa ura3-52 trp1-289 leu2-3,112 bar1::LEU2 rad55:TRP1-P<sub>GAL1</sub>-RAD55 srs2::HYG rad54::NAT PIF1::pif1-m2</i>	NK7208 pYT104/Xhol, URA3 marker looped out after the integration
NK8484	<i>MATa ura3-52 trp1-289 leu2-3,112 bar1::LEU2 rad55:TRP1-P<sub>GAL1</sub>-RAD55</i>	NK8478 <i>sgs1::KAN</i>

	<i>srs2::HYG rad54::NAT Pif1::pif1-m2</i> <i>sgs1::KAN</i>	
NK8540	<i>MATa ura3-52 trp1-289 leu2-3,112</i> <i>bar1::LEU2 rad55:TRP1-P<sub>GAL1</sub>-RAD55</i> <i>srs2::HYG rad54::NAT rad51::rad51-II3A-KAN-RAD51</i>	NK7208 pYT814/Spel
NK8541 NK8542 NK8543	<i>MATa ura3-52 trp1-289 leu2-3,112</i> <i>bar1::LEU2 rad55:TRP1-P<sub>GAL1</sub>-RAD55</i> <i>srs2::HYG rad54::NAT rad51::rad51-II3A-URA3</i>	NK8540 transformed with a <i>URA3</i> cassette (pYT811 with OSM3606 and OSM3607)
NK8544 NK8545 NK8546	<i>MATa ura3-52 trp1-289 leu2-3,112</i> <i>bar1::LEU2 rad55:TRP1-P<sub>GAL1</sub>-RAD55</i> <i>srs2::HYG rad54::NAT rad51::KAN-P<sub>GAL1</sub>-rad51-II3A-URA3</i>	NK8541 <i>rad51-II3A-URA3::KAN-P<sub>GAL1</sub>-rad51-II3A-URA3</i>
NK8994	<i>MATa ura3-52 trp1-289 leu2-3,112</i>	NK7208 <i>sm1::URA3</i>
NK8995	<i>bar1::LEU2 rad55:TRP1-P<sub>GAL1</sub>-RAD55</i> <i>srs2::HYG rad54::NAT sm1::URA3</i>	NK7210 <i>sm1::URA3</i>
NK8997 NK8998	<i>MATa ura3-52 trp1-289 leu2-3,112</i> <i>bar1::LEU2 rad55:TRP1-P<sub>GAL1</sub>-RAD55</i> <i>srs2::HYG rad54::NAT sm1::URA3</i>	NK8994 <i>mec1::KAN</i>
NK8999 NK9000	<i>MATa ura3-52 trp1-289 leu2-3,112</i> <i>bar1::LEU2 rad55:TRP1-P<sub>GAL1</sub>-RAD55</i> <i>srs2::HYG rad54::NAT sm1::URA3</i> <i>mec1::KAN</i>	NK8995 <i>mec1::KAN</i>
NK9001	<i>MATa-inc trp1-289 leu2::P<sub>GAL1</sub>-HO-LEU2</i>	4691 pYT813/Spel
NK9002	<i>ura3-52::KAN-HO site-URA3 rad51::rad51-II3A-TRP-RAD51</i>	4692 pYT813/Spel
NK9003 NK9004 NK9005	<i>MATa-inc trp1-289 leu2::P<sub>GAL1</sub>-HO-LEU2</i> <i>ura3-52::KAN-HO site-URA3 rad51::rad51-II3A-TRP-RAD51</i>	NK9001 transformed with a <i>NAT</i> cassette (pFA6a-NAT with OSM3606 and OSM3607)
NK9006	<i>MATa-inc trp1-289 leu2::P<sub>GAL1</sub>-HO-LEU2</i> <i>ura3-52::KAN-HO site-URA3 rad51::rad51-II3A-TRP-RAD51</i>	NK9002 transformed with a <i>NAT</i> cassette (pFA6a-natMX6 with OSM3606 and OSM3607)
NK9007	<i>MATa-inc trp1-289 leu2::P<sub>GAL1</sub>-HO-LEU2</i>	NK5854 pYT813/Spel
NK9008	<i>ura3-52::KAN-HO site-URA3 srs2::HYG rad51::rad51-II3A-TRP1-RAD51</i>	NK5856 pYT813/Spel
NK9009 NK9010	<i>MATa-inc trp1-289 leu2::P<sub>GAL1</sub>-HO-LEU2</i> <i>ura3-52::KAN-HO site-URA3 srs2::HYG rad51::rad51-II3A-NAT</i>	NK9007 transformed with a <i>NAT</i> cassette (pFA6a-natMX6 with OSM3606 and OSM3607)
NK9011	<i>MATa-inc trp1-289 leu2::P<sub>GAL1</sub>-HO-LEU2</i> <i>ura3-52::KAN-HO site-URA3 srs2::HYG rad51::rad51-II3A-NAT</i>	NK9008 transformed with a <i>NAT</i> cassette (pFA6a-natMX6 with OSM3606 and OSM3607)
NK9019	<i>MATa ura3-52 trp1-289 leu2-3,112</i> <i>bar1::LEU2 rad55:TRP1-PGAL1-RAD55</i> <i>srs2::HYG rad54::NAT exo1::exo1-(aa 1-553)-KAN</i>	NK7210 <i>exo1::exo1-(aa 1-553)-KAN</i>

NK9032	<i>MATa ura3-52 trp1-289 leu2-3,112 bar1::LEU2 rad55:TRP1-PGAL1-RAD55 srs2::HYG rad54::NAT exo1::exo1-(aa 1-702)-KAN</i>	NK7210 <i>exo1::exo1-(aa 1-702)-KAN</i>
NK9044	<i>MATa ura3-52 trp1-289 leu2-3,112 bar1::LEU2 rev3::KAN</i>	NK219 <i>rev3::KAN</i>
NK9045	<i>MATa ura3-52 trp1-289 leu2-3,112 bar1::LEU2 rev3::KAN</i>	
NK9130	<i>MATa ura3-52 trp1-289 leu2-3,112 bar1::LEU2 rev3::KAN rad30::NAT</i>	NK9044 <i>rad30::NAT</i>
NK9132	<i>MATa ura3-52 trp1-289 leu2-3,112 bar1::LEU2 rev3::KAN rad30::NAT</i>	NK9045 <i>rad30::NAT</i>
NK9136	<i>MATa ura3-52 trp1-289 leu2-3,112 bar1::LEU2 hed1::KAN-P<sub>GAL1</sub>-HED1</i>	NK1 <i>hed1::KAN-P<sub>GAL1</sub>-HED1</i>
NK9137		
NK9138		
NK9140	<i>MATa ura3-52 trp1-289 leu2-3,112 bar1::LEU2 rad55:TRP1-P<sub>GAL1</sub>-RAD55 hed1::KAN-P<sub>GAL1</sub>-HED1</i>	NK6933 <i>hed1::KAN-P<sub>GAL1</sub>-HED1</i>
NK9141		
NK9144	<i>MATa ura3-52 trp1-289 leu2-3,112 bar1::LEU2 rad55:TRP1-P<sub>GAL1</sub>-RAD55 srs2::HYG hed1::KAN-P<sub>GAL1</sub>-HED1</i>	NK7204 <i>hed1::KAN-P<sub>GAL1</sub>-HED1</i>
NK9145		
NK9148	<i>MATa ura3-52 trp1-289 leu2-3,112 bar1::LEU2 rad55:TRP1-P<sub>GAL1</sub>-RAD55 srs2::HYG rad54::NAT hed1::KAN-P<sub>GAL1</sub>-HED1</i>	NK7208 <i>hed1::KAN-P<sub>GAL1</sub>-HED1</i>
NK9259	<i>MATa ura3-52 trp1-289 leu2-3,112 bar1::LEU2 rad55:TRP1-P<sub>GAL1</sub>-RAD55 srs2::HYG sgs1::URA</i>	NK7204 <i>sgs1::URA</i>
NK9260		
NK9261	<i>MATa ura3-52 trp1-289 leu2-3,112 bar1::LEU2 rad55:TRP1-P<sub>GAL1</sub>-RAD55 srs2::HYG hed1::KAN-P<sub>GAL1</sub>-HED1 sgs1::URA3</i>	NK9144 <i>sgs1::URA3</i>
NK9263	<i>MATa ura3-52 trp1-289 leu2-3,112 bar1::LEU2 rad55:TRP1-P<sub>GAL1</sub>-RAD55 srs2::HYG rad54::NAT hed1::KAN-P<sub>GAL1</sub>-HED1 sgs1::URA3</i>	NK9148 <i>sgs1::URA3</i>
NK9264		
NK9267	<i>MATa ura3-52 trp1-289 leu2-3,112 bar1::LEU2 rev3::KAN rad30::NAT</i>	NK9130 <i>rev1::URA3</i>
NK9268		
NK9269	<i>rev1::URA3</i>	NK9132 <i>rev1::URA3</i>
NK9270	<i>MATa ura3-52 trp1-289 leu2-3,112 bar1::LEU2 rad55:TRP1-PGAL1-RAD55 srs2::HYG rad54::NAT exo1::exo1-(aa 1-690)-KAN</i>	NK7208 <i>exo1::exo1-(aa 1-690)-KAN</i>
NK9278	<i>MATa ura3-52 trp1-289 leu2-3,112 bar1::LEU2 rad55:TRP1-PGAL1-RAD55 srs2::HYG rad54::NAT exo1::exo1-(aa 1-494)-KAN</i>	NK7208 <i>exo1::exo1-(aa 1-494)-KAN</i>
NK9345	<i>MATa ura3-52 trp1-289 leu2-3,112 bar1::LEU2 rad55:TRP1-P<sub>GAL1</sub>-RAD55 srs2::HYG rad54::NAT hed1::KAN-P<sub>GAL1</sub>-HED1 mph1::TetA(aa 10-125) (pYT1082 URA3 loop-out)</i>	NK9148 <i>mph1::TetA(aa 10-125) (pYT1082 URA3 loop-out)</i>
NK9346		
NK9347	<i>MATa ura3-52 trp1-289 leu2-3,112 bar1::LEU2 rad55:TRP1-P<sub>GAL1</sub>-RAD55 srs2::HYG rad54::NAT hed1::KAN-P<sub>GAL1</sub>-HED1 hrq1::TetA(aa 10-125)</i>	NK9148 <i>hrq1::TetA(aa 10-125) (pYT1082 URA3 loop-out)</i>
NK9348		

NK9349	<i>MAT<math>\alpha</math> ura3-52 trp1-289 leu2-3,112 bar1::LEU2 rad55:TRP1-P<sub>GAL1</sub>-RAD55 srs2::HYG rad54::NAT hed1::KAN-P<sub>GAL1</sub>-HED1 chl1::TetA(aa 10-125)</i>	NK9148 <i>chl1::TetA(aa 10-125) (pYT1082 URA3 loop-out)</i>
NK9351	<i>MAT<math>\alpha</math> ura3-52 trp1-289 leu2-3,112 bar1::LEU2 rad55:TRP1-P<sub>GAL1</sub>-RAD55 srs2::HYG rad54::NAT hed1::KAN-P<sub>GAL1</sub>-HED1 hrq1::TetA(aa 10-125) sgs1::TetA(aa 10-125)</i>	NK9347 <i>sgs1::TetA(aa 10-125) (pYT1082 URA3 loop-out)</i>
NK9353	<i>MAT<math>\alpha</math> ura3-52 trp1-289 leu2-3,112 bar1::LEU2 rad55:TRP1-P<sub>GAL1</sub>-RAD55 srs2::HYG hrq1::NAT</i>	NK7204 <i>hrq1::NAT</i>
NK9355	<i>MAT<math>\alpha</math> ura3-52 trp1-289 leu2-3,112 bar1::LEU2 rad55:TRP1-P<sub>GAL1</sub>-RAD55 srs2::HYG sgs1::URA hrq1::NAT</i>	NK9259 <i>hrq1::NAT</i>
NK9461	<i>MAT<math>\alpha</math> ura3-52 trp1-289 leu2-3,112 bar1::LEU2 rad55:TRP1-PGAL1-RAD55 srs2::HYG rad54::NAT exo1::exo1-(aa 1-660)-KAN</i>	NK7208 <i>exo1::exo1-(aa 1-660)-KAN</i>
NK9464	<i>MAT<math>\alpha</math> ura3-52 trp1-289 leu2-3,112 bar1::LEU2 rad55:TRP1-PGAL1-RAD55 srs2::HYG rad54::NAT exo1::exo1-(aa 1-647)-KAN</i>	NK7208 <i>exo1::exo1-(aa 1-647)-KAN</i>
NK9470	<i>MAT<math>\alpha</math> ura3-52 trp1-289 leu2-3,112 bar1::LEU2 rad55:TRP1-PGAL1-RAD55 srs2::HYG rad54::NAT exo1::exo1-(aa 1-525)-KAN</i>	NK7208 <i>exo1::exo1-(aa 1-525)-KAN</i>
NK9985	<i>MAT<math>\alpha</math>/MAT<math>\alpha</math> ura3-52/ura3-52 trp1-289/trp1-289 leu2-3,112/leu2-3,112</i>	NK78 x NK9267
NK9986		
NK9987	<i>bar1::LEU2/bar1::LEU2 rad51::TRP1/RAD51</i>	NK79 x NK9268
NK9988	<i>REV3/rev3::KAN RAD30/rad30::NAT REV1/rev1::URA3</i>	NK79 x NK9269
NK10075	<i>MAT<math>\alpha</math> ura3-52 trp1-289 leu2-3,112 bar1::LEU2</i>	NK9987 sporulation
NK10076		NK9985 sporulation
NK10077	<i>MAT<math>\alpha</math> ura3-52 trp1-289 leu2-3,112 bar1::LEU2 rad51::TRP1</i>	NK9987 sporulation
NK10078	<i>MAT<math>\alpha</math> ura3-52 trp1-289 leu2-3,112 bar1::LEU2 rad51::TRP1</i>	NK9987 sporulation
NK10079	<i>MAT<math>\alpha</math> ura3-52 trp1-289 leu2-3,112 bar1::LEU2 rad51::TRP1</i>	NK9985 sporulation
NK10080	<i>MAT<math>\alpha</math> ura3-52 trp1-289 leu2-3,112 bar1::LEU2 rev1::URA3 rev3::KAN rad30::NAT</i>	NK9987 sporulation
NK10081	<i>MAT<math>\alpha</math> ura3-52 trp1-289 leu2-3,112 bar1::LEU2 rev1::URA3 rev3::KAN rad30::NAT</i>	NK9987 sporulation
NK10082	<i>MAT<math>\alpha</math> ura3-52 trp1-289 leu2-3,112 bar1::LEU2 rev1::URA3 rev3::KAN rad30::NAT</i>	NK9987 sporulation
NK10083	<i>MAT<math>\alpha</math> ura3-52 trp1-289 leu2-3,112 bar1::LEU2 rad51::TRP1 rev1::URA3 rev3::KAN rad30::NAT</i>	NK9987 sporulation

NK10084	<i>MATa ura3-52 trp1-289 leu2-3,112</i>	NK9985 sporulation
NK10085	<i>bar1::LEU2 rad51::TRP1 rev1::URA3</i> <i>rev3::KAN rad30::NAT</i>	NK9987 sporulation

Table 2.2. Oligonucleotides used in this study

Oligonucleotide number	Sequence (5' to 3')	Purpose
OSM30	TTATGATTGCCCTTTTATTATA TGCTATGTTATTGTGTATGCAAT TAGGAATTGAGCTCGTTAAC	<i>SGS1</i> deletion
OSM 145	AAGAGCAGACGTAGTTATTGTT AAAGGCCTACTAATTGTTATCG TCATCGGATCCCCGGGTTAATT AA	<i>RAD51</i> deletion
OSM146	AGAATTGAAAGTAAACCTGTGTA AATAAATAGAGACAAGAGACCA AATACGAATTGAGCTCGTTAA AC	<i>RAD51</i> deletion
OSM147	CGCGTCATTCGCTATTCTGT CC	To screen for cassette integration at <i>RAD51</i>
OSM189	ACGCCAGAAAATGTTGGTGATG CGCTT	To make <i>ARS1</i> probe
OSM190	ATCCACATCAATGGCTAATGGC AAAACT	To make <i>ARS1</i> probe
OSM289	GGTATCTACCATCTTCTCTCTTA AAAAGGGGCAGCATTCTATG GGTATTGTCCTGGGAATTG AGCTCGTTAAC	To tag Rad53 at the C-terminus
OSM563	GCTCCTTGTGATCTTACGGTCT CACTAACCTCTCTCACTGCTC AATAATTCCCGCTCGGATCCC CGGGTTAAC	<i>SML1</i> deletion
OSM564	GAGAATGTTCGAGAATGACAA CAATAGTAGGACGAGAGTCCCT GAAAAGAAGGGTATCTGAATT GAGCTCGTTAAC	<i>SML1</i> deletion
OSM631	TTAATTAACCCGGGGATCCG	To screen for cassette integrations
OSM642	ACCACATTAAAATAAAGGAGCT CGAAAAAACTGAAAGGCGTAGA	<i>EXO1</i> deletion

	AAGGACGGATCCCCGGGTTAATTAA	
OSM643	CTATTGTGATTGACGTATACCATTCCTCTACTTTTGATTAACGTTGCCGGAATTGAGCTCGTTAAC	<i>EXO1</i> deletion
OSM644	AAAATATCAGGTCCCTGCTCC	To screen for cassette integration at <i>EXO1</i>
OSM653	AGGCTGGACAACAAGAACGACATACACCGCGTAAAGGGCCCACAAAGACTGCCGGATCCCCGGGTTAATTAA	<i>MEC1</i> deletion
OSM654	TGAATTGAGTGGTCCATGTTCTATCGTACATAATTGTTCGATCACATTGAATTGAGCTCGTTAAAC	<i>MEC1</i> deletion
OSM736	AAAACCCGGATCTCAAAATG	To screen for $P_{GAL1}$ at <i>RAD51</i>
OSM801	GTTTAAACGAGCTCGAATTCAACG	To screen for cassette integrations
OSM802	ATTATTGTTG TATATATTAAAGAAATCATA CACGTACACACAAGGCCTGTA CGGATCCCCGGGTTAATTAA	<i>SGS1</i> deletion
OSM803	GATCAATAGAGGGCACTTAGCA	To screen for cassette integration at <i>SGS1</i>
OSM863	AACCAGTTCCACACCAACCA	To screen for $P_{GAL1}$ at <i>RAD51</i>
OSM919	CTCAGAACTTAGCTCTATTCAAAGGTACCATATATATTCCCTATAACTGCGGATCCCCGGGTTAATTAA	<i>RAD54</i> deletion
OSM920	ATCGAATTCTACTTTTGTTTTGTTTATAAGTACATGTATGTAAGAGAGAATTGAGCTCGTTAAAC	<i>RAD54</i> deletion
OSM921	GCGAAGGCCAAACTCTTCT	To screen for cassette integration at <i>RAD54</i>
OSM922	GAGTATCATTCCAATTGATCTTCTACCGGTACTTAGGGATA	<i>SRS2</i> deletion

	GCAACGGATCCCCGGGTTAATT AA	
OSM923	AAATTATAAACCGCCTCCAATAG TTGACGTAGTCAGGCATGAAAG TGCTAGAATTGAGCTCGTTAA AC	SRS2 deletion
OSM939	GGGCAAAATTGGACCAAACCTC AAAAGGCCCGAGAATTGCAA TTTCGCGGATCCCCGGGTTAA TTAA	To tag Rad53 at the C-terminus
OSM940	CTAAGAAGCCGCCAGTTAGC	To screen for the C-terminal tagging cassette integration at <i>RAD53</i>
OSM1006	TGACTGGTACTACCGTAACGGT TC	qPCR at <i>ARO1</i> locus
OSM1007	GAATACCATCTGGTAATTCTGTA GTTTGAC	qPCR at <i>ARO1</i> locus
OSM1068	AGATATTGTGATTCAAGATATAG TAGCTCACTTCAGTTTATTCAA CACAGGATCCCCGGGTTAATTAA	<i>MPH1</i> deletion
OSM1069	TACAGCAGCGTTATTTTGATA GACGCCGACGTATAAGAGTCTC CTATCGAATTGAGCTCGTTAA AC	<i>MPH1</i> deletion
OSM1463	CCCCAGATCTGATTCGGTAAATC TCCGAACAGA	To clone URA3 (to make pYT811)
OSM1489	AAGAGAAAGTATTGAGTCAATA CAAAACTACAAGTTGGCGAA ATAAAATGTTGGAAGGGATCCC CGGGTTAATTAA	<i>REV3</i> deletion
OSM1490	AACGTTATACATAGAAACAAATA ACTACTCATTTGCGAGACA TATCTGTGTCTAGAGAATTGAG CTCGTTAAC	<i>REV3</i> deletion
OSM1491	GCACAGCAGTACAATTATGTAT GT	To screen for cassette integration at <i>REV3</i>
OSM1492	TAGAGGATACGAAGATTCTCA A	To screen for cassette integration at <i>REV3</i>

OSM1493	CGTTATACATATTGAGATGGTTA AGGTCGTAGAAAAGAAATGTTC ATTTGAGAAGGAAAAGGATCCC CGGGTTAATTAA	<i>HRQ1</i> deletion
OSM1494	GAATCTACAAGTAGTAGAATAGA GTATTTATTCGGTTACAAAC TACAAATAGCGTGCAGATTGAG GCTCGTTAAC	<i>HRQ1</i> deletion
OSM1495	GTTGTGAATTGCTCAGAAGAGAA	To screen for cassette integration at <i>HRQ1</i>
OSM1496	ACCTATACCGATTGAGGACATTAA	To screen for cassette integration at <i>HRQ1</i>
OSM1070	TCCATATGAGACAGGAGTCTCTTC	To screen for cassette integration at <i>RAD54</i>
OSM2107	CGCGTGGTGGGACCATAAAGGGGAATAGTGGGGACTGGAGAAA AAATTTCTCAGTTACTGAATTGAGCTCGTTAAC	To integrate $P_{GAL1}$ at <i>RAD51</i>
OSM2108	CGAACCGTTCCGTACTGAAGCTGTGACTCTGATATATGTTGTTCTTGAACTTGAGACATTGAGATCCGGTTTT	To integrate $P_{GAL1}$ at <i>RAD51</i>
OSM2161	TGTGGATATCTTGACTGATTTTCC	To make <i>URA3</i> probe
OSM2162	ATACATGCATTTACTTATAATACAG	To make <i>URA3</i> probe
OSM2233	TGTACTAAACTCACAAATTAGAGC	To monitor non-homologous DNA end cleavage with qPCR
OSM2234	CAACACTCAACCCTATCTCG	To monitor non-homologous DNA end cleavage with qPCR
OSM2365	TTCCTTAAACCCAAAAGAGTAGAAAACCAGGCTAAAAACAGTCA CACTAGTCCAAAAGGATCCCCGGGTAAATTAA	<i>CHL1</i> deletion
OSM2366	AGTTTACTATAATATAGTAGTAATCACAGTATACACGTAAACGT ATTCCCTGAATTGAGCTCGTTAAC	<i>CHL1</i> deletion

OSM2367	TTAATGTCCGGAAGAGAAGTCGC	To screen for cassette integration at <i>CHL1</i>
OSM2368	ACGAGATGATTGAATGATTATGG	To screen for cassette integration at <i>CHL1</i>
OSM2370	ACAAATCAATCTCACAGAACGG TGTGGAAACAAAGTAGTTGAAG GATTCAACGGATCCCCGGGTT AATTAA	<i>RAD17</i> deletion
OSM2371	AATTACCAAATGCTGAATGAAGT TCTCGGTTTCTGCGATGCTGG ATATTGACGAATTGAGCTCGTT TAAAC	<i>RAD17</i> deletion
OSM2372	GCTACTGAAGGAGTGGTGTTAG G	To screen for cassette integration at <i>RAD17</i>
OSM2373	GTTGTTGTCAAGAACTGGGTG C	To screen for cassette integration at <i>RAD17</i>
OSM2489	CCGTCCCAAAAAGGAAATAGCC	To screen for cassette integration at <i>SML1</i>
OSM2562	TTTCGGCTGGCACTTACACG	To screen for cassette integration at <i>RAD54</i>
OSM2681	CCCCCGGCCGATGGCAAGACG CAGATTACCAGACAGACCACCA AATGGAATAGGAGCCGGTGAAC GACCGAGACTGG	To clone the 5' fragment of <i>RAD54</i> with Eagl and Ncol (to make the plasmid pYT477)
OSM2682	CCCCCGGCCGTTTACCCCTTA AGTTATACGATTATAC	To clone the 3' fragment of <i>RAD54</i> with Eagl and Ncol (to make the plasmid pYT477)
OSM2730	AGTTCATGCGTGGTCGATGC	To screen for the C-terminal tagging cassette integration at <i>RAD54</i>
OSM2732	AAATGTCGACATTTAACTCGTT	To check the <i>TRP1-P<sub>GAL1</sub>-RAD55</i> modification
OSM2737	CAGAACTAACACACCTTCAACC CATGGCTCCTGTTATCCATAG ATGTG	To clone the 5' fragment of <i>RAD54</i> with Eagl and Ncol (to make the plasmid pYT477)

OSM2738	CACATCTATGGATAACAAGGAA GCCATGGGTTGAAAGGTTGTT AGTTCTG	To clone the 3' fragment of <i>RAD54</i> with EagI and Ncol (to make the plasmid pYT477)
OSM2745	ACCTCTATACTTTAACGTCAAGG AG	To screen for $P_{GAL1}$ cassette integrations
OSM2870	ACGAGCATCATTACAATGATATC AGTTTGCAATTCAATATATTCA CATCGGATCCCCGGGTTAATTA A	To tag Rad54 at the C-terminus
OSM2871	CGACGATCGAATTCTACTTTTG TTTTTGTGTTATAAGTACATGTAT GTAAGAGAGAATTGAGCTCGT TTAAC	To tag Rad54 at the C-terminus
OSM2934	CTTTTAATCCAGATCCGGAAAAG CCTATCGGTGG	To clone the 3' end of <i>RAD51</i> and introduce K342E mutation with Sall and EagI (to make the plasmid pYT571)
OSM2935	CCACCGATAGGCTTTCCGGAT CTGGATTAAAAG	To clone the 3' end of <i>RAD51</i> and introduce K342E mutation with Sall and EagI (to make the plasmid pYT571)
OSM2936	CCCCGTCGACGGAAGTAGTCAT CGGGAAAGAAG	To clone the 3' end of <i>RAD51</i> with Sall and EagI (to make the plasmids pYT570 and pYT571)
OSM2937	CCCCCGGCCGATATGAGAAGAT CGGAGCTGATTG	To clone the 3' end of <i>RAD51</i> with Sall and EagI (to make the plasmids pYT570 and pYT571)
OSM2938	CAAGCGCGCAATTAAACCCTCAC TAAAGG	To check for a correct integration of the plasmids pYT570 and pYT571
OSM2939	CCTAAAAGGATAAGCCGCGCG G	To check for a correct integration of the plasmids pYT570 and pYT571

OSM3035	CTTCTCATCGCGTTGATATGAA AAATAGAAAAAAATACATAGTAG CATGGAATTGAGCTCGTTAAC C	To integrate $P_{GAL1}$ at $RAD55$
OSM3036	GGCTTGACTTCTACTATTAA TTGGGAAAGTGGTATACCAAGC GACATTTGAGATCCGGGTTTT	To integrate $P_{GAL1}$ at $RAD55$
OSM3234	AAAAATCTCTTATCTGCTGACC TAACATCAAATCCTCAGATTAA AAGTCGGATCCCCGGGTTAATT AA	$MSH2$ deletion
OSM3235	TATATATTATCTATCGATTCTCA CTTAAGATGTCGTTGTAATATTA ATTAGAATTGAGCTCGTTAAA C	$MSH2$ deletion
OSM3236	CCATCAAGTGAACCTAACACAG	To screen for cassette integration at $MSH2$
OSM3237	GGAAAATTGATCTATGACAGAG	To screen for cassette integration at $MSH2$
OSM3516	CCTGTCCTGAATTCACCGAAAA GCTC	To clone the 5' and the promoter of $RAD51$ (to make the plasmid pYT754)
OSM3517	CCCCCGGCCGGGCCTTCTTGA GCATTCCCTGAGC	To clone the 5' and the promoter of $RAD51$ (to make the plasmid pYT754)
OSM3523	TTCAAACAGGACGACAAGCAGA GACATAACGACACTATTTTCCG CTAAATTGAAATTTTTGATTC GG	$RAD4$ deletion
OSM3524	CTTTATTAAAAACATACTTTCTA ATTATTCAAACCGTTTCAGCCTC ATTGGTATAACTGATATAATT	$RAD4$ deletion
OSM3525	GCGGCGGAAAATGGAAAAATGC	To screen for cassette integration at $RAD4$
OSM3526	GCCAACTAAGTTCTCATTCAATT CAAAG	To screen for cassette integration at $RAD4$
OSM3571	CCCCGTTAAACTAATAACTGAT ATAATTAAATTGAAG	To clone $URA3$ (to make the plasmid pYT811)

OSM3594	CGGTGAATTGCGACAGGTAAG TCCCAGC	To clone the 3' end and the terminator of <i>RAD51</i> and introduce R188A, K361A, R371A mutations (to make the plasmid pYT813)
OSM3595	TAATCTTGACATCCCTTACCCCT TCGCGAACCTAACCGCGTGGT GG	To clone the 3' end and the terminator of <i>RAD51</i> and introduce R188A, K361A, R371A mutations (to make the plasmid pYT813)
OSM3596	GGTAAGGGATGTCAAAGATTAT GCGCAGTTGTTGACTCACCTTG CTTACC	To clone the 3' end and the terminator of <i>RAD51</i> and introduce R188A, K361A, R371A mutations (to make the plasmid pYT813)
OSM3597	CTTCTCTGGGTCACCAACACC ATC	To clone the 3' end and the terminator of <i>RAD51</i> and introduce R188A, K361A, R371A mutations (to make the plasmid pYT813)
OSM3598	TCAAAGGTATATCGGAAGCTAA GG	To check for the R188A mutation in <i>RAD51</i>
OSM3599	GACGACTGCAACACCAAATTG	To check for the R188A mutation in <i>RAD51</i>
OSM3600	GATTGGTATCCATAGCTCAGCG GTTC	To check for the K361A mutation in <i>RAD51</i>
OSM3601	ACACACATTAGCCTCTGGTAA GC	To check for the K361A mutation in <i>RAD51</i>
OSM3602	GCAGTCGTCGTTACTAACCAAG TG	To check for the K371A mutation in <i>RAD51</i>
OSM3603	CAGTGGATGGAAATGAAGATAA AAATGTACG	To check for the K371A mutation in <i>RAD51</i>
OSM3606	ACCCATGAAATATATGTATTTT CTACTCTTCTCCGATGACTAC TTCCCGGATCCCCGGGTTAATT AA	To delete the WT <i>RAD51</i> copy and the vector backbone after the pYT813 integration
OSM3607	TTTTCTCTTCACTCCCCCTAAAA GGATAAAGCCCGCGGGACCCCT	To delete the WT <i>RAD51</i> copy and the

	GCAGGAGAATTGAGCTCGTT AAAC	vector backbone after the pYT813 integration
OSM3857	ACAGATTTCTAAAATAATCG ATACTGCATTTCTAGGCATATCC AGCGGGATCCCCGGGTTAATT AA	<i>REV1</i> deletion
OSM3858	TTCGCAAACTGCGTGTACTGT ATGCTGAAATGTTTTTTTTT AATgaattcgagctcgttaaac	<i>REV1</i> deletion
OSM3859	TGAAGTGATCATGCACATCGC	To screen for cassette integration at <i>REV1</i>
OSM3860	CTACTGTTGGTCAAGAATTCTAG	To screen for cassette integration at <i>REV1</i>
OSM3861	TAGCGCAGGCCTGCTCATT GAACGGCTTGATAAAACAAGA CAAAGCCGGATCCCCGGGTTAA TTAA	<i>RAD30</i> deletion
OSM3862	ATCAGGACGTTTAGTGCTGAA GCCATATAATTGTCTATTGGAA TAGGAAATTGAGCTCGTTAA AC	<i>RAD30</i> deletion
OSM3863	CCTGCCGATCATAGGATACC	To screen for cassette integration at <i>RAD30</i>
OSM3864	TTTGATCAAAAGCGAAGTCTC	To screen for cassette integration at <i>RAD30</i>
OSM3865	TTGAAATGCGAGATAGTCC	To screen for cassette integration at <i>MEC1</i>
OSM3866	TCAAATAGATGGAACGCACG	To screen for cassette integration at <i>MEC1</i>
OSM3876	ATGATGACGGTGATGGCGATAC TAGCGAGGATTATAGCGAAACT GCGGAATGAGGCGGCCACTT CTAAA	Exo1-(aa 1-553) truncation
OSM3880	CGGCAGTCAGATCTATCTCCTT GCTTCCCAATTGTTATAAAG GTAAATGAGGCGGCCACTTCT AAA	Exo1-(aa 1-702) WT control
OSM3881	TTTCATTGAAAAATACCTC CGATATGAAACGTGCAGTACTT	Exo1 truncations

	AACTTGAATTCGAGCTCGTTAA AC	
OSM3882	TGATTGCGACGATAACGATG	To check Exo1-(aa 1-690) and Exo1-(aa 1-660) truncations
OSM3883	ATCCCAGAGGAGTATATCGG	To check the Exo1-(aa 1-647) truncation
OSM3884	TTAGAGGATGACGACAACC	To check the Exo1-(aa 1-553) truncation
OSM3885	GGATCATAACCCAAAAGTTGC	To check the Exo1-(aa 1-525) truncation
OSM3888	GATTGACATGAAAAGCGTAG	To check the Exo1-(aa 1-702) WT control
OSM3899	ATATTTATATTTCGTTTTCACG GCTTAATTAGCGTACGTGGTT CTGGAATTGAGCTCGTTAAA C	To integrate $P_{GAL1}$ at <i>HED1</i>
OSM3900	ACCCCGAGTGGTATATAGGAGC AGCTTCTCCTATTGATCTTGT TGCATTTGAGATCCGGGTTTT	To integrate $P_{GAL1}$ at <i>HED1</i>
OSM3902	ACAGTCTTCTTCTACAACG	To screen for $P_{GAL1}$ at <i>HED1</i>
OSM3903	CCCCCGCGCGCTCATCCTCGGCA CCGTCACC	To clone TetA fragments around <i>URA3</i> marker in a pFA6a- <i>URA3</i> plasmid (pYT811) to create a <i>URA3</i> loop-out plasmid (pYT1082)
OSM3904	CCCCAGATCTATCGGTGATGTC GGCGATATAGGC	To clone TetA fragments around <i>URA3</i> marker in a pFA6a- <i>URA3</i> plasmid (pYT811) to create a <i>URA3</i> loop-out plasmid (pYT1082)
OSM3905	TCATCCTCGGCACCGTCACC	To clone TetA fragments around <i>URA3</i> marker in a pFA6a- <i>URA3</i> plasmid (pYT811) to create a

		<i>URA3</i> loop-out plasmid (pYT1082)
OSM3906	CCCCGAGCTCGTTAACATCG GTGATGTCGGCGATAGGC	To clone TetA fragments around <i>URA3</i> marker in a pFA6a- <i>URA3</i> plasmid (pYT811) to create a <i>URA3</i> loop-out plasmid (pYT1082)
OSM3926	GGGACATCGAAACTACTAAGTC AAGCCAAGCTCGGCCGGCAGT CAGATCTTGAGGCGCGCCACTT CTAAA	Exo1-(aa 1-690) truncation
OSM3928	TGGAAGAGCCTGTTCCGAGTC TCAACTATCTACACAAATACCTA GTTCTTGAGGCGCGCCACTTCT AAA	Exo1-(aa 1-494) truncation
OSM3929	TCCAAGAACGTTGAAGGATAC	To check the Exo1-(aa 1-494) truncation
OSM3974	GGTCACAGAGAATTGTGATTGA CATGAAAAGCGTAGATGAACGA AAATCATGAGGCGCGCCACTTC TAAA	Exo1-(aa 1-660) truncation
OSM3975	CGCAAAGGCCATCACTGCGAAA AAGCCTTATTGGTGCCAGGTCA CAGAGATGAGGCGCGCCACTTC TAAA	Exo1-(aa 1-647) truncation
OSM3977	AGGTTTCTGAAGTTGTCAGTGA CATTGAAGAGGACCGAAAGAAT TCTGAATGAGGCGCGCCACTTC TAAA	Exo1-(aa 1-525) truncation

Table 2.3. Plasmids used in this study

Plasmid	Description	Origin
pFA6-kanMX4	To amplify a cassette for gene deletion with <i>KAN</i> marker	(215)
pFA6-TRP1	To amplify a cassette for gene deletion with <i>TRP1</i> marker	(216)

pFA6a-natMX4	To amplify a cassette for gene deletion with <i>NAT</i> marker	(217)
pFA6a-hphMX4	To amplify a cassette for gene deletion with <i>HYG</i> marker	(217)
pFA6a-13Myc-kanMX6	To amplify a cassette for C-terminal tagging or truncation with <i>KAN</i> marker	(217)
pFA6a-13Myc-TRP1	To amplify a cassette for C-terminal tagging or truncation with <i>TRP1</i> marker	(217)
pFA6a-kanMX6-PGAL1	To amplify a cassette with <i>P<sub>GAL1</sub></i> promoter and <i>KAN</i> marker	(217)
pFA6a-TRP1-PGAL1	To amplify a cassette with <i>P<sub>GAL1</sub></i> promoter and <i>TRP1</i> marker	(217)
pyT104	<i>pRS406-pif1-N-m2 (M40A)</i> To introduce the <i>pif1-m2</i> mutation	(218)
pyT191	<i>pRS404-P<sub>GAL1</sub>-PIF1</i>	The plasmid collection of Makovets' laboratory
pyT477	<i>pRS404-rad54(aa 1-192-Ncol site-811-898)-T<sub>RAD54</sub></i> Interrupted <i>RAD54</i> with the endogenous terminator. Integration leads to gene duplication and the creation of one endogenous copy and one copy under the control of the <i>P<sub>GAL1</sub></i> promoter	Three piece ligation: 1) pYT191 digested with PspOMI, 2) PCR product (OSM2681 + OSM2738 + NK1 genomic DNA) digested with Eagl and Ncol, 3) PCR product (OSM2737+OSM2682+NK1 genomic DNA) digested with Eagl and Ncol
pyT570	<i>pRS404-rad51(aa 151-400)-T<sub>RAD51</sub></i> The 3' end of <i>RAD51</i> with the endogenous terminator	PCR product (OSM2936 + OSM2937 + NK1 genomic DNA) digested with Eagl and Sall and ligated into pYT191 digested with Eagl and Sall
pyT571	<i>pRS404-rad51-K342E(aa 151-400)-T<sub>RAD51</sub></i> The 3' end of <i>RAD51</i> encoding the K342E substitution and the endogenous terminator	Recombinant PCR product ((OSM2935 + OSM2937 + NK1 genomic DNA) + (OSM2934 + OSM2936 + NK genomic DNA)) digested with Eagl and Sall and ligated into pYT191 digested with Eagl and Sall
pyT754	<i>pRS404-P<sub>RAD51</sub>-RAD51-T<sub>RAD51</sub></i> <i>RAD51</i> with its endogenous promoter and terminator	PCR product (OSM3516 + OSM3517 + NK1 genomic DNA) digested with Eagl and EcoRI and ligated into pYT570 digested with Eagl and EcoRI

pYT811	<i>pFA6-URA3</i> To amplify a cassette for gene deletion with <i>URA3</i> marker	PCR product (OSM1463 + OSM3571 + NK genomic DNA) digested with BglII and Pmel and ligated into pFA6-TRP1 digested with BglII and Pmel
pYT813	<i>pRS404-P<sub>RAD51</sub>-rad51-II3A(R188A, K361A, K371A)-T<sub>RAD51</sub></i> <i>RAD51</i> with the <i>II3A</i> allele, the endogenous promoter and terminator	Recombinant PCR product ((OSM3594 + OSM3595 + NK1 genomic DNA) + (OSM3603 + OSM3596 + NK1 genomic DNA)); second round of PCR performed with OSM3594 + OSM3597) digested with BstEII and EcoRI and ligated into pYT754 digested with BstEII and EcoRI
pYT814	<i>pRS400-P<sub>RAD51</sub>-rad51-II3A(R188A, K361A, K371A)-T<sub>RAD51</sub></i> <i>RAD51</i> with the <i>II3A</i> allele, the endogenous promoter and terminator	EagI-Sall fragment from pYT813 subcloned into pRS400
pYT1082	<i>pFA6-TetA(aa 10-125)-URA3-TetA(aa 10-125)</i> To amplify a cassette for gene deletion with <i>URA3</i> marker that can be looped out	PCR product (OSM390 + OSM3904) digested with BssHII and BglII was ligated into pYT811 digested with BssHII and BglII. PCR product (OSM3905 + OSM3906) digested with SacI was ligated into the intermediate plasmid digested with SacI and Pmel. A plasmid containing TetA gene from the plasmid collection of Makovets' laboratory was used as a PCR template

## 2.5. Propagation and manipulation of yeast and bacteria

### 2.5.1. Growth media

Recipes for solid and liquid media used in this study are summarised in the Table 2.4. Bacto-yeast extract, bacto-peptone, yeast nitrogen base and bacto-agar solutions were sterilised by autoclaving. Solutions containing the rest of the ingredients were sterilised by filtering and added to the autoclaved components cooled down to approximately 55°C.

Table 2.4. Growth media

Yeast liquid media	
YPD	1% (w/v) bacto-yeast extract, 2% (w/v) bacto-peptone, 2% (w/v) D-glucose
YPRAF	1% (w/v) bacto-yeast extract, 2% (w/v) bacto-peptone, 2% (w/v) D-raffinose
YPGAL	1% (w/v) bacto-yeast extract, 2% (w/v) bacto-peptone, 2% (w/v) D-galactose
YPRAF+G418	1% (w/v) bacto-yeast extract, 2% (w/v) bacto-peptone, 2% (w/v) D-raffinose, 100 µl/mL G418 disulphate (Formedium, G4185)
Yeast solid media (plates)	
YPD agar	1% (w/v) bacto-yeast extract, 2% (w/v) bacto-peptone, 2% (w/v) bacto-agar, 2% (w/v) D-glucose, 0.01% (w/v) adenine sulphate, 0.01% (w/v) L-tryptophan, 0.002% (w/v) uracil
YPRAF agar	1% (w/v) bacto-yeast extract, 2% (w/v) bacto-peptone, 2% (w/v) bacto-agar, 2% (w/v) D-raffinose, 0.01% (w/v) adenine sulphate, 0.01% (w/v) L-tryptophan, 0.002% (w/v) uracil
YPGAL agar	1% (w/v) bacto-yeast extract, 2% (w/v) bacto-peptone, 2% (w/v) bacto-agar, 2% (w/v) D-galactose, 0.01% (w/v) adenine sulphate, 0.01% (w/v) L-tryptophan, 0.002% (w/v) uracil
YPD+G418 agar	1% (w/v) bacto-yeast extract, 2% (w/v) bacto-peptone, 2% (w/v) bacto-agar, 2% (w/v) D-glucose, 0.01% (w/v) adenine sulphate, 0.01% (w/v) L-tryptophan, 0.002% (w/v) uracil, 200 µl/mL G418 disulphate (Formedium, G4185)
YPD+HYG agar	1% (w/v) bacto-yeast extract, 2% (w/v) bacto-peptone, 2% (w/v) bacto-agar, 2% (w/v) D-glucose, 0.01% (w/v) adenine sulphate, 0.01% (w/v) L-tryptophan, 0.002% (w/v) uracil, 300 µg/mL Hygromycin B (Toku-E, H010)
YPD+NAT agar	1% (w/v) bacto-yeast extract, 2% (w/v) bacto-peptone, 2% (w/v) bacto-agar, 2% (w/v) D-glucose, 0.01% (w/v) adenine sulphate, 0.01% (w/v) L-tryptophan, 0.002% (w/v) uracil, 100 µg/mL Nourseothricin (Jena Bioscience, AB-102)

5-FOA agar	0.69% (w/v) yeast nitrogen base without amino acids (Formedium), 2% (w/v) D-glucose, 2% (w/v) bacto-agar, 770 mg/l of complete supplement mixture (CSM) drop-out: -Ura (Formedium), 0.1% (w/v) 5-Fluoroorotic Acid (Formedium), 0.002% (w/v) uracil
-URA agar	0.69% (w/v) yeast nitrogen base without amino acids (Formedium), 2% (w/v) D-glucose, 2% (w/v) bacto-agar, 770 mg/l of complete supplement mixture (CSM) drop-out: -Ura (Formedium)
-TRP agar	0.69% (w/v) yeast nitrogen base without amino acids (Formedium), 2% (w/v) D-glucose, 2% (w/v) bacto-agar, 740 mg/l of complete supplement mixture (CSM) drop-out: -Trp (Formedium)
-TRP -URA agar	0.69% (w/v) yeast nitrogen base without amino acids (Formedium), 2% (w/v) D-glucose, 2% (w/v) bacto-agar, 720 mg/l of complete supplement mixture (CSM) drop-out: -Trp - Ura (Formedium)
Bacterial liquid media	
LB	1% (w/v) bacto-tryptone, 0.5% (w/v) bacto-yeast extract, 1% (w/v) NaCl, pH adjusted to 7.0 with 1 M NaOH
LB+amp	1% (w/v) bacto-tryptone, 0.5% (w/v) bacto-yeast extract, 1% (w/v) NaCl, 100 µg/mL ampicillin sodium salt (Sigma, A0166), pH adjusted to 7.0 with 1 M NaOH
Bacterial solid media (plates)	
LB+amp agar	1% (w/v) bacto-tryptone, 0.5% (w/v) bacto-yeast extract, 2% (w/v) bacto-agar, 1% (w/v) NaCl, 100 µg/mL ampicillin sodium salt (Sigma, A0166), pH adjusted to 7.0 with 1 M NaOH

### **2.5.2. Cell stocks**

#### Materials

- Yeast storage solution: 0.5% (w/v) bacto-yeast extract, 1% (w/v) bacto-peptone, 1% (w/v) D-glucose, 25% (w/v) glycerol

#### Method

Yeast strains to be stored were patched on YPD or appropriate selection plates and incubated overnight at 30°C. Cells from the patches were then resuspended in 2 mL of the storage solution made by mixing 1 mL of YPD broth and 1 mL of 50% sterile glycerol in 2 mL cryogenic vials. Strain stocks were stored at -80°C.

Competent *E. coli* cells were prepared as described in the section 2.5.7 and stored at -80°C.

### **2.5.3. Yeast transformation**

#### Materials

- Wash solution: 0.1 M lithium acetate, pH 7.2
- PEG solution: 40% (w/v) polyethylene glycol (PEG) 3.350, 0.1 M lithium acetate, pH 7.2
- Carrier DNA solution: 10 mg/mL of salmon sperm ssDNA

#### Method

Yeast strains to be transformed were pre-grown on YPD or appropriate selection plates overnight at 30°C. Cells were then resuspended in fresh YPD broth and diluted to approximately OD<sub>600</sub> of 0.1. 10 mL of culture were used per transformation reaction. Cells were incubated at 30°C with appropriate aeration until the mid-log phase was reached (OD<sub>600</sub> ≈ 0.4 - 0.6) and harvested in 50 mL conical centrifuge tubes by centrifugation at 1,741 g for 2 minutes at

RT. The resulting pellets were resuspended in 1 mL of wash solution and transferred to 1.7 mL microcentrifuge tubes. The tubes were then centrifuged at 2,348 g for 2 minutes at RT and the cells were washed with 1 mL of wash solution again. The washed pellets were resuspended in  $(n+1) \times 100 \mu\text{L}$  of wash solution with  $(n+1) \times 10 \mu\text{L}$  of carrier DNA solution, where n is the total number of transformations per strain. The cell suspensions were then aliquoted into 1.7 mL microcentrifuge tubes (110  $\mu\text{L}$  each), one aliquot per transformation and an additional aliquot for the no DNA control. Up to 15  $\mu\text{L}$  of DNA to be transformed were then added to the appropriate cell aliquots. 600  $\mu\text{L}$  of PEG solution were then added into each tube and the samples were mixed by vortexing. The tubes were incubated at 30°C for 40 minutes and heat-shocked at 42°C for 17 minutes. Cells were pelleted by centrifugation at 2,348 g for 2 minutes at RT and washed with 1 mL of YPD broth. The final pellets were resuspended in 100  $\mu\text{L}$  of YPD broth. If auxotrophic markers were used to select for transformants, cells were plated directly on selective agar. When drug resistance markers were employed, cells were plated on YPD agar overnight at 30°C first and then replica-plated on the YPD agar containing the appropriate drug. Plates were incubated at 30°C until colonies were formed.

#### **2.5.4. Yeast mating, sporulation, and tetrad dissection**

##### Materials

- Pre-sporulation medium: 1% (w/v) bacto-yeast extract, 2% (w/v) bacto-peptone, 6% (w/v) D-glucose
- Sporulation medium: 1% (w/v) potassium acetate, 0.05% (w/v) glucose, 0.1% (w/v) bacto-yeast extract, 1x amino-acid mix
- 10x amino-acid mix: adenine sulphate, uracil, L-tryptophan, L-histidine-HCl, L-arginine-HCl, L-methionine, L-tyrosine, L-leucine, L-isoleucine, L-lysine-HCl, L-phenylalanine, L-glutamic acid, L-aspartic acid, L-valine, L-threonine, L-serine (10 mg/mL each)
- 1 mg/mL Zymolyase-20T solution in water (from *Arthrobacter luteus*, MP Biomedicals, 0832092)

## Method

*Yeast mating.* Yeast strains to be mated were pre-grown on YPD agar at 30°C overnight, mixed together into a single patch on a fresh YPD agar and incubated at the same temperature for 8 to 24 hours. Cells from the middle of the patch were then streaked out on an agar selective for diploids and incubated at 30°C for 2 days. Cells from the colonies formed were then tested to confirm they were diploids. For this, two mating type tester strains *MAT $\alpha$*  *bar1Δ* (NK1) and *MAT $\alpha$*  *sst2Δ* (NK1542) were pre-grown on YPD agar at 30°C overnight. Then, a lawn of cells was created for each tester strain by resuspending around 1 OD<sub>600</sub> unit of cells in 100 μL of YPD broth and spreading the suspension on the YPD agar using glass beads. Cells to be tested were then patched onto the two lawns. Both tester strains as well as the parental strains used for the mating were also patched on each lawn in parallel to be used as the mating type controls. Cells of the opposite mating type should inhibit the growth of the lawn around them creating a clear area of growth inhibition called a halo. Diploid cells do not secrete mating pheromones and thus no halo is formed around them on either of the two lawns.

*Sporulation.* To sporulate the diploids, the strains were patched on the YPD agar and pre-grown at 30°C overnight. Cells were then resuspended in 10 mL of the pre-sporulation medium to the optical density of around 0.1 OD<sub>600</sub> and the cultures were incubated at 30°C with an appropriate aeration until the OD<sub>600</sub> reached 1.2 – 1.5. 100 μL of cell culture were then transferred into a 1.7 mL microcentrifuge tube and cells were pelleted by centrifugation at 2,348 g for 2 minutes at RT. Pellets were then washed with 100 μL of the sporulation medium and resuspended in 1 mL of the same solution. Cell samples were transferred into glass test tubes and incubated at 25°C with aeration for 4 to 5 days.

*Dissection.* For tetrad dissection, 15 μL of a sporulated culture were transferred into a 1.7 mL microcentrifuge tube and pelleted by centrifuged at 2,348 g for 2 minutes at RT. The resulting cell pellet was resuspended in 15 μL of 1 mg/mL zymolyase-20T solution and the suspension was incubated at

42°C for 10 minutes. After the incubation, 300 µL of sterile water were added to the sample and the cells were gently resuspended by slowly pipetting the suspension up and down 1-2 times. 15 µL of the suspension was run along the middle of the YPD agar plate in a straight line and tetrads were dissected using Singer MSM 400 dissection microscope. Dissections were performed by Dr Sveta Makovets. Dissected spores were grown at 30°C until colonies of appropriate size were formed. The images of colonies were taken using Gel Doc XR+ imaging system (BioRad). Colony diameters were measured using ImageJ software.

### 2.5.5. Measuring the yeast doubling time

#### Method

To estimate the doubling time of different yeast strains, cells were pre-grown on YPD agar overnight at 30°C. Pre-grown cells were used to start 20 mL 0.1 OD<sub>600</sub> cultures at 30°C in a shaking water bath. Cultures were then incubated for 3 h to allow the cells to enter the exponential growth phase. After that, OD<sub>600</sub> measurements were taken every 45 min for 3 h. Cultures were maintained in the 0.1 – 0.8 OD<sub>600</sub> range. The doubling time was calculated using the following formula:

$$Doubling\ time = \frac{duration * \log(2)}{\log(final\ OD_{600}) - \log(initial\ OD_{600})}$$

### 2.5.6. Yeast spot assay

#### Materials

- A sterile 96-well plate
- A 48-pin frogger

## Method

Strains were pre-grown on an appropriate agar overnight at 30°C. If gene expression from a galactose-inducible promoter was involved, raffinose-containing agar was used, otherwise strains were patched on the YPD agar. The pre-grown cells were resuspended in a broth with an appropriate sugar, and 1 OD<sub>600</sub> unit was harvested for each strain by centrifugation at 2,348 g for 2 minutes at RT. The resulting pellets were resuspended in 200 µL of the same broth (yielding cell concentration of OD<sub>600</sub>=5) and transferred into the first or seventh column of a 96-well plate. The rest of the relevant wells were filled with 160 µL of the appropriate broth. 40 µL of the cell suspensions were then transferred to the neighbouring well on the right, thereby diluting the cell titre 5-fold. Analogous sequential dilutions were performed using six columns of the 96-well plate in total. A 48-pin frogger was then used to transfer approximately 4 µL of cell suspension from each well onto an appropriate agar. Plates were incubated at 30°C until appropriately sized colonies were formed for the most diluted samples. The images of colonies were taken using Gel Doc XR+ imaging system (BioRad).

### **2.5.7. *E. coli* competent cell preparation**

#### Materials

- 0.1 M CaCl<sub>2</sub>
- 20% (w/v) glycerol in 0.1 M CaCl<sub>2</sub>

#### Method

*E. coli* K-12 DH5α cells were streaked on LB agar and grown overnight at 37°C. A single colony was then used to inoculate a 10 mL of LB broth in a 125 mL conical flask and the culture was grown overnight at 37°C with appropriate aeration. The pre-grown *E. coli* culture was then diluted 100-fold in 200 mL of LB broth in a 2 L conical flask. This culture was grown at 37°C

with a vigorous aeration until the cell density reached OD<sub>600</sub> of 0.4-0.5. The culture was then cooled down rapidly by swirling the flask in an ice-water bath for 5 minutes. Cells were then harvested in four 50 mL conical tubes by centrifugation at 1,505 g for 10 minutes at 4°C. The resulting pellets were each resuspended in 25 mL of ice-chilled 0.1 M CaCl<sub>2</sub> and incubated on ice for 1 hour. The four 25 mL suspensions were then combined in two 50 mL conical tubes and centrifuged at 1,505 g for 10 minutes at 4°C. Pellets were then each resuspended in 5 mL of pre-chilled 20% (w/v) glycerol in 0.1 M CaCl<sub>2</sub> and combined in a single 50 mL conical tube. The resulting suspension was aliquoted (100 µL each) into 1.7 mL microcentrifuge tubes pre-chilled at -80°C and kept on dry ice. The aliquots of competent cells were stored at -80°C.

#### **2.5.8. *E. coli* transformation**

##### Method

*E. coli* competent cells prepared as described in the section 2.5.7, were thawed on ice and up to 10 µL of DNA solution (plasmid DNA or ligation reactions) were added to each tube. Cell suspensions and DNA were mixed by pipetting and incubated on ice for 30 minutes. Cells were then heat-shocked at 42°C for 2 minutes and cooled down on ice for another 1 minute. 900 µL of LB broth were then added and the tubes were incubated for 1 hour at 37°C with an appropriate aeration to allow the expression of the plasmid-encoded gene used as a marker for selecting transformants. After the incubation, cells were collected by centrifugation at 2,348 g for 2 minutes at RT. Pellets were resuspended in 100 µL of LB broth and plated on LB agar containing an appropriate antibiotic. Cells were incubated at 37°C overnight.

## **2.6. General manipulation of DNA**

### **2.6.1. The amplification of cassettes for gene deletions and truncations, protein tagging and placing genes under a galactose-inducible promoter**

#### Materials

- 10x PCR buffer: 500 mM KCl, 100 mM Tris-HCl, pH 9.0, 1% (v/v) Triton X-100
- 1 M Tris-HCl, pH 9.0
- 25 mM MgCl<sub>2</sub>
- 10 mg/mL BSA
- 10 mM dNTP mix
- Taq DNA Polymerase, 5000 U/mL (NEB, M0273)
- Vent® DNA polymerase, 2000 U/mL (NEB, M0254)

#### Method

Cassettes for gene deletion, truncation and protein tagging were PCR amplified from previously described pFA6a vectors containing *TRP1*, *HYG*, *NAT* and *KAN* marker genes using 70 base primers where the 50 bases at the 5' end corresponded to the genome sequence for the cassette to recombine with (216, 219). Two derivatives of the pFA6a plasmids were also generated in this study. The first one contained a *URA3* marker. The second plasmid consists of the *URA3* marker flanked by two direct repeats which allow for the marker to be looped out after gene deletion. To loop out the *URA3* marker, strains were pre-grown on the YPD agar at 30°C overnight and then streaked on a 5-FOA agar and grown at 30°C for two days to select for the cells in which the *URA3* marker was lost, presumably through the recombination of the direct repeats. The forward (F) and reverse (R) oligonucleotide primers, PCR reaction mixes and conditions used in this protocol are described below.

## Oligonucleotide primers

Primer	Purpose	Sequence
F1	Gene deletion	5'-(50 bp of gene-specific sequence) CGGATCCCCGGGTTAATTAA-3'
R1	Gene deletion/C-terminal tagging	5'-(50 bp of gene-specific sequence) GAATTCTGAGCTCGTTAAC-3'
F2	C-terminal tagging	5'-(50 bp of gene-specific sequence) CGGATCCCCGGGTTAATTAA-3'
F3	C-terminal truncation	5'-(50 bp of gene-specific sequence) TGAGGCGCGCCACTTCTAAA-3'
F4	The introduction of $P_{GAL1}$	5'-(50 bp of gene-specific sequence) GAATTCTGAGCTCGTTAAC-3'
R2	The introduction of $P_{GAL1}$	5'-(50 bp of gene-specific sequence) CATTGTGAGATCCGGGTTT-3'

## PCR mix

DNA template (stock plasmid diluted 1:10)	1 µl
10x PCR buffer	5 µl
25 mM MgCl <sub>2</sub>	3 µl
1 M Tris, pH 9.0	0.5 µl
10 mg/mL BSA	0.5 µl
10 mM dNTP mix	1 µl
100 µM F primer	0.25 µl
100 µM R primer	0.25 µl
Milli-Q H <sub>2</sub> O	37.5 µl
Taq DNA Polymerase	0.5 µl
Vent® DNA polymerase	0.5 µl
Total volume	50 µl

## PCR conditions

PCR stage	Temperature	Time	Number of cycles
Initial denaturation	94°C	2 min	1
	80°C	2 min	
Denaturation	94°C	1 min	30
Annealing	55°C	45 sec	
Extension	72°C	2.5 min	
Final extension	72°C	10 min	1

### 2.6.2. Yeast colony PCR

#### Materials

- 20 mM NaOH
- Taq PCR Core Kit (Qiagen, 201225)
- 10 mM dNTP mix

#### Method

Disposable pipette tips were used to transfer small amount of cells from individual colonies into 3 µL of 20 mM NaOH in 8-strip PCR tubes. Cells were then incubated at 99°C for 10 min in a PCR machine to release the DNA. A PCR master mix was pre-prepared and added to the heat-treated cells.

### **PCR reaction mix (per 1 sample)**

Cells in 20 mM NaOH	3 µl
5x Q solution	5 µl
10x CoralLoad PCR Buffer	2.5 µl
10 mM dNTP mix	0.5 µl
100 µM F primer	0.25 µl
100 µM R primer	0.25 µl
Milli-Q H <sub>2</sub> O	13.25 µl
Taq DNA Polymerase	0.25 µl
Total volume	25 µl

### **PCR conditions**

PCR stage	Temperature	Time	Number of cycles
Initial denaturation	94°C	2 min	1
Denaturation	94°C	30 sec	40
Annealing	*	30 sec	
Extension	72°C	**	
Final extension	72°C	2 min	1

\*The annealing temperature was derived by subtracting 2°C from the lowest melting temperature of the primers used.

\*\*The extension time was calculated based on the speed of DNA polymerisation by Taq polymerase – 1,000 bases per 1 minute.

### **2.6.3. Molecular cloning**

#### Materials

- Pfu DNA Polymerase, 3000 U/ml (Promega, M7741)
- QIAquick® Gel Extraction Kit (Qiagen, 28706)
- QIAquick® PCR Purification Kit (Qiagen, 28106)
- Restriction enzymes (listed in Table X)
- Calf Intestinal Alkaline Phosphatase (NEB, M0290S)

- T4 DNA Ligase, 400 U/ $\mu$ l (NEB, M0202S)
- 10x T4 DNA Ligase reaction buffer (NEB, B0202S)
- Wizard® Plus SV Miniprep DNA Purification System (Promega, A1460)

### Method

Sequences to be cloned (inserts) were PCR amplified from either genomic or plasmid DNA using Pfu DNA polymerase according to the manufacturer's guidelines. The PCR reactions were investigated using agarose gel electrophoresis (described in the section 2.6.4) and the PCR product of a correct size was extracted from the gel using QIAquick® Gel extraction Kit. Insert and vector DNA was then digested with the appropriate restriction enzymes, based on the manufacturer's guidelines. Vector DNA digests also contained Calf Intestinal Alkaline Phosphatase (5 units per 20  $\mu$ L of reaction) in order to dephosphorylate the DNA ends and prevent the plasmid re-ligation without the insert. Digested inserts were purified using QIAquick® PCR Purification Kit while vector digests were analysed using agarose gel electrophoresis and the fragments of correct sizes were purified using QIAquick® Gel extraction Kit.

15  $\mu$ L total volume ligation reactions were then set up by using 400 units of T4 DNA Ligase and 1.5  $\mu$ L of 10x T4 DNA Ligase reaction buffer. 100 ng of total DNA and 1:3 vector:insert molar ratio were used. Ligation reactions were incubated at RT overnight and then transformed into *E. coli* competent cells (described in sections 2.5.6 and 2.5.7).

The resulting *E. coli* colonies were used to inoculate 4 mL LB+Amp cultures which were grown overnight at 37°C with aeration. Plasmids were then extracted from the overnight cultures using Wizard® Plus SV Minipreps DNA Purification System according to the manufacturer's guidelines. Plasmids were eluted with 50  $\mu$ L of Milli-Q H<sub>2</sub>O and stored at -20°C. The successful outcome of each cloning was verified using restriction digest analysis and DNA sequencing. The services of the GenePool Sanger sequencing facility at the

University of Edinburgh were used and the provided chromatograms were analysed using the FinchTV software.

#### **2.6.4. Agarose gel electrophoresis**

##### Materials

- Agarose, molecular biology grade (Melford, MB1200)
- 1x TBE buffer: 0.089 M Tris, 0.089 M boric acid, 2 mM EDTA, pH 8.0
- Ethidium bromide solution, 10 mg/mL (Fisher Scientific, E/P800/03)
- 6x Gel-Loading buffer: 0.25% (w/v) bromophenol blue, 15% (w/v) Ficoll-400
- 100 bp and 1 kb DNA ladder, 500 µg/mL (NEB, N3231L, N3232L)

##### Method

Agarose gels were prepared by melting agarose powder in 1x TBE buffer using a microwave. Agarose gel concentrations from 0.5% (w/v) to 2% (w/v) were used. Ethidium bromide was added to melted and cooled down agarose, right before the gel pouring, to the final concentration of 0.5 µg/mL. Gels were cast in appropriate trays with the desired combs. Set gels were moved to the running tanks and covered with 1x TBE buffer. DNA samples were mixed with 6x Gel-Loading buffer to the final concentration of 1x and loaded into the gel wells. An appropriate molecular weight DNA size marker (100 bp or 1 kb DNA ladder) was loaded into the wells next to the analysed samples. The gels were run at 5-10 V per cm of the distance between the electrodes. DNA fragments in the gel were visualised using Gel Doc XR+ imaging system (BioRad) and analysed using the Image Lab™ software (Bio-Rad).

## **2.7. General manipulation of proteins**

### **2.7.1. TCA protein precipitation**

#### Materials

- Cell lysis solution: 1.85 M NaOH, 7.4% (v/v)  $\beta$ -mercaptoethanol. Prepared fresh using 10 M NaOH stock and  $\beta$ -mercaptoethanol.
- 50% (v/v) trichloroacetic acid (TCA), 4°C
- 100% Acetone, -20°C
- 4x Laemmli buffer: 200 mM Tris-HCl, pH 6.8, 400 mM DTT, 10% (w/v) SDS, 40% (v/v) glycerol, 0.1% (w/v) bromophenol blue
- Sample buffer: 1x Laemmli buffer, 50mM DTT, 30 mM Tris base (pH not adjusted)

#### Method

A known quantity of cells (1-3 OD<sub>600</sub> units) was collected in 15 mL conical tubes by centrifugation at 1,741 g for 2 minutes at RT. The cell pellets were resuspended in 1 mL of Milli-Q H<sub>2</sub>O and moved to 1.7 mL microcentrifuge tubes. The tubes were centrifuged at 2,348 g for 2 minutes at RT, the supernatants were discarded, and the pellets were stored at -80°C. To extract proteins, cell pellets were thawed on ice and resuspended in 150  $\mu$ L of the cell lysis solution. Tubes were incubated on ice for 10 minutes. 150  $\mu$ L of 50% TCA (4°C) was added, the samples were mixed by vortexing and incubated on ice for 10 minutes. Precipitated proteins were pelleted by centrifugation at 20,817 g for 2 minutes at 4°C. Pellets were then washed with 1 mL of 100% acetone (-20°C) and spun down at 20,817 g for 2 minutes at 4°C. Acetone was removed and the pellets were resuspended in the sample buffer to the final concentration of 0.02 OD<sub>600</sub> units/ $\mu$ L. Samples were incubated at 99°C for 5 minutes, then mixed by vortexing and incubated at 99°C for 3 more minutes. If cells were subjected to crosslinking prior to this protocol, then the samples were incubated at 99°C for additional 30 minutes in a PCR machine. Samples were stored at -80°C.

## **2.7.2. SDS polyacrylamide gel electrophoresis (SDS-PAGE)**

### Materials

- 30% acrylamide/bis-acrylamide solution (37.5:1)
- 1.5 M Tris-HCl, pH 8.8
- 0.5 M Tris-HCl, pH 6.8
- 10% (w/v) SDS
- Resolving gel solution: 375 mM Tris-HCl pH 8.8, 0.1% (w/v) SDS, variable concentration of acrylamide/bis-acrylamide depending on the experimental needs
- Stacking gel solution 5% (v/v) acrylamide/bis-acrylamide, 125 mM Tris-HCl pH 6.8, 0.1% (w/v) SDS
- 10% (w/v) ammonium persulfate (APS)
- Tetramethylethylenediamine (TEMED)
- 10x SDS-PAGE Running Buffer: 250 mM Tris-HCl, pH8.3, 1.92 M glycine, 0.1% (w/v) SDS
- 100% ethanol
- Full Range Rainbow Molecular Weight Protein Marker (GE Healthcare, RPN800E)

### Method

SDS-PAGE was performed using a Bio-Rad Mini-PROTEAN® 3 Cell system. 1.5 mm thickness spacer plates along with 15-well combs were used to cast all SDS-PAGE gels. Resolving and stacking gel solutions were prepared just before usage. APS and TEMED were then added to 1 mL of the resolving gel solution to the final concentration of 0.1% each and the mixture was used to seal the gap at the bottom of glass plates used for gel casting. The gel was allowed to polymerize. APS and TEMED were then added to the remaining volume of the resolving gel solution to the final concentration of 0.1% each and about 7 mL of the mixture were poured between the glass plates. 1 mL of 100% ethanol was pipetted on top, and the gel was left to

polymerase. After gel polymerisation, ethanol was removed and the stacking gel solution with 0.1% APS and 0.1% TEMED was poured on top the resolving gel. A comb was inserted, and the gel was allowed to polymerise. When the gels were ready, a Mini-PROTEAN 3 cell was assembled, the running tank was filled with 1x SDS-PAGE running buffer and the combs were removed.

Protein samples were incubated at 99°C for 5 minutes in a PCR machine and loaded into the wells of an SDS-PAGE gel. Rainbow Molecular Weight Protein Marker was loaded into one of the wells next to the set of samples to be analysed. The gel was run at 100 V at first and then at 200 V after the dye of the sample buffer entered the resolving gel. Gel electrophoresis was stopped after the dye left the bottom of the gel, and the running tank was disassembled.

### **2.7.3. Western blotting**

#### Materials

- Western blotting transfer buffer: 25 mM Tris, 192 mM glycine
- 100% methanol
- 1x TBST: 50 mM Tris-HCl, pH 7.6, 150 mM NaCl, 0.1% (v/v) Tween 20
- Skimmed milk powder (Oxoid, LP0031)
- Immobilon®-FL PVDF Transfer Membrane with 0.45 µm pores (Merck Millipore Ltd.)
- Protran BA83 Nitrocellulose Blotting Membrane, 0.2 µm (Whatman)
- Whatman paper

#### Method

After proteins were resolved using SDS-PAGE, the stacking gel was removed, the remaining resolving gel was rinsed with the transfer buffer and placed on top of three Whatman paper pieces cut to the size of the gel and pre-soaked in the transfer buffer. Transfer membrane cut to the size of the gel

was then placed on top of the gel. PVDF membranes were first activated in 100% methanol and then equilibrated in the transfer buffer. Nitrocellulose membranes were wetted in the transfer buffer directly. Nitrocellulose membrane was used for histone H2B western blotting, while PVDF membrane was used for all other purposes. Three more pre-soaked Whatman paper pieces were placed on top of the membrane. The resulting stack was placed into a transfer cassette with one sponge on each side and moved into a transfer tank filled with the transfer buffer. The protein transfer was carried out at the constant current of 250 mA for 1.5 hours on ice. After the transfer, the setup was disassembled, and the membrane was incubated in 1x TBST with 5% (w/v) skimmed milk on a rocker for 1 hour at RT. The membrane was then placed into a 50 mL conical tube with 4 mL of 1x TBST and an appropriate primary antibody (dilutions indicated in Table 2.5) and incubated overnight at 4°C on a rotator.

Next day, the membrane was washed three times with 1x TBST at RT for 10 minutes in a box placed on an orbital shaker. The membrane was then incubated with 7.5 mL of 1x TBST with a fluorescently labelled secondary antibody (dilutions indicated in Table 2.5) for 1 hour at RT in a container covered with foil and placed on top of a rocker. After the incubation, the membrane was washed twice with 1x TBST at RT for 15 minutes in a foil-covered container on an orbital shaker. Western blotting membranes were scanned using Odyssey® CLx fluorescent scanner (LI-COR®). The resulting images were analysed and quantified using Image Studio™ Lite software.

#### **2.7.4. Antibodies**

Antibodies used in this study are described in Table 2.5. Antibody stocks were stored at -80°C while small aliquots in use were stored at -20°C. Antibody concentrations used in this study were experimentally determined according to the manufacturer's guidelines.

Table 2.5. Antibodies

Antibody	Dilution used for western blotting	Manufacturer
Anti-Rad51 (y-180), rabbit polyclonal	1:200	Santa Cruz Biotechnology (sc-33626)
anti-β-actin, mouse monoclonal	1:50000	Abcam (ab8224)
Anti-c-Myc, mouse monoclonal	1:1000	Thermo Fisher Scientific (13-2500)
Anti-Histone H2B (yeast), rabbit monoclonal	1:2000	Abcam (ab188291)
Goat anti-mouse IgG (H+L) cross-adsorbed secondary antibody, Alexa Fluor 680	1:12500	Thermo Fisher Scientific (A-21057)
Goat anti-rabbit IgG F(c) IRDye800 Conjugated	1:12500	Rockland (611-132-003)

## 2.8. SSA assays

Assays described here were used to estimate the efficiency of SSA in cells harbouring a SSA system described in the section 3.2.

### 2.8.1. Plating assay

Strains were pre-grown on the YPRAF agar at 30°C overnight to de-repress the *P<sub>GAL1</sub>* promoter. Next day, cells were resuspended in the YPRAF broth and the appropriate serial dilutions were plated on the YPD and YPGAL agar. The cells were incubated at 30°C until appropriately sized colonies were formed. To distinguish between the cells that have repaired the break by SSA and NHEJ, the colonies formed on YPGAL agar were replica-plated on YPD+G418 agar. The frequency of DSB repair by SSA was then calculated as a ratio of G418-sensitive colonies from YPGAL agar to the total number of colonies on the corresponding YPD agar.

## **2.8.2. Time-course experiments to assay SSA**

### **2.8.2.1. Cell synchronisation, *P<sub>GAL1</sub>* induction and sample collection**

#### Materials

- 50 mg/mL G418 (Formedium, G4185)
- 5 mg/mL α-factor peptide solution in water (WHWLQLKPGQPMY, Peptide Protein Research Ltd.)
- 20% (w/v) D-galactose
- 3 mg/mL nocodazole in DMSO
- SE solution: 1 M sorbitol, 0.1 M EDTA, pH 8.0

#### Method

The time-course experiments were used to monitor the progression of SSA via analysing the DNA by Southern blotting and qPCR, as well as for protein analyses. Strains were pre-grown on YPRAF agar at 30°C overnight and then used to start 10 mL cultures in YPRAF broth with 100 µg/mL of G418. The cultures were grown at 30°C with aeration for approximately 8 hours while being maintained in the log phase. They were then used to start 105 mL overnight cultures in 500 mL conical flasks using the same type of broth as before. The culture dilutions were calculated so that the yeasts would reach the desired OD<sub>600</sub> next morning. The cultures were incubated at 30°C with appropriate aeration. When the optical density of around 0.3 OD<sub>600</sub> was reached, α-factor was added to the final concentration of 5 µg/mL (*BAR1* cells) to synchronise the cells. After 2.5 hours, 20 mL samples for DNA analysis at the time point -1 h were collected (the processing of the samples is described below) and galactose was added to the remaining cultures to the final concentration of 2%. After an hour, 20 mL samples for the time point 0 h were collected and the rest of the cultures were transferred into 50 mL conical tubes to wash away the α-factor. Cells were pelleted by centrifugation at 1,741 g for 2 minutes at RT and the pellets were resuspended in 35 mL of YPGAL broth.

Cells were then spun down again at 1,741 g for 2 minutes at RT and the pellets were transferred into 500 ml conical flasks with fresh YPGAL broth (same volume as removed). Nocodazole was added to the final concentration of 15 µg/mL to stop the cell division at the next G2/M. The cultures were incubated at 30°C with appropriate aeration. After the release from the α-factor arrest, samples were collected every hour for 4 hours (20 mL for the time point 1 h; 15 mL for the time point 2 h; 10 mL for time points 3 h and 4 h).

All the samples collected for genomic DNA extraction were centrifuged in 50 mL conical tubes at 1,741 g for 2 minutes at RT. Supernatants were discarded, the pellets resuspended in the remaining liquid and transferred into 1.7 mL microcentrifuge tubes. Cells were then pelleted again at 2,348 g for 2 minutes at RT and resuspended in 150 µL of SE. Cell samples were stored at -80°C until further processing.

The sample collection and treatment for western blotting is described in the section 2.7.1.

### **2.8.2.2. Genomic DNA extraction**

#### Materials

- SE solution: 1 M sorbitol, 0.1 M EDTA, pH 8.0
- Zymolyase-100T from *Arthrobacter luteus*, 100 U/mg (MP Biomedicals, 08320932)
- EDS solution: 50 mM EDTA, pH 8.0, 0.2% (w/v) SDS, 2.5 mM NaOH
- 8 M ammonium acetate
- 100% isopropanol
- 70% (v/v) ethanol
- 1x TE solution: 10 mM Tris-HCl, pH 8.0, 1 mM EDTA, pH 8.0
- 20 mg/mL Ribonuclease A (RNase A) from bovine pancreas (Sigma, R4875)

### Method

To extract genomic DNA, samples collected during a time-course experiment described in the section 2.8.2.1 were thawed on ice and 150 µL of SE solution with 0.1 mg/mL of Zymolyase-100T were added to each sample. Cell suspensions were mixed by inverting the tubes and incubated at 37°C for 20 minutes. The tubes were then centrifuged at 2,348 g for 2 minutes, supernatants were removed, and the pellets were resuspended in 300 µL of EDS solution. The tubes were then incubated at 65°C for 30 minutes to inactivate nucleases. 150 µL of 8 M ammonium acetate was then added to each sample to precipitate proteins and the tubes were incubated on ice for 30 minutes. After the incubation, the tubes were centrifuged at 20,238 g for 10 minutes at RT and the resulting supernatants were transferred to fresh 1.7 mL microcentrifuge tubes. DNA was then precipitated using 270 µL of isopropanol and pelleted by centrifugation at 13,523 g for 10 minutes at RT. The resulting pellets were washed with 500 µL of pre-chilled 70% ethanol and spun down at 20,238 g for 5 minutes at RT. Ethanol was removed, the pellets were air-dried for 10 minutes and resuspended in 30 µL of 1x TE with 20 µg/mL of RNase A. The genomic DNA samples were stored at 4°C.

### **2.8.2.3. Labelling of Southern blotting DNA probes with $^{32}\text{P}$**

#### Materials

- QIAquick Gel Extraction Kit (Qiagen)
- Prime-it II Random Primer Labelling Kit (Agilent Technologies, 300385)
- [ $\alpha$ - $^{32}\text{P}$ ]dATP 6,000 Ci/mmol (Perkin Elmer, BLU012Z)
- Illustra MicroSpin G-25 columns (GE Healthcare, 27-5325-01)

#### Method

PCR products used as templates to make the radioactively labelled probes for Southern blotting were obtained by using yeast genomic DNA and

a pair of primers corresponding to the region of interest in the genome. The PCR products were purified using QIAquick® Gel extraction Kit according to the manufacturer's guidelines. The *URA3* probe used to detect DNA fragments from the SSA repair locus was amplified with OSM2161 and OSM2162. Primers OSM189 and OSM190 were used to create a probe specific to the *ARO1* reference locus. Prime-it II Random Primer Labelling Kit was then used to generate radioactively labelled probes. 2.5 µL of the purified PCR product diluted to 2.5 ng/µL were mixed with 2 µL of Milli-Q H<sub>2</sub>O and 2.5 µL of random 9-mer oligonucleotides provided in the labelling kit. The DNA was denatured in the PCR machine at 99°C for 5 minutes and then allowed to cool down at RT. 2.5 µL of 5x reaction buffer from the labelling kit containing dGTP, dTTP, dCTP were then added into the mixture along with 0.5 µL of Exo<sup>-</sup> Klenow polymerase (5 U/mL) and 2.5 µL of [ $\alpha$ -<sup>32</sup>P]dATP. The reaction was incubated at 37°C for 1 hour in a PCR machine. After the incubation, 60 µL of Milli-Q H<sub>2</sub>O were added and the probe was purified from unincorporated nucleotides using a MicroSpin G-25 column according to the manufacturer's guidelines.

#### **2.8.2.4. Southern blotting**

##### Materials

- Depurination solution: 0.25 M HCl
- Denaturing solution: 0.5 M NaOH, 1.5 M NaCl
- Neutralizing solution: 1.5 M NaCl, 0.5 M Tris HCl, 1 mM EDTA; pH 7.2
- 20x SSC solution: 3 M NaCl, 0.3 M tri-sodium citrate; pH 7.0
- 20x SSPE solution: 3 M NaCl, 0.2 M NaH<sub>2</sub>PO<sub>4</sub>, 20 mM EDTA; pH 7.4
- 100x Denhardt's solution: 2% (w/v) bovine serum albumin (BSA), 2% (w/v) polyvinylpyrrolidone (PVP), 2% (w/v) Ficoll400
- Hybridization buffer: 6x SSPE, 0.5% (w/v) SDS, 5x Denhardt's solution
- Wash solution: 0.1x SSPE, 0.1% (w/v) SDS
- Positively charged nylon transfer membrane Amersham Hybond™-N<sup>+</sup> (GE Healthcare, RPN303B)

## Method

5 µL of each genomic DNA sample prepared as described in the section 2.8.2.2 was digested with EcoRI and Sall restriction enzymes according to the manufacturer's guidelines. The DNA fragments were then resolved on 0.6% TBE agarose gels using 3.7 V/cm for 7 hours (agarose gel electrophoresis is described in detail in the section 2.6.4). The gels were visualised using Gel Doc XR+ imaging system (BioRad) and the unnecessary parts of the gels as well as the gel below 1 kb size marker band were cut off. The gel was then sequentially incubated in the depurination solution for 30 minutes, the denaturing solution for 30 minutes and finally in the neutralising solution for 40 minutes in a tray placed on a rocker at RT. Tap water was used to rinse the gel after each incubation. The gel was then flipped up-side-down and placed onto 3-piece Whatman paper wick dipped into 20x SSC solution and positioned on a platform inside a tray with 20x SSC. Positively charged nylon membrane cut to the size of the gel was pre-wetted in 20x SSC solution and placed on top of the gel. Three pieces of Whatman paper were also pre-wetted in 20x SSC solution and placed on top of the membrane. A stack of dry paper towels was then positioned on top of the set-up and the gel was left overnight at RT allowing the DNA from the gel to be transferred onto the membrane by capillary forces. Next day, the membrane was air-dried for 30 minutes, and the transferred DNA was crosslinked to the membrane by exposing it to 1,200 J/m<sup>2</sup> of UV light in the Stratalinker 1800 UV crosslinker (Stratagene).

Crosslinked membranes were incubated in 15 mL of pre-warmed hybridization buffer in glass bottles at 60°C for 1 hour with rotation. During the incubation, 5 µL of each labelled probe (described in the section 2.8.2.3) were mixed with Milli-Q H<sub>2</sub>O to the final volume of 100 µl. The probes were denatured in a PCR machine for 5 minutes at 99°C just before they were needed. After the incubation, the hybridisation buffer was discarded and replaced with 7.5 mL of fresh hybridisation buffer. The probes were then added to the bottles, and the membranes were incubated at 60°C overnight with rotation.

Next day, the membranes were rinsed with 30 mL of pre-warmed wash buffer three times and incubated with 30 mL of the wash buffer at 60°C for 40 minutes with rotation. They were rinsed with 30 mL of pre-warmed wash buffer three more times, taken out of the bottles, wrapped into a plastic film and placed into storage phosphor screen cassettes. Membranes were exposed to the screens for a variable amount of time, depending on the age of the radioactively labelled probes. The screens were scanned using Typhoon FLA 7000 IP2 imager (GE Healthcare) and the images were analysed and quantified using ImageQuant TL software (GE Healthcare).

#### **2.8.2.5. Analysis of flap cleavage by qPCR**

##### Materials

- Brilliant II SYBR® Green QPCR Master mix (Agilent, #600828)

##### Method

Quantitative PCR (qPCR) reactions were performed using Brilliant II SYBR® Green QPCR Master mix according to the manufacturer's guidelines using X3000P Real-Time thermocycler (Agilent Technologies). Two sets of qPCR reactions were run for each genomic DNA sample. The first set was performed with the primers OSM2233 and OSM2234, to amplify the sequence across the cleavage site of the non-homologous DNA flap in the SSA system (described in the section 3.2). The second set of the qPCR reactions was performed with primers OSM1006 and OSM1007 which are specific to the reference locus ARO1. The specificity of the primers was verified by analysing the melting curve. The efficiency of the qPCR reactions was determined from the standard curve (genomic DNA from one of the samples collected at the time point -1 h during the time-course described in the section 2.8.2.1 was used as a template). Each sample was run in triplicate for both sets of the reactions. The reaction mixes and the PCR conditions are described below.

### **qPCR mix per reaction**

Genomic DNA (1:50 dilution)	5 µL
2x Brilliant II SYBR Green QPCR master mix	12.5 µl
F primer (1:10)	0.5 µl
R primer (1:10)	0.5 µl
ROX reference dye (1:500 dilution)	0.375 µl
Molecular grade H <sub>2</sub> O	6.18 µl
Total volume	25 µl

### **qPCR conditions**

qPCR stage	Temperature	Time	Number of cycles
Initial denaturation	95°C	10 min	1
Denaturation	95°C	30 sec	35
Annealing	58°C	30 sec	
Extension	72°C	1 min	
Melting curve	95°C	1 min	1
	55°C	30 sec	
	95°C	30 sec	

## **2.9. Analysis of the cell cycle progression in *P<sub>GAL1</sub>-RAD55 srs2Δ rad54Δ rad53-13Myc* cells**

### **2.9.1. Cell synchronisation, *P<sub>GAL1</sub>* induction and sample collection**

#### Materials

- 10 µg/mL α-factor peptide solution in water (WHWLQLKPGQPMY, Peptide Protein Research Ltd.)
- 3 mg/mL nocodazole in DMSO
- 20% (w/v) D-raffinose
- 20% (w/v) D-galactose

## Method

Cells were pre-grown on the YPRAF agar at 30°C overnight and then used to start a 10 mL culture in the YPRAF broth. The culture was grown at 30°C with aeration for approximately 8 hours while being maintained in the log phase. It was then used to start a 100 mL overnight culture in a 500 mL conical flask using the same medium as before. The culture dilutions were calculated so that the yeasts would reach the desired OD<sub>600</sub> next morning. The culture was incubated at 30°C with appropriate aeration. When the optical density of around 0.3 OD<sub>600</sub> was reached, samples at the time point -3  $\frac{1}{2}$  h were collected, and the culture was split into two (details on the sample collection and processing can be found below). The α-factor to the final concentration of 0.01 µg/mL (*bar1Δ* cells) was then added to the split cultures to synchronise the cells. After 2.5 hours, samples at the time point -1 h were collected and galactose was added to one of the cultures to the final concentration of 2% (the GAL culture). Same volume of 20% (w/v) raffinose solution was added to the second culture (the RAF culture). After an hour, samples at the time point 0 h were collected and the rest of the cultures were separately transferred into 50 mL conical tubes to wash away the α-factor. Cells were pelleted by centrifugation at 1,741 g for 2 minutes at RT and the pellets were resuspended in 35 mL of YPRAF broth. Cells were then spun down again at 1,741 g for 2 minutes at RT and the pellets were transferred to 500 mL conical flasks with fresh YPRAF (the RAF culture) or YPGAL (the GAL culture) broth (same volume as removed). The cultures were incubated at 30°C with appropriate aeration. 40 minutes after the release, fresh α-factor was added to the final concentration of 0.01 µg/mL to stop cells at the next G1 stage. Samples were collected every 40 minutes for 6 hours after the release. After 6 hours of incubation, cultures were separately transferred into 50 mL conical tubes to wash away the α-factor. Cells were pelleted by centrifugation at 1,741 g for 2 minutes at RT and pellets were resuspended in 35 mL of YPRAF broth. Cells were then spun down again at 1,741 g for 2 minutes at RT and the pellets were transferred into 500 mL conical flasks with fresh YPRAF (the RAF culture) or YPGAL (the GAL culture) broth (same volume as removed). Nocodazole

was added to the final concentration of 15 µg/mL to stop cell division at the next G2/M and cells were incubated at 30°C for 2 hours with aeration. After incubation, samples at the time point 8 h were collected. Samples were collected for western blotting and fluorescence-assisted cell sorting (FACS) analysis at each time point. The sample collection and treatment for western blotting and FACS is described in the sections 2.7.1 and 2.9.2 respectively.

### 2.9.2. FACS

#### Materials

- 100% ethanol
- 50 mM sodium citrate
- 20 mg/mL Ribonuclease A (RNase A) from bovine pancreas (Sigma, R4875)
- SYBR™ Green I Nucleic Acid Gel Stain in DMSO (S7563, Thermo Fisher Scientific)

#### Method

Samples for FACS analysis were prepared by centrifuging about 0.6 OD<sub>600</sub> units of cells at 2,348 g for 2 minutes at RT and resuspending them in 1 mL of 100% ethanol. Cells were fixed in ethanol at 4°C overnight. Next day, cells were pelleted at 20,238 g for 2 minutes at RT and washed with 1 mL of 50 mM sodium citrate. The washed cells were resuspended in 1 mL of fresh 50 mM sodium citrate and vortexed at maximum speed for 30 seconds. Cells were then pelleted by centrifugation at 20,238 g for 2 minutes at RT, washed with 1 mL of 50 mM sodium citrate again and finally resuspended in 1 mL of the same solution. 25 µL of 20 mg/mL RNase A were added into each tube and cells were incubated at 37°C overnight on a nutator. Next day, cells were collected by centrifugation at 20,238 g for 2 minutes at RT, washed twice with 1 mL of 50 mM sodium citrate and resuspended in 250 µL of the same solution.

Another 250 µL of 50 mM sodium citrate containing 2 µM of SYBR™ Green dye were added to each sample. Tubes were covered with foil and incubated at RT for 1 hour on a nutator. After the incubation, cells were sonicated using Bioruptor Plus sonicator (Diagenode) for 10 cycles (30 seconds ON / 30 seconds OFF) on the LOW power setting. The samples were analysed using the Attune™ NxT Flow Cytometer (Thermo Fisher Scientific) and the FlowJo software.

## **2.10. Detection of persistent Rad51 chromatin binding in *P<sub>GAL1</sub>-RAD55 srs2Δ rad54Δ* cells**

### **2.10.1. Cell synchronisation, *P<sub>GAL1</sub>* induction and sample collection**

#### Materials

- 10 µg/mL α-factor peptide solution in water (WHWLQLKPGQQPMY, Peptide Protein Research Ltd.)
- 3 mg/mL nocodazole in DMSO
- 20% (w/v) D-raffinose
- 37% formaldehyde solution
- 2.5 M glycine
- PBS: 1.8 mM KH<sub>2</sub>PO<sub>4</sub>, 10 mM Na<sub>2</sub>HPO<sub>4</sub>, pH 7.4, 2.7 mM KCl, 137 mM NaCl
- PBSS: 1.8 mM KH<sub>2</sub>PO<sub>4</sub>, 10 mM Na<sub>2</sub>HPO<sub>4</sub>, pH 7.4, 2.7 mM KCl, 137 mM NaCl, 1.2 M sorbitol

#### Method

Strains were pre-grown on YPRAF agar at 30°C overnight and then used to start 10 mL cultures in the YPRAF broth. The cultures were grown at 30°C with aeration for approximately 8 hours while being maintained in the log phase. They were then used to start 50 mL overnight cultures in 250 mL conical flasks using the same type of broth as before. The culture dilutions were

calculated so that the yeasts would reach the desired OD<sub>600</sub> next morning. The culture was incubated at 30°C with appropriate aeration. When the optical density of around 0.3 OD<sub>600</sub> was reached, α-factor was added to the final concentration of 0.01 µg/mL (*bar1Δ* cells) to synchronise the cells. After 2.5 hours, *P<sub>GAL1</sub>* expression was induced by adding galactose to the final concentration of 2%. Cultures were incubated for another hour and then moved into 50 mL conical tubes to wash away the α-factor. The cells were pelleted by centrifugation at 1,741 g for 2 minutes at RT and pellets were resuspended in 35 mL of the YPGAL broth. Cells were then spun down again at 1,741 g for 2 minutes at RT and the pellets were transferred into 250 mL conical flasks with fresh YPGAL broth (same volume as removed). Nocodazole was added to the final concentration of 15 µg/mL to stop cell division the next G2/M. Cultures were incubated at 30°C with aeration for 2 hours and then diluted to 0.5 OD<sub>600</sub>.

For the fractionation experiments, diluted cells were crosslinked with 1.4% formaldehyde for 10 minutes at 30°C and appropriate shaking. Crosslinking was stopped by adding glycine to the final concentration of 0.25 M and incubating the cultures for 5 minutes. Around 3 and 20 OD<sub>600</sub> units of cells were then collected for the TCA protein precipitation and cell fractionation respectively by centrifuging appropriate volumes of cultures in 50 mL conical tubes at 1,741 g for 2 minutes at RT. Pellets for the cell fractionation were resuspended in 10 mL of Milli-Q H<sub>2</sub>O and transferred to 15 mL conical tubes. The tubes were centrifuged at 1,741 g for 2 minutes at RT, supernatants were discarded, and pellets were frozen at -80°C. Pellets for TCA protein precipitation were resuspended in 1 mL of Milli-Q H<sub>2</sub>O and moved to 1.7 mL microcentrifuge tubes. The tubes were centrifuged at 2,348 g for 2 minutes at RT, supernatants were discarded, and pellets were frozen at -80°C.

## 2.10.2. Cell fractionation

### Materials

- cComplete™, Mini, EDTA-free Protease Inhibitor Cocktail (11836170001, Roche)
- Bead-beating buffer: 20 mM Tris-HCl, pH 7.4, 150 mM NaCl, 1 mM PMSF, 1 cComplete mini tablet per 5 ml of buffer
- Wash buffer: 20 mM Tris-HCl, pH 7.4, 150 mM NaCl, 1 mM PMSF, 1% (w/v) N-Lauroylsarcosine sodium salt, 1 cComplete mini tablet per 5 ml of buffer
- 3x de-crosslinking solution: 1 mM EDTA, 1% (w/v) SDS, 5% (v/v) 2-Mercaptoethanol
- 4x Laemmli buffer: 200 mM Tris-HCl, pH 6.8, 400 mM DTT, 10% (w/v) SDS, 40% (v/v) glycerol, 0.1% (w/v) bromophenol blue
- Glass beads, 0.5 mm diameter (11079105, BioSpec Products)

### Method

Cells prepared as described in the section 2.10.1 were resuspended in 260 µL of the bead-beating buffer. About 260 µL of glass beads were then added and cells were lysed by vortexing (25 cycles: 30 seconds of vortexing, 1 minute of resting on ice). After the bead-beating, samples were separated from the glass beads by introducing a small hole at the bottom of the 15 ml conical tube, placing it into a new 15 ml conical tube, and centrifuging them briefly. Samples were then moved into 1.7 mL microcentrifuge tubes. Membranes were lysed by adding N-Lauroylsarcosine to the final concentration of 1% and incubating the tubes on ice for 10 minutes. Tubes were then centrifuged at 425 g for 2 minutes at 4°C to spin down the debris. The resulting supernatants were transferred into fresh 1.7 mL microcentrifuge tubes and centrifuged at 20,817 g for 15 minutes at 4°C to pellet the crosslinked chromatin. Pellets were resuspended in 1 mL of the wash buffer

and tubes were centrifuged at 20,817 g for 15 minutes at 4°C. Crosslinked chromatin was then resuspended in 100 µL of the wash buffer and sonicated in Bioruptor Plus sonicator (Diagenode) for 10 cycles (30 seconds ON / 30 seconds OFF) on the HIGH power setting. After the sonication, the de-crosslinking solution was added to the final concentration of 1x and the samples were incubated at 99°C for 30 minutes in a PCR machine to de-crosslink the proteins from DNA. After the incubation, 4x Laemmli buffer was added to the final concentration of 1x and the samples were incubated at 99°C for 5 minutes in a PCR machine to denature the proteins. Samples were stored at -80°C.

## **2.11. Statistical analyses**

All statistical analyses in this study were performed using a Student's two-sample one-tailed t-test. If the difference between the standard deviation (SD) values of two averages being compared was less than two-fold – the equal variance t-test was used, otherwise, the unequal variance t-test was employed. P values were presented as follows: ns ( $P > 0.05$ ), \* ( $P \leq 0.05$ ), \*\* ( $P \leq 0.01$ ), \*\*\* ( $P \leq 0.001$ ).

## **Chapter 3. The functional relationship between Srs2 and Rad54 in the regulation of Rad51 during damage-associated DNA synthesis**

### **3.1. Introduction**

Rad51 is one of the most important DNA repair proteins in eukaryotic cells essential for their genome stability (31, 220). The main role of Rad51 is to establish a heteroduplex between the ssDNA originated from the sites of DNA damage, and an intact homologous donor sequence which is to be used for the subsequent steps of repair (31, 220). Although essential for the homology search and the invasion of the donor sequence, Rad51 might interfere with the damage-associated DNA synthesis during later stages of DNA repair (31, 103, 178, 181, 221). As described in the section 1.2.1, DNA synthesis at the repair sites depends on the RFC-mediated PCNA loading on the dsDNA at the dsDNA-ssDNA junction, and this reaction is greatly stimulated by RPA (31, 175, 176, 178, 179, 222-224). Rad51 filament formation around the dsDNA-ssDNA junction not only displaces RPA but might also sterically hinder the loading of PCNA, thereby inhibiting damage-associated DNA synthesis (103, 178).

A genetic system based on SSA has been previously used to demonstrate that a negative Rad51 regulator, Srs2, facilitates DNA synthesis during DSB repair (103). As described in the section 1.1.5.2.7, SSA is a mutagenic DNA repair pathway employed when DSBs are flanked by direct repeats. In brief, after the initial resection of the DNA around a break, the DNA repeats are annealed and non-homologous DNA flaps are cleaved off, leaving two ssDNA gaps which are then filled in by damage-associated DNA synthesis (Figure 3.1A) (31, 103, 225). Unlike other HDR pathways, SSA does not require Rad51 to function. However, Rad51 filaments can form on resected DNA nonetheless and interfere with the repair process. The failure to disassemble these filaments results in the decreased efficiency of repair (103).

Therefore, genetic systems based on SSA are a convenient tool to study negative Rad51 regulators.

It was demonstrated that the efficiency of SSA decreases to about 59% in the absence of Srs2 compared to almost 100% in WT cells (Figure 3.1B) (103). This repair defect can be suppressed by a deletion of *RAD51* suggesting that Srs2 promotes SSA by removing the recombinase. The analysis of DNA flap cleavage during SSA revealed that this or any preceding repair steps are not affected by *SRS2* deletion. Thus, the lack of the helicase most likely leads to problems during DNA synthesis. Together, this suggests that Srs2 facilitates damage-associated DNA synthesis by removing Rad51 from ssDNA.

Although significantly affected, SSA efficiency is still considerably high in *srs2Δ* cells (59%). This signifies the possibility of more proteins being involved in the Rad51 regulation during damage-associated DNA synthesis. One of the best candidates is Rad54 – a Snf2/Swi2 translocase capable of removing Rad51 from dsDNA *in vitro* (199). Rad54 facilitates the invasion of Rad51-ssDNA nucleofilament into a homologous donor sequence during HR (199). *In vitro* evidence suggests that Rad54 also removes Rad51 from the resulting double-stranded heteroduplex DNA (181, 226). This is likely important for the loading of PCNA and the extension of the invading strand by DNA polymerases. Thus, a possible role of Rad54 in damage-associated DNA synthesis and the functional relationship between the translocase and Srs2 helicase are investigated in this chapter.

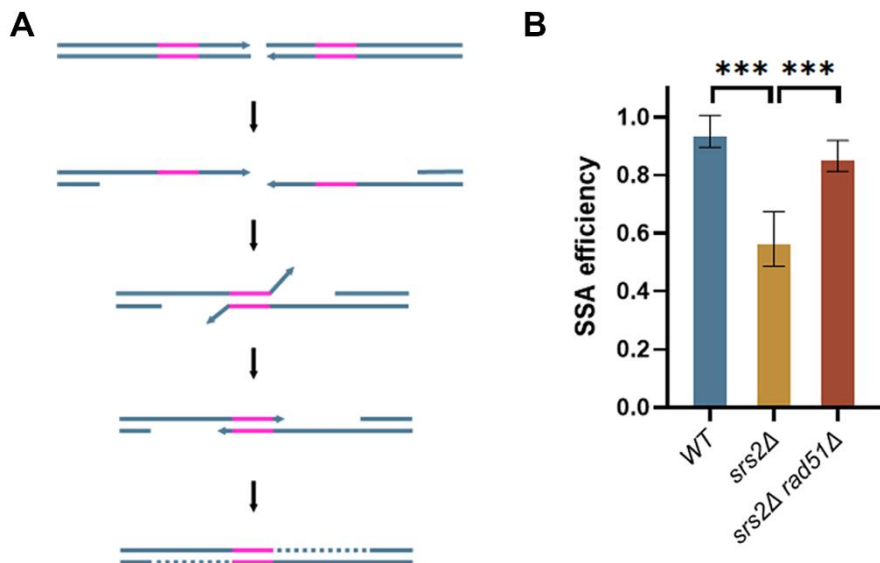


**Figure 3.1. Srs2 is required for SSA**

A. The outline of SSA repair pathway. Solid blue lines represent the two strands of a broken DNA molecule with arrow heads indicating their 3' ends. Solid pink lines represent the homologous sequences used for the DSB repair by SSA. Dashed blue lines show newly synthesised DNA.

B. SSA efficiency values of WT, *srs2* $\Delta$  and *srs2* $\Delta$  *rad51* $\Delta$  cells determined by Vasianovich *et al.* (2017) (103).

### 3.2. The SSA system used to study the damage-associated DNA synthesis

#### The SSA system

The SSA system previously used to investigate Srs2 is also exploited in this study to research a possible role of Rad54 in the promotion of damage-associated DNA synthesis (Figure 3.2A). The genetic system consists of the *ura3-52* and *URA3* alleles flanking a *KAN* marker and a recognition site for the HO endonuclease expressed from a *P<sub>GAL1</sub>* galactose-inducible promoter (103). The DSB induced upon the addition of galactose to the growth media can be repaired by SSA using the homologies provided by *URA3* alleles. The system allows to distinguish between SSA and NHEJ repair events as the *KAN* marker is always lost during the former but rarely during the latter. In addition, most SSA events result in *ura3-52* cells while NHEJ preserves both *URA3* alleles.

Therefore, uracil-dependence is an additional marker which can be used to monitor the repair outcomes genetically. Notice that there is another set of homologies corresponding to the *URA3* sequence on the other side of *Ty1* transposon present in the inactive *ura3-52* allele. If used, a functional *URA3* allele would be preserved after the repair. However, because the transposon is ~6 kb long, the resection reaches this sequence in *ura3::Ty1* much later. Therefore, the first set of homologies highlighted in grey in the Figure 3.2A are used with a much higher frequency and the *URA3 kanΔ* survivors are rare (103).

#### Plating assay to measure the efficiency of SSA

Two different methods can be used to measure the efficiency of SSA. The first one is a plating assay. In brief, strains of interest are pre-grown in the presence of raffinose to derepress the *P<sub>GAL1</sub>* promoter. Cells are then plated on galactose- (break induced) or glucose- (break not induced) containing plates. The number of KAN<sup>S</sup> colonies from galactose-containing plates mostly representing SSA rather than NHEJ repair events and the total number of colonies on glucose-containing plates are then used to calculate the efficiency of SSA.

#### Time-course experiment to monitor SSA at the level of DNA changes

The second method that can be used to estimate the efficiency of SSA consists of a time-course experiment coupled with a Southern blotting analysis (103). This approach allows to monitor the repair at the level of DNA changes. For the time-course experiment, cells are pre-grown in raffinose-containing medium and then synchronised at G1 stage of the cell cycle using α-factor (Figure 3.2B). DSBs are then induced via addition of galactose but the repair by SSA cannot start as it requires DNA resection activity which is greatly reduced in G1 (227). After an hour, α-factor is washed away, and cells are moved into a fresh galactose-containing medium allowing them to progress

into the S phase and start DSB repair by SSA. Samples are then collected every hour for 4 hours. The cell cycle progression is stopped at G2 using nocodazole as the division of cells which have successfully completed the DSB repair might skew the results.

#### Southern blotting analysis of the repair product formation during SSA

The DNA from samples collected throughout the time-course experiment is purified, digested with EcoRI and Sall restriction enzymes and analysed by Southern blotting using an *URA3* hybridisation probe which binds to the homologies highlighted in grey in the Figure 3.2A. Before the addition of galactose, fragments 1 and 2a are detected in the samples (Figure 3.2C). After the induction of HO endonuclease, a DSB is introduced within the sequence of the fragment 2a leading to its disappearance and the formation of the fragment 2. As cells are released into the S phase, they start repairing the break by SSA which results in the disappearance of fragments 1 and 2 as they are being incorporated into the emerging repair product. The repair product is a result of a deletion following SSA, thus, NHEJ cannot contribute to its formation.

The intensities of DNA fragments from the DSB site (*URA3* probe) are normalised using another hybridisation probe that detects a sequence at the *ARS1* locus on chromosome IV which is not involved in the repair (the *URA3* locus and the inserted *KAN*-HO-site are on chromosome V). The ratio between the signals of fragment 2a and fragments detected by *ARS1* probe prior to the break induction corresponds to 100% of cells. Therefore, the relative quantities of the repair product formed throughout the time-course experiment are further normalised to the relative amount of Fragment 2a at the time point -1 h. The resulting numbers represent a fraction of cells which completed the repair within the analysed DNA fragment. For the repair product to be detected in the Southern blot, resected DNA needs to be resynthesised at least up to the closest EcoRI and Sall sites as restriction enzymes do not digest ssDNA. The appearance of the repair product does not necessarily mean that the SSA

repair in cells is completed. However, it was previously observed that the percentage of cells that contain the repair product 4 hours after the release from α-factor arrest is very close to the percentage of cells that repair the DSB by SSA during the plating assay (103). Thus, the efficiency of repair product formation reached by the end of the time-course experiment can be interpreted as the efficiency of SSA.

#### The qPCR analysis of flap cleavage during SSA

SSA consists of multiple steps a defect in any of which could result in the decreased efficiency of DSB repair. It is known that Rad51 has an ability to repress SSA in some situations favouring non-mutagenic repair pathways (225). Therefore, the deletion of enzymes involved in Rad51 removal might lead to a general inhibition of SSA repair pathway instead of affecting only the DNA synthesis step. Furthermore, Rad51 regulators under the investigation might also have other roles in SSA. Thus, their removal might decrease the efficiency of SSA by affecting several stages of the repair. To address these possibilities, the progression of DSB repair by SSA can be investigated in the DNA samples from the time-course experiment described in Figure 3.2B. This is implemented with a qPCR analysis using the primers which amplify the region spanning the cleavage site of the non-homologous DNA flaps. After the cleavage, the DNA sequence can no longer serve as a template for the qPCR reaction (Figure 3.2D). The relative amounts of qPCR signals from the repair site are determined using an unrelated locus *ARO1* as a normaliser. The normalised qPCR signal at time point 0 h corresponds to 100% of cells with uncleaved DNA flaps as the cleavage cannot occur before DNA resection which, in turn, does not start until the release from the G1 arrest. Thus, the rest of the time points are further normalised to the relative qPCR signal at time point 0 h. The resulting numbers are subtracted from 1 and presented as a fraction of cells that have cleaved the non-homologous DNA flaps during SSA. If the cleavage or any preceding steps of SSA are affected by the mutations of

interest, a decrease in the fraction of cells with the cleaved DNA flaps should be observed during the time-course experiment.

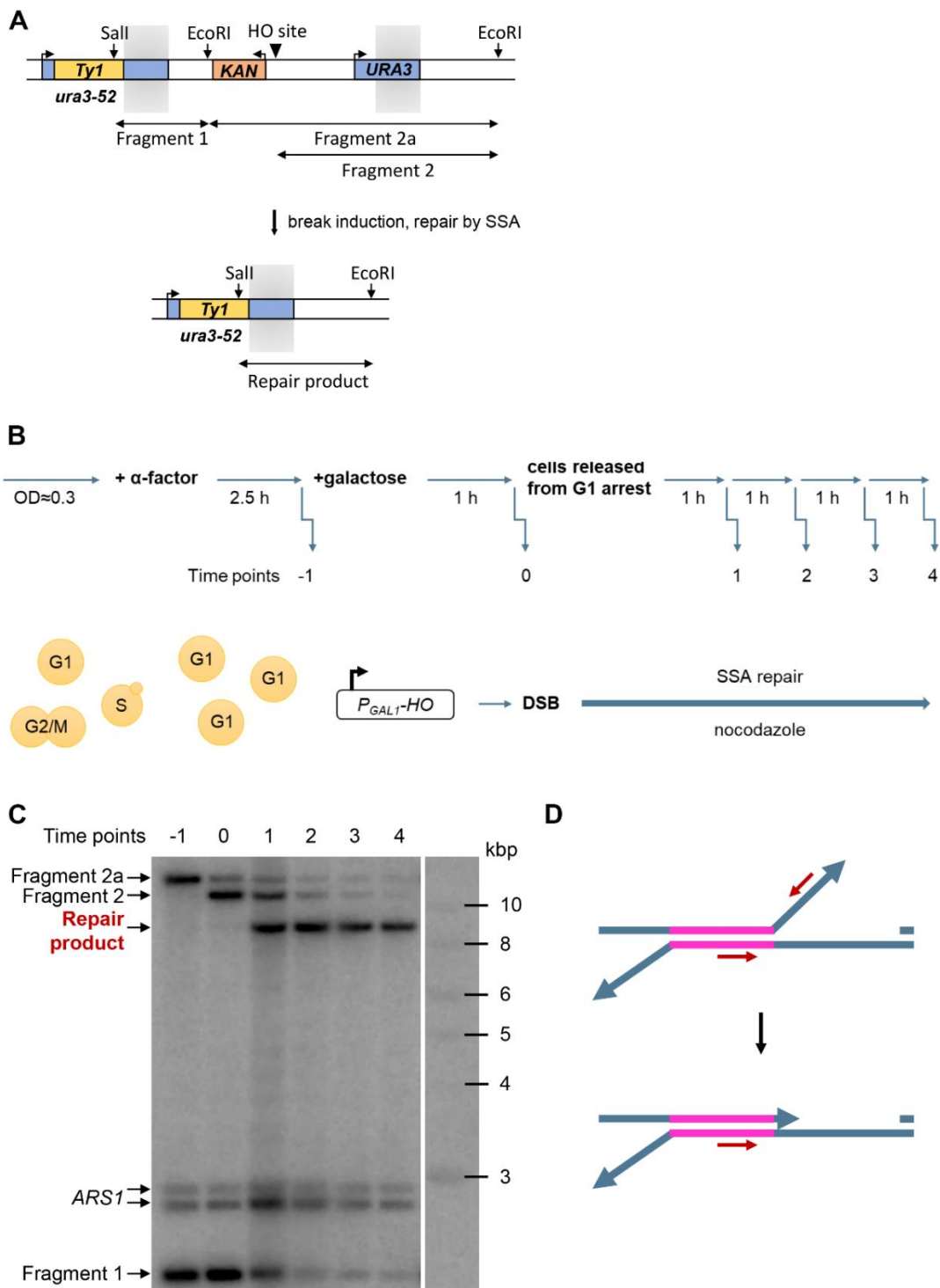


**Figure 3.2. The SSA system for studying DNA repair**

A. A schematic of the SSA system used in this study. The grey shadows mark the homologies most frequently used for SSA. The cleavage sites of HO and restriction

endonucleases as well as the DNA fragments detected by Southern blotting analysis are also indicated. Schematic adapted from Vasianovich *et al.* (2017) (103).

**B.** An outline of the time-course experiment used to determine the SSA efficiency. Time points correspond to the amount of time (in hours) before (negative) and after (positive) the release from α-factor arrest. Yellow circular shapes represent yeast cells at different stages of the cell cycle.

**C.** An exemplary image of a Southern blotting analysis performed on samples collected during the time-course experiment (Figure 3.2B).

**D.** A schematic representation of the annealing sites of the primers used to monitor the cleavage of the DNA flaps in the SSA system used in this work. The schematics on the top and bottom show the DNA structure prior to and after the non-homologous end cleavage respectively. Solid blue lines represent DNA strands in general, while solid pink lines indicate homologous sequences used for the SSA repair. Solid red lines represent primers used for the qPCR analysis. Arrow heads indicate the 3' ends of the DNA molecules.

### 3.3. The lack of Srs2 and/or Rad54 leads to a decreased SSA efficiency in the *P<sub>GAL1</sub>-RAD51* background

Cells lacking Srs2 and Rad54 are not viable unless Rad51 nucleofilament formation is disrupted (204). Thus, to investigate the role of Rad54 in the promotion of damage-associated DNA synthesis, *RAD51* was replaced with a conditional allele, *P<sub>GAL1</sub>-RAD51*, in the strains containing the SSA system (indicated as SSA in the genotype description). This enabled the propagation of *srs2Δ rad54Δ* double mutants as well as the simultaneous induction of the HO endonuclease-mediated DSB and *RAD51* expression during experiments.

The efficiency of SSA in different strains was first measured using a plating assay described in the section 3.2. Consistent with previously published findings (103), the *P<sub>GAL1</sub>-RAD51 srs2Δ* SSA strains were found to have a profound defect in SSA with only 43% of mutants completing the repair compared to 90% of *P<sub>GAL1</sub>-RAD51* SSA cells (Figure 3.3A). A smaller but statistically significant decrease was also observed in *P<sub>GAL1</sub>-RAD51 rad54Δ* SSA strains exhibiting 79% SSA repair efficiency. Unfortunately, *P<sub>GAL1</sub>-RAD51 srs2Δ rad54Δ* SSA cells cannot be examined using this method as they die and thus never form colonies on galactose-containing plates. Therefore, the efficiency of SSA in the strains of interest was also estimated using a time-

course experiment which does not require cell viability after the  $P_{GAL1}$  induction (described in the section 3.2).

A dramatic decrease in the efficiency of SSA (the formation of the repair product) was detected during the time-course experiment in the absence of Srs2 and Rad54 (Figures 3.3B and 3.3C). While 94% of  $P_{GAL1}\text{-RAD51}$  SSA cells managed to form the repair product, this number was decreased to 24% and 42% in  $P_{GAL1}\text{-RAD51 } srs2\Delta$  SSA and  $P_{GAL1}\text{-RAD51 } rad54\Delta$  SSA mutants respectively. Furthermore, when the mutations were combined, SSA efficiency was further reduced to only 8%. Together, this evidence highlights the involvement of Rad54 in SSA and its possible functional overlap with Srs2.

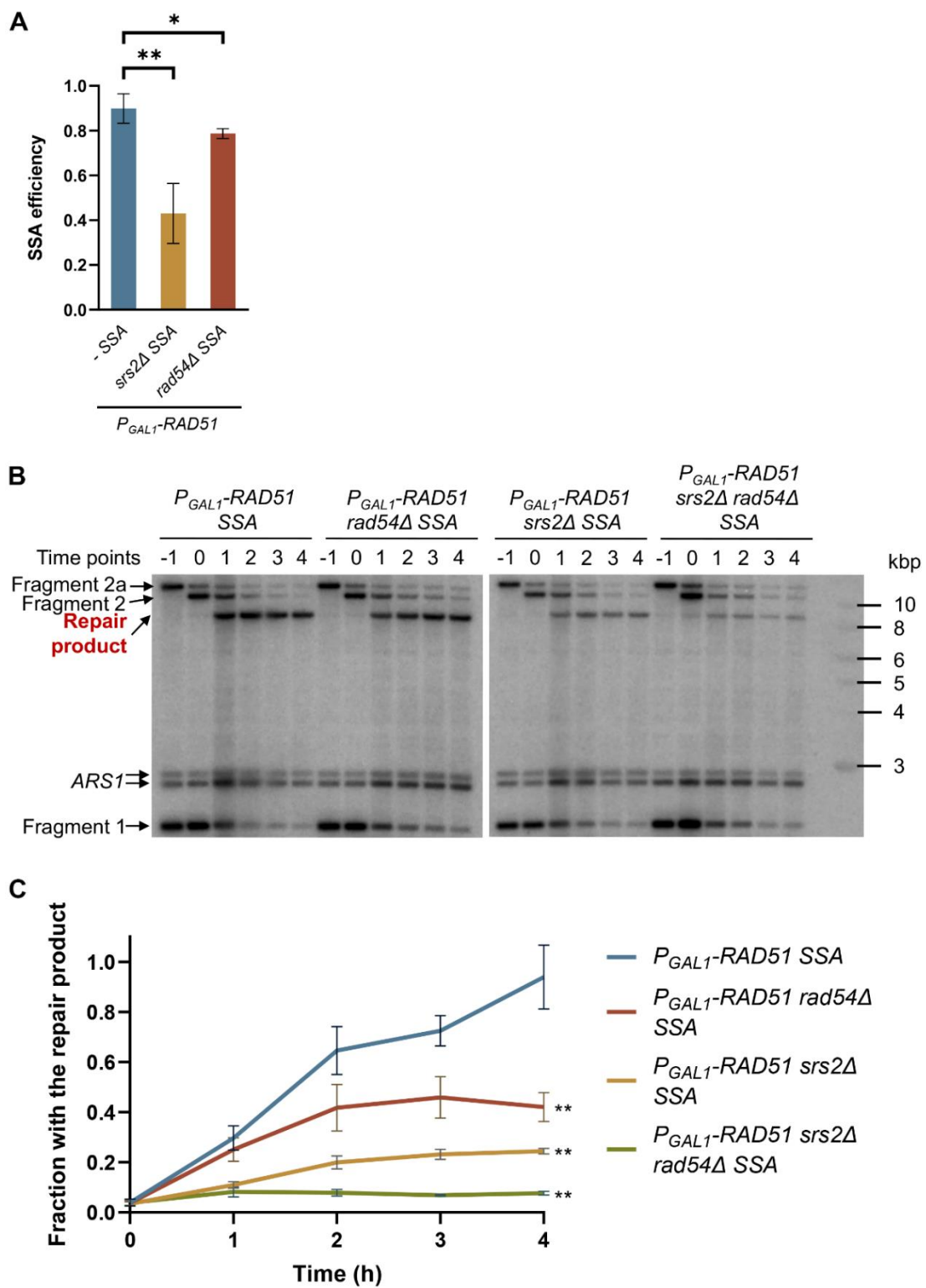


**Figure 3.3. Rad54 is required for SSA**

A. SSA efficiency values of  $P_{GAL1}$ -RAD51 cells lacking Srs2 or Rad54 determined by the plating assay. The average  $\pm$ SD of at least three biological repeats is shown for each genotype. Strains used: NK5858-NK5860 ( $P_{GAL1}$ -RAD51 SSA); NK5861-NK5863 ( $P_{GAL1}$ -RAD51  $srs2\Delta$  SSA); NK5864-NK5866 ( $P_{GAL1}$ -RAD51  $rad54\Delta$  SSA)

**B.** Representative images of a Southern blotting analysis performed on samples collected during the time-course experiments.

**D.** A quantification of the repair product formation in samples from the time-course experiments. The average  $\pm$ SD of at least three biological repeats is shown for each time point of each genotype. Asterisks describe the statistical significance of a difference between the value of the  $P_{GAL1}$ -RAD51 control and the value of each mutant strain at the time point 4 h. Strains used: NK5858-NK5860 ( $P_{GAL1}$ -RAD51 SSA); NK5861-NK5863 ( $P_{GAL1}$ -RAD51  $srs2\Delta$  SSA); NK5864-NK5866 ( $P_{GAL1}$ -RAD51  $rad54\Delta$  SSA); NK5868-NK5870 ( $P_{GAL1}$ -RAD51  $rad54\Delta$   $srs2\Delta$  SSA).

### **3.4. The elimination of Srs2 and/or Rad54 affects the earlier stages of SSA in the $P_{GAL1}$ -RAD51 background**

Although the controlled expression of RAD51 from the galactose-inducible promoter enables the propagation of  $srs2\Delta$   $rad54\Delta$  double mutants, it might be disrupting the balance of the recombination factors. It appears that in the plating assay both  $srs2\Delta$  and  $rad54\Delta$  cells show significantly lower SSA efficiency values when RAD51 is under the control of  $P_{GAL1}$  rather than the endogenous promoter (Figure 3.4A). Furthermore, the SSA values estimated from the time-course experiments are even lower. This is inconsistent with the results from the study which originally described the SSA system exploited here (103). When RAD51 is under its endogenous promoter SSA efficiency values in  $srs2\Delta$  cells match closely regardless which method, the plating assay or the time-course experiment, is used (103).

The lower SSA efficiency observed in the  $P_{GAL1}$ -RAD51 background might be explained by a possible RAD51 overexpression. The increased levels of Rad51 could enhance its inhibitory effect on both, the damage-associated DNA synthesis and the SSA repair pathway in general (104, 228). To analyse this in more detail, the progression of SSA was investigated by quantifying the cleavage of non-homologous DNA flaps in the samples from the time-course experiments as described in the section 3.2.

Indeed, all mutant strains exhibited a statistically significant decrease in the fraction of cells which have processed the DNA flaps four hours after the release from the  $\alpha$ -factor arrest (Figure 3.4B). While 94% of  $P_{GAL1}$ -RAD51 SSA cells had non-homologous DNA flaps cleaved, this number is decreased to

88%, 85% and 78% in  $P_{GAL1}$ -RAD51  $rad54\Delta$  SSA,  $P_{GAL1}$ -RAD51  $srs2\Delta$  SSA and  $P_{GAL1}$ -RAD51  $srs2\Delta$   $rad54\Delta$  SSA mutants respectively. Such observations are inconsistent with the previously published results showing that the progression of SSA repair up to the DNA synthesis step in  $srs2\Delta$  strains is identical to that of the WT cells (103). This suggests that the SSA pathway might be partially repressed in the  $P_{GAL1}$ -RAD51 background when Srs2 and/or Rad54 are missing, possibly because of the Rad51 overproduction.

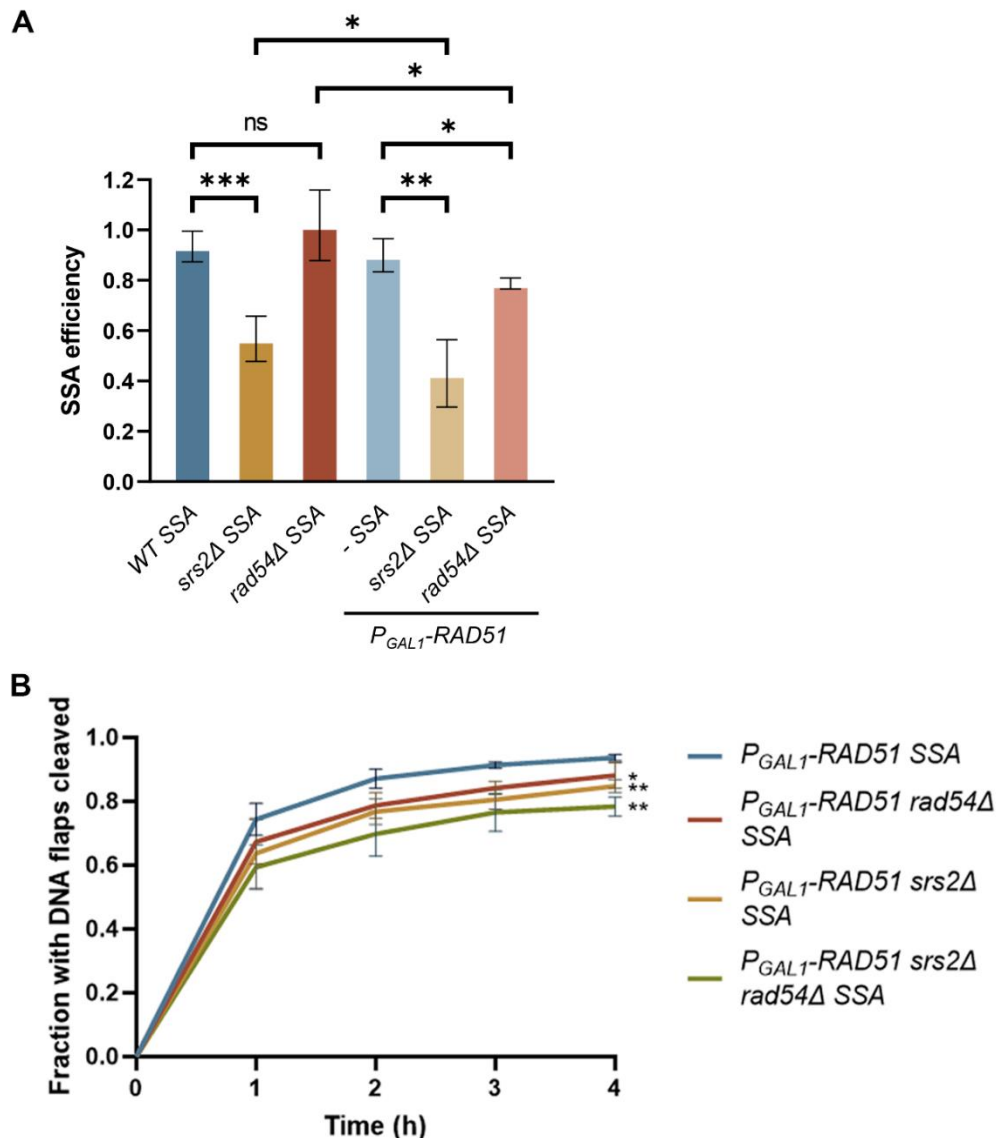


**Figure 3.4. SSA defects resulting from *SRS2* and/or *RAD54* deletions are exacerbated by  $P_{GAL1}$ -RAD51**

**A.** A comparison of SSA efficiency values between the RAD51 and  $P_{GAL1}$ -RAD51 backgrounds. The average  $\pm$ SD of at least three biological repeats is shown for each

genotype. Strains used: NK4691-NK4695 (*WT* SSA); NK4805-NK4808, NK5854-NK5857 (*srs2Δ* SSA); NK6390-NK6392 (*rad54Δ* SSA); NK5858-NK5860 (*P<sub>GAL1</sub>-RAD51* SSA); NK5861-NK5863 (*P<sub>GAL1</sub>-RAD51 srs2Δ* SSA); NK5864-NK5866 (*P<sub>GAL1</sub>-RAD51 rad54Δ* SSA).

**B.** The analysis of DNA flap cleavage using quantitative PCR. Results are presented as a fraction of the cells with non-homologous DNA flaps cleaved over the time-course. Asterisks describe the statistical significance of a difference between the value of *P<sub>GAL1</sub>-RAD51* control and the values of each mutant strain at the time point 4 h. The average  $\pm$ SD of at least three biological repeats is shown for each time point of each genotype. Strains used: NK5858-NK5860 (*P<sub>GAL1</sub>-RAD51* SSA); NK5861-NK5863 (*P<sub>GAL1</sub>-RAD51 srs2Δ* SSA); NK5864-NK5866 (*P<sub>GAL1</sub>-RAD51 rad54Δ* SSA); NK5868-NK5870 (*P<sub>GAL1</sub>-RAD51 rad54Δ srs2Δ* SSA).

### **3.5. *RAD51* expression from *P<sub>GAL1</sub>* leads to excessive protein levels**

To confirm the possible *RAD51* overexpression, a time-course experiment described in the section 3.2 was carried out using the SSA strains with or without *P<sub>GAL1</sub>-RAD51* and the samples for the western blotting analysis were collected (Figure 3.5A). Relative amounts of Rad51 were determined using actin and then normalised to the average value of the WT cells at the time point -1 h. It was observed that when compared to WT strains, Rad51 was overexpressed about four times in the *P<sub>GAL1</sub>-RAD51* background by the time the α-factor was washed away, and the cells could start repairing DSBs (Figure 3.5B). As the time-course progressed, the Rad51 levels increased further and appeared to plateau at the protein level seven times higher than that of the WT yeast. Such overexpression could explain the decreased SSA efficiency in the *P<sub>GAL1</sub>-RAD51* background as the higher levels of Rad51 might exert stronger inhibition of damage-associated DNA synthesis and SSA in general. Furthermore, a progressive increase in the Rad51 level might explain the discrepancies observed between the measuring methods. In the plating assay, the cells can start repairing the induced break by SSA immediately provided they are not in G1, while in the time-course experiment, the α-factor arrest delays the onset of repair by an hour allowing more Rad51 to accumulate. Together, this raises a question of whether *RAD54* deletion would aggravate the SSA defect in *srs2Δ* cells under the normal circumstances, or it is just an artifact stemming from the Rad51 overproduction.

To solve this ambiguity, the feasibility of manipulating Rad51 levels in the *P<sub>GAL1</sub>-RAD51* background was investigated by adjusting the protocol of the time-course experiment. Cells with the DSBs induced were moved into a glucose- rather than galactose- containing medium after the release from α-factor arrest to stop further *RAD51* expression. A shorter induction period of half an hour was also tested. Unfortunately, Rad51 was still greatly overproduced in both situations (Figure 3.5C). Thus, an alternative strategy must be employed to overcome the issues caused by the *RAD51* overexpression.

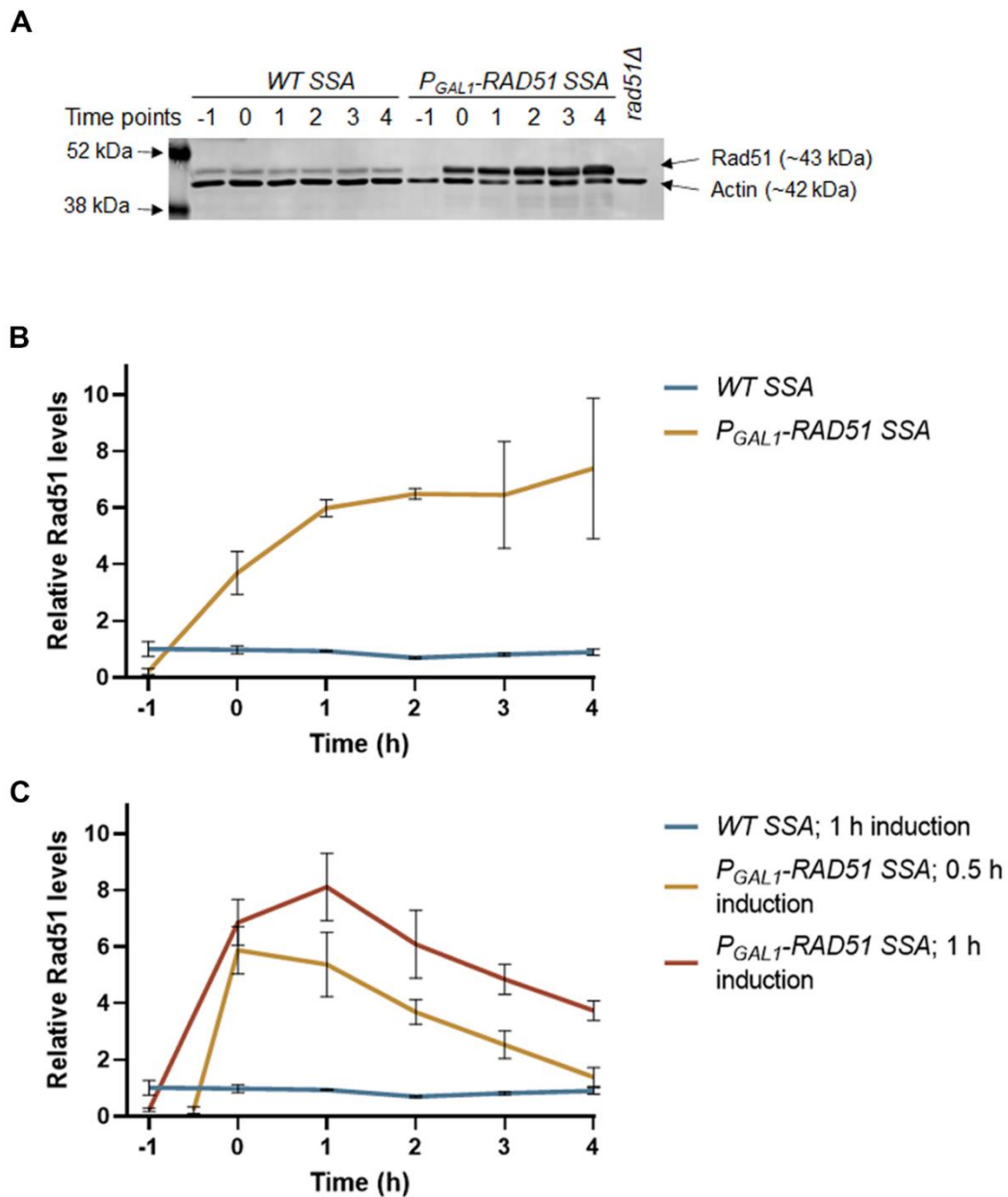


**Figure 3.5. RAD51 overexpression in the  $P_{GAL1}$ -RAD51 background**

**A.** A representative image of the western blotting analysis performed to determine the relative amounts of Rad51 in the  $P_{GAL1}$ -RAD51 background.

**B.** A quantification of Rad51 levels throughout the time-course experiment in cells with  $P_{GAL1}$ -RAD51 and WT RAD51 expression. The average  $\pm$ SD of at least three biological repeats is shown for each time point of each genotype. Strains used: NK4691-NK4693 (WT SSA); NK5858-NK5860 ( $P_{GAL1}$ -RAD51  $srs2\Delta$  SSA).

**C.** A quantification of attempts to modify RAD51 expression from the  $P_{GAL1}$  promoter by releasing cells into a medium containing glucose after the initial induction with galactose. Half an hour and one hour induction times were tested. The average  $\pm$ SD of at least three biological repeats is shown for each time point of each genotype. Strains used: NK4691-NK4693 (WT SSA); NK5858-NK5860 ( $P_{GAL1}$ -RAD51  $srs2\Delta$  SSA).

### **3.6. In the *P<sub>GAL1</sub>-RAD55* background, the deletion of *RAD54* decreases the efficiency of SSA only when combined with *srs2Δ***

The synthetic lethality of *srs2Δ* and *rad54Δ* mutations can be suppressed by the removal of Rad51 or its mediators (204). These include the Rad51 paralogs Rad55 and Rad57 which function as an obligate heterodimer required for the formation of stable Rad51 nucleofilaments (65, 69, 70). It was demonstrated that the absolute majority of cellular Rad55 and Rad57 exist as a complex in *S. cerevisiae* (68). Hence, presumably even if one of the components is overexpressed, the total amount of the functional Rad55-Rad57 unit should remain the same or change very slightly and thus not affect the balance of the DNA repair factors dramatically.

Consistent with published results (204), *P<sub>GAL1</sub>-RAD55* modification enabled a conditional lethality of the *srs2Δ rad54Δ* strains which can be induced using galactose-containing media (Figure 3.6A). Thus, the *P<sub>GAL1</sub>-RAD55* allele was introduced into the strains of interest containing the SSA system. The SSA efficiency values of *P<sub>GAL1</sub>-RAD55* cells determined using a plating assay described in the section 3.2 have closely resembled the pattern observed in cells with the WT *RAD55* expression (Figure 3.6B). While the lack of Srs2 led to a significant SSA defect in the *P<sub>GAL1</sub>-RAD55* background, *RAD54* deletion did not have an effect. This contrasts with the *P<sub>GAL1</sub>-RAD51* background where the removal of Rad54 results in a decreased repair efficiency. Thus, it appears that unlike that of *RAD51*, *RAD55* expression from a galactose-inducible promoter does not exacerbate the effect of *SRS2* and *RAD54* deletions. It is important to note that *P<sub>GAL1</sub>-RAD55 srs2Δ* strains had a slightly higher SSA efficiency than *srs2Δ* cells. This suggests that *RAD55* expression from the galactose-inducible promoter might be interfering with the formation of the Rad51 nucleofilaments. However, this effect seems to be very mild and does not suppress the *srs2Δ* and *rad54Δ* synthetic lethality (Figure 3.6A).

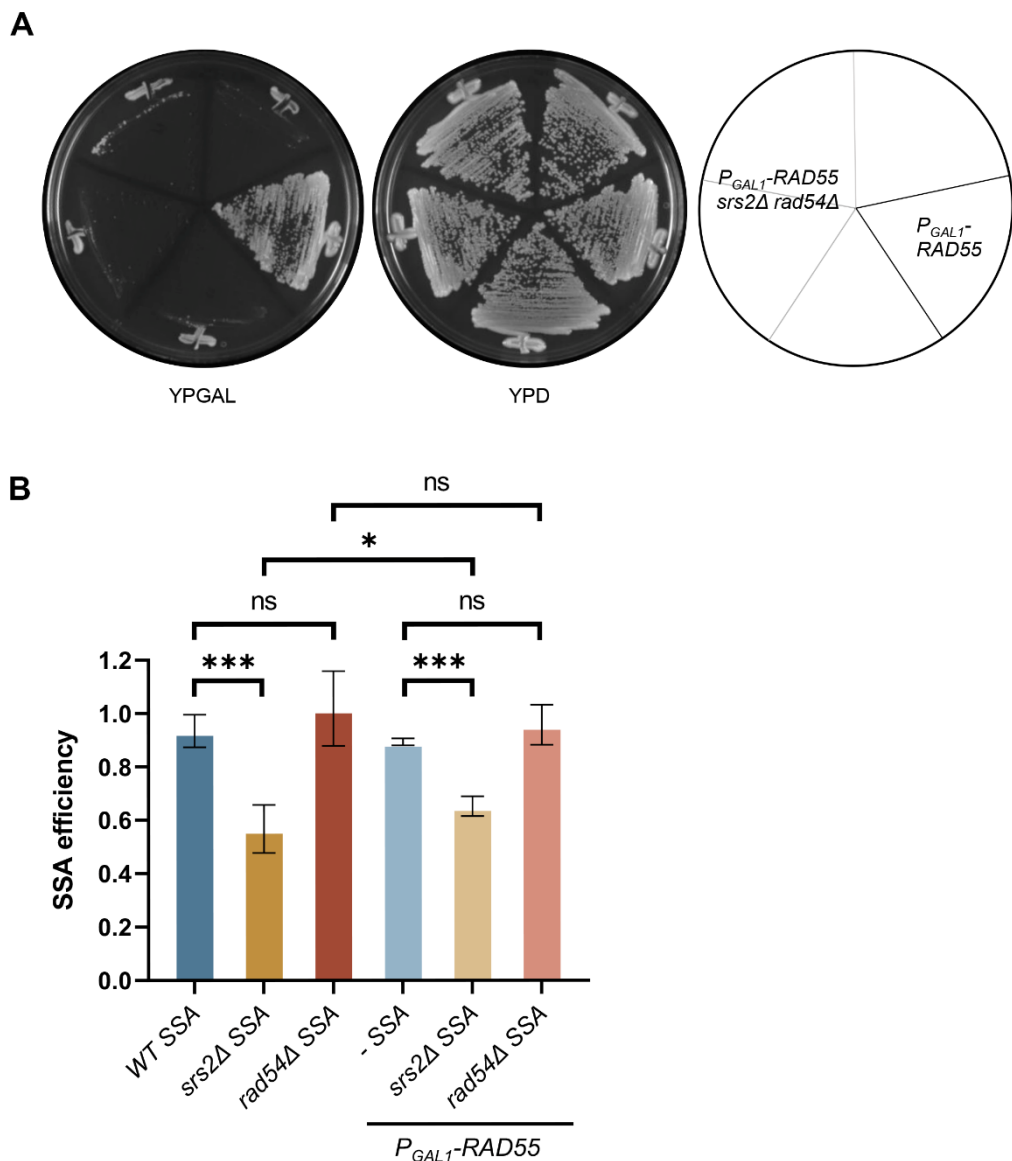


**Figure 3.6.**  $P_{GAL1}$ -RAD55 does not exacerbate the SSA defects in  $srs2\Delta$  and  $rad54\Delta$  cells

**A.**  $P_{GAL1}$ -RAD55 modification enables the propagation of  $srs2\Delta$   $rad54\Delta$  cells, as well as a controlled induction of the lethality. In YPD,  $P_{GAL1}$ -RAD55  $srs2\Delta$   $rad54\Delta$  mutants can grow as  $P_{GAL1}$  is repressed and the cells cannot form stable Rad51 nucleofilaments. In the presence of galactose, RAD55 is expressed leading to the cell death due to the synthetic lethality of  $srs2\Delta$  and  $rad54\Delta$  mutations.

**B.** A comparison of SSA efficiency between the  $P_{GAL1}$ -RAD55 background and the strains with WT RAD55 expression. The average  $\pm$ SD of at least three biological repeats is shown for each genotype. Strains used: NK4691-NK4695 (WT SSA); NK4805-NK4808, NK5854-NK5857 ( $srs2\Delta$  SSA); NK6390-NK6392 ( $rad54\Delta$  SSA); NK6724-NK6726 ( $P_{GAL1}$ -RAD55 SSA); NK7291-NK7293, NK7424-NK7428 ( $P_{GAL1}$ -RAD55  $srs2\Delta$  SSA); NK7188-NK7190 ( $P_{GAL1}$ -RAD55  $rad54\Delta$  SSA).

The SSA efficiency in the strains with the  $P_{GAL1}$ -RAD55 background was then investigated using a time-course experiment as described in the section 3.2. While virtually all of  $P_{GAL1}$ -RAD55 SSA and  $P_{GAL1}$ -RAD55  $rad54\Delta$  SSA cells appeared to form the repair product four hours after the release from the α-factor arrest, only 62% of  $P_{GAL1}$ -RAD55  $srs2\Delta$  SSA mutants managed to do the same (Figures 3.7A and 3.7B). These results are consistent with the SSA efficiency values established in the plating experiments reinforcing their reliability. Importantly, when the  $srs2\Delta$  and  $rad54\Delta$  mutations were combined in the  $P_{GAL1}$ -RAD55 background, the SSA efficiency decreased even further – to 24%.

To test the possibility of Rad55 expression from a galactose-inducible promoter having a negative effect on the SSA pathway at the earlier stages, the cleavage of non-homologous DNA flaps was quantified in the samples from the  $P_{GAL1}$ -RAD55 set of strains collected during the time-course experiment as described in the section 3.2. No significant difference in the progression of the non-homologous DNA flap cleavage was observed between the  $P_{GAL1}$ -RAD55 control and the  $P_{GAL1}$ -RAD55 strains lacking Srs2 and/or Rad54 (Figure 3.7C). Together, this suggests that Rad54 facilitates damage-associated DNA synthesis during SSA along with Srs2.

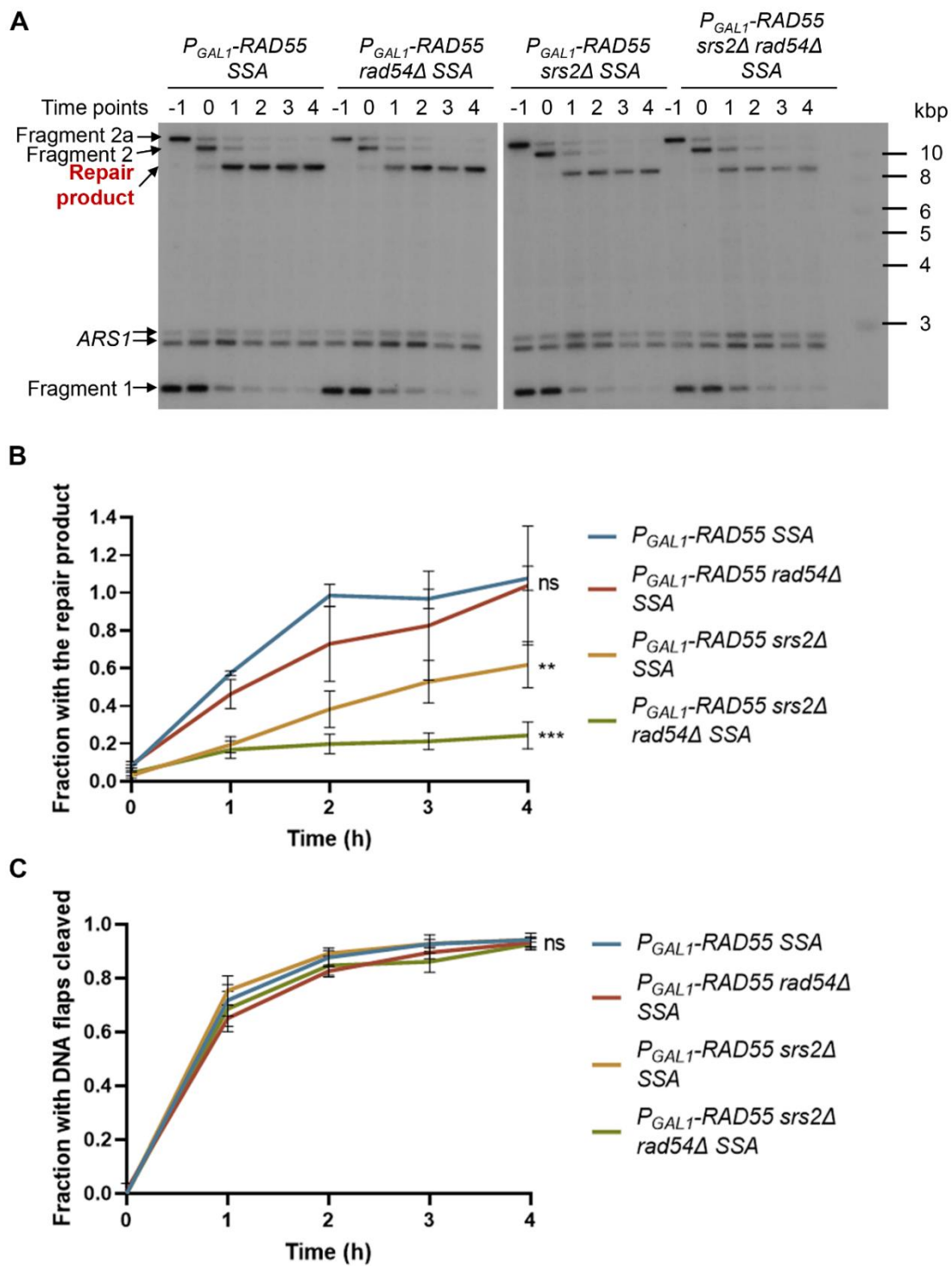


**Figure 3.7. Rad54 facilitates damage-associated DNA synthesis along with Srs2**

**A.** Representative images of a Southern blotting analysis performed on samples from the *P<sub>GAL1</sub>-RAD55* set of strains collected during the time-course experiments.

**B.** A quantification of the repair product formation in the *P<sub>GAL1</sub>-RAD55* background in the samples from the time-course experiments. The average  $\pm$ SD of at least three biological repeats is shown for each time point of each genotype. Asterisks describe the statistical significance of a difference between the value of *P<sub>GAL1</sub>-RAD55* control

and the value of each mutant strain at the time point 4 h. Strains used: NK6724-NK6726 ( $P_{GAL1}$ -RAD51 SSA); NK7291-NK7293 ( $P_{GAL1}$ -RAD51  $srs2\Delta$  SSA); NK7188-NK7190 ( $P_{GAL1}$ -RAD51  $rad54\Delta$  SSA); NK7295-NK7297 ( $P_{GAL1}$ -RAD51  $rad54\Delta$   $srs2\Delta$  SSA).

C. The analysis of DNA flap cleavage in the  $P_{GAL1}$ -RAD55 background using quantitative PCR. Results are presented as a fraction of cells with non-homologous DNA flaps cleaved. Asterisks describe the statistical significance of a difference between the value of  $P_{GAL1}$ -RAD55 control and the values of each mutant strain at the time point 4 h. The average  $\pm$ SD of at least three biological repeats is shown for each time point of each genotype. Strains used: NK6724-NK6726 ( $P_{GAL1}$ -RAD51 SSA); NK7291-NK7293 ( $P_{GAL1}$ -RAD51  $srs2\Delta$  SSA); NK7188-NK7190 ( $P_{GAL1}$ -RAD51  $rad54\Delta$  SSA); NK7295-NK7297 ( $P_{GAL1}$ -RAD51  $rad54\Delta$   $srs2\Delta$  SSA).

### 3.7. Rad54 cannot effectively substitute for the Srs2 function in damage-associated DNA synthesis

It appears that both Srs2 and Rad54 can facilitate damage-associated DNA synthesis (Figure 3.7). However, the relationship between the two proteins in this process is not immediately obvious considering they remove Rad51 from different substrates. Srs2 has been demonstrated to strip Rad51 from ssDNA while Rad54 acts on dsDNA (71, 199). Nonetheless, as established in the previous sections, the  $srs2\Delta$   $rad54\Delta$  double mutants have a more severe SSA defect than the cells missing only Srs2 (Figure 3.7). This raises a question whether Srs2 and Rad54 work in parallel pathways or have redundant activities.

To test the possibility of Rad54 directly substituting for the Srs2 function during damage-associated DNA synthesis, *RAD54* was overexpressed in *srs2\Delta* cells. To achieve this, the endogenous copy of Rad54 was first tagged with 13Myc in the WT cells containing the SSA system. The activity of the tagged Rad54 version was confirmed using a DNA damaging drug sensitivity assay (Figure 3.8A). A plasmid containing an interrupted *rad54* gene under the control of a galactose-inducible promoter was then integrated in the *RAD54* locus (Figure 3.8B). This led to a duplication of the gene while reconstituting the endogenous *RAD54* copy and introducing a  $P_{GAL1}$ -*rad54*-13Myc allele. *SRS2* was then deleted as the presence of a WT *RAD54* gene prevented the lethality. A time-course experiment described in the section 3.2 was performed

to examine Rad54-13Myc overproduction using western blotting. Actin was used to determine the relative protein amounts, and the values were normalised to the average value of Rad54-13Myc in *rad54-13Myc srs2Δ* SSA cells at the time point -1 h (Figure 3.8C). Compared to the expression from the endogenous promoter, the level of Rad54-13Myc was found to be about 45 times higher when expressed from a galactose-inducible promoter (Figure 3.8D).

The ability of Rad54 to substitute for Srs2 during damage-associated DNA synthesis during SSA was then tested using a plating assay as described in the section 3.2. The control *rad54-13Myc srs2Δ* SSA strains were found to have the SSA efficiency of 58% which is essentially the same as that observed in *srs2Δ* SSA cells (Figure 3.8E). A small but statistically significant increase of six percentage points in the SSA efficiency was detected in *srs2Δ* cells overproducing Rad54-13Myc. Such a marginal improvement suggests that Rad54 cannot effectively substitute for the Srs2 function.

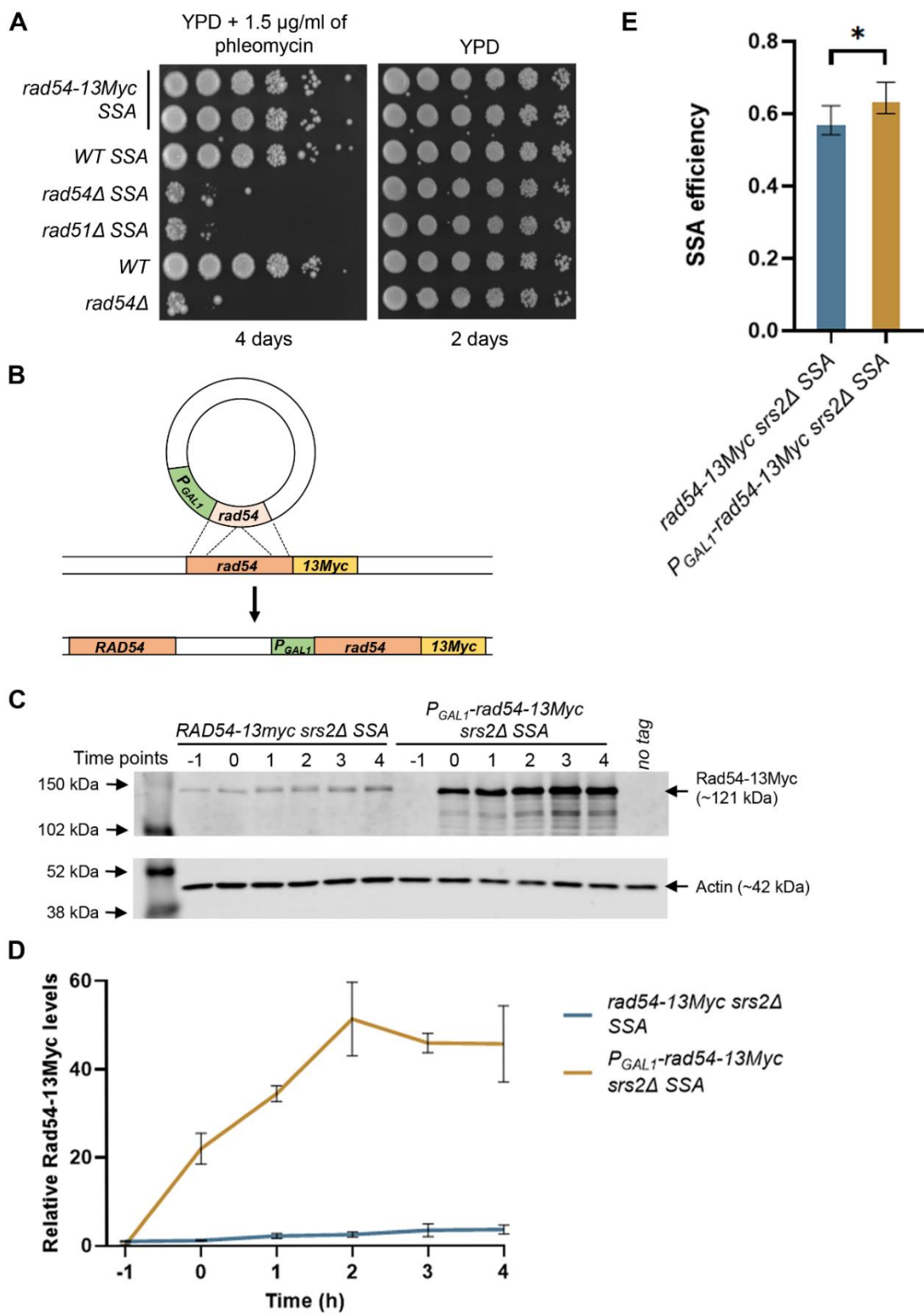


**Figure 3.8. Rad54 and Srs2 functions are mostly complementary rather than redundant**

**A.** A drug sensitivity assay to test the functionality of Rad54-13Myc. Strains used: NK6397, NK6399 (*rad54-13Myc SSA*); NK4691 (*WT SSA*); NK6390 (*rad54Δ SSA*); NK5081 (*rad51Δ SSA*); NK1 (*WT*); NK5895 (*rad54Δ*).

**B.** A schematic describing how Rad54 overexpression was achieved. A plasmid containing a galactose-inducible promoter along with 5' and 3' ends of *RAD54* gene (indicated with dashed black lines) was integrated into the *RAD54* locus. Gap repair of the interrupted *rad54* gene resulted in a duplication recreating the original copy and introducing a *P<sub>GAL1</sub>-rad54-13Myc* allele.

**C.** A representative image of the western blotting analysis performed to determine the relative amounts of Rad54-13Myc in the *P<sub>GAL1</sub>-rad54-13Myc* background. Strains used: NK6591 (*rad54-13Myc srs2Δ*); NK6525 (*P<sub>GAL1</sub>-rad54-13Myc srs2Δ*).

**D.** A quantification of Rad54-13Myc levels throughout the time-course experiment in *rad54-13Myc srs2Δ* and *P<sub>GAL1</sub>-rad54-13Myc srs2Δ* strains. The average ±SD of at least three biological repeats is shown for each time point of each genotype. Strains used: NK6590-NK6592 (*rad54-13Myc srs2Δ*); NK6524-NK6526 (*P<sub>GAL1</sub>-RAD51 srs2Δ SSA*).

**E.** SSA efficiency values of *rad54-13Myc srs2Δ* and *P<sub>GAL1</sub>-rad54-13Myc srs2Δ* strains determined by the plating assay. The average ±SD of at least three biological repeats is shown for each genotype. Strains used: NK6735, NK6736, NK6738 (*rad54-13Myc srs2Δ*); NK6525, NK6526, NK6809-NK6811, NK6813-NK6815 (*P<sub>GAL1</sub>-rad54-13Myc srs2Δ*).

### 3.8. Discussion

Rad51 is one of the key DNA repair proteins (31, 220). However, its binding to DNA can interfere with the recruitment of DNA polymerases and thus the completion of the repair (31, 103, 178, 181, 221). Srs2 has been demonstrated to alleviate this Rad51-dependent inhibition of damage-associated DNA synthesis in *S. cerevisiae* (103). Based on the data presented in this chapter it appears that Rad54 has a similar function.

The deletion of *RAD54* alone does not lead to a defect in SSA. However, its involvement in the process is unmasked by the removal of Srs2. In the *P<sub>GAL1</sub>-RAD55* background, cells lacking both Srs2 and Rad54 exhibit a significantly lower SSA efficiency than the strains with only *SRS2* deleted (Figure 3.7B). The analysis of the DNA flap cleavage revealed that the progression of SSA up to the DNA synthesis step is not affected by the removal of Rad54 (Figure 3.7C). This suggests that Rad54 is not required for the earlier stages of SSA and most likely acts during the DNA synthesis step.

The SSA defect observed in *srs2Δ* cells can be suppressed by *RAD51* deletion signifying the importance of the Srs2-mediated recombinase removal in this process (103). However, the equivalent cannot be tested in the *rad54Δ*

cells as they do not have a SSA defect *per se*. This ambiguity is resolved by the *RAD51* overexpression. It was observed that the SSA defects of *srs2Δ* and *srs2Δ rad54Δ* cells were exacerbated in the *P<sub>GAL1</sub>-RAD51* background (Figure 3.3C). Furthermore, even *rad54Δ* single mutant exhibited a repair defect at higher levels of Rad51. This suggests, that Rad54 indeed performs its function in SSA by acting on Rad51. It is important to note that in strains lacking Srs2 and/or Rad54, *RAD51* overexpression led to a decrease in a fraction of cells that managed to cleave non-homologous DNA flaps in a four-hour period (Figure 3.4B). As mentioned earlier, Rad51 can inhibit Rad52-mediated DNA annealing which precedes flap cleavage during SSA (104, 228). Thus, the observed effect of *RAD51* overexpression is most likely a result of fewer cells completing the strand annealing step due to the inhibition exerted by the higher levels of Rad51. Either way, the decrease in the DNA flap cleavage can only account for a smaller part of the more substantial decrease in the efficiency of SSA observed in *P<sub>GAL1</sub>-RAD51* cells lacking Srs2 and/or Rad54 compared to their *P<sub>GAL1</sub>-RAD55* equivalents. Together, this evidence suggests that Rad54, along with Srs2, facilitates damage-associated DNA synthesis by removing Rad51 from DNA.

The nature of the Srs2 and Rad54 functional relationship in the damage-associated DNA synthesis remains to be elucidated further. *RAD54* overexpression does slightly suppress the SSA defect in *srs2Δ* cells (Figure 3.8E). It is possible that Rad54 catalysed reactions are simply not functioning to their maximum capacity at the WT levels of Rad54. Thus, *RAD54* overexpression could possibly increase the efficiency of these reactions and, in turn, the efficiency of SSA in *srs2Δ* cells. Alternatively, it is possible that Rad54 is directly substituting for the Srs2 function in the removal of Rad51 from ssDNA. This is also in line with a peculiar observation that *RAD54* deletion in the strains overproducing Rad51 leads to a slight defect in the earlier stages of SSA (Figure 3.4B). Such an effect is expected in cells lacking Srs2 as the helicase can remove Rad51 from resected DNA promoting Rad52-mediated ssDNA annealing which can be partially inhibited by the higher levels of Rad51. It is difficult to imagine how Rad54 could do the same without being

able to remove Rad51 from ssDNA. However, it is not clear whether the excessive Rad51 binding to the dsDNA in the vicinity of the resected regions in *rad54Δ* cells overproducing Rad51 could affect the Rad52-mediated annealing during SSA.

Based on the Rad54 overexpression experiment, even if Rad54 can directly substitute for the Srs2 function in the damage-associated DNA synthesis, this ability appears to be very limited (Figure 3.8E). Nonetheless, *RAD54* deletion in *srs2Δ* cells leads to a considerable drop in the SSA efficiency (Figure 3.7B). Together, this suggest that Srs2 and Rad54 functions are mostly complementary rather than redundant.

Rad51 filaments are normally initiated on ssDNA but they are likely to spread to the surrounding dsDNA regions (30, 31, 220). This blocks the access of RFC/PCNA/DNA polymerases to the dsDNA-ssDNA junction and inhibits DNA synthesis (31, 103, 178, 181, 221). It is possible that Srs2 removes Rad51 from ssDNA while Rad54 clears up the neighbouring dsDNA exposing the junction and promoting damage-associated DNA synthesis (Figure 3.9). In the absence of Srs2, Rad54 brings the end of the Rad51 filament to the dsDNA-ssDNA junction. This might promote the stochastic exchange between Rad51 and RPA at the neighbouring ssDNA as Rad51 monomers appear to primarily dissociate from the ends of the filament rather than internal sites (229). Likewise, the Srs2-mediated Rad51 removal from the ssDNA at the junction might promote the dissociation of Rad51 from dsDNA enabling the loading of PCNA and the recruitment of DNA polymerases. This might explain how non-redundant, complementary functions of Srs2 and Rad54 might contribute to the outcome of the same process – damage-associated DNA synthesis.

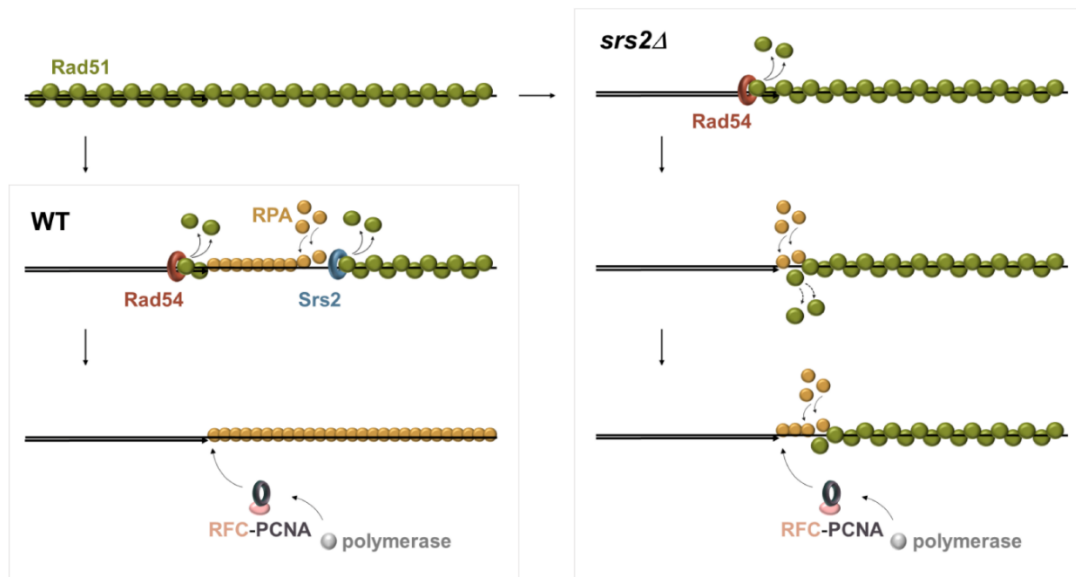


**Figure 3.9. A hypothetical model for the complementary functions of Srs2 and Rad54 in the damage-associated DNA synthesis**

In wild-type cells Srs2 and Rad54 enable the recruitment of DNA polymerases by removing Rad51 from single-stranded and double-stranded DNA respectively. In the absence of Srs2, Rad54 removes Rad51 from dsDNA bringing the end of the Rad51 filament to the dsDNA-ssDNA junction. This might promote the stochastic exchange between Rad51 and RPA on the neighbouring ssDNA and enable the loading of PCNA and the subsequent DNA synthesis. Figure adapted from Andriuskevicius *et al.* (2018) (31).

## **Chapter 4. The molecular aspects of the *srs2Δ* and *rad54Δ* synthetic lethality**

### **4.1. Introduction**

As discussed in the section 1.2.5, the *srs2Δ* and *rad54Δ* synthetic lethality is most likely caused by defective ssDNA gap repair. Without Rad54, Rad51 filaments formed on ssDNA gaps cannot invade a homologous donor and thus the repair is unable to proceed via a recombination-based mechanism. In the concurrent absence of Srs2, these filaments also cannot be disassembled obstructing the use of other repair pathways. This presumably results in an unproductive and persistent Rad51 binding to DNA. Although such assumption is supported by the ability of *rad51Δ* to suppress the *srs2Δ* and *rad54Δ* synthetic lethality (204), it has not been addressed directly and thus is examined in this chapter.

A previously reported observation that the inactivation of 9-1-1 complex can suppress the *srs2Δ* and *rad54Δ* synthetic lethality has led to a suggestion that the persistent DNA damage results in a permanent cell-cycle arrest in *srs2Δ rad54Δ* cells causing their death. Consequentially, the disruption of the 9-1-1 signalling restores cell division, thereby rescuing cell viability (204). However, the deletion of *RAD9*, a gene required for a robust DNA damage checkpoint, did not produce the same results making such an explanation inconsistent with the experimental data (152, 155, 163, 204). In order to understand the molecular events leading to the cell death in the *srs2Δ rad54Δ* genetic background, the cell cycle progression of *P<sub>GAL1</sub>-RAD55 srs2Δ rad54Δ* strains grown in the presence of galactose was investigated and described in this chapter.

#### **4.2. *P<sub>GAL1</sub>-RAD55 srs2Δ rad54Δ* cells grown in galactose accumulate chromatin-bound Rad51**

To test the assumption that *srs2Δ rad54Δ* cells accumulate Rad51 persistently bound to DNA, *P<sub>GAL1</sub>-RAD55* cells lacking Srs2 and/or Rad54 as well as *P<sub>GAL1</sub>-RAD55*, *rad52Δ* and *rad51Δ* controls were analysed in a following manner. Cells pre-grown over night in a raffinose-containing medium were synchronised in G1 using α-factor. Galactose was then added to induce the expression of *RAD55* from the *P<sub>GAL1</sub>* promoter. After an hour of incubation, α-factor was washed away allowing the cells to enter the S phase. The cell cycle progression was blocked again at G2/M by adding nocodazole after the G1 release. Two hours after the release from α-factor arrest, cells were crosslinked with formaldehyde and samples were collected for TCA protein precipitation (total protein) and cell fractionation (chromatin fraction) to test for Rad51 bound to DNA after a single round of replication. The chromatin fraction was prepared by breaking the cells with glass beads, lysing the membranes with an ionic detergent, and collecting the insoluble material (including crosslinked chromatin) by centrifugation. The crosslinking was then reversed, and the Rad51 amounts in the total cell lysates and chromatin fractions were analysed using western blotting (Figure 4.1A). Actin and histone H2B were used as quality control markers (soluble and chromatin-bound proteins respectively) during the cell fractionation. The relative Rad51 levels were determined by normalising Rad51 to the histone H2B. The relative values were then normalised to that of the *P<sub>GAL1</sub>-RAD55* genotype for the total protein and the chromatin fractions separately.

When compared to *P<sub>GAL1</sub>-RAD55*, *P<sub>GAL1</sub>-RAD55 srs2Δ* and *rad52Δ* cells, the *P<sub>GAL1</sub>-RAD55 rad54Δ* and *P<sub>GAL1</sub>-RAD55 srs2Δ rad54Δ* strains appeared to have 17% and 27% more of Rad51 in their total cell lysates respectively (Figure 4.1B). However, these differences were not statistically significant. As expected, both actin and histone H2B were detected in total cell lysates.

While the histone H2B was present in the chromatin fractions of the strains investigated, actin was not detected. This confirmed a successful separation of insoluble (crosslinked chromatin) and soluble (proteins not bound to DNA) fractions. Rad51 signal was observed in the chromatin fractions of all the strains except the *rad51Δ* control (Figure 4.1B). As Rad52 is required for the formation of Rad51 filaments and *rad52Δ* cells cannot form detectable damage induced Rad51 foci, it is most likely that the Rad51 signal present in the chromatin fraction of these cells represents the unspecific crosslinking of Rad51 to DNA and sets the background level of Rad51 detection in the chromatin fraction (65-67). *P<sub>GAL1</sub>-RAD55* and *P<sub>GAL1</sub>-RAD55 srs2Δ* strains were found to have the same amount of Rad51 crosslinked to their chromatin as *RAD52* knockouts (the background level) suggesting that the Rad51 filaments are generally not persistent in these cells. The *P<sub>GAL1</sub>-RAD55 rad54Δ* strains had on average around 20% more of Rad51 in their chromatin fraction than the background level. However, this difference was not statistically significant. In contrast, *P<sub>GAL1</sub>-RAD55 srs2Δ rad54Δ* cells exhibited a statistically significant 2-fold increase in the amount of Rad51 crosslinked to their chromatin. This suggests that the concurrent absence of Srs2 and Rad54 indeed leads to the accumulation of persistent Rad51 nucleofilaments in the nucleus. It is difficult to evaluate the fold increase over the *P<sub>GAL1</sub>-RAD55* strains because they do not show any detectable increase in the chromatin-bound Rad51 over the background level. Therefore, what appears as a 2-fold increase in comparison with the background, might, in fact, represent a much higher increase in the DNA-bound Rad51 relative to the *P<sub>GAL1</sub>-RAD55* control.

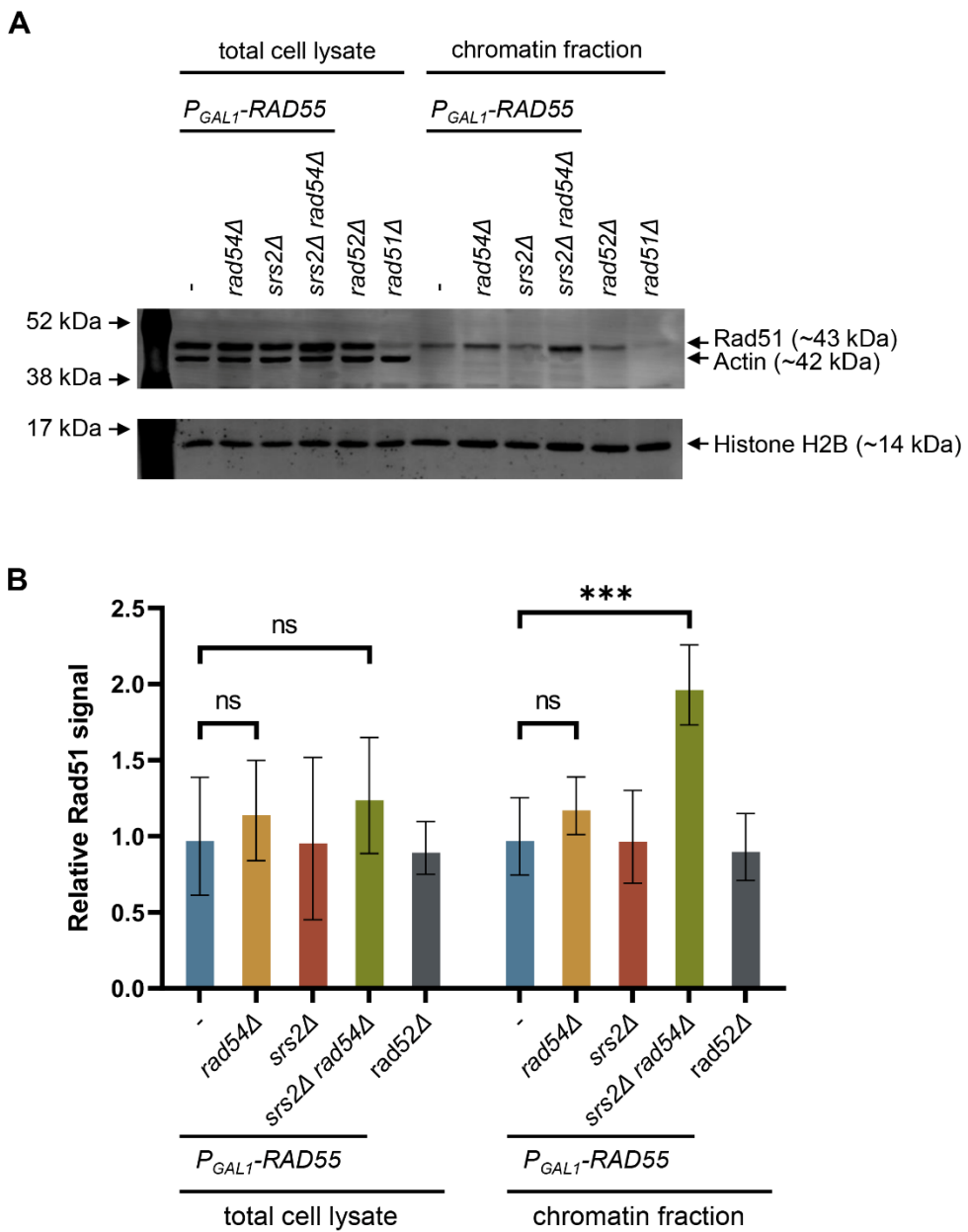


**Figure 4.1. Cells lacking Srs2 and Rad54 accumulate Rad51 nucleofilaments**

**A.** A representative western blotting image of an experiment performed to test for a persistent DNA binding of Rad51 in cells lacking Srs2 and Rad54. Strains used: NK6935 (*P<sub>GAL1</sub>-RAD55*); NK7202 (*P<sub>GAL1</sub>-RAD55 rad54Δ*); NK7206 (*P<sub>GAL1</sub>-RAD55 srs2Δ*); NK7210 (*P<sub>GAL1</sub>-RAD55 srs2Δ rad54Δ*); NK81 (*rad52Δ*); NK78 (*rad51Δ*).

**B.** A data summary plot for the relative Rad51 levels in the total cell lysates and chromatin fractions of galactose-induced *P<sub>GAL1</sub>-RAD55 srs2Δ rad54Δ* cells and the appropriate controls. Histone H2B was used to determine the relative amounts of Rad51. The values were normalised to the average value of *P<sub>GAL1</sub>-RAD55* strains for the total protein and chromatin fractions separately. The average  $\pm$ SD of three biological repeats is shown for each strain with the *P<sub>GAL1</sub>-RAD55* background and three technical repeats for the *rad52Δ* control. Strains used: NK6933-NK6935 (*P<sub>GAL1</sub>-RAD55*); NK7200-NK7202 (*P<sub>GAL1</sub>-RAD55 rad54Δ*); NK7204-NK7206 (*P<sub>GAL1</sub>-RAD55 srs2Δ*); NK7208-NK7210 (*P<sub>GAL1</sub>-RAD55 srs2Δ rad54Δ*); NK81 (*rad52Δ*).

#### **4.3. After the addition of galactose, *P<sub>GAL1</sub>-RAD55 srs2Δ rad54Δ* mutants activate the DNA damage checkpoint in the first cell cycle**

To investigate the cell cycle progression and the dynamics of the DNA damage checkpoint in the mutants lacking both Srs2 and Rad54, the phosphorylation status of the DNA damage signalling kinase Rad53 was used as a readout. To this end, Rad53 was tagged with 13Myc and the functionality of the tagged Rad53 protein was tested. A *rad53-13Myc* modification was introduced into the WT yeast cells which were then examined in a drug sensitivity assay. Strains expressing Rad53-13Myc were found to be as resistant to the DNA damaging agents as the WT control (Figure 4.2A). This suggests that the tagging did not affect the activity of Rad53.

After the functionality of Rad53-13Myc was confirmed, the checkpoint kinase was tagged in *P<sub>GAL1</sub>-RAD55 srs2Δ rad54Δ* cells. The resulting mutants were examined in a time-course experiment (Figure 4.2B). For this, a *P<sub>GAL1</sub>-RAD55 srs2Δ rad54Δ rad53-13Myc* strain was pre-grown overnight in a raffinose-containing medium where *RAD55* was not expressed suppressing the *srs2Δ* and *rad54Δ* synthetic lethality. At the beginning of the experiment, a sample of an asynchronous population was collected, the culture was then split into two and the cells were arrested in G1 using α-factor. After the G1-synchronisation, galactose was added into one of the cultures (designated as GAL) to activate the expression of *RAD55* from the *P<sub>GAL1</sub>* promoter, thereby enabling the formation of Rad51 nucleofilaments and initiating the processes that lead to death in the *srs2Δ rad54Δ* background. The same amount of raffinose was added into the second culture (designated as RAF) which was used as a control. One hour later, α-factor was washed away, and the cells were transferred into fresh media with the appropriate sugar allowing them to progress into the S phase. Samples for FACS and Rad53 analyses were collected every 40 minutes for 6 hours. Approximately 50 minutes after the release from the G1 arrest, fresh α-factor was added to stop cells at the beginning of the next cell cycle. Once the 6-hour incubation was complete, α-factor was washed away, and the cells were transferred into the fresh media (same carbon source) with nocodazole allowing them to progress through the

second cell cycle until the G2/M phase. Samples were collected 2 hours after the second G1 release (see Figure 4.2B for a full graphical description of this experiment). Replication profiles of cells from the samples collected throughout the time-course experiment were analysed using FACS. Rad53-13Myc western blotting was performed to examine the state of the DNA damage checkpoint.

The FACS analysis revealed that the cell synchronisation and the release from the α-factor arrest during the time-course experiment were efficient and timely (Figure 4.2C). Cells grown in both raffinose- and galactose-containing media appeared to progress through the first S phase without any noticeable differences and completed their bulk genome duplication in about 40 minutes. This is in line with the results from similar FACS experiments published in the scientific literature suggesting it takes about 30 – 60 minutes for *S. cerevisiae* to complete one round of DNA replication (230-234). As it could be expected, the majority of cells grown in the raffinose-containing medium reached the next G1 within 2 hours (Figure 4.2C, time point 2 h). In contrast, in the presence of galactose, *P<sub>GAL1</sub>-RAD55 srs2Δ rad54Δ rad53-13Myc* cells appeared to arrest at G2/M for at least additional 40 minutes (Figure 4.2C, time point 2 $\frac{2}{3}$  h). Nonetheless, most of them have also divided and reached the next G1 approximately 3 hours and 20 minutes after the release from the first α-factor arrest (Figure 4.2C, time point 3 $\frac{1}{3}$  h). At this time point a sub-G1 peak was detected in the replication profile of the cells grown in galactose. This indicates a possible loss of genetic information due to the DNA damage. As it could be expected, once the cells were released from the second α-factor block, *P<sub>GAL1</sub>-RAD55 srs2Δ rad54Δ rad53-13Myc* mutants grown in the raffinose-containing medium resumed the cell cycle and reached the following G2/M phase (Figure 4.2C, time point 8 h). In contrast, cells grown in the presence of galactose failed to duplicate their DNA as indicated by the lack of the G2 peak. Instead, the G1 release led to the disappearance of the G1 peak suggesting that entering the S-phase by the cells with the 1N DNA content led to DNA loss, presumably through the nucleolytic degradation.

The western blotting analysis of the Rad53-13Myc phosphorylation has revealed that *P<sub>GAL1</sub>-RAD55 srs2Δ rad54Δ rad53-13Myc* cells grown in galactose activated their DNA damage checkpoint approximately 80 minutes after the release from the first α-factor arrest (Figure 4.2D). In combination with the FACS data (Figure 4.2C, time point  $1\frac{1}{3}$  h), this suggests that the DNA damage in these cells was detected after the bulk genome duplication and led to an arrest in G2 rather than S-phase. The hyper-phosphorylation of Rad53-13Myc was evident in the cells grown in the galactose-containing medium throughout the remainder of the time-course experiment. However, this western blotting analysis was not quantitative, thus, the relative phosphorylation levels at different time points could not be assessed. As expected, *P<sub>GAL1</sub>-RAD55 srs2Δ rad54Δ rad53-13Myc* cells grown in the raffinose-containing medium did not activate the DNA damage checkpoint (Figure 4.2D).

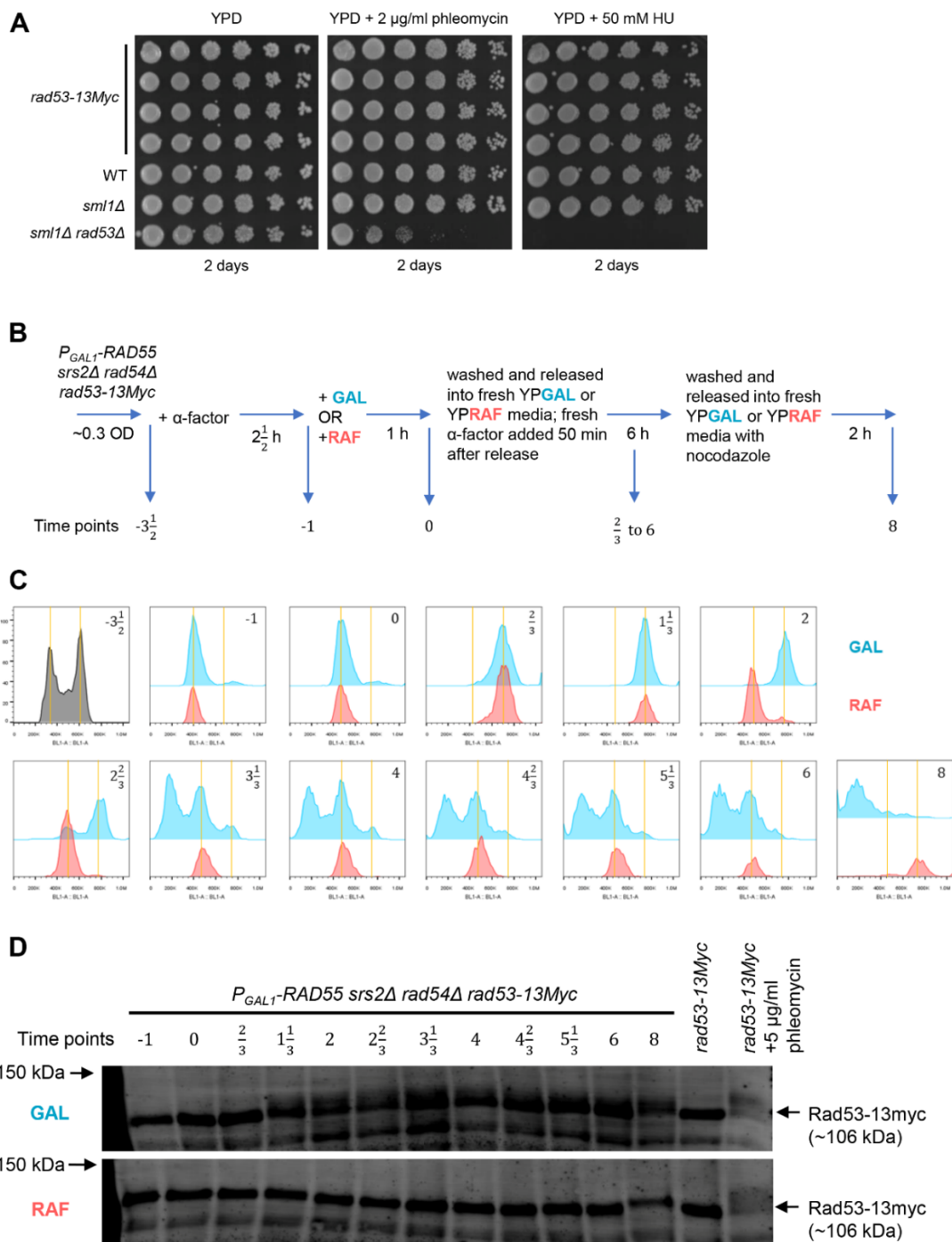


**Figure 4.2.** *P<sub>GAL1</sub>-RAD55 srs2Δ rad54Δ rad53-13Myc* cells grown in galactose initially arrest at G2/M but escape the arrest and lose their DNA upon cell division

**A.** A DNA damage sensitivity plating assay used to test the functionality of Rad53-13Myc. Strains used: NK9282-NK9285 (*rad53-13Myc*); NK1 (WT); NK947 (*sml1Δ*); NK1277 (*sml1Δ rad53Δ*).

**B.** A schematic of the time-course experiments performed to investigate the cell cycle progression and the DNA damage checkpoint dynamics of *P<sub>GAL1</sub>-RAD55 srs2Δ rad54Δ rad53-13Myc* mutants. Time points correspond to the time (in hours) before

(negative) and after (positive) the release from the first α-factor arrest. Strain used: NK9135 ( $P_{GAL1}$ -RAD55  $srs2\Delta$   $rad54\Delta$   $rad53-13Myc$ ).

**C.** Replication profiles of the samples collected during the time-course experiment (Figure 4.2B). Vertical yellow lines specify the positions of G1 and G2 peaks from left to right respectively. Treatments with α-factor and nocodazole lead to the changes in cell morphology which are known to cause the drifting of replication profiles to the right (235, 236). Thus, the positions of the yellow lines had to be slightly adjusted for each time-point individually.

**D.** Western blotting analysis performed to test for the hyper-phosphorylation of Rad53-13Myc characteristic of the DNA damage checkpoint activation. The time points correspond to the ones in the panels B and C.

#### **4.4. Postreplicative repair by HR and TLS is not essential for cell viability**

The time-course experiment described in the section 4.3 has revealed that after the induction of *RAD55* expression, the majority of  $P_{GAL1}$ -RAD55  $srs2\Delta$   $rad54\Delta$  cells arrest at the following G2/M. This suggests that the ssDNA regions bound by the recombination machinery arise in *S. cerevisiae* cells every cell cycle and while they are likely to be rapidly resolved in WT conditions, they cannot be efficiently repaired without Srs2 and Rad54.

As discussed in the section 1.2.5, ssDNA gaps rather than DSBs or compromised replication forks most likely underlie the  $srs2\Delta$  and  $rad54\Delta$  synthetic lethality. Arguably, the repriming of DNA synthesis in response to DNA polymerase blocks is the most probable source of these structures. In the scientific literature, the postreplicative repair of ssDNA gaps is attributed to HR (TS and the salvage pathway) and TLS. However, postreplicative repair is usually studied using the DNA damaging agents which make the phenotypes of postreplicative repair mutants more pronounced (119, 120). As discussed in the section 1.1.6.4, DNA synthesis can also be re-primed in response to non-damage polymerase barriers such as R-loops and secondary DNA structures. The resulting ssDNA gaps could be filled in by not only translesion but also replicative DNA polymerases as soon as the DNA synthesis blocks are resolved.

If the ssDNA structures which appear to arise every cell cycle and become long-lived in *srs2Δ rad54Δ* mutants represent postreplicative gaps formed in response to damaged DNA, *S. cerevisiae* cells deficient in HR and TLS should have a viability problem. Without these repair pathways, the spontaneous DNA damage could not be bypassed, and the ssDNA gaps would persist (119, 120). To test this hypothesis, mutants lacking TLS machinery (*rev1Δ rev3Δ rad30Δ*) were crossed to the *rad51Δ* cells defective in HR. The resulting quadruple heterozygous diploids were sporulated to test the viability of the quadruple haploid mutants deficient in both repair pathways.

After the tetrad dissection, the genotypes of the spores were determined by examining the presence of the genetic markers employed to delete the genes of interest. These were then used to infer the genotypes of the spores that did not form visible colonies in the tetrads where 3 out of the 4 spores formed colonies. It has been observed that *rad51Δ rev1Δ rev3Δ rad30Δ* quadruple mutants are viable (Figure 4.3A). Nonetheless, 2 out of 23 *rad51Δ rev1Δ rev3Δ rad30Δ* spores (8.7%) did not form visible colonies. It is possible that the ssDNA gaps prompted by DNA damage have formed during the first cell cycle of these spores leading to their death due to the absence of HR and TLS repair pathways. However, there were 11 out of 276 spores in total (4%) that did not form visible colonies during the dissection experiment. These included spores with the WT genotype as well as the mutants lacking only one of the TLS polymerases. This raises a possibility that the death of the spores that did not form visible colonies during the experiment including the *rad51Δ rev1Δ rev3Δ rad30Δ* mutants might be independent of the spore genotype and reflect the probability of cell death during meiosis or the dissection process.

It was additionally observed that the genotypes of the spores strongly correlated with the size of the colonies they formed during the experiment (Figure 4.3B). Therefore, the diameters of the colonies formed by spores with relevant genotypes were measured and presented as an average colony size relative to that of the colonies formed by the WT spores (Figure 4.3C). No difference has been observed between the WT cells and the mutants lacking the TLS machinery (*rev1Δ rev3Δ rad30Δ*). In contrast, the absence of *RAD51*

caused a statistically significant decrease in the average colony size. A further decrease was observed when the TLS polymerases were missing along with *RAD51* and this decrease was statistically significant when compared to *rad51Δ* cells. These results suggest that the efficient growth of unchallenged *S. cerevisiae* cells depends on Rad51 while the TLS machinery is dispensable. However, in the absence of the recombinase, the TLS polymerases can partially compensate for the lack of Rad51 activity in the promotion of cell growth.

The colonies formed by spores with the *rad51Δ rev1Δ* and *rad51Δ rev3Δ* but not *rad51Δ rad30Δ* genotypes exhibited the same average sizes as those formed by the *rad51Δ rev1Δ rev3Δ rad30Δ* cells. This is consistent with the previously described observations on the importance of different TLS polymerases. Rev3-Rev7 is considered to be the main TLS polymerase in *S. cerevisiae*, while Rev1 mostly serves as a regulatory platform required for the activities of the Rev3-Rev7 and Rad30. Thus, both Rev3 and Rev1 are necessary for the efficient TLS. In contrast, Rad30 is specialised in bypassing UV-induced damage which is essentially irrelevant in unchallenged yeast cells grown in laboratory conditions (121).

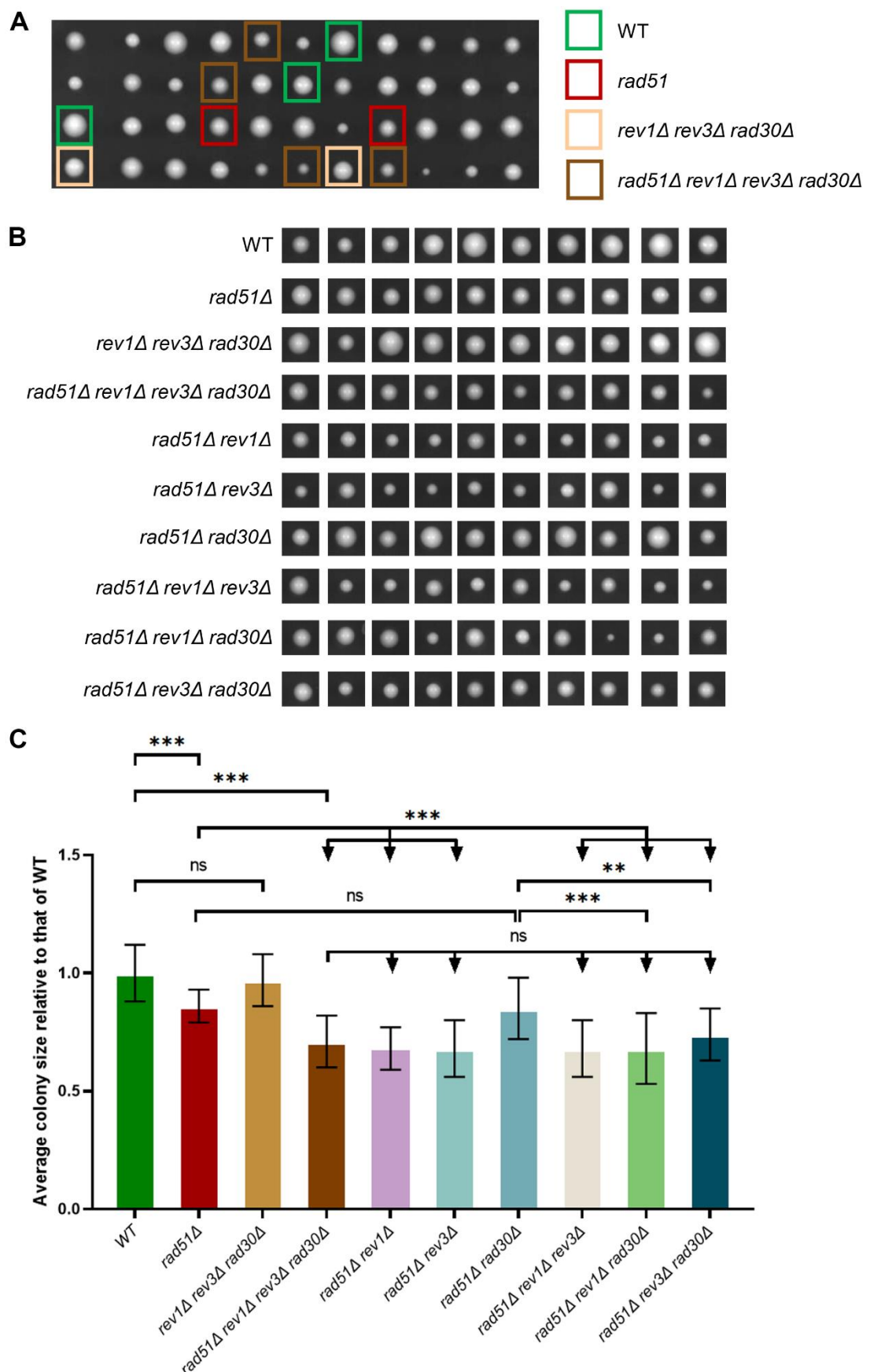


**Figure 4.3. Cells lacking Rad51 and TLS polymerases are viable but have a growth defect**

**A.** Sporulation tetrad dissection experiment performed to test the viability of *rad51Δ rev1Δ rev3Δ rad30Δ* cells. Each set of 4 colonies in a column originate from 4 spores of a single tetrad. 276 spores analysed in total.

**B.** Comparison of the sizes of the colonies formed by the spores with different genotypes. All images are taken 48 h after tetrad dissection.

**C.** Colony size analysis plot. The average ±SD of at least 14 colonies is shown for each genotype.

Strains used for the dissection: NK9985, NK9986, NK9987, NK9988 (*RAD51/rad51Δ REV1/rev1Δ REV3/rev3Δ RAD30/rad30Δ*).

To verify the growth defects of *rad51Δ* and *rad51Δ rev1Δ rev3Δ rad30Δ* cells observed during the dissection experiment, doubling times of the relevant strains were determined using logarithmically growing YPD broth cultures. Indeed, *rad51Δ* mutants have a significantly longer doubling time than the WT cells while the removal of the TLS machinery on its own (*rev1Δ rev3Δ rad30Δ*) does not influence the rate of the cell growth (Figure 4.4A). Consistent with the previous observations (Figure 4.3C), the doubling time of the quadruple *rad51Δ rev1Δ rev3Δ rad30Δ* mutants was found to be significantly longer than that of *rad51Δ* cells.

Mutants lacking HR and/or TLS repair pathways were also examined using FACS analysis. The replication profiles of unsynchronised exponentially growing WT and *rev1Δ rev3Δ rad30Δ* cells closely resembled each other (Figure 4.4B). In contrast, a sub-G1 peak was detected in *rad51Δ rev1Δ rev3Δ rad30Δ* mutants. The presence of cells with less than 1N DNA content can be explained by excessive DNA resection in the absence of successful repair of postreplicative gaps. A less profound sub-G1 peak was also observed in the *rad51Δ* mutants. It is possible that some lesions which prompt the formation of ssDNA gaps cannot be bypassed by TLS polymerases. Alternatively, TLS machinery can fully compensate for the lack of Rad51 in postreplicative gap repair and the sub-G1 peak in the *rad51Δ* mutants appears due to the resection of spontaneous DSBs which cannot be efficiently repaired without Rad51. Either way, the fact that *rad51Δ rev1Δ rev3Δ rad30Δ* cells are viable

suggests that the ssDNA gaps prompted by DNA damage do not arise every cell cycle and the majority of postreplicative gaps formed in unchallenged *S. cerevisiae* cells are formed in response to non-damage replication barriers. However, it cannot be excluded that there is an unidentified alternative pathway, independent of both Rad51 and TLS polymerases, which is involved in the repair of ssDNA gaps prompted by DNA damage.

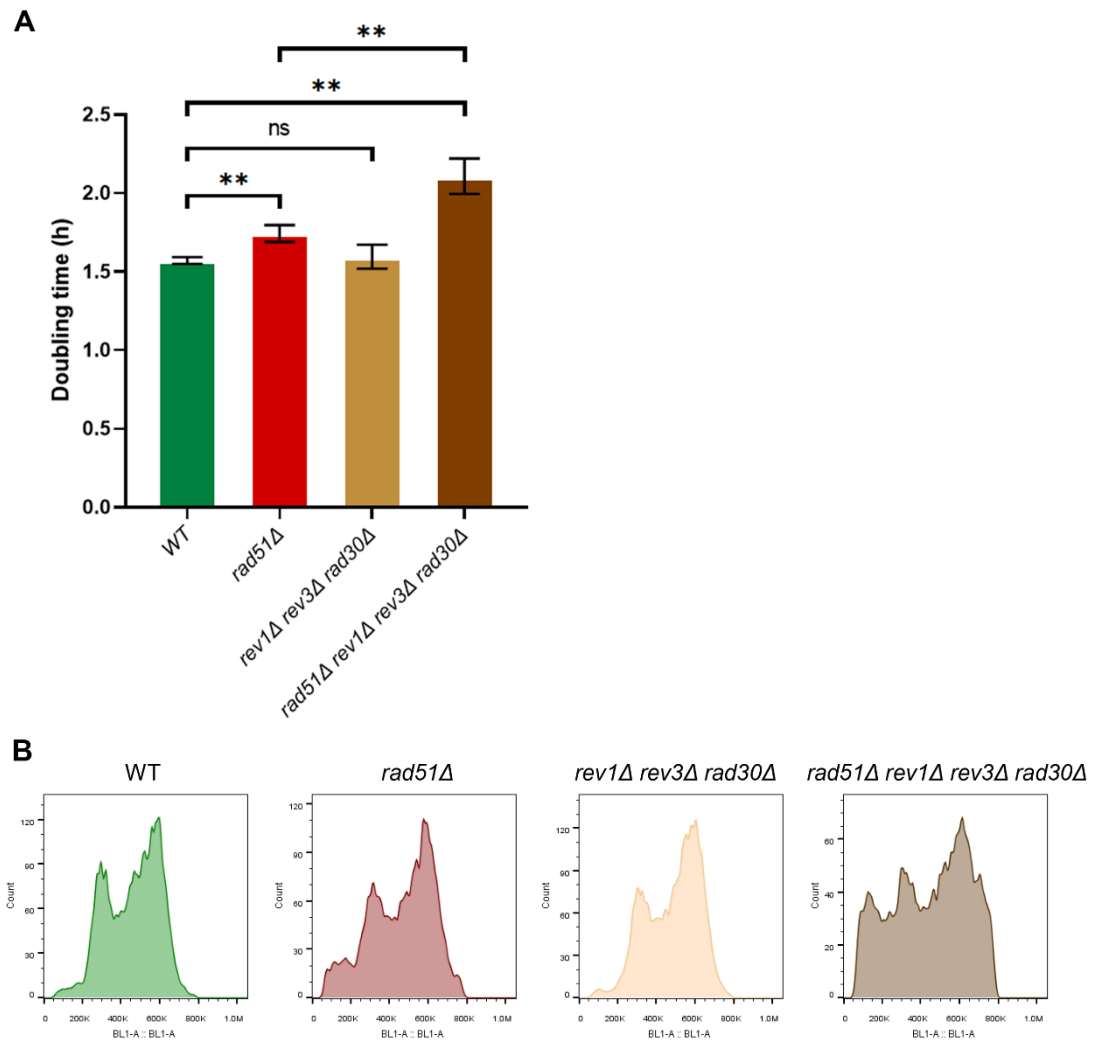


**Figure 4.4. The growth defect of *rad51Δ rev1Δ rev3Δ rad30Δ* mutants is associated with a sub-population of cells experiencing extensive DNA loss**

**A.** Doubling times of WT, *rad51Δ*, *rev1Δ rev3Δ rad30Δ* and *rad51Δ rev1Δ rev3Δ rad30Δ* cells. The average  $\pm$ SD of 3 biological repeats is shown for each genotype.

**B.** Representative FACS replication profiles of unsynchronised, exponentially growing WT, *rad51Δ*, *rev1Δ rev3Δ rad30Δ* and *rad51Δ rev1Δ rev3Δ rad30Δ* cells. Three

biological repeats were analysed for each genotype and produced identical results (not shown).

Strain used: NK1, NK10075, NK10076 (WT); NK10077, NK10078, NK10079 (*rad51Δ*); NK10080, NK10081, NK10082 (*rev1Δ rev3Δ rad30Δ*); NK10083, NK10084, NK10085 (*rad51Δ rev1Δ rev3Δ rad30Δ*).

#### 4.5. Discussion

As predicted by the genetic studies (204), the simultaneous lack of Srs2 and Rad54 results in the accumulation of long-lived Rad51 nucleofilaments. During the fractionation experiment described in the section 4.2, the amount of Rad51 crosslinked to chromatin in *P<sub>GAL1</sub>-RAD55 srs2Δ rad54Δ* cells grown in galactose was found to be considerably higher than the background levels observed in the *P<sub>GAL1</sub>-RAD55*, *P<sub>GAL1</sub>-RAD55 srs2Δ* and *rad52Δ* controls (Figure 4.1B). *P<sub>GAL1</sub>-RAD55 rad54Δ* cells have also exhibited slightly elevated levels of Rad51 in their chromatin fraction but this difference was not statistically significant. Both *P<sub>GAL1</sub>-RAD55 rad54Δ* and *P<sub>GAL1</sub>-RAD55 srs2Δ rad54Δ* mutants were found to have increased amounts of Rad51 in their total cell lysates compared to *P<sub>GAL1</sub>-RAD55*, *P<sub>GAL1</sub>-RAD55 srs2Δ* and *rad52Δ* strains. However, these changes were also not statistically significant. In *P<sub>GAL1</sub>-RAD55 rad54Δ*, the Rad51 levels in the total cell lysate and the chromatin fraction appeared to rise to a very similar extent. Thus, even if the statistical significance in these cases was not detected due to the insufficient sample size, it is possible that the higher amount of Rad51 crosslinked to chromatin in *P<sub>GAL1</sub>-RAD55 rad54Δ* mutants is a result of elevated total levels of the recombinase. In contrast, *P<sub>GAL1</sub>-RAD55 srs2Δ rad54Δ* cells exhibited a disproportionately greater increase in the relative levels of Rad51 crosslinked to their chromatin in comparison to the total cell lysate. This suggests that the higher amount of Rad51 found in the chromatin fraction of the cells lacking both Srs2 and Rad54 after a single round of genome duplication is indeed a result of persistent Rad51 binding to DNA.

The time-course experiment described in the section 4.3 has revealed that the expression of *RAD55* in *P<sub>GAL1</sub>-RAD55 srs2Δ rad54Δ rad53-13Myc*

cells does not appear to affect their progression through the S phase but leads to the activation of the DNA damage checkpoint later on resulting in the G2/M arrest (Figures 4.2C). Rad53 hyperphosphorylation is only detectable after the completion of the bulk genome duplication (Figure 4.2D) supporting the arguments presented in the section 1.2.5 that the absence of Srs2 and Rad54 primarily causes problems at ssDNA gaps rather than replication forks.

During the time-course experiment, the majority of the *P<sub>GAL1</sub>-RAD55 srs2Δ rad54Δ rad53-13Myc* cells overcame the G2/M arrest which lasted somewhere between 40 to 80 minutes and underwent mitosis (Figure 4.2C). Once Rad53 was initially activated after the bulk genome replication in induced mutants, the hyperphosphorylation of the kinase was observed in the samples from all of the remaining time points (Figure 4.2D). Because western blotting represents the Rad53 status at the population rather than single-cell level, it is not clear whether Rad53 remains phosphorylated during the transition to the next cell cycle or is dephosphorylated just before the division and activated again in the following G1, assuming the G1 cells still carry the ssDNA gaps.

A sub-G1 peak was detected in the replication profiles of the *P<sub>GAL1</sub>-RAD55 srs2Δ rad54Δ rad53-13Myc* cells after the first cell division in galactose (Figure 4.2C). This might be caused by the extensive resection of ssDNA gaps in a fraction of population, which would lead to a significant loss of fluorescent signal as the dye used for the FACS analysis is less efficient at binding ssDNA. A subpopulation of these cells that did not lose detectable amounts of genetic material (the G1 peak) still seemed to fail replicating their genomes during the second cell cycle. It is tempting to speculate that during the second S phase, replication forks ran into the ssDNA gaps unresolved since the previous cell cycle and collapsed. The resulting single-ended DSBs would be resected but could not be repaired due to the absence of Rad54 leading to the death of the *srs2Δ rad54Δ* mutants. A similar sub-G1 peak is observed in the replication profiles of exponentially growing *rad51Δ rev1Δ rev3Δ rad30Δ* cells incapable of repairing postreplicative gaps prompted by damaged DNA (Figure 4.4B). This reinforces the hypothesis that the defective repair of ssDNA gaps underlies the synthetic lethality of *srs2Δ* and *rad54Δ*. Together these results

suggest that in the absence of Srs2 and Rad54, ssDNA gaps cannot be adequately repaired, most likely due to the persistent binding of Rad51 which prevents the recruitment of the replication machinery and reconstitution of the DNA double-strandedness throughout the genome.

*S. cerevisiae* can adapt to persistent unrepaired damage and override DNA damage checkpoint resuming the cell division. However, this usually occurs only after 8-15 hours of G2/M arrest and involves dephosphorylation of Rad53 (152, 160). Thus, further research is required to determine how *srs2Δ rad54Δ* cells overcome the cell cycle arrest relatively quickly despite being unable to efficiently repair ssDNA gaps.

During the time-course experiment described in the section 4.3, the absolute majority of *P<sub>GAL1</sub>-RAD55 srs2Δ rad54Δ* cells arrested at the following G2/M after *RAD55* was expressed (Figure 4.2C). This suggests that ssDNA gaps that become long-lived in the absence of Srs2 and Rad54 might be formed during every cell cycle but are likely quickly repaired in WT yeast cells. DNA synthesis repriming is arguably the most likely source of these gaps. A tetrad dissection experiment described in the section 4.4 revealed that *S. cerevisiae* mutants deficient in HR and TLS are viable (Figure 4.3A). These two repair pathways are necessary to bypass DNA lesions making it unlikely that ssDNA gaps formed in response to damaged DNA arise every cell cycle in unchallenged yeast cells (119, 120). Instead, it is possible that *S. cerevisiae* cells might routinely reprime DNA synthesis downstream of non-damage replication barriers leaving ssDNA gaps which can be filled-in postreplicatively by not only HR and TLS but also replicative DNA polymerases, provided the replication impediments were resolved by designated enzymes (e.g., the unwinding of G-quadruplexes by Pif1). In *srs2Δ rad54Δ* cells these gaps cannot be repaired due to the Rad51-mediated inhibition of the damage-associated DNA synthesis, which leads to cell death.

## Chapter 5. Suppressors of the *srs2Δ* and *rad54Δ* synthetic lethality

### 5.1. Introduction

Genetic modifications that can suppress synthetically lethal interactions between a group of genes might provide insights into the mechanisms leading to the synthetic lethality. All known suppressors of the *srs2Δ* and *rad54Δ* synthetic lethality can be categorised into two groups. The first one includes the genes coding for Rad51 and its mediators Rad52, Rad55 and Rad57 (204). The identification of these suppressors has led to the conclusion that Rad51 filament formation becomes a problem when both Srs2 and Rad54 are absent (151, 204). As discussed in the section 1.2.5, defective ssDNA gap repair most likely underlies the lethality. Without Rad54, the Rad51 filaments formed on ssDNA gaps cannot invade a homologous donor and thus the repair cannot proceed via homology-based mechanisms. Srs2 is likely required to disassemble these filaments allowing the gaps to be filled in by DNA polymerases. Thus, in the absence of both proteins, the gap repair is stuck at the presynaptic Rad51 nucleofilament stage.

As demonstrated in chapter 3, Rad54-mediated Rad51 removal can facilitate damage-associated DNA synthesis. Thus, it is likely that Rad54 can participate in the alternative pathway of postreplicative repair and promote ssDNA gap filling by DNA polymerases by destabilising the Rad51 filaments along with Srs2. This makes it unclear whether the *srs2Δ* and *rad54Δ* synthetic lethality is caused by the lack of the Rad54 activity in strand invasion, Rad51 removal or both. Unfortunately, separation of function mutations for Rad54 have not been identified. Thus, alternative strategies are explored here to address this ambiguity.

A second class of *srs2Δ* and *rad54Δ* synthetic lethality suppressors includes the genes coding for the components of the 9-1-1 complex, Rad17, Mec3, and Ddc1, as well as Rad24 required for the loading of the checkpoint

clamp on DNA (204). It has been suggested that the disruption of the DNA damage checkpoint allows *srs2Δ rad54Δ* cells to divide instead of being permanently arrested in response to a persistent DNA damage, thereby suppressing the lethality (204). However, the deletion of *RAD9* gene which is required for a robust cell cycle arrest could not rescue the viability of the *srs2Δ rad54Δ* double mutants (152, 204). Furthermore, as demonstrated in section 4.3, *P<sub>GAL1</sub>-RAD55 srs2Δ rad54Δ* strains grown in galactose do resume cell division relatively quickly after the initial arrest. Together, this evidence argues that the elimination of the 9-1-1 function likely suppresses the *srs2Δ* and *rad54Δ* synthetic lethality by a mechanism other than the disruption of the DNA damage checkpoint. Possible alternative explanations for the suppression are explored in this chapter.

## 5.2. Rad51-II3A cannot effectively inhibit damage-associated DNA synthesis

The Rad54 activities in strand invasion and Rad51 removal are mediated by direct functional interactions between the two proteins and do not involve any additional factors (199, 203, 237). This makes it difficult to disrupt one Rad54 activity without affecting the other. As mentioned earlier, the Rad54 separation of function mutants are not available. Thus, the Rad54-mediated processes must be hijacked from the Rad51 point of view. Rad51 mutant protein Rad51-II3A (R188A, K361A and K371A) might be suitable for this purpose. Rad51-II3A has a defective secondary DNA binding site, which prevents it from binding a homologous donor and therefore specifically affect the strand invasion step. Cells harbouring the *rad51-II3A* allele are as sensitive to the DSB-inducing γ radiation as the *RAD51* knock-out cells suggesting they are deficient in HR (238). Rad51-II3A seems to retain a substantial activity at the primary DNA binding site and is able to form filaments *in vitro* and *in vivo*. However, these filaments appear to be less stable (76, 238).

In the cells harbouring *rad51-II3A* allele, the Rad54 activity in strand invasion can be ignored as it is irrelevant without the Rad51-mediated binding

of homologous donor sequences. Nonetheless, Rad54 should still be able to facilitate damage-associated DNA synthesis by removing Rad51 from DNA. Thus, if the lack of the Rad54 activity in strand invasion but not Rad51 removal underlies the *srs2Δ* and *rad54Δ* synthetic lethality, then *rad51-II3A srs2Δ* cells should be inviable. The same could be expected if both Rad54-mediated processes are essential in the absence of Srs2. However, to be suitable for the dissection of the Rad54 roles, Rad51-II3A must be able to inhibit damage-associated DNA synthesis the same way as its WT counterpart. This ability might be compromised by the reportedly lower stability of the Rad51-II3A filaments (76, 238). To investigate this, *rad51-II3A* was introduced into *P<sub>GAL1</sub>-RAD55 srs2Δ rad54Δ* strains which were then tested for viability. Unfortunately, it appears that *rad51-II3A* mutation suppresses *srs2Δ* and *rad54Δ* synthetic lethality (Figure 5.1A). To possibly compensate for the less stable Rad51-II3A DNA binding, the strains expressing the mutant allele from the *P<sub>GAL1</sub>* promoter were constructed. However, *P<sub>GAL1</sub>-RAD55 srs2Δ rad54Δ P<sub>GAL1</sub>-rad51-II3A* strains were also viable (Figure 5.1B).

To confirm that the observed effect is not due to the complete disruption of *RAD51* expression, the strains were investigated by western blotting (Figure 5.1C). It was observed that the mutant protein is produced to the same extent as its WT equivalent in *rad51-II3A* cells and is overproduced about 4.3 times in *P<sub>GAL1</sub>-rad51-II3A* strains.

Together, these results suggest that Rad51-II3A filaments are not stable enough to inhibit the damage-associated DNA synthesis even at higher protein levels. Consistently, *rad51-II3A* was found to fully suppress the *srs2Δ* defect in the SSA assay (Figure 5.1D). Thus, Rad51-II3A cannot be used to dissect the relative importance of Rad54 functions in the context of *srs2Δ* and *rad54Δ* synthetic lethality.

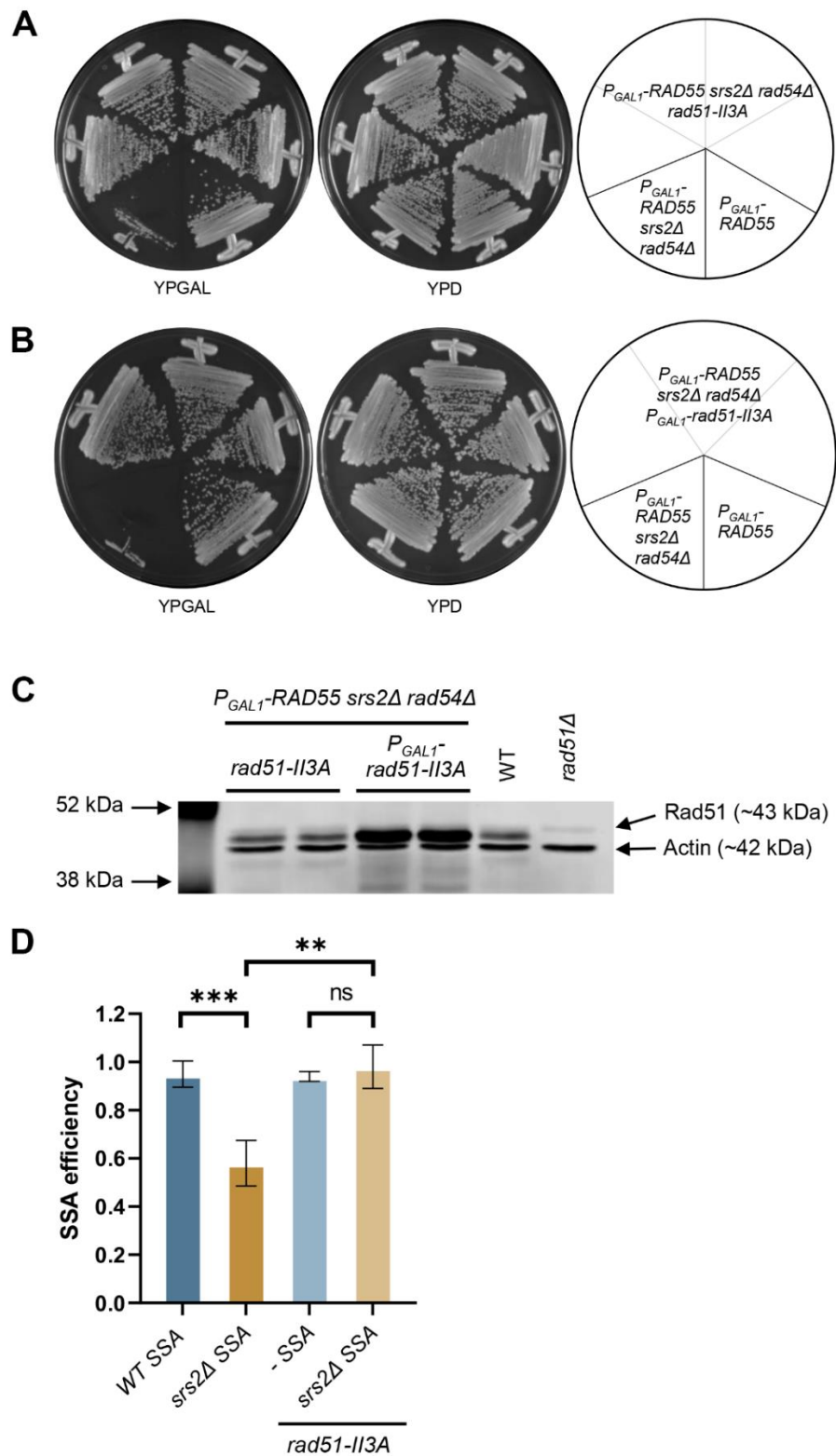


**Figure 5.1. The *rad51-II3A* allele suppresses the *srs2 $\Delta$*  and *rad54 $\Delta$*  synthetic lethality**

**A.** The viability test for  $P_{GAL1}\text{-RAD55 } srs2\Delta \text{ rad54}\Delta \text{ rad51-II3A}$  strains. Strains used: NK8541-NK8543 and one more biological repeat that was not saved ( $P_{GAL1}\text{-RAD51}$

*srs2Δ rad54Δ rad51-II3A*); NK7208 ( $P_{GAL1}$ -RAD51 *srs2Δ rad54Δ*); NK8419 ( $P_{GAL1}$ -RAD51 *srs2Δ rad54Δ rad51Δ*).

**B.** The viability test for  $P_{GAL1}$ -RAD55 *srs2Δ rad54Δ P<sub>GAL1</sub>-rad51-II3A* strains. Strains used: NK8544-NK8546 ( $P_{GAL1}$ -RAD51 *srs2Δ rad54Δ P<sub>GAL1</sub>-rad51-II3A*); NK7208 ( $P_{GAL1}$ -RAD51 *srs2Δ rad54Δ*); NK8419 ( $P_{GAL1}$ -RAD51 *srs2Δ rad54Δ rad51Δ*).

**C.** The *rad51-II3A* expression and overexpression analysed by western blotting. Strains used: NK8541, NK8542 ( $P_{GAL1}$ -RAD51 *srs2Δ rad54Δ rad51-II3A*); NK8544, NK8545 ( $P_{GAL1}$ -RAD51 *srs2Δ rad54Δ P<sub>GAL1</sub>-rad51-II3A*); NK7208 ( $P_{GAL1}$ -RAD51 *srs2Δ rad54Δ*); NK8419 ( $P_{GAL1}$ -RAD51 *srs2Δ rad54Δ rad51Δ*).

**D.** SSA assay with the strains harbouring the *rad51-II3A* allele. The average  $\pm$ SD of at least three biological repeats is shown for each genotype. Strains used: NK4691-NK4695 (*WT* SSA); NK4805-NK4808 (*srs2Δ* SSA); NK9003-NK9006 (*rad51-II3A* SSA); NK9009-NK9011 (*rad51-II3A srs2Δ* SSA).

### **5.3. The lack of the Rad54 function in the damage-associated DNA synthesis significantly contributes to the *srs2Δ* and *rad54Δ* synthetic lethality**

Another feasible approach to differentiate between the Rad54 activities in strand invasion and Rad51 removal is to specifically suppress one of the defects caused by *RAD54* deletion. Rad54 is absolutely necessary for the strand invasion step during HR. Therefore, there is no obvious way to compensate for the lack of its activity in this process. In contrast, the Rad54 function in Rad51 removal could possibly be substituted by a partial destabilisation of Rad51 filaments. Ideally, this would specifically suppress the contribution of *RAD54* deletion towards the damage-associated DNA synthesis defect in *srs2Δ rad54Δ* cells. If the lack of the Rad54 function in Rad51 removal contributes to the death of *srs2Δ rad54Δ* mutants, such partial destabilisation of Rad51 filaments should rescue their viability.

The mutant allele *rad51-K342E* could possibly be used to partially compromise the stability of Rad51 nucleofilaments. Rad51-K342E has a mutation in its primary DNA binding site which greatly disrupts its ability to bind dsDNA while the interaction with ssDNA is less affected. It also has a higher total ATPase activity and can form filaments in the absence of DNA *in vitro*.

(46). This could possibly affect Rad51 nucleofilaments by enhancing the Rad51 turnover or decreasing the number of available monomers.

To test the ability of *rad51-K342E* to suppress the *srs2Δ* and *rad54Δ* synthetic lethality, an integration plasmid carrying the mutation was introduced into *WT SSA*, *rad54Δ SSA* and *srs2Δ SSA* strains replacing the endogenous *RAD51* allele. Control strains were created with an analogous plasmid but without the mutation. *RAD54* was then deleted in *rad51-K342E srs2Δ SSA* strains generating triple mutants which had a slightly slower growth rate than the control strains but were viable nonetheless (Figure 5.2A). This led to a conclusion that *rad51-K342E* can suppress the *srs2Δ* and *rad54Δ* synthetic lethality.

SSA efficiency values were then determined for these strains using a plating assay (Figure 5.2B). It was observed that *rad51-K342E* partially suppresses the SSA defect in *srs2Δ* cells, likely reflecting the less efficient ssDNA binding of the mutant Rad51 protein. As described in chapter 3, the elimination of Rad54 significantly decreases the efficiency of damage-associated DNA synthesis in cells already lacking Srs2. However, it was observed that the *srs2Δ rad54Δ SSA* strains carrying the *rad51-K342E* mutation exhibited the SSA efficiency (55%) statistically indistinguishable from that of *srs2Δ SSA* cells (57%). Thus, *rad51-K342E* effectively negates the contribution of *RAD54* deletion towards the damage-associated DNA synthesis defect in *srs2Δ rad54Δ* cells. As this appears to be enough to suppress the synthetic lethality, it can be extrapolated that the Rad54-mediated facilitation of the damage-associated DNA synthesis would be sufficient to support cell viability in the absence of Srs2. Thus, the lack of the Rad54 function in Rad51 removal significantly contributes to the *srs2Δ* and *rad54Δ* synthetic lethality.

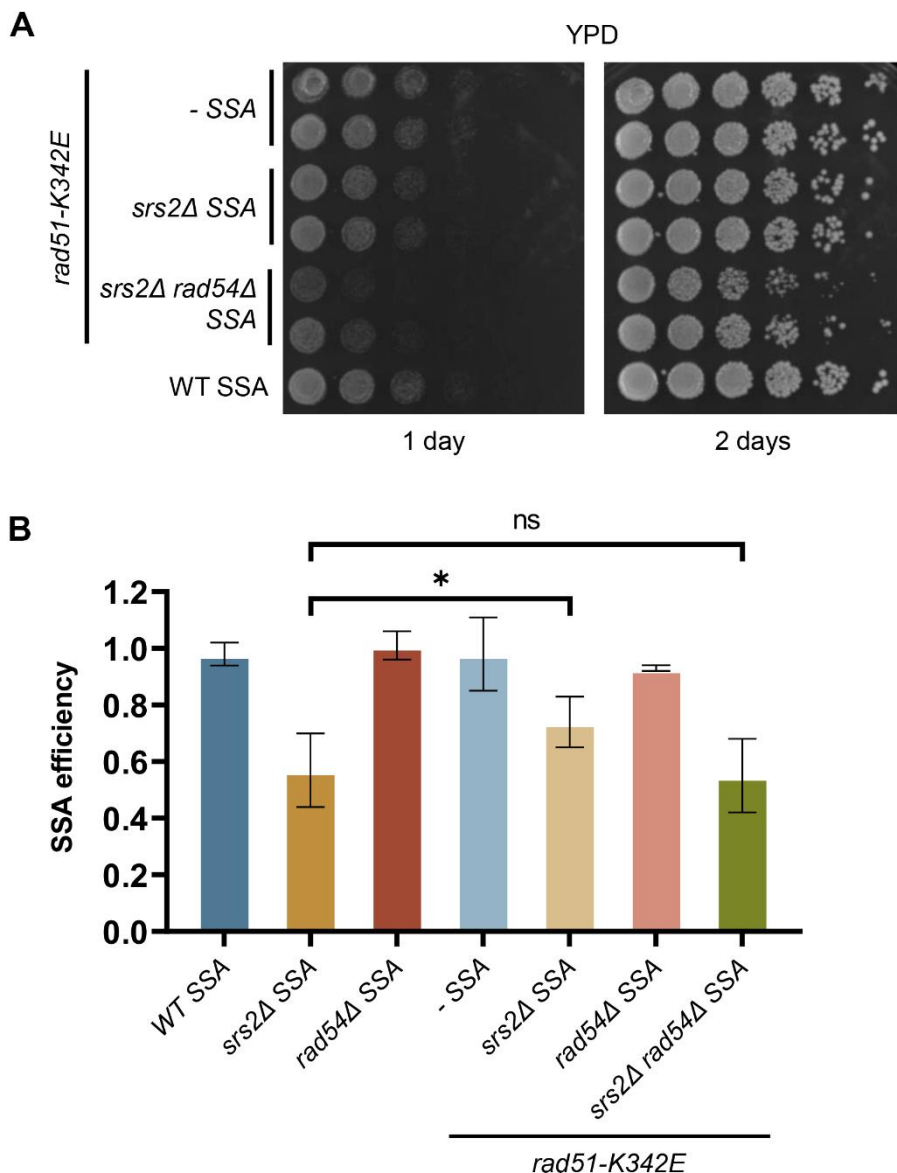


**Figure 5.2. The mutant *rad51-K342E* allele restores the viability of the *srs2Δ rad54Δ* cells and partially suppresses their SSA defect**

**A.** A spot test demonstrating the growth of the cells harbouring the *rad51-K342E* mutation. Strains used: NK6509, NK6511 (*rad51-K342E* SSA); NK6517, NK6519 (*rad51-K342E srs2Δ* SSA); NK6527, NK6530 (*rad51-K342E srs2Δ rad54Δ* SSA); NK4691 (WT SSA).

**B.** SSA efficiency values of *srs2Δ* and/or *rad54Δ* cells with or without the *rad51-K342E* allele. The average  $\pm$ SD of at least three biological repeats is shown for each genotype. Strains used: NK6505-NK6508 (WT SSA); NK6513-NK6515 (*srs2Δ* SSA); NK7182-NK7184 (*rad54Δ* SSA); NK6509-NK6511 (*rad51-K342E* SSA); NK6517-NK6519, NK7580-NK7583 (*rad51-K342E srs2Δ* SSA); NK7185-NK7187 (*rad51-K342E rad54Δ* SSA); NK6528-NK6531 (*rad51-K342E srs2Δ rad54Δ* SSA).

#### **5.4. NER and MMR do not significantly contribute to the generation of expanded ssDNA gaps in unchallenged yeast cells**

As discussed in sections 1.2.5 and 5.1, defective ssDNA gap repair most likely underlies the *srs2Δ* and *rad54Δ* synthetic lethality. These gaps can be created during replication as a result of DNA synthesis repriming downstream of DNA lesions or structures blocking the movement of DNA polymerases (described in detail in the section 1.1.6.4). In addition, ssDNA gaps may also be formed as intermediates in certain repair pathways, such as NER and MMR. It has been demonstrated that Exo1 competes with DNA synthesis during NER and can generate expanded ssDNA gaps if the polymerases are delayed by closely opposing blocks (239). Such gaps could possibly be covered by Rad51 and thus their repair would require Srs2 and/or Rad54 needed to remove the recombinase. Exo1 is also involved in the generation of ssDNA gaps during MMR raising a possibility of an analogous scenario.

If NER or MMR significantly contribute to the generation of DNA repair intermediates that eventually cause death in the cells lacking Srs2 and Rad54, the elimination of these repair pathways could be expected to suppress the *srs2Δ* and *rad54Δ* synthetic lethality. To test this, the two repair pathways were disrupted in *P<sub>GAL1</sub>-RAD55 srs2Δ rad54Δ* strains by deleting *RAD4* and *MSH2* which are essential for NER (section 1.1.2) and MMR (section 1.1.4) respectively. The viability tests revealed that neither single knockouts nor their combination could suppress the *srs2Δ* and *rad54Δ* synthetic lethality (Figure 5.3). This suggests that in unchallenged cells, the NER and MMR activities do not significantly contribute to the creation of expanded ssDNA gaps capable of supporting the Rad51 filament formation.

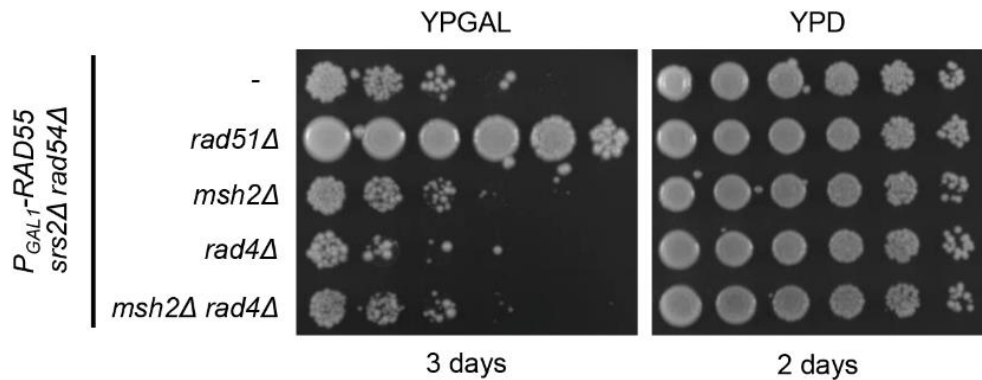


**Figure 5.3. The disruption of NER and MMR cannot suppress the synthetic lethality between *srs2Δ* and *rad54Δ***

A viability test showing the effect of *MSH2* (MMR) and *RAD4* (NER) deletions on the growth of *P<sub>GAL1</sub>-RAD55 srs2Δ rad54Δ* cells. Strains used: NK7208 (*P<sub>GAL1</sub>-RAD55 srs2Δ rad54Δ*); NK8420 (*P<sub>GAL1</sub>-RAD55 srs2Δ rad54Δ rad51Δ*); NK8285 (*P<sub>GAL1</sub>-RAD55 srs2Δ rad54Δ msh2Δ*); NK8288 (*P<sub>GAL1</sub>-RAD55 srs2Δ rad54Δ rad4Δ*); NK8443 (*P<sub>GAL1</sub>-RAD55 srs2Δ rad54Δ msh2Δ rad4Δ*). A second viability test with another set of biological repeats was also performed and produced identical results (not shown).

### 5.5. The 9-1-1 complex may primarily cause the cell death of *srs2Δ rad54Δ* mutants through Exo1-dependent resection rather than DNA damage checkpoint signalling

As mentioned in the section 5.1, a loss of the 9-1-1 complex suppresses the *srs2Δ* and *rad54Δ* synthetic lethality. However, a deletion of *RAD9* does not have the same effect suggesting that the 9-1-1 complex promotes the death of *srs2Δ rad54Δ* cells via a mechanism other than the activation of the DNA damage checkpoint (204). To investigate this further, the DNA damage signalling pathway was disrupted in *P<sub>GAL1</sub>-RAD55 srs2Δ rad54Δ* cells by deleting *MEC1*. Cells are not viable without *Mec1* as it is required for the destruction of *Sml1* upon the entry into the S phase. *Sml1* is an inhibitor of ribonucleotide reductase required for the *de novo* synthesis of dNTPs. If *Sml1* is not removed, the dNTP pool becomes depleted during the S phase leading to the permanent arrest of replication forks and cell death (240). Thus, *SML1* was deleted in the strains of interest to suppress the lethality of *MEC1* deletion.

The viability of *P<sub>GAL1</sub>-RAD55 srs2Δ rad54Δ* cells in a galactose-containing medium was not affected by *SML1* deletion alone but was partially

restored in the absence of Mec1 (Figure 5.4A). However, the elimination of the 9-1-1 complex (*rad17Δ*) produced a significantly stronger suppression of the *srs2Δ* and *rad54Δ* synthetic lethality than the disruption of the DNA damage checkpoint by *MEC1* deletion (Figure 5.4C). This suggests that a defect in DNA damage signalling can only partially account for the suppression of the lethality observed in the absence of the 9-1-1 complex.

Apart from the activation of the DNA damage checkpoint, the 9-1-1 complex is also involved in the regulation of resection. As described in the section 1.1.6.4, it recruits Exo1 to post-replicative ssDNA gaps stimulating their expansion which promotes the formation of Rad51 nucleofilaments. Thus, the contribution of the resection machinery towards the death of *P<sub>GAL1</sub>-RAD55* *srs2Δ rad54Δ* strains grown in galactose was tested. Both players involved in the long-range resection of DSBs, Exo1 and Sgs1-Dna2, were investigated. As the helicase Pif1 was also implicated in the expansion of ssDNA gaps, its relevance for the *srs2Δ* and *rad54Δ* synthetic lethality was explored as well using the *pif1-m2* allele which eliminates the nuclear but not the mitochondrial version of the protein (150, 241).

The viability tests revealed that *exo1Δ* is capable of suppressing the *srs2Δ* and *rad54Δ* synthetic lethality to the same extent as the *RAD17* deletion (Figures 5.4B and 5.4C). In contrast, neither *sgs1Δ* nor *pif1-m2* could do the same (Figure 5.4B). Together, this evidence suggests that the 9-1-1 complex might be causing the death of *srs2Δ rad54Δ* cells primarily by recruiting Exo1 and stimulating its activity rather than activating the DNA damage checkpoint.

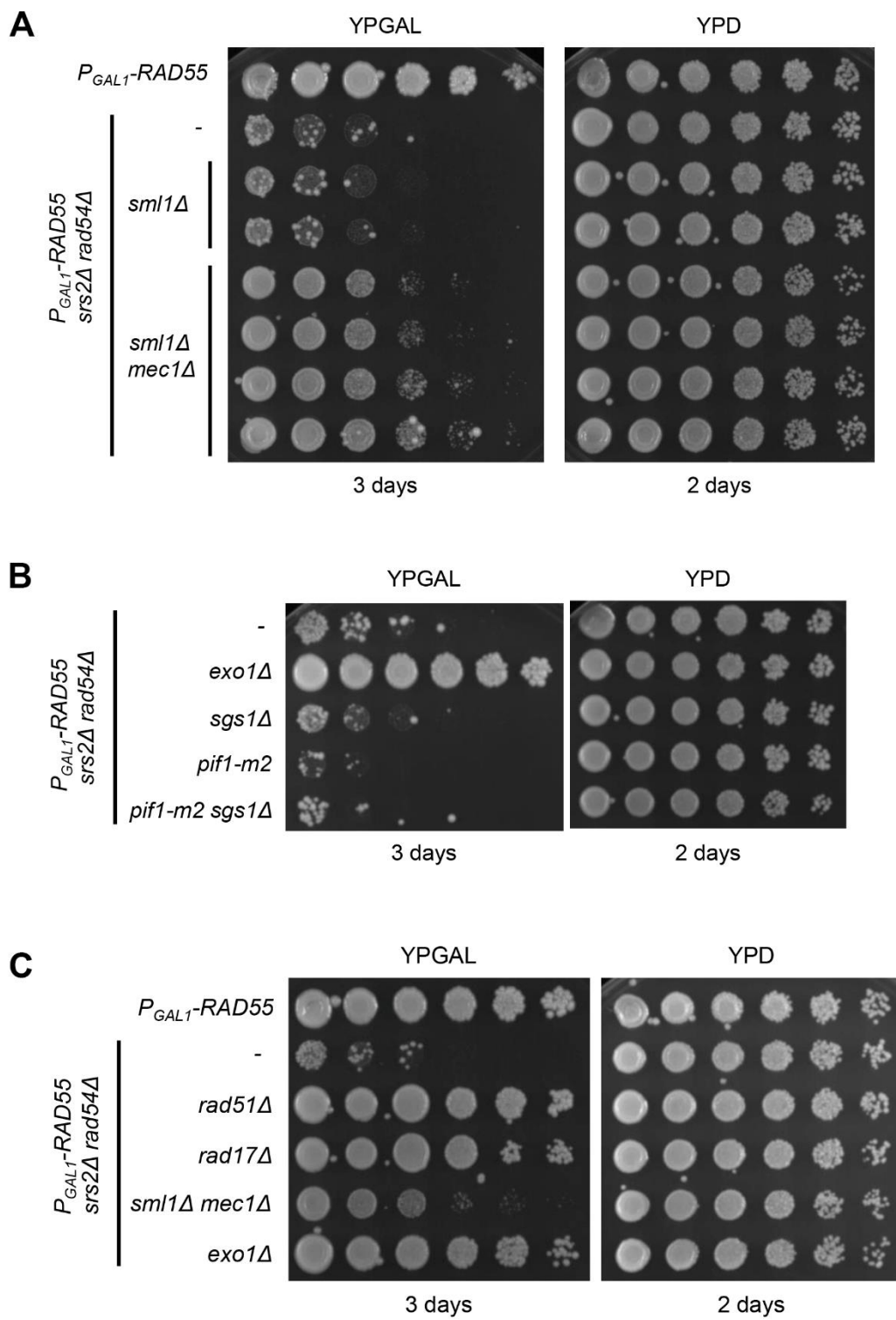


**Figure 5.4. MEC1 and EXO1 deletions can differentially suppress the *srs2Δ* and *rad54Δ* synthetic lethality**

**A.** A viability test demonstrating the effect of *MEC1* deletion on the *srs2Δ* and *rad54Δ* synthetic lethality. Strains used: NK6933 ( $P_{GAL1}$ -RAD55); NK7208 ( $P_{GAL1}$ -RAD55 *srs2Δ rad54Δ*); NK8994, NK8995 ( $P_{GAL1}$ -RAD55 *srs2Δ rad54Δ sml1Δ*); NK8997-NK9000 ( $P_{GAL1}$ -RAD55 *srs2Δ rad54Δ sml1Δ mec1Δ*).

**B.** A viability test demonstrating the contribution of the resection machinery towards the death of  $P_{GAL1}$ -RAD55  $srs2\Delta$   $rad54\Delta$  cells grown in galactose. Strains used: NK7208 ( $P_{GAL1}$ -RAD55  $srs2\Delta$   $rad54\Delta$ ); NK8279 ( $P_{GAL1}$ -RAD55  $srs2\Delta$   $rad54\Delta$   $exo1\Delta$ ); NK8276 ( $P_{GAL1}$ -RAD55  $srs2\Delta$   $rad54\Delta$   $sgs1\Delta$ ); NK8478 ( $P_{GAL1}$ -RAD55  $srs2\Delta$   $rad54\Delta$   $pif1-m2$ ); NK8484 ( $P_{GAL1}$ -RAD55  $srs2\Delta$   $rad54\Delta$   $pif1-m2$   $sgs1\Delta$ ). A second viability test with another set of biological repeats was also performed and produced identical results (not shown).

**C.** A comparative analysis of the different suppressor mutations. Strains used: NK6934 ( $P_{GAL1}$ -RAD55); NK7210 ( $P_{GAL1}$ -RAD55  $srs2\Delta$   $rad54\Delta$ ); NK8421 ( $P_{GAL1}$ -RAD55  $srs2\Delta$   $rad54\Delta$   $rad51\Delta$ ); NK8425 ( $P_{GAL1}$ -RAD55  $srs2\Delta$   $rad54\Delta$   $rad17\Delta$ ); NK8999 ( $P_{GAL1}$ -RAD55  $srs2\Delta$   $rad54\Delta$   $smf1\Delta$   $mec1\Delta$ ); NK8435 ( $P_{GAL1}$ -RAD55  $srs2\Delta$   $rad54\Delta$   $exo1\Delta$ ). A second viability test with another set of biological repeats was also performed and produced identical results (not shown).

## 5.6. Identifying the hypothetical Mec3-interacting regions in Exo1

As demonstrated in the section 5.5, the 9-1-1 complex might cause the death of  $srs2\Delta$   $rad54\Delta$  cells by recruiting Exo1 and stimulating its activity. Thus, the disruption of the physical interaction between the two factors should theoretically suppress the  $srs2\Delta$  and  $rad54\Delta$  synthetic lethality. This makes  $P_{GAL1}$ -RAD55  $srs2\Delta$   $rad54\Delta$  strains an attractive system to easily pinpoint the Exo1 region responsible for the interaction with the Mec3 subunit of the 9-1-1 complex (145).

The C-terminus of Exo1 contains several protein-protein interacting regions including Mlh1-Interacting-Peptide (MIP) and Msh2-Interacting-Peptide (SHIP) boxes (242). Thus, it was suspected that Mec3-interacting sequence might also be in this part of the protein. To address this hypothesis, multiple Exo1 C-terminal truncations were introduced into  $P_{GAL1}$ -RAD55  $srs2\Delta$   $rad54\Delta$  cells. The mutants carrying the Exo1 truncations lacking the Mec3-interacting region were expected to be viable. A gene truncation cassette was introduced immediately after the 702 amino-acid open reading frame of the *EXO1* in the negative control and the coding sequence was knocked out completely in the positive control.

A viability test revealed a three-step improvement in the growth of  $P_{GAL1}$ -RAD55  $srs2\Delta$   $rad54\Delta$  mutants carrying different Exo1 truncations (Figure 5.5A). The first one was observed when the protein was truncated from full length (702 amino acids) to the amino acid 690. The second improvement was

evident when amino acids 648-660 were removed and the third one when amino acids 495-525 were eliminated. This suggests that there might be three separate regions in Exo1 involved in the interaction with Mec3 (Figure 5.5B).

The Exo1 protein sequence between amino acids 690 and 702 is mostly occupied by one of the SHIP boxes (Figure 5.5B) (242). As demonstrated in the section 5.4, the deletion of Msh2 has no effect on the viability of *P<sub>GAL1</sub>-RAD55 srs2Δ rad54Δ* cells grown in galactose. This suggests that the Msh2-Exo1 interaction is not relevant to the Exo1-dependent suppression of the *srs2Δ* and *rad54Δ* synthetic lethality. However, it is possible that the Mec3-interacting sequence of Exo1 overlaps with the SHIP box or that the removal of 12 C-terminal amino acids affects the Exo1 stability in general leading to a weak suppression of the said lethality.

Apart from Exo1, Mcm10 is one other protein known to physically interact with Mec3 (243). The Mec3-interacting region of Mcm10 was previously investigated using a yeast two-hybrid system. It was discovered that the removal of first 150 but not 100 amino acids of Mcm10 disrupts the interaction. However, the internal deletion of the amino acids 100-150 failed to fully eliminate the Mcm10-Mec3 binding (243). This suggests that Mcm10 might also contain several Mec3-intercating sequences. Thus, the two candidate Mec3-interacting regions of Exo1 described above were aligned with the first 150 amino acids of Mcm10. Indeed, the sequences similar to those in Exo1 were identified in Mcm10 (Figure 5.5B). The first region was found to within the first 50 amino acids of Mcm10 while the second one was located between the amino acids 100 and 150. This might explain the previously described observations on the Mcm10-Mec3 binding.

The effect of the Exo1 truncations on the viability of *P<sub>GAL1</sub>-RAD55 srs2Δ rad54Δ* cells grown in the presence of galactose might be due to the disrupted Exo1 interaction with the 9-1-1 complex. However, the truncations might also affect Exo1 activity or protein levels leading to the suppression of the *srs2Δ* and *rad54Δ* synthetic lethality. Thus, further research is required to mutate the

candidate Mec3-interacting regions of Exo1 identified in this study and test their importance for the resection and Exo1 recruitment to DNA.

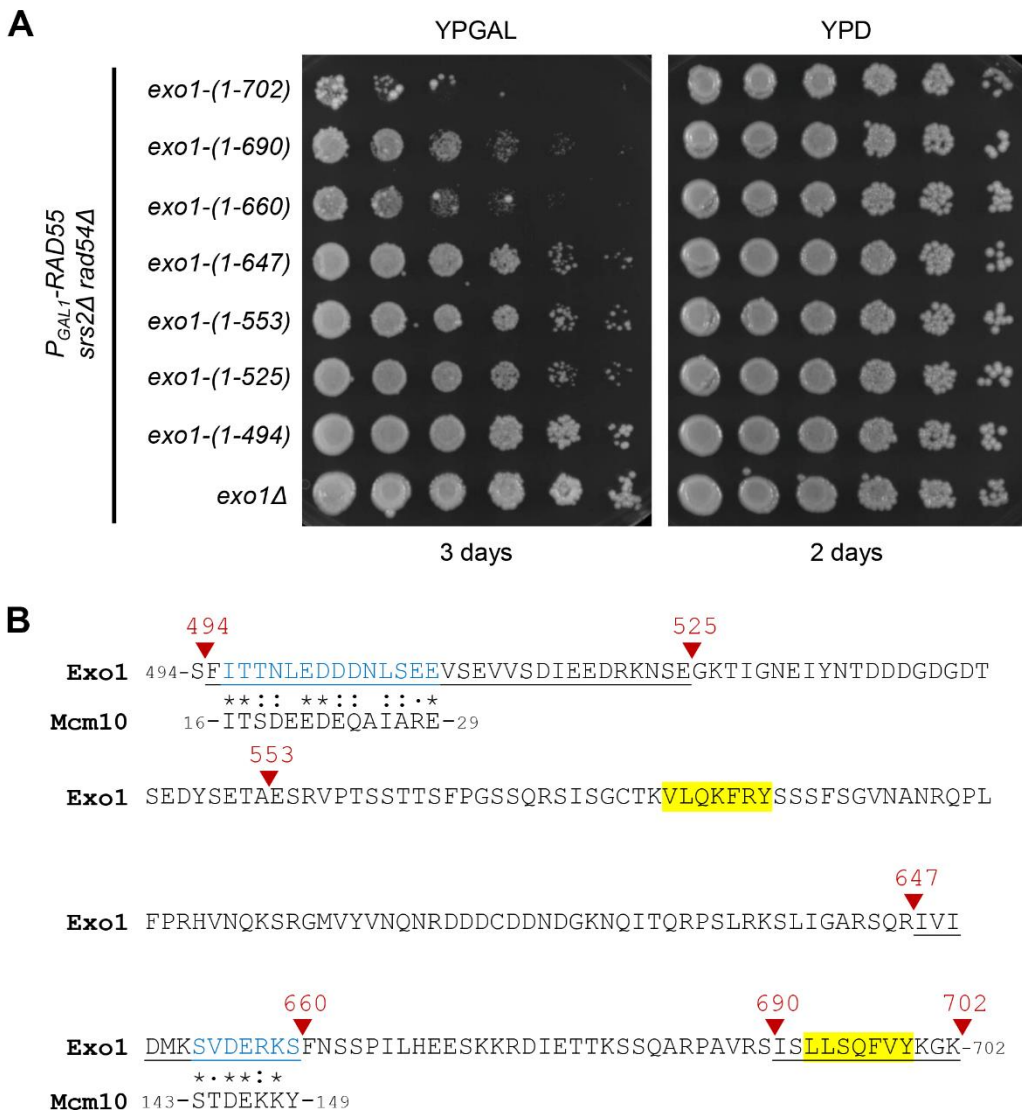


**Figure 5.5. Exo1 C-terminal truncations differentially suppress the *srs2Δ* and *rad54Δ* synthetic lethality**

**A.** A viability test demonstrating the effect of Exo1 truncations on the growth of *P<sub>GAL1</sub>-RAD55 srs2Δ rad54Δ* mutants. Strains used: NK9032 (*P<sub>GAL1</sub>-RAD55 srs2Δ rad54Δ exo1-(1-702)*); NK9270 (*P<sub>GAL1</sub>-RAD55 srs2Δ rad54Δ exo1-(1-690)*); NK9461 (*P<sub>GAL1</sub>-RAD55 srs2Δ rad54Δ exo1-(1-660)*); NK9464 (*P<sub>GAL1</sub>-RAD55 srs2Δ rad54Δ exo1-(1-647)*); NK9019 (*P<sub>GAL1</sub>-RAD55 srs2Δ rad54Δ exo1-(1-553)*); NK9470 (*P<sub>GAL1</sub>-RAD55 srs2Δ rad54Δ exo1-(1-525)*); NK9278 (*P<sub>GAL1</sub>-RAD55 srs2Δ rad54Δ exo1-(1-494)*); NK9279 (*P<sub>GAL1</sub>-RAD55 srs2Δ rad54Δ exo1Δ*). At least two biological repeats were tested for each truncation and produced identical results.

**B.** The C-terminus sequence of Exo1 from amino acid 494 to the end. Red triangles indicate the positions of the truncations investigated. Sequences highlighted in yellow specify two SHIP boxes. Underlined letters indicate the possible Mec3-interacting regions determined by assessing the growth of  $P_{GAL1}$ -RAD55  $srs2\Delta$   $rad54\Delta$  cells carrying different Exo1 truncations (Figure 5.5A). Blue letters specify the hypothetical Mec3-interacting motifs shared by Exo1 and Mcm10. An asterisk (\*) identifies fully conserved residues, while a colon (:) and a period (.) specify conservation between amino acids with strongly and weakly similar properties respectively. Alignments were performed using T-Coffee multiple sequence alignment program (244, 245).

### 5.7. *HED1* expression suppresses the *srs2Δ* and *rad54Δ* synthetic lethality

As described in section 1.1.5.2.8, the meiosis-specific *S. cerevisiae* protein Hed1 can block the Rad54 interaction with Rad51 and inhibit the strand invasion during homology-based repair (111, 116, 117). Thus, the Hed1 expression might effectively mimic the deletion of *RAD54* and might be useful in the investigation of the *srs2Δ* and *rad54Δ* synthetic lethality.

To explore this possibility, a galactose-inducible promoter was introduced upstream of *HED1* in WT cells. Firstly, the expression of Hed1 from the  $P_{GAL1}$  promoter was confirmed indirectly by using a drug sensitivity assay. Consistent with the reported ability of Hed1 to inhibit Rad54-mediated strand invasion,  $P_{GAL1}$ -*HED1* strains were sensitive to DNA damaging agents when grown on a medium containing galactose (Figure 5.6A).

The  $P_{GAL1}$ -*HED1* allele was then introduced into the  $P_{GAL1}$ -RAD55 background.  $P_{GAL1}$ -*HED1*  $P_{GAL1}$ -RAD55 mutants were found to have a slight growth defect in a galactose-containing medium when compared to the  $P_{GAL1}$ -RAD55 control (Figure 5.6B). The removal of Srs2 in the  $P_{GAL1}$ -RAD55 cells did not lead to a notable growth defect on YPGAL plates. In contrast, the deletion of *SRS2* in  $P_{GAL1}$ -*HED1*  $P_{GAL1}$ -RAD55 mutants caused a slight decrease in the cell viability (Figure 5.6B). This suggests that the growth of haploid yeast cells expressing *HED1* partially depends on Srs2.

Unexpectedly, the *HED1* expression suppressed the *srs2Δ* and *rad54Δ* synthetic lethality (Figure 5.6B). Hed1 has only one function reported in the literature so far – the inhibition of the Rad54 and Rad51 interaction (section

1.1.5.2.8). Thus, the *HED1* expression was not expected to have any effect on the viability of *P<sub>GAL1</sub>-RAD55 srs2Δ rad54Δ* cells grown in galactose as they already lack Rad54. The growth of *P<sub>GAL1</sub>-RAD55 P<sub>GAL1</sub>-HED1 srs2Δ rad54Δ* cells on galactose-containing plates was indistinguishable from that of *P<sub>GAL1</sub>-RAD55 P<sub>GAL1</sub>-HED1 srs2Δ* mutants (Figure 5.6B). This suggests that the presence of Rad54 is irrelevant when *HED1* is expressed, which is consistent with the ability of Hed1 to inhibit Rad54-Rad51 interaction.

The simplest way how Hed1 could be suppressing the *srs2Δ* and *rad54Δ* synthetic lethality is by disrupting Rad51 nucleofilament formation. However, the *in vitro* studies suggest that Hed1 does not alter the Rad51 binding to DNA or even has a stabilising effect (111, 117). Another possibility is that Hed1 enables or promotes Rad51 filament disassembly by other factors. Apart from Srs2, Sgs1 is one other *S. cerevisiae* protein which has a demonstrated ability of removing Rad51 from ssDNA *in vitro* (187). Thus, the effect of *SGS1* deletion on the growth of *P<sub>GAL1</sub>-RAD55 P<sub>GAL1</sub>-HED1 srs2Δ rad54Δ* cells in the presence of galactose was investigated. Indeed, the growth of these strains partially depends on Sgs1 as it is significantly poorer in the absence of the helicase (Figure 5.6C).

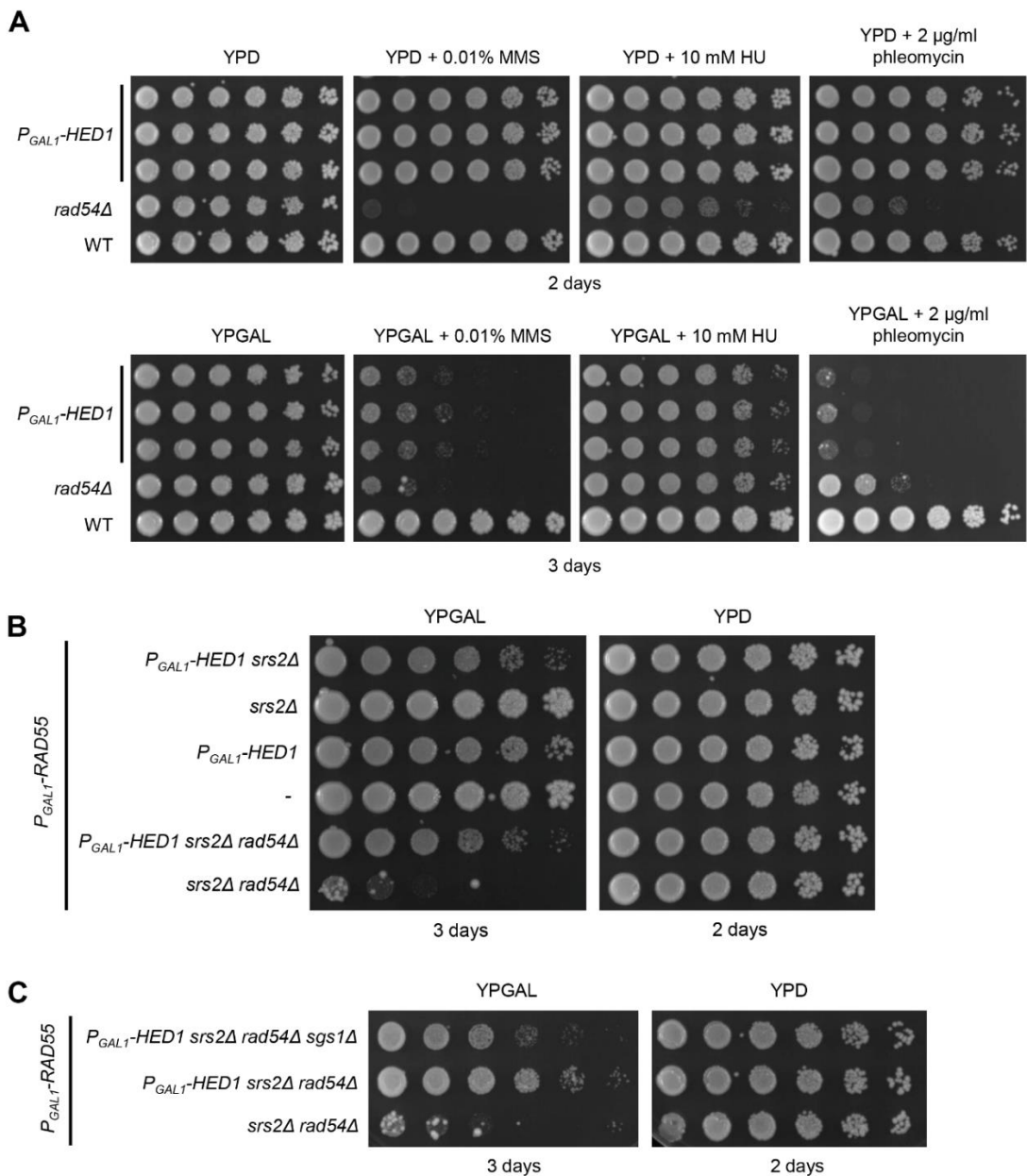


**Figure 5.6. Hed1 suppresses the *srs2Δ* and *rad54Δ* synthetic lethality**

**A.** A drug sensitivity assay used to indirectly test the expression of Hed1 from  $P_{GAL1}$  promoter. Strains used: NK9136-NK9138 ( $P_{GAL1}$ -HED1); NK5895 (*rad54Δ*); NK1 (WT).

**B.** The suppression of the *srs2Δ* and *rad54Δ* synthetic lethality by the presence of Hed1. Strains used: NK9144, NK9145 ( $P_{GAL1}$ -RAD55  $P_{GAL1}$ -HED1 *srs2Δ*); NK7204 ( $P_{GAL1}$ -RAD55 *srs2Δ*); NK9141 ( $P_{GAL1}$ -RAD55  $P_{GAL1}$ -HED1); NK6933 ( $P_{GAL1}$ -RAD55); NK9148 ( $P_{GAL1}$ -RAD55  $P_{GAL1}$ -HED1 *srs2Δ rad54Δ*); NK7208 ( $P_{GAL1}$ -RAD55 *srs2Δ rad54Δ*). A second viability test with another set of biological repeats was also performed and produced identical results (not shown).

**C.** A spot test demonstrating the effect of SGS1 deletion on the growth of  $P_{GAL1}$ -RAD55  $P_{GAL1}$ -HED1 *srs2Δ rad54Δ* cells on media containing galactose. Strains used: NK9263 ( $P_{GAL1}$ -RAD55  $P_{GAL1}$ -HED1 *srs2Δ rad54Δ sgs1Δ*); NK9148 ( $P_{GAL1}$ -RAD55

$P_{GAL1}$ -*HED1* *srs2Δ rad54Δ*; NK7208 ( $P_{GAL1}$ -*RAD55* *srs2Δ rad54Δ*). A second spot test with another set of biological repeats was also performed and produced identical results (not shown).

To test if more helicases are involved in this process, another RecQ helicase of *S. cerevisiae*, Hrq1, along with two other DNA repair helicases, Mph1 and Chl1, were investigated (246-251). The growth of  $P_{GAL1}$ -*RAD55*  $P_{GAL1}$ -*HED1* *srs2Δ rad54Δ* cells in the presence of galactose greatly depended on Hrq1, while Mph1 and Chl1 were dispensable (Figure 5.7A). The simultaneous lack of both RecQ helicases produced an even stronger effect than the removal of either single one, leading to a severe growth retardation of the  $P_{GAL1}$ -*RAD55*  $P_{GAL1}$ -*HED1* *srs2Δ rad54Δ sgs1Δ hrq1Δ* mutants grown in the presence of galactose (Figure 5.7B). This suggests that Sgs1 and Hrq1 might be working in parallel to facilitate the growth of *srs2Δ rad54Δ* cells expressing *HED1*.

It is known that the combination of *srs2Δ* and *sgs1Δ* leads to a synthetic growth defect in *S. cerevisiae* (151, 252, 253). Thus, the effect of *SGS1* deletion on the growth of  $P_{GAL1}$ -*RAD55*  $P_{GAL1}$ -*HED1* *srs2Δ rad54Δ* cells might be due to this negative interaction and have nothing to do with Hed1. Therefore, synthetic interactions between *srs2Δ*, *sgs1Δ* and *hrq1Δ* were investigated. Consistently with the published observations, a growth defect was observed when *srs2Δ* and *sgs1Δ* were combined in the  $P_{GAL1}$ -*RAD55* background (Figure 5.7C). In contrast, the deletion of *HRQ1* showed no negative interactions in any of the combinations tested.

As discussed in sections 1.1.5.2.5 and 1.1.6.2, Sgs1-Top3 and Mus81-Mms4 comprise the two main pathways for the resolution of the recombination intermediates during DNA repair. Srs2 has been shown to promote Mus81-Mms4 activity by stimulating it directly and providing access for the nuclease by removing Rad51 from DNA (89, 90). Thus, the synthetic growth defect of *srs2Δ* and *sgs1Δ* might be a result of a compromised resolution of recombination intermediates (151, 252). Indeed, the growth of the cells lacking these two proteins is restored when Rad51 or its mediators are eliminated

(151). Therefore, the *srs2Δ* and *sgs1Δ* synthetic interactions might be suppressed in the *P<sub>GAL1</sub>-RAD55 P<sub>GAL1</sub>-HED1 srs2Δ rad54Δ* strains grown on galactose as they lack Rad54 and thus cannot form recombination intermediates. Unfortunately, this cannot be tested directly as *srs2Δ sgs1Δ rad54Δ* triple mutants would not be viable due to the *srs2Δ* and *rad54Δ* synthetic lethality. However, *sgs1Δ* and *mus81Δ* negative interactions are indeed suppressed by the *RAD54* deletion (151). Overall, this evidence suggests that the effect of *sgs1Δ* on the growth of *P<sub>GAL1</sub>-RAD55 P<sub>GAL1</sub>-HED1 srs2Δ rad54Δ* cells grown in the presence of galactose is likely specific to Hed1 rather than being a result of negative interactions with *srs2Δ*. Together, the evidence presented in this section suggests that the RecQ helicases might have a weak ability to negatively regulate Rad51 nucleofilaments and this ability is enhanced by the presence of Hed1 via an unknown mechanism. Nonetheless, further research is required to test this new hypothetical pathway.

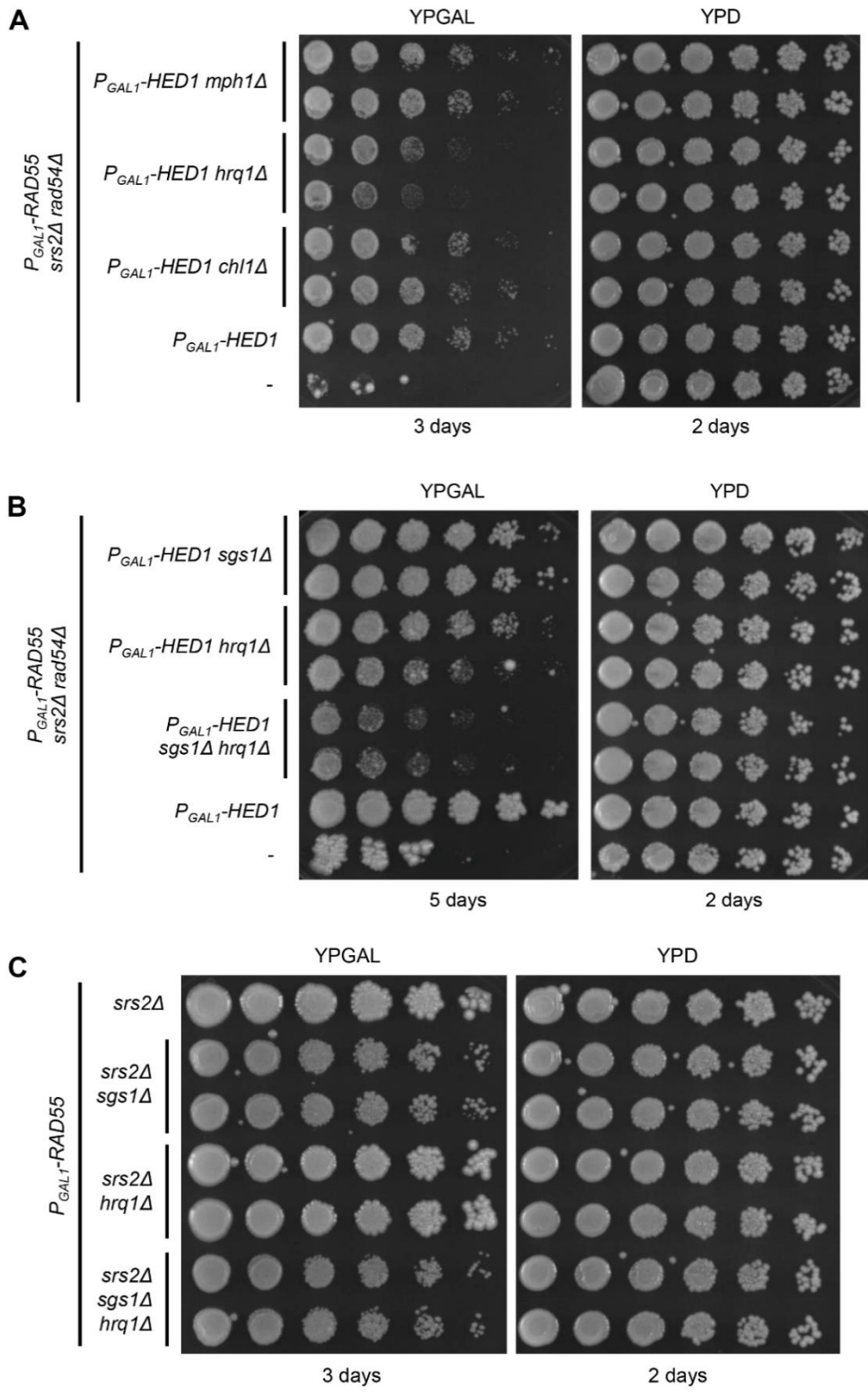


**Figure 5.7. The growth of  $P_{GAL1}\text{-}RAD55\ P_{GAL1}\text{-}HED1\ srs2\Delta\ rad54\Delta$  cells in the presence of galactose strongly depends on RecQ helicases**

**A.** A spot test demonstrating the effect of *MPH1*, *HRQ1* and *CHL1* deletions on the growth of  $P_{GAL1}\text{-}RAD55\ P_{GAL1}\text{-}HED1\ srs2\Delta\ rad54\Delta$  cells. Strains used: NK9345, NK9346 ( $P_{GAL1}\text{-}RAD55\ P_{GAL1}\text{-}HED1\ srs2\Delta\ rad54\Delta\ mph1\Delta$ ); NK9347, NK9348 ( $P_{GAL1}\text{-}$

*RAD55 P<sub>GAL1</sub>-HED1 srs2Δ rad54Δ hrq1Δ*; NK9349, NK9350 (*P<sub>GAL1</sub>-RAD55 P<sub>GAL1</sub>-HED1 srs2Δ rad54Δ chl1Δ*); NK9148 (*P<sub>GAL1</sub>-RAD55 P<sub>GAL1</sub>-HED1 srs2Δ rad54Δ*); NK7208 (*P<sub>GAL1</sub>-RAD55 srs2Δ rad54Δ*).

**B.** A spot test showing the severity of growth retardation in the induced *P<sub>GAL1</sub>-RAD55 P<sub>GAL1</sub>-HED1 srs2Δ rad54Δ* cells in the absence of Sgs1, Hrq1 or both. Strains used: NK9263, NK9264 (*P<sub>GAL1</sub>-RAD55 P<sub>GAL1</sub>-HED1 srs2Δ rad54Δ sgs1Δ*); NK9347, NK9348 (*P<sub>GAL1</sub>-RAD55 P<sub>GAL1</sub>-HED1 srs2Δ rad54Δ hrq1Δ*); NK9351, NK9352 (*P<sub>GAL1</sub>-RAD55 P<sub>GAL1</sub>-HED1 srs2Δ rad54Δ sgs1Δ hrq1Δ*); NK9148 (*P<sub>GAL1</sub>-RAD55 P<sub>GAL1</sub>-HED1 srs2Δ rad54Δ*); NK7208 (*P<sub>GAL1</sub>-RAD55 srs2Δ rad54Δ*).

**C.** A spot test demonstrating the synthetic interactions between *srs2Δ*, *sgs1Δ* and *hrq1Δ* in *P<sub>GAL1</sub>-RAD55* background. Strains used: NK7204 (*P<sub>GAL1</sub>-RAD55 srs2Δ*); NK9259, NK9260 (*P<sub>GAL1</sub>-RAD55 srs2Δ sgs1Δ*); NK9353, NK9354 (*P<sub>GAL1</sub>-RAD55 srs2Δ hrq1Δ*); NK9355, NK9356 (*P<sub>GAL1</sub>-RAD55 srs2Δ sgs1Δ hrq1Δ*).

## 5.8. Discussion

The *srs2Δ* and *rad54Δ* synthetic lethality is most likely caused by a defective repair of ssDNA gaps (section 1.2.5). Neither NER nor MMR appear to contribute significantly to the generation of these gaps (section 5.4) leaving the DNA repriming during replication as their most probable source. Postreplicative gaps are preferentially repaired by TS which involves the formation of Rad51 filaments and Rad54-mediated invasion into a homologous donor (119, 120). Alternatively, Rad51 can be removed from ssDNA by Srs2 allowing the gaps to be filled in by DNA polymerases (151). It is generally believed that the simultaneous lack of these two processes leads to the synthetic lethality between *srs2Δ* and *rad54Δ* (151). However, the data presented in chapter 3 demonstrate that the Rad54-mediated Rad51 removal is also important for the damage-associated DNA synthesis and thus might play a role in the postreplicative gap filling by DNA polymerases. As demonstrated in the section 5.3, the lack of the Rad54 activity in Rad51 removal can be specifically compensated for by the *rad51-K342E* mutation which compromises the ability of Rad51 to bind DNA (Figure 5.2B). It appears that raising the efficiency of the damage-associated DNA synthesis in the cells lacking Srs2 and Rad54 to the level observed in *srs2Δ* strains is sufficient to rescue the cell viability (Figure 5.2A). As *rad51-K342E srs2Δ rad54Δ* triple mutants still lack the strand invasion activity, it can be argued that the lack of the Rad54 function in Rad51 removal from dsDNA significantly contributes to

the *srs2Δ* and *rad54Δ* synthetic lethality. It is not clear whether a restoration of the Rad54 activity in strand invasion only could also rescue cell viability as such a *RAD54* separation of function allele has not been described so far.

It appears that all known suppressor mutations of the *srs2Δ* and *rad54Δ* synthetic lethality act by either preventing the formation of Rad51 nucleofilaments or promoting their disassembly. It is obvious how this is achieved by deleting the genes coding for Rad51 or its mediators. However, it is less straight forward explaining the suppression by the loss of the 9-1-1 complex. As presented in this chapter, the disruption of the DNA damage checkpoint by *MEC1* deletion only moderately rescues the viability of the *P<sub>GAL1</sub>-RAD55 srs2Δ rad54Δ* cells grown in galactose-containing media (Figure 5.3C). This suggests that a defective DNA damage signalling can only partially account for the suppression of the *srs2Δ* and *rad54Δ* synthetic lethality observed in the absence of the 9-1-1 complex. Apart from the DNA damage checkpoint, the 9-1-1 complex is also involved in the regulation of Exo1 activity during resection (145, 147). The deletion of *EXO1* suppressed the *srs2Δ* and *rad54Δ* lethality to the same extent as the removal of the 9-1-1 complex (Figure 5.3C). This suggests that the 9-1-1 complex might primarily be promoting the death of *srs2Δ rad54Δ* cells by recruiting Exo1 to ssDNA gaps and stimulating their expansion, which would then promote the formation of Rad51 nucleofilaments (145, 149). The partial suppression of the *srs2Δ* and *rad54Δ* synthetic lethality by *MEC1* deletion might also be explained by a compromised Rad51 filament assembly. Mec1 is required for the phosphorylation of Rad51 and Rad55 in response to DNA damage and these modifications appear to be important for the proper functioning of the recombination machinery (254-256). Therefore, in the absence of the DNA damage checkpoint the formation of Rad51 filaments might be suboptimal.

As discussed above, the *srs2Δ* and *rad54Δ* synthetic lethality can be suppressed by the removal of Exo1, most likely because it is required for the expansion of ssDNA gaps and the subsequent formation of Rad51 filaments. The lack of Sgs1 and Pif1 did not have the same effect suggesting that their

contribution to the process was insignificant (Figure 5.4B). This is not surprising for Pif1 as its ability to expand ssDNA gaps appears to be very subtle (150). In contrast, both Sgs1-Dna2 and Exo1 are major players in the long-range resection of DSBs (34). It is possible that Sgs1-Dna2 is simply not recruited to postreplicative gaps. Alternatively, the cell-cycle dependent regulation of the Dna2 activity might place it outside of the time window of dealing with the ssDNA gaps. The Dna2 levels are low during G1 and early S but substantially increase during late S and G2 phases (257). Thus, it is possible that ssDNA gaps could be resected by Dna2 in late S and G2. In *P<sub>GAL1</sub>-RAD55 srs2Δ rad54Δ sgs1Δ* cells, Exo1 still expands postreplicative gaps during early S phase promoting the formation of Rad51 filaments and the eventual cell death. As described in the section 4.4, ssDNA gaps prompted by non-damage replication barriers most likely underlie the *srs2Δ* and *rad54Δ* synthetic lethality. Theoretically, these gaps could be filled in by replicative DNA polymerases as soon as the replication impediments are resolved. This is in contrast to TLS which mostly takes place during the late S and G2 (119, 120) In *P<sub>GAL1</sub>-RAD55 srs2Δ rad54Δ exo1Δ* strains, the lack of Exo1-mediated expansion of ssDNA gaps prevents the efficient formation of Rad51 nucleofilaments enabling the filling of ssDNA gaps by DNA polymerases. This might occur before the Dna2 levels increase explaining why the presence of Sgs1-Dna2 does not compromise the viability of *P<sub>GAL1</sub>-RAD55 srs2Δ rad54Δ exo1Δ* cells grown in galactose.

As described in the section 5.7, Hed1 expression in mitotic cells led to a surprising suppression of the *srs2Δ* and *rad54Δ* synthetic lethality. Hed1 does not affect Rad51 binding to DNA and might even stabilise it *in vitro* (111, 117). However, the findings presented in this study suggest that Rad51 filaments must be disassembled to successfully complete genome duplication. How could these two statements go along? The growth of Hed1-expressing *srs2Δ rad54Δ* mutants heavily depends on the RecQ helicases Sgs1 and Hrq1. Sgs1 has been shown to remove Rad51 from ssDNA *in vitro* (187). This raises a possibility that Hed1 might be suppressing the *srs2Δ* and *rad54Δ* synthetic lethality by promoting the disassembly of Rad51 nucleofilaments by Sgs1 and

Hrq1. It is not clear why the RecQ helicases might need Hed1 to perform this function. Possibly, Sgs1 and Hrq1 can specifically remove Rad51-Hed1 complexes from DNA. Alternatively, Hed1 might condition Rad51 filaments into a particular conformation susceptible for the disassembly by the RecQ helicases. Further research is required to fully decipher the mechanism of how Hed1 suppresses the *srs2Δ* and *rad54Δ* synthetic lethality. Furthermore, the ability of Hrq1 to remove Rad51 from DNA is yet to be tested.

## Chapter 6. Summary and general discussion

DNA repair is essential to ensure genome stability and the continuity of life. The eukaryotic recombinase Rad51 is one of the most pivotal proteins providing the means for the faithful maintenance of genetic material. It is required for the identification and utilisation of homologous donors during HR. However, *S. cerevisiae* cells lacking Srs2, a helicase capable of removing Rad51 from ssDNA, exhibit decreased efficiency of SSA repair pathway for which the recombinase is not required. A closer analysis of these mutants has revealed that the elimination of Srs2 affects the DNA synthesis step of SSA, and the repair defect in *srs2Δ* mutants can be reversed by the deletion of *RAD51* (103). Thus, Rad51 recombinase appears to be a two-edged sword: it enables the usage of the error-free repair pathways but it can also hinder damage-associated DNA synthesis required for the completion of DNA repair. Therefore, a timely removal of Rad51 from DNA might be as important as the recombination events facilitated by the recombinase. This study was dedicated to investigating the functional relationship between Srs2 and the translocase Rad54 in the negative regulation of Rad51, often using the synthetic lethality of *srs2Δ* and *rad54Δ* as a genetic tool to address this question. Understanding what goes wrong in the double mutants helped placing the relevant functions of Srs2 and Rad54 in the context of both DNA repair and normal DNA metabolism in the cell. To do this, a system where the synthetic lethality is conditional was developed by placing the *RAD55* under the control of a galactose-inducible promoter. This allowed the *srs2Δ rad54Δ* double mutants to grow in the glucose- and raffinose-containing media as Rad51 filaments cannot form without Rad55, thereby preventing the lethality. In the presence of galactose, the expression of *RAD55* was induced making the cells inviable and allowing to study the processes underlying the *srs2Δ* and *rad54Δ* synthetic lethality.

## 6.1. Srs2 and Rad54 have complementary functions in the negative regulation of Rad51

The evidence presented in the chapter 3 suggests that similar to Srs2, the Snf2/Swi2 translocase Rad54 alleviates the Rad51-dependent inhibition of the damage-associated DNA synthesis assayed in the system for SSA. Although the elimination of Rad54 did not produce a defect in SSA on its own, the involvement of Rad54 in this repair mechanism was unmasked by *SRS2* deletion (Figure 3.7B). The DNA synthesis step of SSA was significantly more impaired in the *S. cerevisiae* cells lacking both Srs2 and Rad54 than in *SRS2* single knockouts. *RAD51* overexpression not only exacerbated the DNA repair issues in *srs2Δ* and *srs2Δ rad54Δ* strains but also led to a SSA defect in *rad54Δ* cells (Figure 3.3C). Together, this evidence suggests that Rad54 indeed facilitates damage-associated DNA synthesis by removing Rad51 from DNA.

While Srs2 disassembles Rad51 filaments formed on ssDNA, Rad54 has been demonstrated to remove Rad51 from dsDNA (182, 199). This makes it less obvious how the two proteins can facilitate the same process. The overexpression of *RAD54* provides only a marginal suppression of the damage-associated DNA synthesis defect in *srs2Δ* cells (Figure 3.8E). This suggests that Srs2 and Rad54 functions are mostly complementary rather than redundant. To enable damage-associated DNA synthesis, PCNA needs to be loaded on dsDNA at the dsDNA-ssDNA junction and this reaction greatly depends on the presence of RPA (described in detail in the section 1.2.1). It is likely that the Rad51 nucleofilaments formed on ssDNA can spread into the surrounding dsDNA regions. Srs2 and Rad54 might then work in parallel to remove Rad51 from ssDNA and dsDNA respectively. This would not only enable the binding of RPA but would also eliminate the steric hindrance Rad51 filaments might pose for the loading of PCNA. In the absence of Srs2, Rad54 could still remove Rad51 from dsDNA to bring the end of the nucleofilament to the dsDNA-ssDNA junction possibly promoting the dissociation of Rad51 monomers bound to the vicinal ssDNA (Figure 3.9). The opposite could be expected in *rad54Δ* cells. This could explain how Srs2 and Rad54 can both

facilitate damage-associated DNA synthesis without having redundant molecular functions – each can disassemble the filament to the dsDNA-ssDNA junction where stochastic dissociation of Rad51 monomers from the remaining end of the filament might be a sufficient enough force to clear the junction from Rad51 and enable PCNA recruitment and the initiation of DNA synthesis.

## **6.2. In the absence of the strand invasion, Rad51 nucleofilaments need to be enzymatically disassembled to complete the genome duplication**

*S. cerevisiae* cells lacking Srs2 and Rad54 are not viable unless *RAD51* is deleted (204). It has been suggested that without Rad54, Rad51 filaments cannot invade a homologous donor preventing further progression of HR. In the concurrent absence of Srs2, the filaments cannot be disassembled either hindering the use of other repair pathways. This results in the accumulation of toxic recombination intermediates causing the death of *srs2Δ rad54Δ* double mutants (151). The hypothesis of persistent Rad51 binding to DNA in the cells lacking both Srs2 and Rad54 has been tested in this study. Rad51 indeed accumulates in the chromatin fraction of *P<sub>GAL1</sub>-RAD55 srs2Δ rad54Δ* strains grown in galactose after just a single round of genome duplication (Figure 4.1B).

The formation of Rad51 nucleofilaments that become long-lived in the absence of Srs2 and Rad54 requires ssDNA which can be generated during the resection of DSBs. However, it was estimated that *S. cerevisiae* cells experience only 0.12 spontaneous DSBs per cell cycle making these lesions simply not frequent enough to explain the unviability of *srs2Δ rad54Δ* cells (209-211). Another major source of ssDNA is replication forks. However, mutations that disrupt the interaction of Srs2 with PCNA and thus prevent the recruitment of the helicase to replication forks are not synthetically lethal with *rad54Δ* (212, 213). Furthermore, a time-course experiment described in the section 4.3 demonstrated that after the induction of the *RAD55* expression via the addition of galactose, *P<sub>GAL1</sub>-RAD55 srs2Δ rad54Δ* mutants progress

through the first S phase with dynamics very similar to those of the control cells grown in raffinose (Figure 4.2C). In addition, they activate the DNA damage checkpoint only after the completion of the bulk genome duplication (Figure 4.2D). Thus, it seems unlikely that the compromised replication forks are the primary cause of the *srs2Δ* and *rad54Δ* synthetic lethality. This leaves ssDNA gaps as the most probable source of ssDNA needed for the formation of Rad51 nucleofilaments which become long-lived in the absence of Srs2 and Rad54.

NER (section 1.1.2) and MMR (section 1.1.4) involve ssDNA gap intermediates. However, the elimination of either one or both repair pathways cannot suppress the synthetic lethality of *srs2Δ* and *rad54Δ* (Figure 5.3). This indicates that in unchallenged conditions, NER and MMR do not contribute significantly towards the generation of ssDNA gaps that support the formation of Rad51 nucleofilaments and lead to cell death in *srs2Δ rad54Δ* mutants. The only remaining feasible source of ssDNA gaps is the repriming of synthesis during DNA replication. As described in sections 1.1.6.2 and 1.1.6.4, postreplicative ssDNA gaps are preferentially repaired by TS which involves the formation of Rad51 nucleofilaments and thus can lead to problems in the absence of Srs2 and Rad54.

A time-course experiment described in the section 4.3 has revealed that the absolute majority of *P<sub>GAL1</sub>-RAD55 srs2Δ rad54Δ* cells arrest at the first G2/M after the induction of the *RAD55* expression (Figure 4.2C). This indicates that the ssDNA gaps that cannot be efficiently repaired in the absence of Srs2 and Rad54 are formed every cell cycle. However, *S. cerevisiae* mutants deficient in HR (TS and the salvage pathway) and TLS were found to be viable in this study (Figure 4.3). These repair mechanisms are necessary to resolve postreplicative ssDNA gaps formed in response to damaged DNA (119, 120). In contrast, the gaps without any DNA lesions could still be filled in by replicative DNA polymerases as soon as the replication impediments which prompted the formation of ssDNA gaps are resolved. This suggests that the majority of ssDNA gaps routinely arising in unchallenged *S. cerevisiae* cells might be formed in response to non-damage replication barriers (G-quadruplexes, R-loops etc.). Cells may prioritise the completion of bulk

genome duplication over the continuity of the newly synthesised strands and thus restarting DNA synthesis downstream of these structures could be a common strategy during routine DNA replication. The resulting ssDNA gaps are then repaired postreplicatively by TS in WT cells but cannot be resolved and accumulate in *srs2Δ rad54Δ* mutants.

In *rad54Δ* cells, TS is unavailable. Thus, postreplicative gaps are likely channelled into an alternative repair pathway by Srs2 which disassembles Rad51 nucleofilaments allowing for the gaps to be filled in by DNA polymerases (151). The fact that Rad54 can alleviate Rad51-dependent inhibition of the DNA synthesis suggests that the translocase might participate in the alternative gap filling pathway along with Srs2. It was discovered in this study that the efficiency of the damage-associated DNA synthesis in the cells lacking Srs2 and Rad54 can be elevated to the level seen in the *srs2Δ* mutants by employing a *rad51-K342E* mutation (Figure 5.2B). This effectively compensates for the lack of the Rad54 function in Rad51 removal during the damage-associated DNA synthesis. Therefore, *rad51-K342E srs2Δ rad54Δ* mutants can be regarded as *srs2Δ* cells with Rad54 translocase defective in strand invasion but not Rad51 removal. As these cells are viable (Figure 5.2A), it can be extrapolated that in the absence of the Srs2 activity, the Rad54-mediated Rad51 removal would be sufficient to support an adequate filling of ssDNA gaps by DNA polymerases. Thus, it appears that Rad54 can significantly contribute to both pathways of postreplicative repair – TS and gap filling by polymerases.

As mentioned earlier, in *srs2Δ rad54Δ* cells ssDNA gaps cannot be resolved by TS as the Rad51 nucleofilaments are unable to invade a homologous donor without Rad54. It was discovered in this study that the simultaneous absence of Srs2- and Rad54-mediated Rad51 removal appears to result in a strong inhibition of damage-associated DNA synthesis, which prevents an adequate filling of postreplicative gaps by DNA polymerases. *P<sub>GAL1</sub>-RAD55 srs2Δ rad54Δ* cells expressing *RAD55* divide with unrepaired ssDNA gaps which are extensively resected in G1 as evident from the FACS analysis showing the accumulation of cells with sub-1N DNA content (Figure

4.2C). In addition, any attempts to replicate DNA with the gaps appear to cause further loss of genetic material, possibly because of the resection of DSBs formed after replication forks run into unrepaired ssDNA gaps. Thus, it can be deduced that in the absence of the strand invasion, the enzymatic disassembly of Rad51 nucleofilaments is necessary to complete genome duplication. The situation when Rad51 filaments form on postreplicative gaps but cannot invade a homologous donor is probably mostly artificial in *S. cerevisiae* (created by *RAD54* deletion). However, instances when homology is not available can theoretically arise in WT conditions as well, for example, when ssDNA gaps are formed on both daughter strands in close proximity.

### **6.3. Enzymatic Rad51 removal might be required for the completion of genome duplication even when strand invasion is functional**

As mentioned earlier, separation of function mutations are not available for *RAD54*. Thus, there is no obvious way to test whether the lack of the Srs2 and Rad54 activities in the Rad51 removal would result in cell death in the *S. cerevisiae* mutants still proficient in strand invasion. According to the current model of TS, the DNA strand with a discontinuity is repaired by using a donor strand displaced by the invasion of Rad51 nucleofilament (Figure 6.1). The displaced strand is initially covered by RPA. Thus, it is not clear whether Rad51 filaments can form on the displaced strand in time to exert and inhibitory effect on DNA synthesis before PCNA is loaded, DNA synthesis is initiated, and the ssDNA gap repair is completed.

Several *in vivo* experiments suggest that it takes about 20-40 minutes for DNA synthesis to start after the strand invasion during DSB repair by GC (258-260). It has been proposed that this might reflect the time needed for the initial recruitment and assembly of the DNA synthesis machinery (258). Rad51 can be detected at DSB loci around 10 minutes after the appearance of the RPA signal suggesting the approximate time necessary for some Rad51 nucleofilaments to assemble *in vivo* (261). Therefore, assuming that the

dynamics of the initiation of DNA synthesis during TS and GC are similar, it is plausible that Rad51 filaments can form on the displaced strand after the establishment of TS recombination intermediates but before the start of DNA synthesis. This suggests that even if the strand invasion was functional in *srs2Δ rad54Δ* mutants, the completion of the postreplicative gap repair by TS might be prevented by the extensive inhibition of the damage-associated DNA synthesis caused by the Rad51 filaments in the absence of the Srs2- and Rad54-mediated Rad51 clearance. As discussed in the section 6.2, ssDNA gaps appear to arise every cell cycle and are preferentially repaired by TS. Thus, it is tempting to speculate that the enzymatic removal of Rad51 might be required to complete the genome duplication during every cell cycle in *S. cerevisiae*. However, further research is needed to obtain more direct evidence for this hypothesis.

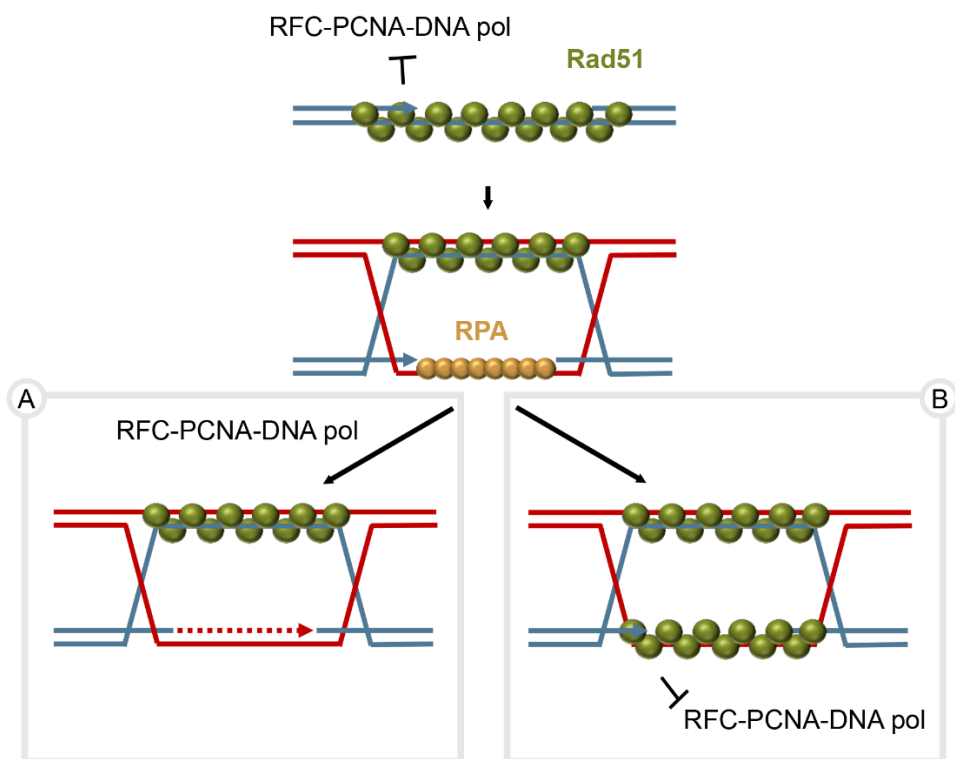


**Figure 6.1. The hypothetical outcomes of TS in the absence of Srs2- and Rad54-mediated Rad51 removal from DNA**

In cells deficient in Rad51 removal from DNA but proficient in the strand invasion during HR, a ssDNA gap could not be directly filled in by DNA polymerases due to the

Rad51-dependent inhibition of PCNA loading but a TS intermediate could be formed. During TS, the invasion of Rad51 nucleofilament into the donor duplex displaces a non-complementary strand which is then used as a template for the repair. The displaced strand is first covered by RPA. If the damage-associated DNA synthesis occurred before the formation of a Rad51 nucleofilament, Rad51 removal from DNA would not be required and the gap could be filled in by DNA polymerases (A). If the formation of Rad51 nucleofilaments preceded the recruitment of the replication machinery, the filling of a ssDNA gap in the TS intermediate would be prevented in the absence of Srs2- and Rad54-mediated Rad51 removal due to the inhibition of PCNA loading (B). Solid blue and red lines represent the strands of two sister chromatids. Arrow heads depict the 3' ends of DNA. Dotted lines represent newly synthesised DNA, and their colour indicates which DNA molecule was used as a template.

#### **6.4. The synthetic lethality of *srs2Δ* and *rad54Δ* is suppressed when the formation of stable Rad51 nucleofilaments is prevented**

As discussed above, persistent Rad51 binding to DNA hinders the repair of postreplicative gaps in *srs2Δ rad54Δ* mutants leading to their death. Consistent with this explanation, the viability of the double mutants can be restored by removing Rad51 or its mediators (204). It has been previously discovered that disrupting the function of the 9-1-1 complex involved in the DNA damage signalling also suppresses the synthetic lethality of *srs2Δ* and *rad54Δ*. This has led to a suggestion that *srs2Δ rad54Δ* mutants permanently arrest due to persistent ssDNA and the genetic elimination of the DNA damage checkpoint restores the cell viability by enabling their cell cycle progression (204). However, a time-course experiment described in the section 4.3 revealed that *P<sub>GAL1</sub>-RAD55 srs2Δ rad54Δ* mutants expressing *RAD55* do resume cell division after a relatively short G2/M arrest despite not being able to efficiently repair ssDNA gaps (Figure 4.2C). Furthermore, it was demonstrated in this study that the removal of Mec1, a protein immediately downstream of the 9-1-1 complex in the DNA damage checkpoint activation cascade, produces only a partial suppression of the *srs2Δ* and *rad54Δ* synthetic lethality (Figure 5.4C). In contrast, a loss of Exo1 nuclease which is recruited to DNA damage sites by the 9-1-1 complex (145-147) was found to strongly restore the viability of *P<sub>GAL1</sub>-RAD55 srs2Δ rad54Δ* cells grown in the presence of galactose (Figure 5.4C). Both 9-1-1 and Exo1 are involved in the

TS pathway. The *sgs1Δ* cells exposed to the ssDNA gap-inducing drug MMS accumulate TS intermediates which are normally resolved by Sgs1 (145, 148, 149). The accumulation of these recombination structures can be drastically reduced by removing either the 9-1-1 complex or Exo1 (145, 148, 149), probably because the nucleolytic expansion of ssDNA gaps is needed to produce a longer stretch of RPA-coated ssDNA capable of supporting a successful formation of Rad51 nucleofilaments. Thus, the mutations in the genes coding for Exo1 or the components of the 9-1-1 complex might suppress the synthetic lethality of *srs2Δ* and *rad54Δ* by preventing the formation of the Rad51 filaments on postreplicative gaps. The deletion of *MEC1* partially restores the viability of *srs2Δ rad54Δ* mutants, perhaps by decreasing the stability of the Rad51 nucleofilaments as the DNA damage checkpoint is required for their optimal assembly (254, 255).

A surprising observation was made in this study that the expression of meiosis-specific gene *HED1* can suppress the *srs2Δ* and *rad54Δ* synthetic lethality (Figure 5.6B). The main known function of Hed1 is to inhibit the interaction between Rad51 and Rad54 thus promoting the Dmc1-guided HR between homologous chromosomes (111, 116, 117). However, Rad54 is already missing in *srs2Δ rad54Δ* cells. It was further discovered that the growth of *P<sub>GAL1</sub>-RAD55 P<sub>GAL1</sub>-HED1 srs2Δ rad54Δ* mutants in galactose greatly depends on the RecQ helicases Sgs1 and Hrq1 (Figure 5.7B). Sgs1 has a reported ability to remove Rad51 from ssDNA *in vitro* (187). Thus, it is tempting to speculate that Hed1 binding might promote or enable the Rad51 filament disassembly by RecQ helicases *in vivo*. However, further research is required to determine how the expression of *HED1* suppresses the *srs2Δ* and *rad54Δ* synthetic lethality, what role RecQ helicases have in this process and if the RecQ helicases have a meiosis-specific role in the regulation of the Rad51 filaments.

## **6.5. The mechanistic model explaining the synthetic lethality of *srs2Δ* and *rad54Δ***

To summarise the main advances of this study, a model is proposed to describe the molecular events that take place during the postreplicative gap repair in WT cells and different mutants, explaining the genetic interactions involving *srs2Δ* and *rad54Δ* (Figure 6.2). Every S phase, DNA polymerases encounter non-damage replication barriers like secondary DNA structures, R-loops, etc. Cells likely prioritise the completion of bulk genome duplication and thus restart DNA synthesis downstream of replication impediments. The resulting ssDNA gaps are first detected and initially processed by MRX complex (143). The 9-1-1 complex is then loaded and recruits Exo1 which expands postreplicative gaps further enabling the formation of Rad51 nucleofilaments. The subsequent Rad54-mediated strand invasion allows for the gaps to be repaired by TS using sister chromatids as templates. Replication impediments could possibly be resolved before or after the filling of postreplicative gaps by TS.

Without Rad54, TS cannot occur, but the Rad51 nucleofilaments can be disassembled by Srs2, which enables the filling of ssDNA gaps by DNA polymerases as soon as replication blocks are resolved (for example, G-quadruplexes unwound by Pif1). In *srs2Δ rad54Δ* cells the simultaneous lack of Rad54- and Srs2-mediated Rad51 removal results in an inefficient damage-associated DNA synthesis incapable of supporting an adequate filling of postreplicative gaps. This leads to the accumulation of persistent and unproductive Rad51 nucleofilaments as well as excessive DNA resection by Exo1. As suggested by the experiments described in this study, *srs2Δ rad54Δ* cells appear to divide with unrepaired ssDNA gaps which are then either extensively resected or cause a collapse of replication forks during the next round of genome duplication. Without Rad54, the resulting DSBs cannot be repaired leading to cell death.

The elimination of Rad51, Rad52, Rad55, Rad57, 9-1-1 complex or Exo1 prevents the formation of Rad51 filaments. Without Rad51-mediated

inhibition of damage-associated DNA synthesis ssDNA gaps can be readily filled in by replicative DNA polymerases provided the replication impediments are resolved.

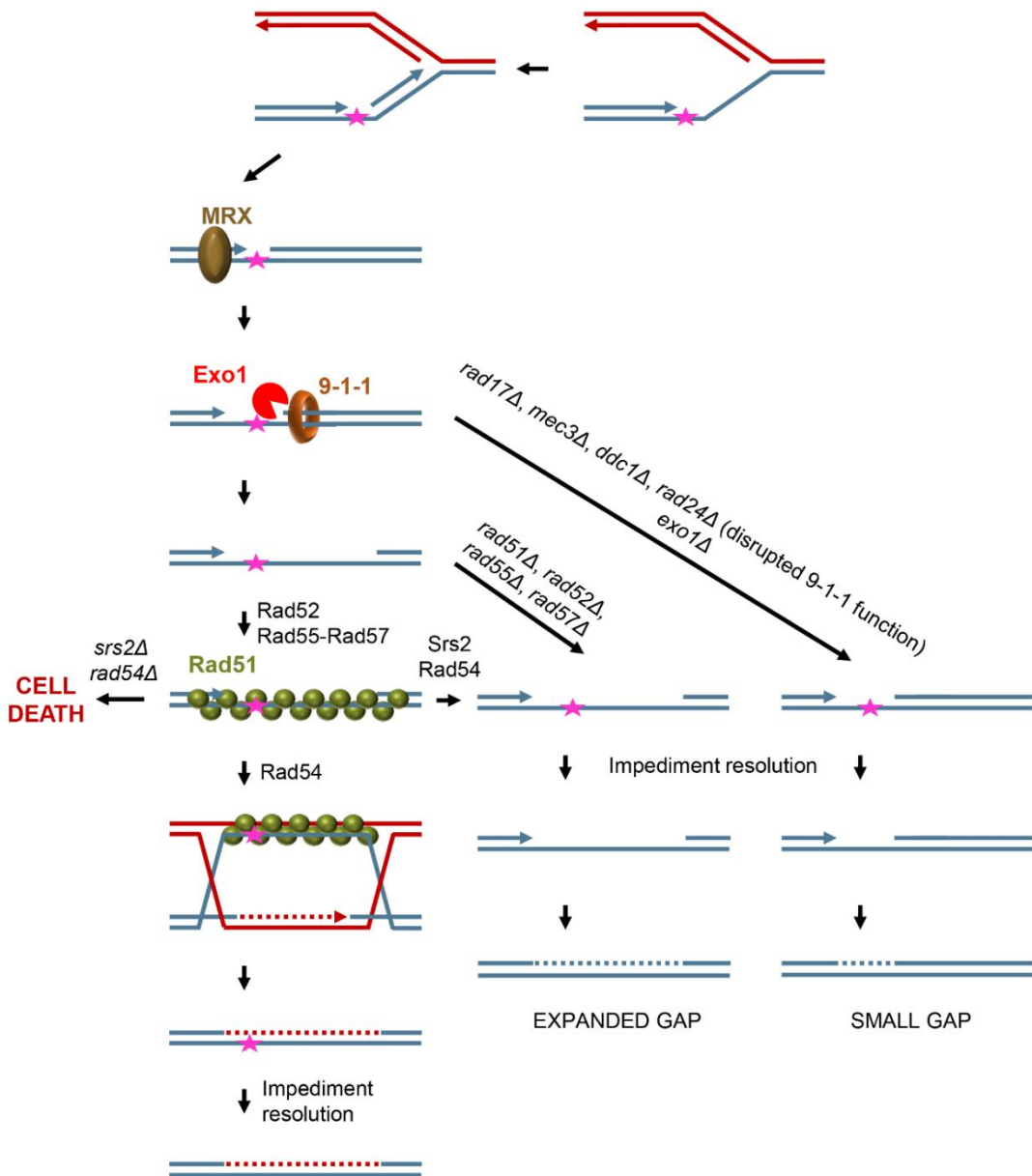


**Figure 6.2. The mechanistic model explaining the synthetic lethality of *srs2Δ* and *rad54Δ***

During DNA replication, DNA synthesis is routinely restarted downstream of endogenous non-damage replication barriers. The resulting ssDNA gaps are detected and initially processed by MRX. The 9-1-1 complex is then loaded and recruits Exo1 which expands postreplicative gaps further enabling the efficient formation of Rad51

nucleofilaments. Rad54 then catalyses the invasion of the Rad51 filaments into sister chromatids and gaps are repaired by TS. Replication impediments can be resolved before or after the repair of ssDNA gaps by TS. In the absence of strand invasion, Rad54 and Srs2 can remove Rad51 from DNA enabling gap filling by DNA polymerases as soon as the replication blocks are resolved. In *srs2Δ rad54Δ* cells, Rad51 filaments can neither invade a homologous donor nor be enzymatically disassembled making them trapped in this state for an extended period of time and thus obstructing any further repair. Genetic removal of Rad51, its mediators, 9-1-1 complex or Exo1 prevents the formation of Rad51 nucleofilaments. This eliminates the Rad51-dependent inhibition of the damage-associated DNA synthesis enabling an adequate filling of postreplicative gaps by DNA polymerases and thus suppressing the *srs2Δ* and *rad54Δ* synthetic lethality. Solid blue and red lines represent the strands of two sister chromatids. Arrow heads depict the 3' ends of DNA. Dotted lines represent newly synthesised DNA, and their colour indicates which DNA molecule was used as a template. Pink star depicts a replication impediment.

Overall, the investigation of the processes that take place during the death of *srs2Δ rad54Δ* double mutants described in this study further emphasises the importance of the enzymatic disassembly of Rad51 nucleofilaments during DNA repair. Moreover, experiments performed here imply that *S. cerevisiae* cells frequently restart DNA synthesis downstream of endogenous non-damage replication barriers during DNA replication generating ssDNA gaps which are preferentially repaired by Rad51-mediated recombination. This suggests that the Srs2- and Rad54-mediated disassembly of Rad51 nucleofilaments is required not only in response to DNA damage but also during normal cellular physiology and might be essential for the cell survival.

## References

1. Jackson SP, Bartek J. The DNA-damage response in human biology and disease. *Nature*. 2009;461(7267):1071-8.
2. Roos WP, Thomas AD, Kaina B. DNA damage and the balance between survival and death in cancer biology. *Nat Rev Cancer*. 2016;16(1):20-33.
3. Chatterjee N, Walker GC. Mechanisms of DNA damage, repair, and mutagenesis. *Environ Mol Mutagen*. 2017;58(5):235-63.
4. Taylor EM, Lehmann AR. Conservation of eukaryotic DNA repair mechanisms. *Int J Radiat Biol*. 1998;74(3):277-86.
5. Swenberg JA, Lu K, Moeller BC, Gao L, Upton PB, Nakamura J, et al. Endogenous versus exogenous DNA adducts: their role in carcinogenesis, epidemiology, and risk assessment. *Toxicol Sci*. 2011;120 Suppl 1:S130-45.
6. De Bont R, van Larebeke N. Endogenous DNA damage in humans: a review of quantitative data. *Mutagenesis*. 2004;19(3):169-85.
7. Boiteux S, Jinks-Robertson S. DNA repair mechanisms and the bypass of DNA damage in *Saccharomyces cerevisiae*. *Genetics*. 2013;193(4):1025-64.
8. Kelley MR, Kow YW, Wilson DM, 3rd. Disparity between DNA base excision repair in yeast and mammals: translational implications. *Cancer Res*. 2003;63(3):549-54.
9. Tatum D, Li S. Nucleotide Excision Repair in *S. cerevisiae*. *DNA Repair - On the Pathways to Fixing DNA Damage and Errors* 2011.
10. Xie Z. Roles of Rad23 protein in yeast nucleotide excision repair. *Nucleic Acids Research*. 2004;32(20):5981-90.
11. Dulk Bd, Sun SM, de Ruijter M, Brandsma JA, Brouwer J. Rad33, a new factor involved in nucleotide excision repair in *Saccharomyces cerevisiae*. *DNA Repair*. 2006;5(6):683-92.
12. Koch SC, Kuper J, Gasteiger KL, Simon N, Strasser R, Eisen D, et al. Structural insights into the recognition of cisplatin and AAF-dG lesion by Rad14 (XPA). *Proc Natl Acad Sci U S A*. 2015;112(27):8272-7.
13. Sugasawa K. A multistep damage recognition mechanism for global genomic nucleotide excision repair. *Genes & Development*. 2001;15(5):507-21.
14. Nick McElhinny SA, Watts BE, Kumar D, Watt DL, Lundstrom EB, Burgers PMJ, et al. Abundant ribonucleotide incorporation into DNA by yeast replicative polymerases. *Proceedings of the National Academy of Sciences*. 2010;107(11):4949-54.
15. Sparks Justin L, Chon H, Cerritelli Susana M, Kunkel Thomas A, Johansson E, Crouch Robert J, et al. RNase H2-Initiated Ribonucleotide Excision Repair. *Molecular Cell*. 2012;47(6):980-6.
16. Fishel R. Mismatch repair. *J Biol Chem*. 2015;290(44):26395-403.
17. Pluciennik A, Dzantiev L, Iyer RR, Constantin N, Kadyrov FA, Modrich P. PCNA function in the activation and strand direction of MutLalpha endonuclease in mismatch repair. *Proc Natl Acad Sci U S A*. 2010;107(37):16066-71.
18. Ghodgaonkar Medini M, Lazzaro F, Olivera-Pimentel M, Artola-Borán M, Cejka P, Reijns Martin A, et al. Ribonucleotides Misincorporated into DNA Act as Strand-Discrimination Signals in Eukaryotic Mismatch Repair. *Molecular Cell*. 2013;50(3):323-32.
19. Lujan Scott A, Williams Jessica S, Clausen Anders R, Clark Alan B, Kunkel Thomas A. Ribonucleotides Are Signals for Mismatch Repair of Leading-Strand Replication Errors. *Molecular Cell*. 2013;50(3):437-43.
20. Paques F, Haber JE. Multiple pathways of recombination induced by double-strand breaks in *Saccharomyces cerevisiae*. *Microbiol Mol Biol Rev*. 1999;63(2):349-404.

21. Chapman JR, Taylor Martin RG, Boulton Simon J. Playing the End Game: DNA Double-Strand Break Repair Pathway Choice. *Molecular Cell*. 2012;47(4):497-510.
22. Jackson SP. Sensing and repairing DNA double-strand breaks. *Carcinogenesis*. 2002;23(5):687-96.
23. Emerson CH, Bertuch AA. Consider the workhorse: Nonhomologous end-joining in budding yeast. *Biochemistry and Cell Biology*. 2016;94(5):396-406.
24. Wu D, Topper LM, Wilson TE. Recruitment and Dissociation of Nonhomologous End Joining Proteins at a DNA Double-Strand Break in *Saccharomyces cerevisiae*. *Genetics*. 2008;178(3):1237-49.
25. Gobbini E, Cassani C, Villa M, Bonetti D, Longhese M. Functions and regulation of the MRX complex at DNA double-strand breaks. *Microbial Cell*. 2016;3(8):329-37.
26. Daley JM, Palmbos PL, Wu D, Wilson TE. Nonhomologous end joining in yeast. *Annu Rev Genet*. 2005;39:431-51.
27. Karanam K, Kafri R, Loewer A, Lahav G. Quantitative Live Cell Imaging Reveals a Gradual Shift between DNA Repair Mechanisms and a Maximal Use of HR in Mid S Phase. *Molecular Cell*. 2012;47(2):320-9.
28. Sfeir A, Symington LS. Microhomology-Mediated End Joining: A Back-up Survival Mechanism or Dedicated Pathway? *Trends in Biochemical Sciences*. 2015;40(11):701-14.
29. Dudášová Z, Dudáš A, Chovanec M. Non-homologous end-joining factors of *Saccharomyces cerevisiae*. *FEMS Microbiology Reviews*. 2004;28(5):581-601.
30. Krejci L, Altmannova V, Spirek M, Zhao X. Homologous recombination and its regulation. *Nucleic Acids Res*. 2012;40(13):5795-818.
31. Andriuskevicius T, Kotenko O, Makovets S. Putting together and taking apart: assembly and disassembly of the Rad51 nucleoprotein filament in DNA repair and genome stability. *Cell Stress*. 2018;2(5):96-112.
32. Symington LS. Mechanism and regulation of DNA end resection in eukaryotes. *Critical Reviews in Biochemistry and Molecular Biology*. 2016;51(3):195-212.
33. Donniani RA, Symington LS. Break-induced replication occurs by conservative DNA synthesis. *Proceedings of the National Academy of Sciences*. 2013;110(33):13475-80.
34. Zhu Z, Chung W-H, Shim EY, Lee SE, Ira G. Sgs1 Helicase and Two Nucleases Dna2 and Exo1 Resect DNA Double-Strand Break Ends. *Cell*. 2008;134(6):981-94.
35. Game JC, Mortimer RK. A genetic study of X-ray sensitive mutants in yeast. *Mutation Research/Fundamental and Molecular Mechanisms of Mutagenesis*. 1974;24(3):281-92.
36. Malkova A, Ivanov EL, Haber JE. Double-strand break repair in the absence of RAD51 in yeast: a possible role for break-induced DNA replication. *Proceedings of the National Academy of Sciences*. 1996;93(14):7131-6.
37. Lim DS, Hasty P. A mutation in mouse rad51 results in an early embryonic lethal that is suppressed by a mutation in p53. *Molecular and Cellular Biology*. 1996;16(12):7133-43.
38. Sonoda E. Rad51-deficient vertebrate cells accumulate chromosomal breaks prior to cell death. *The EMBO Journal*. 1998;17(2):598-608.
39. Shinohara A, Ogawa H, Ogawa T. Rad51 protein involved in repair and recombination in *S. cerevisiae* is a RecA-like protein. *Cell*. 1992;69(3):457-70.
40. Yu X, Jacobs SA, West SC, Ogawa T, Egelman EH. Domain structure and dynamics in the helical filaments formed by RecA and Rad51 on DNA. *Proceedings of the National Academy of Sciences*. 2001;98(15):8419-24.
41. Danilowicz C, Peacock-Villada A, Vlassakis J, Facon A, Feinstein E, Kleckner N, et al. The differential extension in dsDNA bound to Rad51 filaments may play important roles in homology recognition and strand exchange. *Nucleic Acids Research*. 2014;42(1):526-33.

42. Short JM, Liu Y, Chen S, Soni N, Madhusudhan MS, Shivji MKK, et al. High-resolution structure of the presynaptic RAD51 filament on single-stranded DNA by electron cryo-microscopy. *Nucleic Acids Research*. 2016.
43. Conway AB, Lynch TW, Zhang Y, Fortin GS, Fung CW, Symington LS, et al. Crystal structure of a Rad51 filament. *Nature Structural & Molecular Biology*. 2004;11(8):791-6.
44. Ma CJ, Gibb B, Kwon Y, Sung P, Greene EC. Protein dynamics of human RPA and RAD51 on ssDNA during assembly and disassembly of the RAD51 filament. *Nucleic Acids Research*. 2017;45(2):749-61.
45. Prasad TK, Yeykal CC, Greene EC. Visualizing the Assembly of Human Rad51 Filaments on Double-stranded DNA. *Journal of Molecular Biology*. 2006;363(3):713-28.
46. Zhang X-P, Galkin VE, Yu X, Egelman EH, Heyer W-D. Loop 2 in *Saccharomyces cerevisiae* Rad51 protein regulates filament formation and ATPase activity. *Nucleic Acids Research*. 2009;37(1):158-71.
47. Matsuo Y, Sakane I, Takizawa Y, Takahashi M, Kurumizaka H. Roles of the human Rad51 L1 and L2 loops in DNA binding. *FEBS Journal*. 2006;273(14):3148-59.
48. Baumann P, Benson FE, West SC. Human Rad51 Protein Promotes ATP-Dependent Homologous Pairing and Strand Transfer Reactions In Vitro. *Cell*. 1996;87(4):757-66.
49. Sung P. Catalysis of ATP-dependent homologous DNA pairing and strand exchange by yeast RAD51 protein. *Science*. 1994;265(5176):1241-3.
50. Sung P, Robberson DL. DNA strand exchange mediated by a RAD51-ssDNA nucleoprotein filament with polarity opposite to that of RecA. *Cell*. 1995;82(3):453-61.
51. Benson FE, Stasiak A, West SC. Purification and characterization of the human Rad51 protein, an analogue of *E. coli* RecA. *EMBO J*. 1994;13(23):5764-71.
52. Ogawa T, Yu X, Shinohara A, Egelman E. Similarity of the yeast RAD51 filament to the bacterial RecA filament. *Science*. 1993;259(5103):1896-9.
53. Morrison C, Shinohara A, Sonoda E, Yamaguchi-Iwai Y, Takata M, Weichselbaum RR, et al. The Essential Functions of Human Rad51 Are Independent of ATP Hydrolysis. *Molecular and Cellular Biology*. 1999;19(10):6891-7.
54. Sung P, Stratton SA. Yeast Rad51 Recombinase Mediates Polar DNA Strand Exchange in the Absence of ATP Hydrolysis. *Journal of Biological Chemistry*. 1996;271(45):27983-6.
55. Antony E, Tomko EJ, Xiao Q, Krejci L, Lohman TM, Ellenberger T. Srs2 Disassembles Rad51 Filaments by a Protein-Protein Interaction Triggering ATP Turnover and Dissociation of Rad51 from DNA. *Molecular Cell*. 2009;35(1):105-15.
56. Shim K-S, Schmutte C, Yoder K, Fishel R. Defining the salt effect on human RAD51 activities. *DNA Repair*. 2006;5(6):718-30.
57. Chi P, Van Komen S, Sehorn MG, Sigurdsson S, Sung P. Roles of ATP binding and ATP hydrolysis in human Rad51 recombinase function. *DNA Repair*. 2006;5(3):381-91.
58. Wang X, Haber JE. Role of *Saccharomyces* Single-Stranded DNA-Binding Protein RPA in the Strand Invasion Step of Double-Strand Break Repair. *PLoS Biology*. 2004;2(1).
59. Sung P. Function of Yeast Rad52 Protein as a Mediator between Replication Protein A and the Rad51 Recombinase. *Journal of Biological Chemistry*. 1997;272(45):28194-7.
60. Milne GT, Weaver DT. Dominant negative alleles of RAD52 reveal a DNA repair/recombination complex including Rad51 and Rad52. *Genes & Development*. 1993;7(9):1755-65.
61. Shinohara A, Shinohara M, Ohta T, Matsuda S, Ogawa T. Rad52 forms ring structures and co-operates with RPA in single-strand DNA annealing. *Genes to Cells*. 2003;3(3):145-56.

62. Hays SL, Firmenich AA, Massey P, Banerjee R, Berg P. Studies of the Interaction between Rad52 Protein and the Yeast Single-Stranded DNA Binding Protein RPA. *Molecular and Cellular Biology*. 1998;18(7):4400-6.
63. Stauffer ME, Chazin WJ. Physical Interaction between Replication Protein A and Rad51 Promotes Exchange on Single-stranded DNA. *Journal of Biological Chemistry*. 2004;279(24):25638-45.
64. Gibb B, Ye LF, Kwon Y, Niu H, Sung P, Greene EC. Protein dynamics during presynaptic-complex assembly on individual single-stranded DNA molecules. *Nature Structural & Molecular Biology*. 2014;21(10):893-900.
65. Sugawara N, Wang X, Haber JE. In vivo roles of Rad52, Rad54, and Rad55 proteins in Rad51-mediated recombination. *Mol Cell*. 2003;12(1):209-19.
66. Miyazaki T, Bressan DA, Shinohara M, Haber JE, Shinohara A. In vivo assembly and disassembly of Rad51 and Rad52 complexes during double-strand break repair. *The EMBO Journal*. 2004;23(4):939-49.
67. Lisby M, Barlow JH, Burgess RC, Rothstein R. Choreography of the DNA Damage Response. *Cell*. 2004;118(6):699-713.
68. Sung P. Yeast Rad55 and Rad57 proteins form a heterodimer that functions with replication protein A to promote DNA strand exchange by Rad51 recombinase. *Genes Dev*. 1997;11(9):1111-21.
69. Hays SL, Firmenich AA, Berg P. Complex formation in yeast double-strand break repair: participation of Rad51, Rad52, Rad55, and Rad57 proteins. *Proc Natl Acad Sci U S A*. 1995;92(15):6925-9.
70. Fortin GS, Symington LS. Mutations in yeast Rad51 that partially bypass the requirement for Rad55 and Rad57 in DNA repair by increasing the stability of Rad51-DNA complexes. *EMBO J*. 2002;21(12):3160-70.
71. Liu J, Renault L, Veaute X, Fabre F, Stahlberg H, Heyer W-D. Rad51 paralogues Rad55–Rad57 balance the antirecombinase Srs2 in Rad51 filament formation. *Nature*. 2011;479(7372):245-8.
72. Roy U, Kwon Y, Marie L, Symington L, Sung P, Lisby M, et al. The Rad51 paralog complex Rad55-Rad57 acts as a molecular chaperone during homologous recombination. *Molecular Cell*. 2021;81(5):1043-57.e8.
73. Fung CW, Mozlin AM, Symington LS. Suppression of the Double-Strand-Break-Repair Defect of the *Saccharomyces cerevisiae rad57* mutant. *Genetics*. 2009;181(4):1195-206.
74. Tavares EM, Wright WD, Heyer W-D, Le Cam E, Dupaigne P. In vitro role of Rad54 in Rad51-ssDNA filament-dependent homology search and synaptic complexes formation. *Nature Communications*. 2019;10(1).
75. Qi Z, Redding S, Lee Ja Y, Gibb B, Kwon Y, Niu H, et al. DNA Sequence Alignment by Microhomology Sampling during Homologous Recombination. *Cell*. 2015;160(5):856-69.
76. Renkawitz J, Lademann Claudio A, Kalocsay M, Jentsch S. Monitoring Homology Search during DNA Double-Strand Break Repair In Vivo. *Molecular Cell*. 2013;50(2):261-72.
77. Renkawitz J, Lademann CA, Jentsch S. Mechanisms and principles of homology search during recombination. *Nature Reviews Molecular Cell Biology*. 2014;15(6):369-83.
78. Sung P, Krejci L, Van Komen S, Sehorn MG. Rad51 Recombinase and Recombination Mediators. *Journal of Biological Chemistry*. 2003;278(44):42729-32.
79. Sinha M, Peterson CL. A Rad51 Presynaptic Filament Is Sufficient to Capture Nucleosomal Homology during Recombinational Repair of a DNA Double-Strand Break. *Molecular Cell*. 2008;30(6):803-10.
80. Zhang Z, Fan H-Y, Goldman JA, Kingston RE. Homology-driven chromatin remodeling by human RAD54. *Nature Structural & Molecular Biology*. 2007;14(5):397-405.

81. Petukhova G, Van Komen S, Vergano S, Klein H, Sung P. Yeast Rad54 Promotes Rad51-dependent Homologous DNA Pairing via ATP Hydrolysis-driven Change in DNA Double Helix Conformation. *Journal of Biological Chemistry*. 1999;274(41):29453-62.
82. Ristic D, Wyman C, Paulusma C, Kanaar R. The architecture of the human Rad54-DNA complex provides evidence for protein translocation along DNA. *Proceedings of the National Academy of Sciences*. 2001;98(15):8454-60.
83. Van Komen S, Petukhova G, Sigurdsson S, Stratton S, Sung P. Superhelicity-Driven Homologous DNA Pairing by Yeast Recombination Factors Rad51 and Rad54. *Molecular Cell*. 2000;6(3):563-72.
84. Chen J-M, Cooper DN, Chuzhanova N, Férec C, Patrinos GP. Gene conversion: mechanisms, evolution and human disease. *Nature Reviews Genetics*. 2007;8(10):762-75.
85. Jain S, Sugawara N, Haber JE. Role of Double-Strand Break End-Tethering during Gene Conversion in *Saccharomyces cerevisiae*. *PLOS Genetics*. 2016;12(4).
86. Matos J, West SC. Holliday junction resolution: Regulation in space and time. *DNA Repair*. 2014;19:176-81.
87. Ashton TM, Mankouri HW, Heidenblut A, McHugh PJ, Hickson ID. Pathways for Holliday Junction Processing during Homologous Recombination in *Saccharomyces cerevisiae*. *Molecular and Cellular Biology*. 2011;31(9):1921-33.
88. San-Segundo PA, Clemente-Blanco A. Resolvases, Dissolvases, and Helicases in Homologous Recombination: Clearing the Road for Chromosome Segregation. *Genes*. 2020;11(1).
89. Chavdarova M, Marini V, Sisakova A, Sedlackova H, Vigasova D, Brill SJ, et al. Srs2 promotes Mus81–Mms4-mediated resolution of recombination intermediates. *Nucleic Acids Research*. 2015;43(7):3626-42.
90. Keyamura K, Arai K, Hishida T. Srs2 and Mus81–Mms4 Prevent Accumulation of Toxic Inter-Homolog Recombination Intermediates. *PLOS Genetics*. 2016;12(7).
91. Liu J, Ede C, Wright WD, Gore SK, Jenkins SS, Freudenthal BD, et al. Srs2 promotes synthesis-dependent strand annealing by disrupting DNA polymerase δ-extending D-loops. *eLife*. 2017;6.
92. Mitchel K, Lehner K, Jinks-Robertson S. Heteroduplex DNA Position Defines the Roles of the Sgs1, Srs2, and Mph1 Helicases in Promoting Distinct Recombination Outcomes. *PLoS Genetics*. 2013;9(3).
93. Matos J, Blanco Miguel G, Maslen S, Skehel JM, West Stephen C. Regulatory Control of the Resolution of DNA Recombination Intermediates during Meiosis and Mitosis. *Cell*. 2011;147(1):158-72.
94. Saini N, Ramakrishnan S, Elango R, Ayyar S, Zhang Y, Deem A, et al. Migrating bubble during break-induced replication drives conservative DNA synthesis. *Nature*. 2013;502(7471):389-92.
95. Rodgers K, McVey M. Error-Prone Repair of DNA Double-Strand Breaks. *Journal of Cellular Physiology*. 2016;231(1):15-24.
96. Bhargava R, Onyango DO, Stark JM. Regulation of Single-Strand Annealing and its Role in Genome Maintenance. *Trends in Genetics*. 2016;32(9):566-75.
97. Sugiyama T, New JH, Kowalczykowski SC. DNA annealing by Rad52 Protein is stimulated by specific interaction with the complex of replication protein A and single-stranded DNA. *Proceedings of the National Academy of Sciences*. 1998;95(11):6049-54.
98. So A, Muhammad A, Chailleux C, Sanz LS, Ragu S, Le Cam E, et al. Mammalian RAD51 prevents non-conservative alternative end-joining and single strand annealing through non-catalytic mechanisms. *bioRxiv*. 2019;768887.
99. Davis AP, Symington LS. The yeast recombinational repair protein Rad59 interacts with Rad52 and stimulates single-strand annealing. *Genetics*. 2001;159(2):515-25.

100. Davies AA, Friedberg EC, Tomkinson AE, Wood RD, West SC. Role of the Rad1 and Rad10 Proteins in Nucleotide Excision Repair and Recombination. *Journal of Biological Chemistry*. 1995;270(42):24638-41.
101. Sugawara N, Ira G, Haber JE. DNA Length Dependence of the Single-Strand Annealing Pathway and the Role of *Saccharomyces cerevisiae* RAD59 in Double-Strand Break Repair. *Molecular and Cellular Biology*. 2000;20(14):5300-9.
102. Pohl TJ, Nickoloff JA. Rad51-Independent Interchromosomal Double-Strand Break Repair by Gene Conversion Requires Rad52 but Not Rad55, Rad57, or Dmc1. *Molecular and Cellular Biology*. 2008;28(3):897-906.
103. Vasianovich Y, Altmannova V, Kotenko O, Newton MD, Krejci L, Makovets S. Unloading of homologous recombination factors is required for restoring double-stranded DNA at damage repair loci. *EMBO J*. 2017;36(2):213-31.
104. Wu Y, Kantake N, Sugiyama T, Kowalczykowski SC. Rad51 protein controls Rad52-mediated DNA annealing. *J Biol Chem*. 2008;283(21):14883-92.
105. McIlwraith MJ, West SC. DNA Repair Synthesis Facilitates RAD52-Mediated Second-End Capture during DSB Repair. *Molecular Cell*. 2008;29(4):510-6.
106. Wilson TE. A genomics-based screen for yeast mutants with an altered recombination/end-joining repair ratio. *Genetics*. 2002;162(2):677-88.
107. Brown MS, Bishop DK. DNA Strand Exchange and RecA Homologs in Meiosis. *Cold Spring Harbor Perspectives in Biology*. 2015;7(1).
108. Yadav VK, Claeys Bouuaert C. Mechanism and Control of Meiotic DNA Double-Strand Break Formation in *S. cerevisiae*. *Frontiers in Cell and Developmental Biology*. 2021;9.
109. Symington LS. End Resection at Double-Strand Breaks: Mechanism and Regulation. *Cold Spring Harbor Perspectives in Biology*. 2014;6(8):a016436-a.
110. Shinohara M, Shita-Yamaguchi E, Buerstedde JM, Shinagawa H, Ogawa H, Shinohara A. Characterization of the roles of the *Saccharomyces cerevisiae* RAD54 gene and a homologue of RAD54, RDH54/TID1, in mitosis and meiosis. *Genetics*. 1997;147(4):1545-56.
111. Crickard JB, Kaniecki K, Kwon Y, Sung P, Lisby M, Greene EC. Regulation of Hed1 and Rad54 binding during maturation of the meiosis-specific presynaptic complex. *The EMBO Journal*. 2018;37(7).
112. Chi P, Kwon Y, Moses DN, Seong C, Sehorn MG, Singh AK, et al. Functional interactions of meiotic recombination factors Rdh54 and Dmc1. *DNA Repair*. 2009;8(2):279-84.
113. Allers T, Lichten M. Differential Timing and Control of Noncrossover and Crossover Recombination during Meiosis. *Cell*. 2001;106(1):47-57.
114. Bishop DK, Zickler D. Early Decision: Meiotic Crossover Interference prior to Stable Strand Exchange and Synapsis. *Cell*. 2004;117(1):9-15.
115. Lao JP, Cloud V, Huang C-C, Grubb J, Thacker D, Lee C-Y, et al. Meiotic Crossover Control by Concerted Action of Rad51-Dmc1 in Homolog Template Bias and Robust Homeostatic Regulation. *PLoS Genetics*. 2013;9(12).
116. Busygina V, Sehorn MG, Shi IY, Tsubouchi H, Roeder GS, Sung P. Hed1 regulates Rad51-mediated recombination via a novel mechanism. *Genes & Development*. 2008;22(6):786-95.
117. Busygina V, Saro D, Williams G, Leung W-K, Say AF, Sehorn MG, et al. Novel Attributes of Hed1 Affect Dynamics and Activity of the Rad51 Presynaptic Filament during Meiotic Recombination\*. *Journal of Biological Chemistry*. 2012;287(2):1566-75.
118. Zeman MK, Cimprich KA. Causes and consequences of replication stress. *Nature Cell Biology*. 2013;16(1):2-9.

119. Prado F. Homologous recombination maintenance of genome integrity during DNA damage tolerance. *Molecular & Cellular Oncology*. 2014;1(2).
120. Bi X. Mechanism of DNA damage tolerance. *World Journal of Biological Chemistry*. 2015;6(3).
121. Waters LS, Minesinger BK, Wiltzout ME, D'Souza S, Woodruff RV, Walker GC. Eukaryotic Translesion Polymerases and Their Roles and Regulation in DNA Damage Tolerance. *Microbiology and Molecular Biology Reviews*. 2009;73(1):134-54.
122. Mankouri HW, Ngo H-P, Hickson ID, Bickmore W. Shu Proteins Promote the Formation of Homologous Recombination Intermediates That Are Processed by Sgs1-Rmi1-Top3. *Molecular Biology of the Cell*. 2007;18(10):4062-73.
123. Mankouri HW, Ashton TM, Hickson ID. Holliday junction-containing DNA structures persist in cells lacking Sgs1 or Top3 following exposure to DNA damage. *Proceedings of the National Academy of Sciences*. 2011;108(12):4944-9.
124. Szakal B, Branzei D. Premature Cdk1/Cdc5/Mus81 pathway activation induces aberrant replication and deleterious crossover. *The EMBO Journal*. 2013;32(8):1155-67.
125. Hoege C, Pfander B, Moldovan G-L, Pyrowolakis G, Jentsch S. RAD6-dependent DNA repair is linked to modification of PCNA by ubiquitin and SUMO. *Nature*. 2002;419(6903):135-41.
126. Karras GI, Jentsch S. The RAD6 DNA Damage Tolerance Pathway Operates Uncoupled from the Replication Fork and Is Functional Beyond S Phase. *Cell*. 2010;141(2):255-67.
127. Urulangodi M, Sebesta M, Menolfi D, Szakal B, Sollier J, Sisakova A, et al. Local regulation of the Srs2 helicase by the SUMO-like domain protein Esc2 promotes recombination at sites of stalled replication. *Genes & Development*. 2015;29(19):2067-80.
128. Neelsen KJ, Lopes M. Replication fork reversal in eukaryotes: from dead end to dynamic response. *Nature Reviews Molecular Cell Biology*. 2015;16(4):207-20.
129. Meng X, Zhao X. Replication fork regression and its regulation. *FEMS Yeast Research*. 2016.
130. Lopes M, Foiani M, Sogo JM. Multiple Mechanisms Control Chromosome Integrity after Replication Fork Uncoupling and Restart at Irreparable UV Lesions. *Molecular Cell*. 2006;21(1):15-27.
131. Hashimoto Y, Ray Chaudhuri A, Lopes M, Costanzo V. Rad51 protects nascent DNA from Mre11-dependent degradation and promotes continuous DNA synthesis. *Nature Structural & Molecular Biology*. 2010;17(11):1305-11.
132. Branzei D, Foiani M. Maintaining genome stability at the replication fork. *Nature Reviews Molecular Cell Biology*. 2010;11(3):208-19.
133. Daigaku Y, Davies AA, Ulrich HD. Ubiquitin-dependent DNA damage bypass is separable from genome replication. *Nature*. 2010;465(7300):951-5.
134. Wong RP, García-Rodríguez N, Zilio N, Hanulová M, Ulrich HD. Processing of DNA Polymerase-Blocking Lesions during Genome Replication Is Spatially and Temporally Segregated from Replication Forks. *Molecular Cell*. 2020;77(1):3-16.e4.
135. Maffia A, Ranise C, Sabbioneda S. From R-Loops to G-Quadruplexes: Emerging New Threats for the Replication Fork. *International Journal of Molecular Sciences*. 2020;21(4).
136. Schiavone D, Jozwiakowski SK, Romanello M, Guilbaud G, Guilliam TA, Bailey LJ, et al. PrimPol Is Required for Replicative Tolerance of G Quadruplexes in Vertebrate Cells. *Molecular Cell*. 2016;61(1):161-9.
137. Švirković S, Crisp A, Tan-Wong SM, Guilliam TA, Doherty AJ, Proudfoot NJ, et al. R-loop formation during S phase is restricted by PrimPol-mediated repriming. *The EMBO Journal*. 2018;38(3).

138. Fumasoni M, Zwicky K, Vanoli F, Lopes M, Branzei D. Error-Free DNA Damage Tolerance and Sister Chromatid Proximity during DNA Replication Rely on the Pol $\alpha$ /Primase/Ctf4 Complex. *Molecular Cell*. 2015;57(5):812-23.
139. Paeschke K, Capra John A, Zakian Virginia A. DNA Replication through G-Quadruplex Motifs Is Promoted by the *Saccharomyces cerevisiae* Pif1 DNA Helicase. *Cell*. 2011;145(5):678-91.
140. Lockhart A, Pires VB, Bento F, Kellner V, Luke-Glaser S, Yakoub G, et al. RNase H1 and H2 Are Differentially Regulated to Process RNA-DNA Hybrids. *Cell Reports*. 2019;29(9):2890-900.e5.
141. Piberger AL, Bowry A, Kelly RDW, Walker AK, González-Acosta D, Bailey LJ, et al. PrimPol-dependent single-stranded gap formation mediates homologous recombination at bulky DNA adducts. *Nature Communications*. 2020;11(1).
142. Kolinjivadi AM, Sannino V, de Antoni A, Técher H, Baldi G, Costanzo V. Moonlighting at replication forks - a new life for homologous recombination proteins BRCA1, BRCA2 and RAD51. *FEBS Letters*. 2017;591(8):1083-100.
143. Ball LG, Hanna MD, Lambrecht AD, Mitchell BA, Ziola B, Cobb JA, et al. The Mre11-Rad50-Xrs2 Complex Is Required for Yeast DNA Postreplication Repair. *PLoS ONE*. 2014;9(10).
144. Pages V, Santa Maria SR, Prakash L, Prakash S. Role of DNA damage-induced replication checkpoint in promoting lesion bypass by translesion synthesis in yeast. *Genes & Development*. 2009;23(12):1438-49.
145. Karras Georgios I, Fumasoni M, Sienski G, Vanoli F, Branzei D, Jentsch S. Noncanonical Role of the 9-1-1 Clamp in the Error-Free DNA Damage Tolerance Pathway. *Molecular Cell*. 2013;49(3):536-46.
146. Ngo GHP, Lydall D. The 9-1-1 checkpoint clamp coordinates resection at DNA double strand breaks. *Nucleic Acids Research*. 2015;43(10):5017-32.
147. Ngo GHP, Balakrishnan L, Dubarry M, Campbell JL, Lydall D. The 9-1-1 checkpoint clamp stimulates DNA resection by Dna2-Sgs1 and Exo1. *Nucleic Acids Research*. 2014;42(16):10516-28.
148. Korolev S, Ball LG, Hanna MD, Lambrecht AD, Mitchell BA, Ziola B, et al. The Mre11-Rad50-Xrs2 Complex Is Required for Yeast DNA Postreplication Repair. *PLoS ONE*. 2014;9(10).
149. Vanoli F, Fumasoni M, Szakal B, Maloisel L, Branzei D. Replication and Recombination Factors Contributing to Recombination-Dependent Bypass of DNA Lesions by Template Switch. *PLoS Genetics*. 2010;6(11).
150. García-Rodríguez N, Wong RP, Ulrich HD. The helicase Pif1 functions in the template switching pathway of DNA damage bypass. *Nucleic Acids Research*. 2018;46(16):8347-56.
151. Fabre F, Chan A, Heyer WD, Gangloff S. Alternate pathways involving Sgs1/Top3, Mus81/ Mms4, and Srs2 prevent formation of toxic recombination intermediates from single-stranded gaps created by DNA replication. *Proceedings of the National Academy of Sciences*. 2002;99(26):16887-92.
152. Waterman DP, Haber JE, Smolka MB. Checkpoint Responses to DNA Double-Strand Breaks. *Annual Review of Biochemistry*. 2020;89(1):103-33.
153. Finn K, Lowndes NF, Grenon M. Eukaryotic DNA damage checkpoint activation in response to double-strand breaks. *Cellular and Molecular Life Sciences*. 2011;69(9):1447-73.
154. Mantiero D, Clerici M, Lucchini G, Longhese MP. Dual role for *Saccharomyces cerevisiae* Tel1 in the checkpoint response to double-strand breaks. *EMBO reports*. 2007;8(4):380-7.

155. Navadgi-Patil VM, Burgers PM. The Unstructured C-Terminal Tail of the 9-1-1 Clamp Subunit Ddc1 Activates Mec1/ATR via Two Distinct Mechanisms. *Molecular Cell*. 2009;36(5):743-53.
156. Puddu F, Granata M, Di Nola L, Balestrini A, Piergiovanni G, Lazzaro F, et al. Phosphorylation of the Budding Yeast 9-1-1 Complex Is Required for Dpb11 Function in the Full Activation of the UV-Induced DNA Damage Checkpoint. *Molecular and Cellular Biology*. 2008;28(15):4782-93.
157. Pfander B, Diffley JFX. Dpb11 coordinates Mec1 kinase activation with cell cycle-regulated Rad9 recruitment. *The EMBO Journal*. 2011;30(24):4897-907.
158. Sanchez Y. Control of the DNA Damage Checkpoint by Chk1 and Rad53 Protein Kinases Through Distinct Mechanisms. *Science*. 1999;286(5442):1166-71.
159. Surana U, Lim HH, Shi I, Chia DB, Yam Candice Qiu X. Dun1, a Chk2-related kinase, is the central regulator of securin-separase dynamics during DNA damage signaling. *Nucleic Acids Research*. 2020;48(11):6092-107.
160. Pellicoli A, Lee SE, Lucca C, Foiani M, Haber JE. Regulation of *Saccharomyces* Rad53 checkpoint kinase during adaptation from DNA damage-induced G2/M arrest. *Mol Cell*. 2001;7(2):293-300.
161. Balogun FO, Truman AW, Kron SJ. DNA resection proteins Sgs1 and Exo1 are required for G1 checkpoint activation in budding yeast. *DNA Repair*. 2013;12(9):751-60.
162. Gerald JN, Benjamin JM, Kron SJ. Robust G1 checkpoint arrest in budding yeast: dependence on DNA damage signaling and repair. *J Cell Sci*. 2002;115(Pt 8):1749-57.
163. Al-Moghrabi NM. The *Saccharomyces cerevisiae* RAD9 cell cycle checkpoint gene is required for optimal repair of UV-induced pyrimidine dimers in both G1 and G2/M phases of the cell cycle. *Nucleic Acids Research*. 2001;29(10):2020-5.
164. Jossen R, Bermejo R. The DNA damage checkpoint response to replication stress: A Game of Forks. *Frontiers in Genetics*. 2013;4.
165. Paulovich AG, Margulies RU, Garvik BM, Hartwell LH. RAD9, RAD17, and RAD24 are required for S phase regulation in *Saccharomyces cerevisiae* in response to DNA damage. *Genetics*. 1997;145(1):45-62.
166. Zou L. Four pillars of the S-phase checkpoint. *Genes & Development*. 2013;27(3):227-33.
167. Kumar S, Burgers PM. Lagging strand maturation factor Dna2 is a component of the replication checkpoint initiation machinery. *Genes & Development*. 2013;27(3):313-21.
168. Moldovan G-L, Pfander B, Jentsch S. PCNA, the Maestro of the Replication Fork. *Cell*. 2007;129(4):665-79.
169. Maga G, Hübscher U. Proliferating cell nuclear antigen (PCNA): a dancer with many partners. *Journal of Cell Science*. 2003;116(15):3051-60.
170. Podust VN, Tiwari N, Stephan S, Fanning E. Replication Factor C Disengages from Proliferating Cell Nuclear Antigen (PCNA) upon Sliding Clamp Formation, and PCNA Itself Tethers DNA Polymerase δ to DNA. *Journal of Biological Chemistry*. 1998;273(48):31992-9.
171. Prakash S. Translesion DNA synthesis in eukaryotes: A one- or two-polymerase affair. *Genes & Development*. 2002;16(15):1872-83.
172. Li X, Stith CM, Burgers PM, Heyer W-D. PCNA Is Required for Initiation of Recombination-Associated DNA Synthesis by DNA Polymerase δ. *Molecular Cell*. 2009;36(4):704-13.
173. Shiomi Y, Nishitani H. Control of Genome Integrity by RFC Complexes; Conductors of PCNA Loading onto and Unloading from Chromatin during DNA Replication. *Genes*. 2017;8(2).

174. Bylund GrO, Burgers PMJ. Replication Protein A-Directed Unloading of PCNA by the Ctf18 Cohesion Establishment Complex. *Molecular and Cellular Biology*. 2005;25(13):5445-55.
175. Cai J, Uhlmann F, Gibbs E, Flores-Rozas H, Lee CG, Phillips B, et al. Reconstitution of human replication factor C from its five subunits in baculovirus-infected insect cells. *Proc Natl Acad Sci U S A*. 1996;93(23):12896-901.
176. Waga S, Stillman B. Cyclin-dependent kinase inhibitor p21 modulates the DNA primer-template recognition complex. *Mol Cell Biol*. 1998;18(7):4177-87.
177. Gary R, Kim K, Cornelius HL, Park MS, Matsumoto Y. Proliferating Cell Nuclear Antigen Facilitates Excision in Long-patch Base Excision Repair. *Journal of Biological Chemistry*. 1999;274(7):4354-63.
178. Li J, Holzschu DL, Sugiyama T. PCNA is efficiently loaded on the DNA recombination intermediate to modulate polymerase delta, eta, and zeta activities. *Proc Natl Acad Sci U S A*. 2013;110(19):7672-7.
179. Yuzhakov A, Kelman Z, Hurwitz J, O'Donnell M. Multiple competition reactions for RPA order the assembly of the DNA polymerase delta holoenzyme. *EMBO J*. 1999;18(21):6189-99.
180. Sneeden JL, Grossi SM, Tappin I, Hurwitz J, Heyer W-D. Reconstitution of recombination-associated DNA synthesis with human proteins. *Nucleic Acids Research*. 2013;41(9):4913-25.
181. Li X, Heyer WD. RAD54 controls access to the invading 3'-OH end after RAD51-mediated DNA strand invasion in homologous recombination in *Saccharomyces cerevisiae*. *Nucleic Acids Res*. 2009;37(2):638-46.
182. Marini V, Krejci L. Srs2: The "Odd-Job Man" in DNA repair. *DNA Repair*. 2010;9(3):268-75.
183. Kaniecki K, De Tullio L, Gibb B, Kwon Y, Sung P, Greene EC. Dissociation of Rad51 Presynaptic Complexes and Heteroduplex DNA Joints by Tandem Assemblies of Srs2. *Cell Reports*. 2017;21(11):3166-77.
184. Armstrong AA, Mohideen F, Lima CD. Recognition of SUMO-modified PCNA requires tandem receptor motifs in Srs2. *Nature*. 2012;483(7387):59-63.
185. Burgess RC, Lisby M, Altmannova V, Krejci L, Sung P, Rothstein R. Localization of recombination proteins and Srs2 reveals anti-recombinase function in vivo. *Journal of Cell Biology*. 2009;185(6):969-81.
186. Carter SD, Vigasova D, Chen J, Chovanec M, Astrom SU. Nej1 recruits the Srs2 helicase to DNA double-strand breaks and supports repair by a single-strand annealing-like mechanism. *Proceedings of the National Academy of Sciences*. 2009;106(29):12037-42.
187. Crickard J B, Xue C, Wang W, Kwon Y, Sung P, Greene Eric C. The RecQ helicase Sgs1 drives ATP-dependent disruption of Rad51 filaments. *Nucleic Acids Research*. 2019;47(9):4694-706.
188. Bernstein KA, Shor E, Sunjevaric I, Fumasoni M, Burgess RC, Foiani M, et al. Sgs1 function in the repair of DNA replication intermediates is separable from its role in homologous recombinational repair. *The EMBO Journal*. 2009;28(7):915-25.
189. Lo Y-C, Paffett KS, Amit O, Clikeman JA, Sterk R, Brenneman MA, et al. Sgs1 Regulates Gene Conversion Tract Lengths and Crossovers Independently of Its Helicase Activity. *Molecular and Cellular Biology*. 2006;26(11):4086-94.
190. Ira G, Malkova A, Liberi G, Foiani M, Haber JE. Srs2 and Sgs1-Top3 suppress crossovers during double-strand break repair in yeast. *Cell*. 2003;115(4):401-11.
191. Moldovan G-L, Dejsuphong D, Petalcorin Mark IR, Hofmann K, Takeda S, Boulton Simon J, et al. Inhibition of Homologous Recombination by the PCNA-Interacting Protein PARI. *Molecular Cell*. 2012;45(1):75-86.

192. Bugreev DV, Yu X, Egelman EH, Mazin AV. Novel pro- and anti-recombination activities of the Bloom's syndrome helicase. *Genes & Development*. 2007;21(23):3085-94.
193. Hu Y, Raynard S, Sehorn MG, Lu X, Bussen W, Zheng L, et al. RECQL5/Recql5 helicase regulates homologous recombination and suppresses tumor formation via disruption of Rad51 presynaptic filaments. *Genes & Development*. 2007;21(23):3073-84.
194. Simandlova J, Zagelbaum J, Payne MJ, Chu WK, Shevelev I, Hanada K, et al. FBH1 Helicase Disrupts RAD51 Filaments in Vitro and Modulates Homologous Recombination in Mammalian Cells. *Journal of Biological Chemistry*. 2013;288(47):34168-80.
195. Sommers JA, Rawtani N, Gupta R, Bugreev DV, Mazin AV, Cantor SB, et al. FANCI Uses Its Motor ATPase to Destabilize Protein-DNA Complexes, Unwind Triplets, and Inhibit RAD51 Strand Exchange. *Journal of Biological Chemistry*. 2009;284(12):7505-17.
196. Fugger K, Mistrik M, Danielsen JR, Dinant C, Falck J, Bartek J, et al. Human Fbh1 helicase contributes to genome maintenance via pro- and anti-recombinase activities. *Journal of Cell Biology*. 2009;186(5):655-63.
197. Traverso G, Bettegowda C, Kraus J, Speicher MR, Kinzler KW, Vogelstein B, et al. Hyper-recombination and genetic instability in BLM-deficient epithelial cells. *Cancer Res*. 2003;63(24):8578-81.
198. Hu Y, Lu X, Barnes E, Yan M, Lou H, Luo G. Recql5 and Blm RecQ DNA Helicases Have Nonredundant Roles in Suppressing Crossovers. *Molecular and Cellular Biology*. 2005;25(9):3431-42.
199. Solinger JA, Kianitsa K, Heyer WD. Rad54, a Swi2/Snf2-like recombinational repair protein, disassembles Rad51:dsDNA filaments. *Mol Cell*. 2002;10(5):1175-88.
200. Chi P, Kwon Y, Seong C, Epshtain A, Lam I, Sung P, et al. Yeast Recombination Factor Rdh54 Functionally Interacts with the Rad51 Recombinase and Catalyzes Rad51 Removal from DNA. *Journal of Biological Chemistry*. 2006;281(36):26268-79.
201. Shah PP, Zheng X, Epshtain A, Carey JN, Bishop DK, Klein HL. Swi2/Snf2-Related Translocases Prevent Accumulation of Toxic Rad51 Complexes during Mitotic Growth. *Molecular Cell*. 2010;39(6):862-72.
202. Mason JM, Dusad K, Wright WD, Grubb J, Budke B, Heyer W-D, et al. RAD54 family translocases counter genotoxic effects of RAD51 in human tumor cells. *Nucleic Acids Research*. 2015;43(6):3180-96.
203. Mazin AV, Mazina OM, Bugreev DV, Rossi MJ. Rad54, the motor of homologous recombination. *DNA Repair*. 2010;9(3):286-302.
204. Klein HL. Mutations in recombinational repair and in checkpoint control genes suppress the lethal combination of srs2Delta with other DNA repair genes in *Saccharomyces cerevisiae*. *Genetics*. 2001;157(2):557-65.
205. Gaines WA, Godin SK, Kabbinavar FF, Rao T, VanDemark AP, Sung P, et al. Promotion of presynaptic filament assembly by the ensemble of *S. cerevisiae* Rad51 paralogues with Rad52. *Nature Communications*. 2015;6(1).
206. Burgess RC, Sebesta M, Sisakova A, Marini VP, Lisby M, Damborsky J, et al. The PCNA Interaction Protein Box Sequence in Rad54 Is an Integral Part of Its ATPase Domain and Is Required for Efficient DNA Repair and Recombination. *PLoS ONE*. 2013;8(12).
207. Doe CL. The involvement of Srs2 in post-replication repair and homologous recombination in fission yeast. *Nucleic Acids Research*. 2004;32(4):1480-91.
208. Veaute X, Jeusset J, Soustelle C, Kowalczykowski SC, Le Cam E, Fabre F. The Srs2 helicase prevents recombination by disrupting Rad51 nucleoprotein filaments. *Nature*. 2003;423(6937):309-12.
209. Coic E, Feldman T, Landman AS, Haber JE. Mechanisms of Rad52-Independent Spontaneous and UV-Induced Mitotic Recombination in *Saccharomyces cerevisiae*. *Genetics*. 2008;179(1):199-211.

210. Mehta A, Haber JE. Sources of DNA Double-Strand Breaks and Models of Recombinational DNA Repair. *Cold Spring Harbor Perspectives in Biology*. 2014;6(9):a016428-a.
211. Claussin C, Porubský D, Spierings DCJ, Halsema N, Rentas S, Guryev V, et al. Genome-wide mapping of sister chromatid exchange events in single yeast cells using Strand-seq. *eLife*. 2017;6.
212. Kolesar P, Altmannova V, Silva S, Lisby M, Krejci L. Pro-recombination Role of Srs2 Protein Requires SUMO (Small Ubiquitin-like Modifier) but Is Independent of PCNA (Proliferating Cell Nuclear Antigen) Interaction. *Journal of Biological Chemistry*. 2016;291(14):7594-607.
213. Le Breton C, Dupaigne P, Robert T, Le Cam E, Gangloff S, Fabre F, et al. Srs2 removes deadly recombination intermediates independently of its interaction with SUMO-modified PCNA. *Nucleic Acids Research*. 2008;36(15):4964-74.
214. Makovets S, Herskowitz I, Blackburn EH. Anatomy and Dynamics of DNA Replication Fork Movement in Yeast Telomeric Regions. *Molecular and Cellular Biology*. 2004;24(9):4019-31.
215. Wach A, Brachat A, Pöhlmann R, Philippson P. New heterologous modules for classical or PCR-based gene disruptions in *Saccharomyces cerevisiae*. *Yeast*. 1994;10(13):1793-808.
216. Longtine MS, McKenzie Iii A, Demarini DJ, Shah NG, Wach A, Brachat A, et al. Additional modules for versatile and economical PCR-based gene deletion and modification in *Saccharomyces cerevisiae*. *Yeast*. 1998;14(10):953-61.
217. Goldstein AL, McCusker JH. Three new dominant drug resistance cassettes for gene disruption in *Saccharomyces cerevisiae*. *Yeast*. 1999;15(14):1541-53.
218. Makovets S, Blackburn EH. DNA damage signalling prevents deleterious telomere addition at DNA breaks. *Nature Cell Biology*. 2009;11(11):1383-6.
219. Van Driessche B, Tafforeau L, Hentges P, Carr AM, Vandenhoute J. Additional vectors for PCR-based gene tagging in *Saccharomyces cerevisiae* and *Schizosaccharomyces pombe* using nourseothricin resistance. *Yeast*. 2005;22(13):1061-8.
220. Bonilla B, Hengel SR, Grundy MK, Bernstein KA. RAD51 Gene Family Structure and Function. *Annu Rev Genet*. 2020;54:25-46.
221. Solinger JA, Heyer WD. Rad54 protein stimulates the postsynaptic phase of Rad51 protein-mediated DNA strand exchange. *Proc Natl Acad Sci U S A*. 2001;98(15):8447-53.
222. Tsurimoto T, Stillman B. Functions of replication factor C and proliferating-cell nuclear antigen: functional similarity of DNA polymerase accessory proteins from human cells and bacteriophage T4. *Proc Natl Acad Sci U S A*. 1990;87(3):1023-7.
223. Hingorani MM, Coman MM. On the specificity of interaction between the *Saccharomyces cerevisiae* clamp loader replication factor C and primed DNA templates during DNA replication. *J Biol Chem*. 2002;277(49):47213-24.
224. Boehm EM, Gildenberg MS, Washington MT. The Many Roles of PCNA in Eukaryotic DNA Replication. *Enzymes*. 2016;39:231-54.
225. Ceccaldi R, Rondinelli B, D'Andrea AD. Repair Pathway Choices and Consequences at the Double-Strand Break. *Trends Cell Biol*. 2016;26(1):52-64.
226. Heyer WD, Li X, Rolfsmeier M, Zhang XP. Rad54: the Swiss Army knife of homologous recombination? *Nucleic Acids Res*. 2006;34(15):4115-25.
227. Barlow JH, Lisby M, Rothstein R. Differential regulation of the cellular response to DNA double-strand breaks in G1. *Mol Cell*. 2008;30(1):73-85.
228. Ira G, Haber JE. Characterization of RAD51-independent break-induced replication that acts preferentially with short homologous sequences. *Mol Cell Biol*. 2002;22(18):6384-92.

229. van der Heijden T, Seidel R, Modesti M, Kanaar R, Wyman C, Dekker C. Real-time assembly and disassembly of human RAD51 filaments on individual DNA molecules. *Nucleic Acids Res.* 2007;35(17):5646-57.
230. Donaldson AD, Fangman WL, Brewer BJ. Cdc7 is required throughout the yeast S phase to activate replication origins. *Genes & Development.* 1998;12(4):491-501.
231. Vogelauer M, Rubbi L, Lucas I, Brewer BJ, Grunstein M. Histone Acetylation Regulates the Time of Replication Origin Firing. *Molecular Cell.* 2002;10(5):1223-33.
232. Osborn AJ. Mrc1 is a replication fork component whose phosphorylation in response to DNA replication stress activates Rad53. *Genes & Development.* 2003;17(14):1755-67.
233. Amin A, Wu R, Cheung MH, Scott JF, Wang Z, Zhou Z, et al. An Essential and Cell-Cycle-Dependent ORC Dimerization Cycle Regulates Eukaryotic Chromosomal DNA Replication. *Cell Reports.* 2020;30(10):3323-38.e6.
234. Tercero JA. DNA synthesis at individual replication forks requires the essential initiation factor Cdc45p. *The EMBO Journal.* 2000;19(9):2082-93.
235. Haase SB, Reed SI. Improved Flow Cytometric Analysis of the Budding Yeast Cell Cycle. *Cell Cycle.* 2014;1(2):117-21.
236. Woppard A, Basi G, Nurse P. A novel S phase inhibitor in fission yeast. *EMBO J.* 1996;15(17):4603-12.
237. Heyer W-D, Li X, Rolfsmeier M, Zhang X-P. Rad54: the Swiss Army knife of homologous recombination? *Nucleic Acids Research.* 2006;34(15):4115-25.
238. Cloud V, Chan YL, Grubb J, Budke B, Bishop DK. Rad51 Is an Accessory Factor for Dmc1-Mediated Joint Molecule Formation During Meiosis. *Science.* 2012;337(6099):1222-5.
239. Giannattasio M, Follonier C, Tourrière H, Puddu F, Lazzaro F, Pasero P, et al. Exo1 Competes with Repair Synthesis, Converts NER Intermediates to Long ssDNA Gaps, and Promotes Checkpoint Activation. *Molecular Cell.* 2010;40(1):50-62.
240. Corcoles-Saez I, Dong K, Johnson AL, Waskiewicz E, Costanzo M, Boone C, et al. Essential Function of Mec1, the Budding Yeast ATM/ATR Checkpoint-Response Kinase, in Protein Homeostasis. *Developmental Cell.* 2018;46(4):495-503.e2.
241. Budd ME, Reis CC, Smith S, Myung K, Campbell JL. Evidence Suggesting that Pif1 Helicase Functions in DNA Replication with the Dna2 Helicase/Nuclease and DNA Polymerase δ. *Molecular and Cellular Biology.* 2006;26(7):2490-500.
242. Goellner EM, Putnam CD, Graham WJ, Rahal CM, Li B-Z, Kolodner RD. Identification of Exo1-Msh2 interaction motifs in DNA mismatch repair and new Msh2-binding partners. *Nature Structural & Molecular Biology.* 2018;25(8):650-9.
243. Alver RC, Zhang T, Josephrajan A, Fultz BL, Hendrix CJ, Das-Bradoo S, et al. The N-terminus of Mcm10 is important for interaction with the 9-1-1 clamp and in resistance to DNA damage. *Nucleic Acids Research.* 2014;42(13):8389-404.
244. EMBL-EBI. T-Coffee multiple sequence alignment program [Available from: <https://www.ebi.ac.uk/Tools/msa/tcoffee/>.]
245. Duggan K. Bioinformatics Tools FAQ; EMBL-EBI 2019 [Available from: <https://www.ebi.ac.uk/seqdb/confluence/display/JDSAT/Bioinformatics+Tools+FAQ>.]
246. Choi D-H, Lee R, Kwon S-H, Bae S-H. Hrq1 functions independently of Sgs1 to preserve genome integrity in *Saccharomyces cerevisiae*. *Journal of Microbiology.* 2013;51(1):105-12.
247. Barea F, Tessaro S, Bonatto D. In silico analyses of a new group of fungal and plant RecQ4-homologous proteins. *Computational Biology and Chemistry.* 2008;32(5):349-58.
248. Schurer KA. Yeast MPH1 Gene Functions in an Error-Free DNA Damage Bypass Pathway That Requires Genes From Homologous Recombination, but Not From Postreplicative Repair. *Genetics.* 2004;166(4):1673-86.

249. Panico ER, Ede C, Schildmann M, Schürer KA, Kramer W. Genetic evidence for a role of *Saccharomyces cerevisiae*Mph1 in recombinational DNA repair under replicative stress. *Yeast.* 2010;27(1):11-27.
250. Laha S, Das SP, Hajra S, Sau S, Sinha P. The budding yeast protein Chl1p is required to preserve genome integrity upon DNA damage in S-phase. *Nucleic Acids Research.* 2006;34(20):5880-91.
251. Ogiwara H, Ui A, Lai MS, Enomoto T, Seki M. Chl1 and Ctf4 are required for damage-induced recombinations. *Biochemical and Biophysical Research Communications.* 2007;354(1):222-6.
252. Gangloff S, Soustelle C, Fabre F. Homologous recombination is responsible for cell death in the absence of the Sgs1 and Srs2 helicases. *Nature Genetics.* 2000;25(2):192-4.
253. McVey M, Kaeberlein M, Tissenbaum HA, Guarente L. The short life span of *Saccharomyces cerevisiae* sgs1 and srs2 mutants is a composite of normal aging processes and mitotic arrest due to defective recombination. *Genetics.* 2001;157(4):1531-42.
254. Bashkirov VI, King JS, Bashkirova EV, Schmuckli-Maurer J, Heyer W-D. DNA Repair Protein Rad55 Is a Terminal Substrate of the DNA Damage Checkpoints. *Molecular and Cellular Biology.* 2000;20(12):4393-404.
255. Bashkirov VI, Herzberg K, Haghnazari E, Vlasenko AS, Heyer WD. DNA Damage-Induced Phosphorylation of Rad55 Protein as a Sentinel for DNA Damage Checkpoint Activation in *S. cerevisiae*. *DNA Repair, Part B. Methods in Enzymology*2006. p. 166-82.
256. Flott S, Kwon Y, Pigli YZ, Rice PA, Sung P, Jackson SP. Regulation of Rad51 function by phosphorylation. *EMBO reports.* 2011;12(8):833-9.
257. Ranjha L, Levikova M, Altmannova V, Krejci L, Cejka P. Sumoylation regulates the stability and nuclease activity of *Saccharomyces cerevisiae* Dna2. *Communications Biology.* 2019;2(1).
258. Hicks WM, Yamaguchi M, Haber JE. Real-time analysis of double-strand DNA break repair by homologous recombination. *Proceedings of the National Academy of Sciences.* 2011;108(8):3108-15.
259. Chung W-H, Zhu Z, Papusha A, Malkova A, Ira G. Defective Resection at DNA Double-Strand Breaks Leads to De Novo Telomere Formation and Enhances Gene Targeting. *PLoS Genetics.* 2010;6(5).
260. Jain S, Sugawara N, Lydeard J, Vaze M, Tanguy Le Gac N, Haber JE. A recombination execution checkpoint regulates the choice of homologous recombination pathway during DNA double-strand break repair. *Genes & Development.* 2009;23(3):291-303.
261. Steven W, Wang X, Haber JE. Role of *Saccharomyces* Single-Stranded DNA-Binding Protein RPA in the Strand Invasion Step of Double-Strand Break Repair. *PLoS Biology.* 2004;2(1).